THE UNIVERSITY OF OKLAHOMA

GRADUATE COLLEGE

FLOW INSTABILITY THRESHOLDS IN A NATURAL-CIRCULATION LOOP

A DISSERTATION

SUBMITTED TO THE GRADUATE FACULTY

in partial fulfillment of the requirements for the

degree of

DOCTOR OF PHILOSOPHY

BY

BILLY JAY WALKER

Norman, Oklahoma

1967

FLOW INSTABILITY THRESHOLDS IN A

NATURAL-CIRCULATION LOOP

APPROVED BY

Darrel G. Harden

W. Ewbank

W. N. Huff

J. T. Sone

C. M. Sliepcevich

DISSERTATION COMMITTEE

ABSTRACT

An analytical and experimental investigation was made of the flow instability threshold in a closed natural-circulation loop. The "density effect" model formulated by Boure was utilized to predict the instability threshold in terms of dimensionless parameters. Comparison with experimental data showed that the model which is based on large density changes as the sole driving mechanism for the oscillations was sufficiently accurate to predict pressure and flow instabilities.

The various vibrational modes of the loop were calculated and compared with the experimental oscillations. Results showed that the loop tended to vibrate at frequencies comparable to the natural frequencies of the various modes of vibration of the loop.

ACKNOWLEDGEMENTS

This research was sponsored by the National Science Foundation (Grant Number GK-742). The financial support of this organization is gratefully acknowledged.

The author also acknowledges the financial support given him by the National Aeronautics and Space Administration through the NASA traineeship.

The author also wishes to express his gratitude and sincere appreciation to Dr. D. G. Harden whose encouragement, patience and guidance has made this dissertation possible.

Sincere appreciation is extended to the author's graduate committee: Dr. T. J. Love, Dr. C. M. Sliepcevich, Professor W. J. Ewbank and Dr. W. N. Huff for their suggestions and criticism. The author also wishes to acknowledge the work of D. C. Nelson for his help with the experimental apparatus.

Special thanks go to the author's family for their continued encouragement throughout his academic career.

Finally, to my wife, Mary Ann, for her understanding, encouragement and especially her patience, I am sincerely grateful.

TABLE OF CONTENTS

LIST OF TABLES

LIST OF ILLUSTRATIONS

NOMENCLATURE

Model Parameters

Dimensional Quantities		Corresponding Non-Dimensional Quantities
F	- Friction factor, Dimensionless	f
G	- Acceleration of gravity, ft/sec^2	g
H	- Fluid enthalpy, Btu/lb_m	h
L	- Pipe section length, ft	ℓ
R	- Fluid density, lb_m/ft^3	ρ
T	- Time, sec	t
U	- Fluid velocity, ft/sec	u
V	- Transient velocity, ft/sec	v
W	- Volumetric heat flux, $Btu/ft^3 sec$	w
Z	- Axial coordinate, ft	z
ΔP	- Pressure drop, psid	Δp
Θ	- Time parameter, sec	θ
Ω	- Frequency, rad/sec	ω

(These quantities defined by Equations (1 - 12), pp. 33-45)

---

a_i - Defined by Equations (IV-7, IV-10, IV-13)

B_i - Defined by Equations (III-45, III-54, III-56)

b_i - Defined by Equations (IV-8, IV-11, IV-14)

c - Complex constant

D - Hydraulic diameter, ft

E_s - Defined by Equation (III-1)

E_y - Defined by Equation (III-23)

K - Defined by Equation (IV-3)

k - Defined by Equation (II-10)

M_i - Defined by Equations (III-35) - (III-43)

m - Defined by Equation (II-10)

r - Real constant

S - Defined by Equation (IV-3)

s - Subcooling, defined by Equation (40)

Y - Defined by Equation (IV-3)

y - Defined by Equation (III-23)

ζ - Defined by Equation (I-6)

η - Defined by Equation (I-6)

λ - Defined by Equation (41)

ξ - Defined by Equation (I-6)

τ - Defined by Equation (36)

Subscripts

∞ - Steady state stream properties

o - Refers to upstream properties and steady state values

c - Refers to heater section

ss - Steady state values

1 - Refers to downstream properties

D.A.S. - Downstream adiabatic section

D.H.S. - Downstream heated section

H.S. - Heated section

U.A.S. - Upstream adiabatic section

U.H.S. - Upstream heated section

Other Than Model Parameters

a - Sonic velocity, ft/sec

C_p - Specific heat, Btu/lb_m ^oF

f - Frequency, sec^{-1}

g - Gravitational acceleration, ft/sec^2

g_c - Gravitational constant, $\frac{lb_m \cdot ft}{lb_f\ sec^2}$

h - Enthalpy, Btu/lb_m

$\bar{h}$ - Convective heat transfer coefficient, Btu/ft^2sec ^oF

L - Length, ft

m - Mass, lb_m

P - Pressure, psia

Q - Heat transfer rate, Btu/sec

T - Temperature, ^oF

t - Time, sec

W - Total heat transfer, Btu/sec

x - Axial coordinate, ft

ρ - Density, lb_m/ft^3

ω - Circular frequency, rad/sec

Subscripts

L - Liquid

max - Maximum

n - Natural frequency

s - Constant entropy

v - Vapor

FLOW INSTABILITY THRESHOLDS IN A NATURAL-CIRCULATION LOOP

CHAPTER I

INTRODUCTION

The onset of combined pressure and flow oscillations in natural-circulation loops and various other fluid flow systems under certain operating conditions are of importance to designers in various areas. Some of the areas where research has been and is now being carried on are: (a) regenerative heating of a rocket nozzle, (b) supercritical conventional and nuclear powerplants, (c) seawater desalination plants, (d) boiling water reactors, (e) emergency cooling of nuclear reactors, and (f) cool down of helium cryopanels. Since there are several areas where the problem of combined pressure and flow oscillations is of great importance, it is necessary that (i) the mechanism which causes these oscillations be understood, and (ii) the occurrence of these oscillations be predictable.

This study was carried on primarily in the critical and supercritical thermodynamic regions. The purpose of this study was to predict an instability envelope which a designer can utilize in the development and operation of devices where these oscillations are important.

Oscillations occurring during heat transfer to a supercritical fluid were first mentioned by Schmidt *et al*[25]. They reported that pressure and temperature fluctuated very much in time during a study made to determine apparent conductivity coefficients. Their study was made utilizing a natural convection loop employing ammonia as the heat transfer fluid. These oscillations occurred near the thermodynamic critical point and made their measurements difficult and in part impossible. They also found these oscillations quite severe since they noted that at approximately 118 atm (P_{cr} = 112.1 atm), the pressure suddenly rose by about 5 atm. Since this group was interested in apparent conductivity coefficients, they did not study these oscillations in any detail except to note an increase in heat transfer near the critical state.

Several investigators[17,25,26] noted the occurrence of combined pressure and flow oscillations but they were generally considered as a nuisance.

In 1956 Wissler *et al*[31] made the first important theoretical and experimental study of oscillations of the type mentioned above. In this investigation a natural-circulation loop was built which utilized water as the heat transfer fluid. The loop was operated in the two-phase region and a study of the resulting periodic oscillations of flow rate and fluid temperature was made. The experimental results showed that stable operation was possible at both low power and at high power. At low power stable operation was possible when the temperature in the riser did not exceed the boiling point. At high power stable operation was possible when the entire riser contained a water-steam mixture. It was also found that intermediate power resulted in oscillatory modes of operation. The period of oscillations was found to be inversely proportional to the mean velocity provided that some steam was in the riser at all times. When the presence of the steam was intermittent, the periods were found to be much longer.

The analytical results of Wissler et al showed that the product of the coefficient of expansion of the fluid $\frac{d\rho}{dh}$ and the vertical height of the riser must exceed a certain value if the flow perturbation is to be sustained. Their results also showed that the period of oscillations is approximately equal to the residence time of the fluid in the heater and vertical riser. In order to predict the period of oscillation, the basic equations, i.e. the conservation equations and an equation of state, were applied to the loop and were solved on an analog computer. This analysis gave similar shaped oscillations but the periods were less than the experimentally observed values. The probable reason for the discrepancies was the representation of the equation of state. However, the trends predicted by this study lent support to the general conclusions of the stability analysis.

Garlid et al[12] devised mathematical models of the transient behavior of two-phase natural-circulation loops. The initial portion of this work produced solutions from an analog computer which patterned the geometry and operating conditions after those of the University of Minnesota loop originally studied by Wissler as mentioned above. Since many simplifying assumptions had to be made, more sophisticated models were formulated to be solved on a high speed digital computer.

The mathematical model utilized consisted of writing the conservation equations in finite difference form and applying a forward differencing technique* to solve the resulting set of partial differential equations. This study showed that it was difficult to establish rigorously that the numerical procedure was stable to round off error and did not give spurious oscillations. Therefore, there is considerable doubt concerning the use of numerical methods in stability problems. This study also showed that slip (ratio of vapor velocity to liquid velocity) was a very important parameter in the analysis. Further, this study showed a significant deviation between the calculated and experimentally measured period of oscillations.

Quandt[24] studied flow instabilities in a parallel flow channel both experimentally and analytically. This analysis starts from the four basic transient equations in two-phase flow in a heated channel. The equations are linearized and small perturbations are applied. The perturbed equations are integrated and the Laplace transforms of the integrated equations are taken. In order to apply this technique, several restrictive assumptions were made. Two of the most restrictive were: (a) the period of oscillations is significantly (at least four times) longer than the residence time in the two-phase region, and (b) the mass flow rate varies linearly between the entrance and exit of the channel. Results from other studies show that the period of oscillations is approximately one and one-half times longer than the residence time.

This study emphasized the importance of the term $\frac{d\rho}{dh}$. However, this term was arbitrarily adjusted to obtain agreement between analytical

*This technique does not always permit convergence and recently a new differencing technique has been utilized in problems of this type. cf. Ref. 22.

prediction and experimental results. Another result from this study was that there is a certain minimum value of $\frac{d\rho}{dh}$ which would make an oscillatory behavior impossible for a single-phase fluid. However, this conclusion was probably made without considering single-phase supercritical fluids. Another cause of flow oscillations discussed, but not studied, was non-uniform heating of the channel.

Wallis and Heasley[30] made an important contribution by mathematically studying three modes of oscillation of a two-phase flow natural-circulation loop. In addition to the mathematical study, attempts were made to explain the oscillations in physical terms. The qualitative descriptions were supported by their experimental observations of a glass natural-circulation loop utilizing pentane as the heat transfer fluid.

Their approach was to consider the loop as a dynamic system of non-linear time delays, storage elements (capacitors), and resistances. The equations were formulated in Lagrangian terms (i.e. following the particle), linearized, and then small perturbation techniques were applied. The utilization of Lagrangian variables results in eliminating the usual trouble experienced with mixed partial differential equations in time and space by expressing the position of a fluid particle in terms of a "residence time" in various parts of the loop and integrals over time. They distinguished three possible mechanisms: (a) oscillations due to changes in riser buoyancy, (b) oscillations excited by the heater section, and (c) oscillations caused by a restriction at the top of the riser. The first two were investigated analytically and general conditions for stability were enumerated although the solutions were not applied to any particular physical problem.

Hines and Wolf[16] studied pressure oscillations occurring when RP-1 (kerosene) and DECH (diethylcyclohexane) were circulated through a test section which was electrically heated at supercritical pressures and wall temperatures. The dominant frequencies varied from 1200 to 7500 cps with principal minor frequencies ranging from 600 to 15,000 cps. The amplitude of the oscillations varied from 55 to 380 psi. Sharp increases in the heat transfer coefficient were observed near the critical temperature. When the pressure was increased from 700 to 2000 psia, no increase in heat transfer was obtained. Audible noises which were described as high-pitched screams accompanied the increased heat transfer and could be heard at distances of 200 yards from the test cell.

Assuming a sonic velocity, fundamental longitudinal acoustic resonance frequencies were calculated for the test section. These frequencies were 320-350 cps for a closed pipe and 650-700 cps for an open pipe. Therefore, it was concluded that the pressure oscillations were not simple, resonant, acoustic oscillations similar to those reported by McCarthy and Wolf[23].

It was concluded from the experiments that the basic supercritical vibration phenomenon can arise in a liquid regardless of the damping placed on the tube wall but that resultant damage to the tube was a function of wall strength and damping.

The authors also suggested a hypothesis which utilizes a variable viscosity to account for the experimentally observed oscillations. It was suggested that a sudden moderate increase in wall temperature causes an appreciable thinning of the laminar boundary layer. Thinning of the boundary layer results in a wall temperature drop and a corresponding rise in viscosity with a resultant increase in the laminar boundary layer. This would produce a wall temperature rise and the cycle would be repeated. However, no measurements of heater wall temperature could be made with the recording equipment employed in their series of tests.

Gouse and Andrysiak[14] built a closed, transparent forced and natural-circulation loop which was resistance heated with parallel, vertical test sections utilizing Freon-113 as the heat transfer fluid. Results from this study showed the following:

(a) The range of periods of measured flow oscillations were of the same order of magnitude as the range of natural periods calculated for the system.

(b) If the flow rate was large enough, there were no oscillations at any inlet temperatures.

(c) Subcooling was the most useful single independent variable in determining whether or not the flow would fluctuate.

(d) Boiling must be taking place in the test sections for flow oscillations to occur.

(e) For any particular heat flux, loop geometry, and liquid flow rate, there is a definite range of subcooling within which the flow would oscillate.

Harden[15] investigated pressure and flow transients in a natural-circulation loop operating in the critical and supercritical thermodynamic regions which utilized Freon-114 as the heat transfer fluid. He concluded from other investigations in the field that the equation of state was very important in the prediction of pressure and flow transients. Upon close examination of the experimental data, it was concluded that the oscillations seemed to occur when the fluid attained a maximum energy density (energy/unit volume). Therefore, on the basis of the experimental evidence it was concluded that pressure and flow oscillations occur near the density-enthalpy (ρh) maximum as a function of temperature, density, or enthalpy.

In the analytical portion of this investigation Harden attempted to obtain sustained pressure and flow oscillations by solving the flow equations on a digital computer utilizing a finite difference technique. Sustained oscillatory solutions were obtained by this technique but as mentioned previously, this method proves to be difficult in differentiating between an actual instability and a machine-generated instability. Therefore, some doubt is cast on the analytical results obtained.

Walker and Harden[29] constructed a natural-circulation loop and experimentally investigated the pressure and flow instabilities occurring in the critical and supercritical thermodynamic regions. Since most researchers in the area had concluded either directly or indirectly that the equation of state was very instrumental in the behavior of oscillatory flows, four fluids were chosen to be investigated experimentally. Three of the fluids were chosen on the basis that they had previously been observed to exhibit an oscillatory behavior when utilized as the heat transfer fluid in a natural-circulation loop (H_2O, Freon-12, and Freon-114). The other fluid, CO_2, was chosen since no instabilities had been reported in the literature when it had been utilized as the heat transfer fluid in a series of experiments with this fluid in the critical region by Smith and co-workers[9,18,20]. Results from this investigation showed that pressure and flow oscillations did occur for each fluid near the $\rho h(T)$ maximum for all four fluids. These results also showed that instabilities did occur when utilizing CO_2 as the heat transfer fluid in a natural-circulation loop. The instabilities proved to be easier to locate for the four fluids in the following order: (1) Freon-114, (2) Freon-12, (3) H_2O, (4) CO_2. The reason for this will be shown in Chapter V.

Cornelius and Parker[11] studied pressure and flow oscillations in both natural convection and forced flow in the critical and supercritical thermodynamic regions. It was concluded that there were two dominant types of oscillations that occur. One was of an acoustic nature which produced pressure and flow oscillations in the frequency range from 5 to 30 cps. The second was termed a slow oscillation and exhibited frequencies from 0.05 to 0.1 cps. It was concluded that the basic cause of both types of oscillatory behavior originated in the heated boundary layer. A behavior very similar to that of Hines and Wolf[16] was postulated. A pressure wave passes the heated surface and compresses the boundary layer thereby improving the thermal conductivity. This results in an increased heat transfer rate from the wall to the fluid. A rarefaction wave would have caused the boundary layer to expand and thermal conductivity to decrease and resulted in a decreased heat transfer rate to the fluid. This pressure-dependent heat transfer rate could have caused the resonant acoustic oscillation to be maintained.

A sudden improvement in the heat transfer coefficient which was attributed to a "boiling-like" behavior was also postulated. This behavior would result in an oscillatory wall temperature and an oscillatory transfer of heat from the wall to the fluid.

An attempt was made to formulate a model which would exhibit a sustained oscillation. A model quite similar to that of Harden[15] was utilized. A numerical solution was attempted utilizing an implicit differencing technique. In order to simulate the observed "boiling-like" behavior, the heat transfer coefficient - mass flow ratio was given a step increase to approximate the experimentally observed wall temperature variation. It does not appear surprising that a sustained oscillation would result in view of the fact that a "forcing function" was incorporated in the model. This theory is somewhat in doubt since some investigators[15,24] and this author found sustained pressure and flow oscillations with no apparent cycling of wall temperature.

The problems encountered by Cornelius[10] concerning flow rate measurement with a venturi were not experienced in this investigation and recent work in this area by Jain[19] shows that a venturi gives a valid flow measurement even during an oscillatory flow. This subject will be discussed in more detail in Chapter II which deals with the experimental apparatus.

Boure[8] made an excellent theoretical study of pressure and flow oscillations in a heated channel. Although this study is primarily theoretical, some comparisons were made with data from other studies which primarily include water at low pressures. The equation of state is predominant in the model utilized and the mechanism of oscillations is postulated to be the behavior of the equation of state or the "density effect". This model showed that the density effect, with its delay times, was sufficient to cause the system to oscillate and to explain the experimentally observed oscillations.

This model utilized the simplifications afforded by the use of

Lagrangian coordinates which were mentioned earlier to formulate the problem. The flow equations were formulated, linearized, and the method of small perturbations applied to the resulting equations. The methods of control theory were then utilized to predict stability. Physical interpretations of the parameters which resulted from the mathematics were given and the effect of each term was investigated.

A stability map was given in terms of the system parameters and some special flow effects were studied. The model utilized was a single-phase model and these restrictions as applied to a two-phase model were discussed.

Maulbetsch and Griffith[21] presented a somewhat novel approach to the stability problem by introducing an energy storage mechanism assumed to be that of a compressible volume upstream of the heated test section. Small perturbations were applied and a Laplace transform of the system of equations was obtained. Marginal stability was assumed and an expression for the oscillatory frequency obtained. A critical slope of the pressure drop - flow rate curve in the heated section was computed. Results showed that steady state measurements of pressure drop - flow rate curve may be used to describe the unsteady behavior with sufficient accuracy to draw meaningful conclusions concerning system stability.

All of the previous studies lead to the following conclusions:

(1) The equation of state is of fundamental importance in the study of combined pressure and flow oscillations.

(2) It should be possible to enumerate instability thresholds to include first order effects.

(3) Numerical techniques appear to be unreliable in the study of oscillatory flow.

CHAPTER II

EXPERIMENTAL APPARATUS

The natural-circulation loop utilized in this investigation had already been designed and built to accommodate the four heat transfer fluids used in this investigation. A description of this basic loop can be found in Walker[28]. For this investigation, the loop was redesigned somewhat to allow for transient instrumentation and to more closely approach the equation of state used in the analytical model while at the same time giving more control of the loop operating parameters. Therefore, only a description of the additional apparatus and the modifications of the basic loop will be included.

A. Description of the Added Equipment

A hydraulic accumulator was the single piece of equipment added to the basic loop for this investigation. This accumulator consisted of a stainless steel cylinder which housed a rubber diaphram. The five gallon capacity accumulator kept pressure relatively constant by absorbing pressure surges. The accumulator was connected to the loop at a point just downstream of the second heat exchanger through a 0.25 inch O.D. stainless steel tube. The accumulator was pressurized to system pressure with nitrogen gas. Figure (1) shows a schematic of the accumulator as it was integrated into the loop.

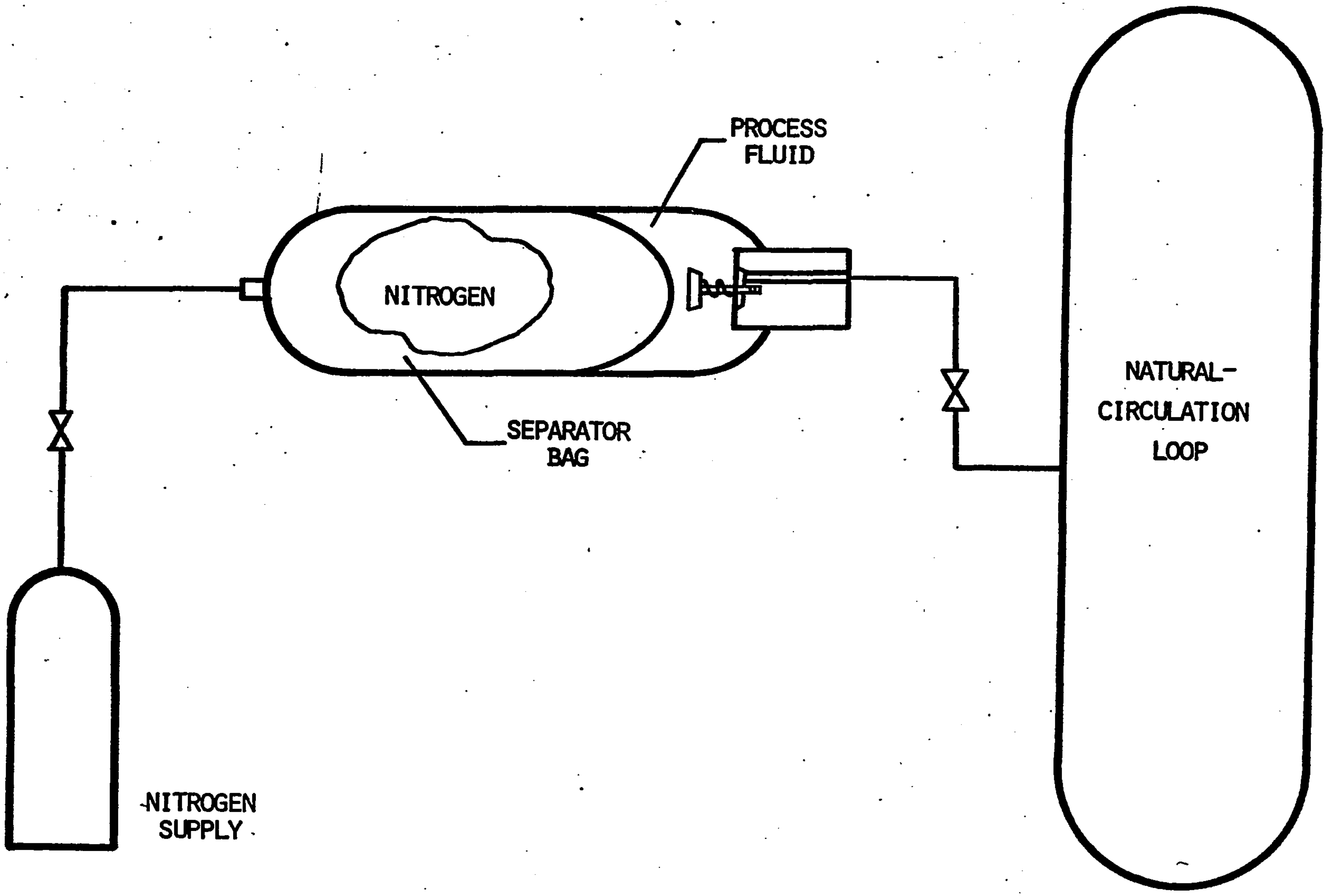

FIGURE (1) ACCUMULATOR SCHEMATIC

Addition of the accumulator to the system and the addition of transient instrumentation required that the circulation loop piping be extensively redesigned. The final design utilized in this investigation is shown in Figure (2). Notice in this figure that an alternate position is available to connect the differential pressure transducer to the venturi. This arrangement allows an evaluation of what effect line length has on the output of the transducer. Cornelius[10] reported that oscillations of up to 120 psi amplitude were observed while using a venturi for flow measurement and the amplitude did not exceed 30 psi for the same type of oscillation after a Pottermeter (Potter Aeronautical Corporation) was installed. Jain[19] ran a series of tests where both a venturi and a Pottermeter were used to simultaneously measure the flow. These tests showed that the maximum flow rates using both devices matched quite well. Since there was some disagreement, the alternate piping was included in the redesign of the loop.

Several new valves were installed that were not included in the original design and a vacuum pump was utilized to make certain the loop was completely evacuated before starting a test series after fluid had been added to the system.

B. Instrumentation

The principal reason for the piping redesign mentioned in the above section was to accommodate the transient instrumentation added to the loop. Figure (3) shows the loop instrumentation schematic. Figure (2) shows the location of some steady state temperature instrumentation while transient instrumentation is shown in Figure (3).

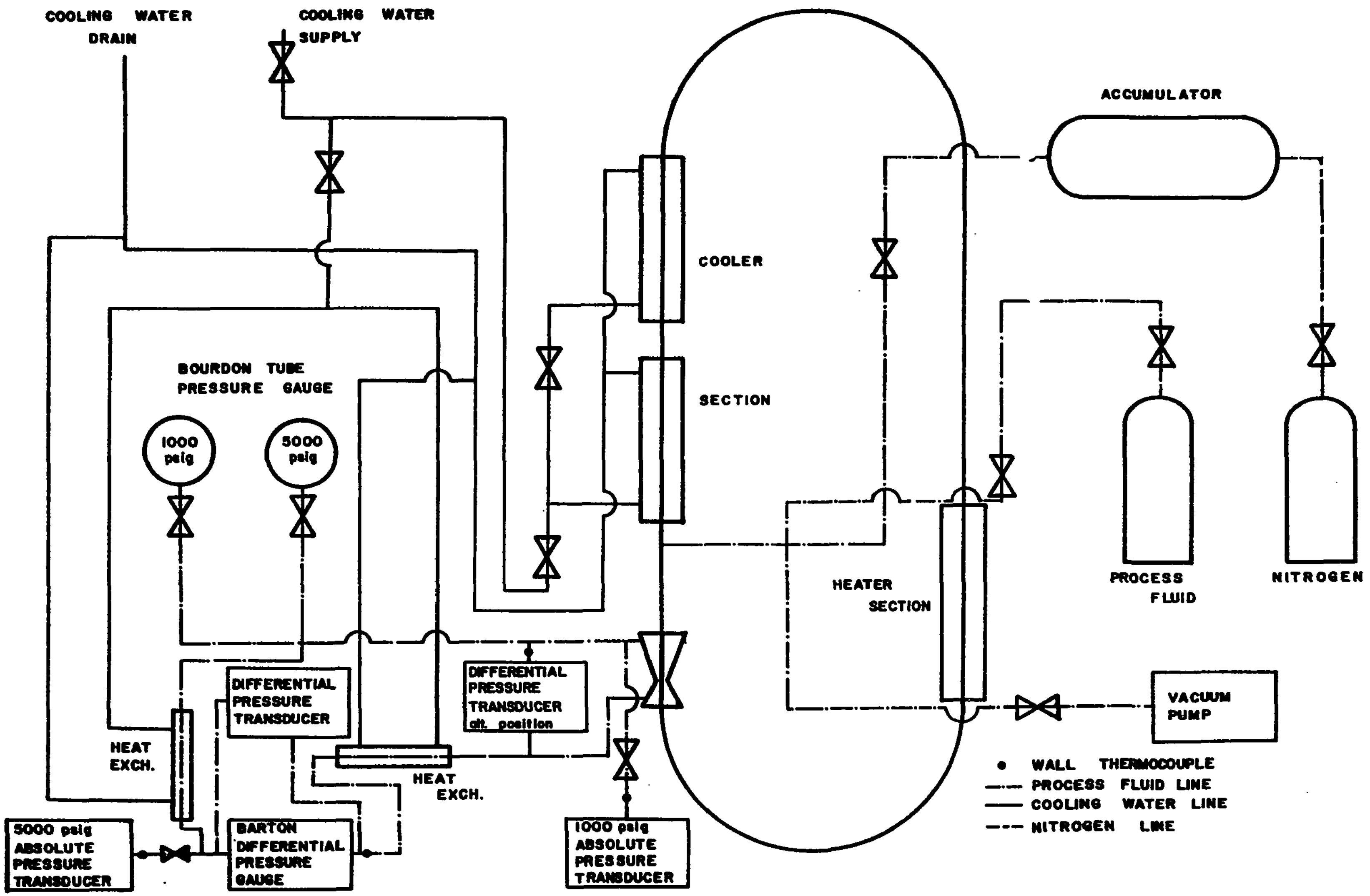

FIGURE (2) CIRCULATION LOOP PIPING DETAIL

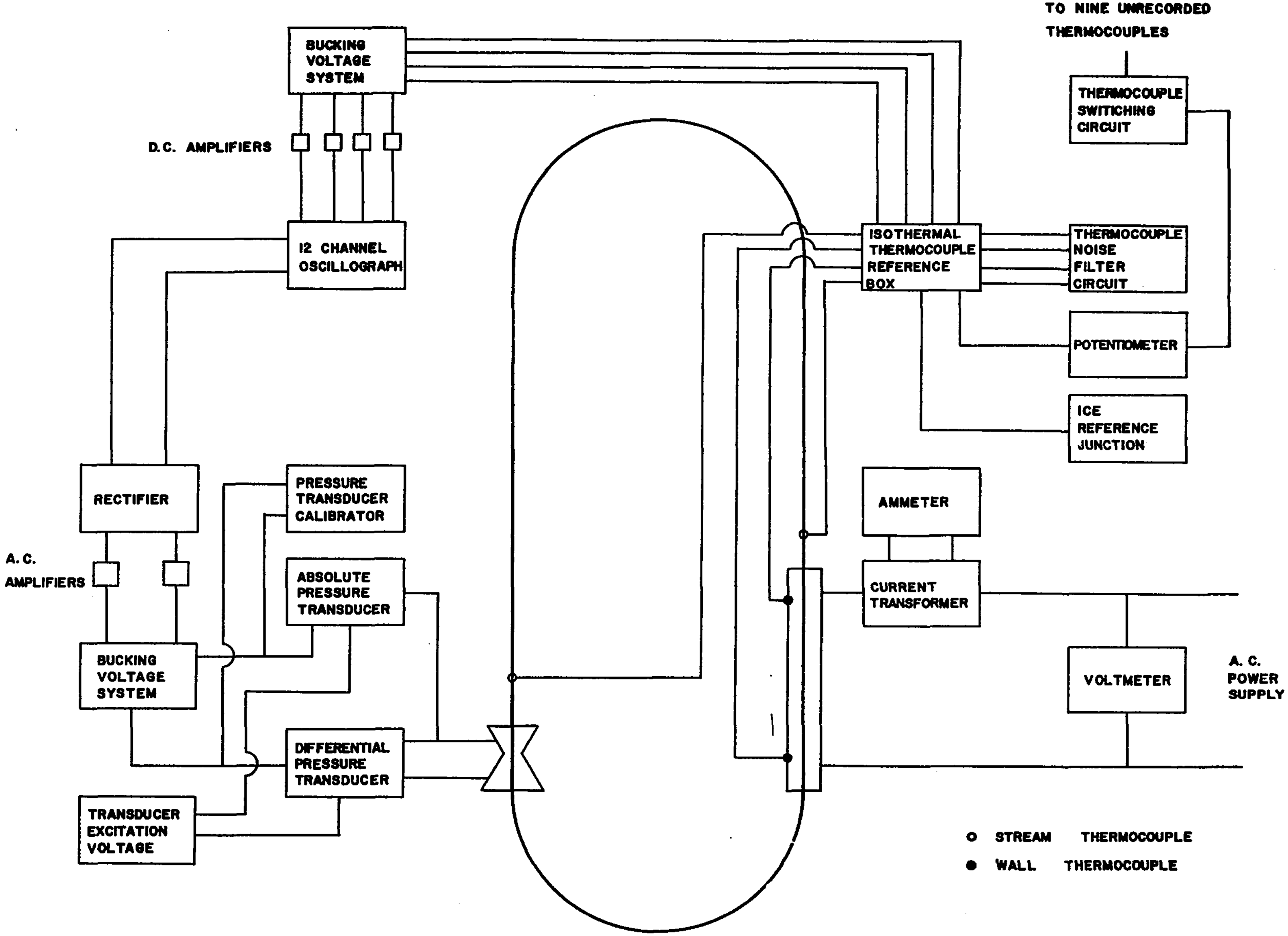

FIGURE (3) INSTRUMENTATION SCHEMATIC

1. Flow Measurement

The flow was measured with a calibrated venturi. Calibrations and specifications for this venturi can be found in Walker[28]. A 5.0 psid differential pressure transducer was connected across the outlet taps of the venturi. Cornelius[10] found that during rapid pressure oscillations measurements indicated that differential pressure oscillations whose amplitude exceeded the average value (flow reversal) were present. He suspected that the large venturi pressure drop amplitudes were due to the phase relationship of the absolute pressure at the venturi taps although subsequent analysis indicated to him that this was not entirely the reason for the large amplitude oscillations encountered in his experimental work.

Jain[19] showed the existence of a flow reversal in oscillatory flow was a reality. The problem was not one of instrumentation but was, in fact, a flow reversal. Several flow reversals were encountered in the present study and several were also encountered during the experimental investigations of Harden[15].

2. Pressure Measurement

In addition to the 1000 psig and 5000 psig bourdon-tube pressure gauges, a 1000 psig and a 5000 psig pressure transducer were utilized. The transducer circuit for both the absolute and differential type transducers are shown in Figure (4). Checking of the transducers can be accomplished without the use of a standard pressure source by utilizing the Honeywell carrier amplifier. This checking is effected by electrically shorting out one leg of the transducer bridge and is explained in

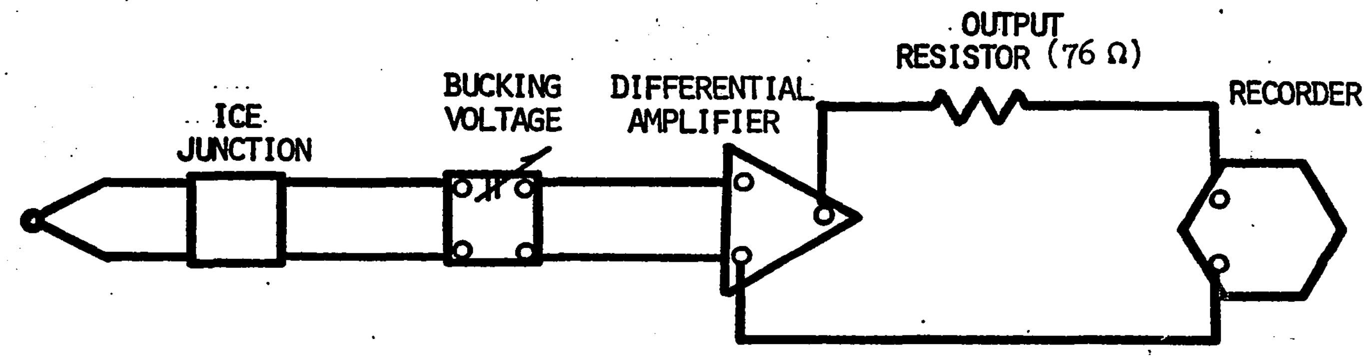

A) THERMOCOUPLE CIRCUIT

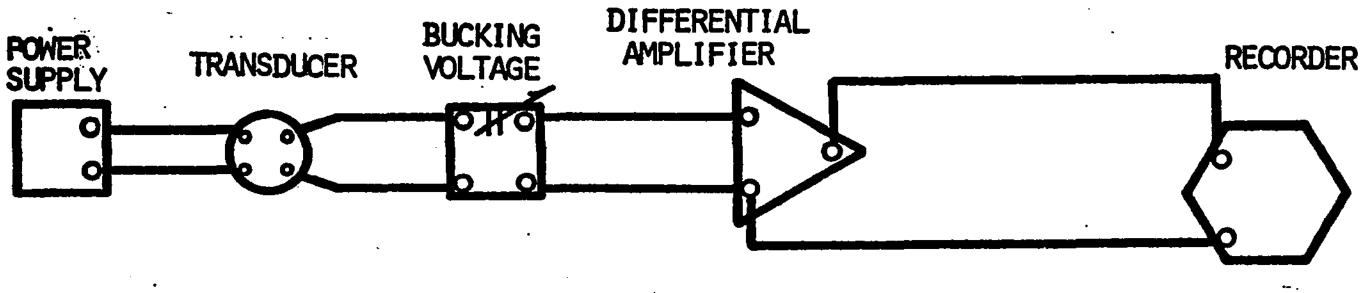

B) TRANSDUCER CIRCUIT

FIGURE (4) INDIVIDUAL CIRCUIT SCHEMATIC FOR A PRESSURE AND
A TEMPERATURE MEASURING CHANNEL

detail in Appendix VIII. This method can also be used for the differential pressure transducer.

3. Wall-Temperature Measurement

Wall temperatures were measured and recorded for the electrically heated section of the loop. The heater section temperature was monitored at the two locations shown in Figure (3). The exact placement varied slightly with the particular test series. Thirty gauge chromel-alumel thermocouples were placed on a thin mica sheet and the mica sheet was placed on the heater section wall. Then a strip of Durabla asbestos was wrapped around the thermocouple bead which was lying on the mica sheet which in turn was lying on the heater section wall. The purpose of the mica sheet was to electrically insulate the heater section from the thermocouple in order to reduce noise pickup. Noise on the thermocouple channels proved to be quite a problem with a considerable effort going into reduction of this noise level. Various low pass LR and RC filter circuits were employed in an effort to reduce the noise level. In addition, extensive shielding was also employed. Finally, these filters were discarded and a single 1500 μ-fd capacitor was installed in parallel with the thermocouple as shown in Figure (5). The reason for the excessive noise problem in this particular test apparatus was due to the power supply. This power supply is a single phase, high ampereage, A.C. transformer. Because of this, there is essentially a 100% ripple factor. Most power supplies utilized in laboratories where it is necessary to record transient parameters that emanate from a very low voltage signal, such as that of a thermocouple, utilize D.C. current. Generally, these power supplies are three-phase transformers that rectify the A.C. current.

This type power supply nominally has only a 5% ripple factor. Therefore, further noise reduction will probably necessitate acquisition of a D.C. power supply. Several other temperatures describing the loop operation were taken but not recorded since they were essentially steady state readings. Several of these were monitored so that the maximum temperatures of the fluid entering the various instruments would not be exceeded. The location of these thermocouples is shown in Figure (2). All were attached to the stainless steel piping with a condenser discharge type thermocouple welder and then covered with an epoxy for maximum strength.

4. Stream Temperature Measurement

The bulk fluid temperatures were measured downstream of the heater section and upstream of the venturi as shown in Figure (3). The thermocouples were designed similar to those shown in Figure (5) of Walker[28] which were purchased from Minneapolis-Honeywell (Part No. 2K1M13E6-5). The thermocouples were fabricated in the shop utilizing 0.25 inch O.D. type 304 seamless stainless steel tubing having a wall thickness of 0.028 inch. A high temperature ceramic adhesive was used inside the tubing to separate the thermocouple wires and to separate the wires from the inside tubing wall. The thermocouple measuring junction was left exposed in the stream in order to improve the response time. The response time was estimated to be on the order of 0.1 to 0.2 sec. thereby eliminating detection of temperature transients of frequency greater than 10 cps. Thirty gauge chromel-alumel thermocouples were utilized. Noise was also a problem for these two thermocouple channels and a capacitor had to be utilized to suppress the noise to an acceptable level. An isothermal thermocouple reference box was designed and built and is shown in

Figure (5). This reference junction box provided an isothermal point where the thermocouple wires could be replaced by copper wires going to the potentiometer and the amplifiers. Note that the potentiometer and the amplifiers are connected in parallel permitting simultaneous monitoring of the thermocouples utilizing the potentiometer for steady state readings and recording the transient signals on the oscillograph.

Figure (5) also shows the design of the common reference junction for the four measuring junctions being recorded.

The thermocouples fabricated in the shop had to be replaced while operating with Freon-114 as the heat transfer fluid. The operating temperatures that the thermocouples were exposed to exceeded the value that the epoxy pressure sealant could withstand. Two similar thermocouples were purchased from Minneapolis-Honeywell (Part No. 2K4M15-E6-6) which would seal to temperatures up to 1000 F.

5. Recording Instrumentation

Transient recording instrumentation is a necessity for the study of an oscillatory flow system. This type instrumentation was assembled and placed in a mobile cabinet in order that it could be utilized by more than one project and could be adapted to another system simply by the connection of the inlet signal and the 110 V. wall plug.

This system consists of a 12-channel recording oscillograph (Minneapolis-Honeywell visicorder), a two-channel carrier amplifier and power supply (Minneapolis-Honeywell), four differential D.C. amplifiers (Hewlett-Packard), and a D.C. bucking voltage system.

Figure (6) shows the complete instrumentation package. Figure (4) shows the individual circuit diagram for both a pressure measuring

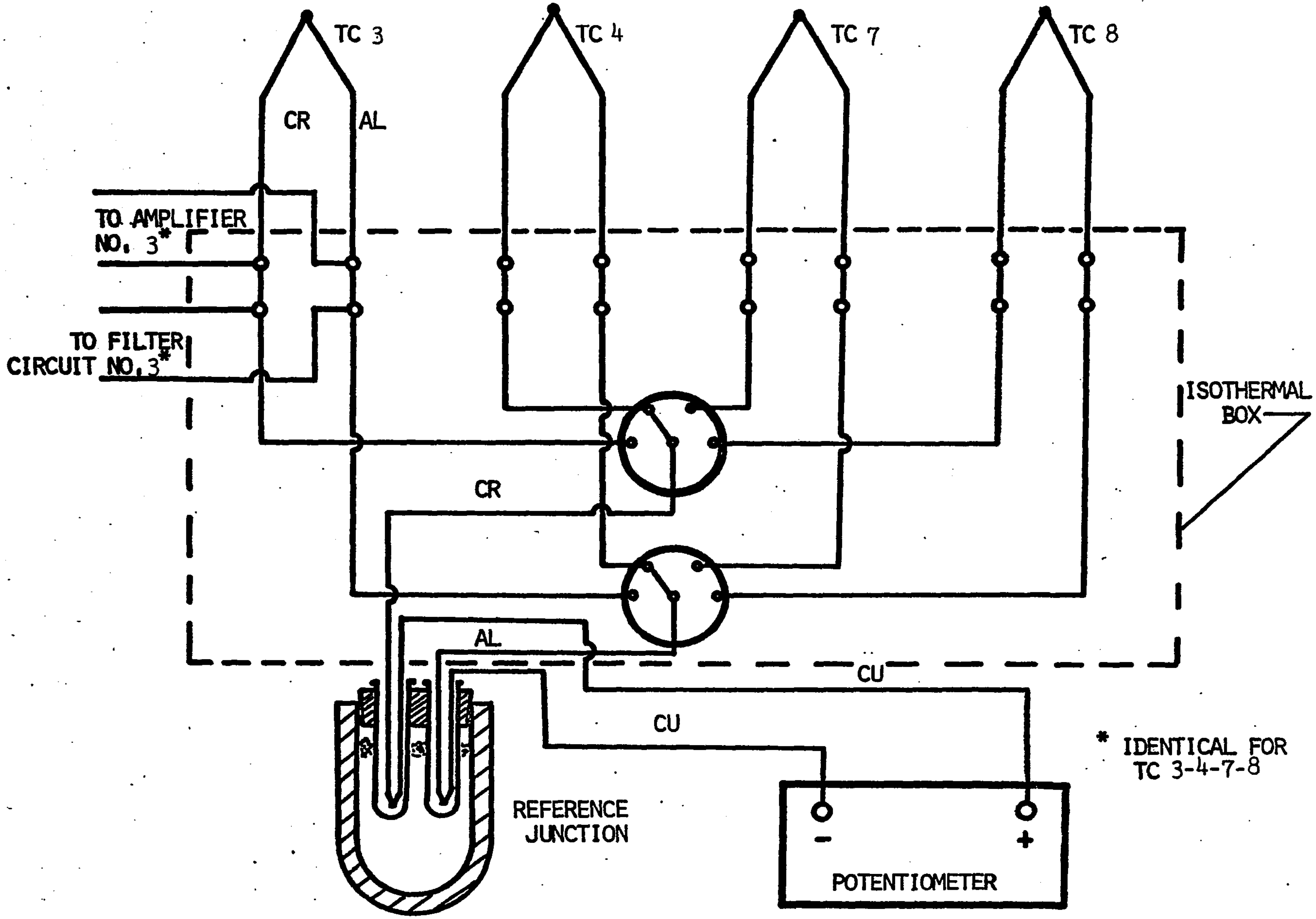

FIGURE (5) CIRCUIT DIAGRAM OF ISOTHERMAL THERMOCOUPLE REFERENCE BOX channel and a temperature measuring channel. Shielding was utilized throughout this system (although not shown in the circuit diagram of Figure (4)). The shielding was tied to a common ground point - the ground plug of the 110 V. line.

A bucking voltage system was designed and built for the four temperature channels which are fed into the Hewlett-Packard differential amplifiers. The controls for this system are shown in Figure (7) and the circuit diagram for one channel of the four-channel system is shown in Figure (8). This system was necessary to protect the optical galvanometers used in the visicorder. The galvanometers used in this investigation were fluid damped galvanometers (Minneapolis-Honeywell Part No. M-1650) which were current limited to 100 ma for short time operation and 80 ma for continuous operation. This bucking voltage system is capable of bucking out a signal up to 40 mv, hence, its use insures that an overvoltage will not be applied to the optical galvanometers. Further, this system is convenient since it allows the galvanometer light image to be conveniently placed on the photographic paper.

A bucking voltage system is built into the carrier amplifier which provides the two pressure channels with the same ease of operation that the bucking voltage system provides for the four temperature channels except that the galvanometer light image cannot be placed on the photographic paper with this system without turning the optical galvanometers themselves.

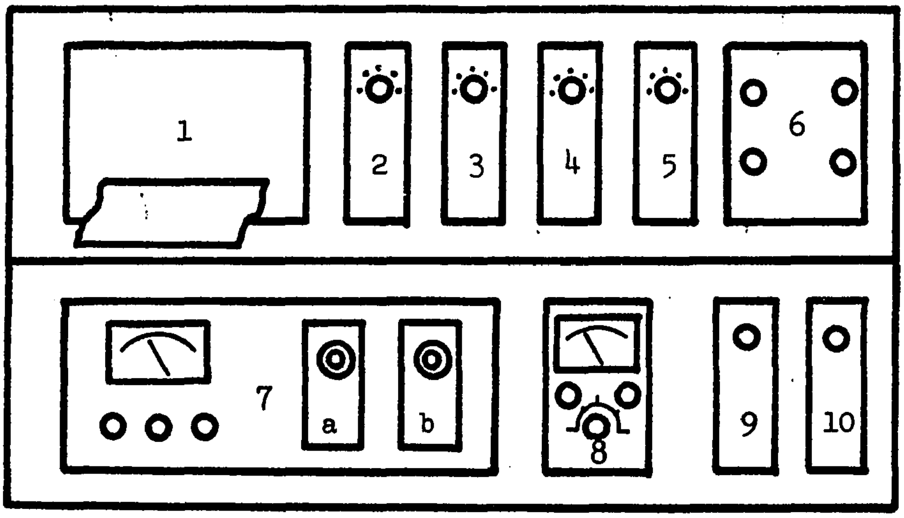

1. Recording Oscillograph, Minneapolis Honeywell Visicorder, Model 906C.

2-5. D.C. Differential Amplifier, Hewlett-Packard, Model 8875A.

6. Zero Offset Voltage System, Described elsewhere in this chapter.

7. Carrier Amplifier, Minneapolis Honeywell, Model 131-2C (Power Supply and two D.C. Amplifiers a and b).

8. Voltmeter, Hewlett-Packard, Model 410B.

9-10. Attenuator*, Minneapolis Honeywell, Accudata VII.

*This equipment not utilized in this investigation.

The following instrumentation was used but not shown in this figure.

A. Ammeter, Weston, Model 370.

B. Current Transformer, Westinghouse, Model PC-137.

FIGURE (6) MOBILE INSTRUMENTATION SYSTEM

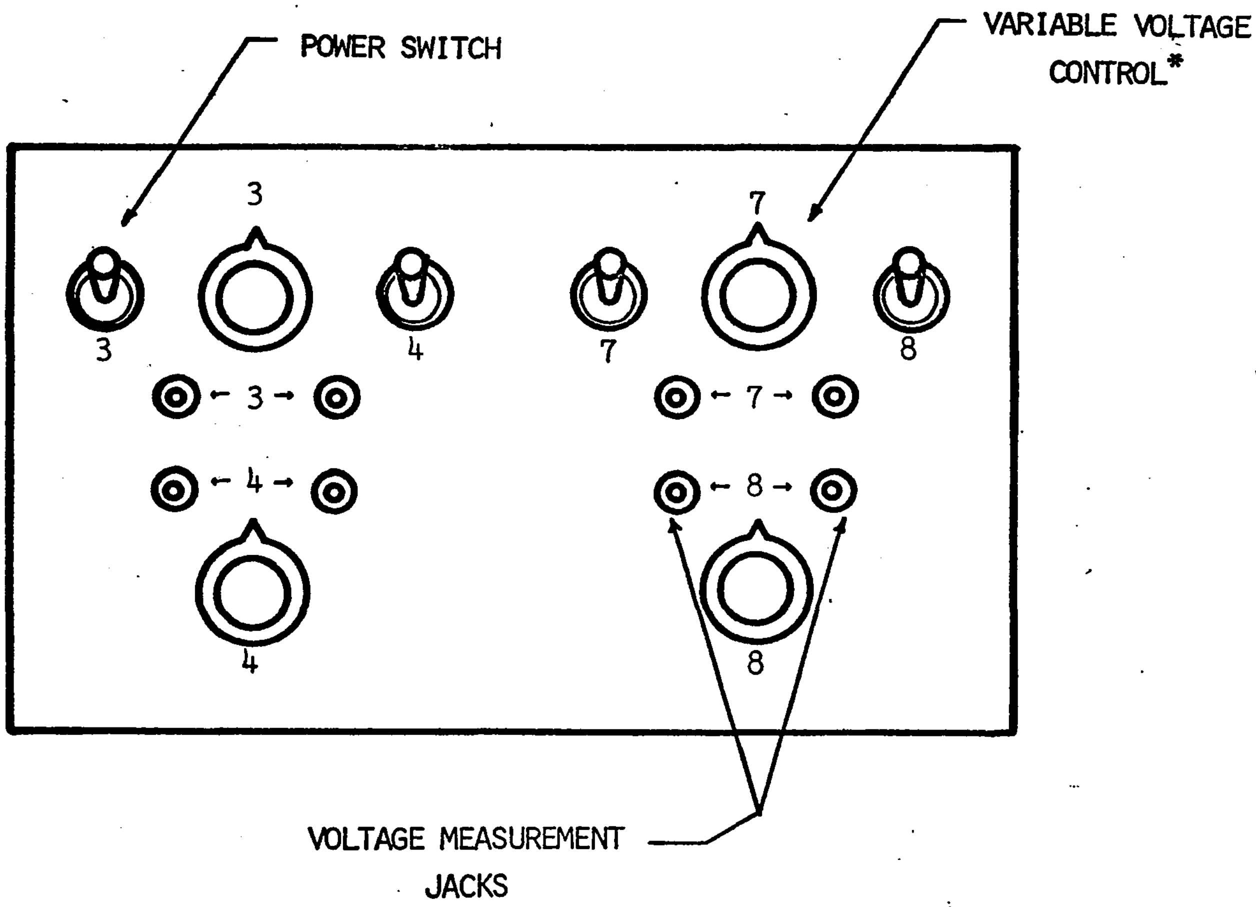

*VOLTAGE INCREASES BY TURNING CLOCKWISE FOR CHANNELS 3 AND 7, COUNTERCLOCKWISE FOR CHANNELS 4 AND 8.

FIGURE (7) FRONT VIEW OF BUCKING VOLTAGE SYSTEM

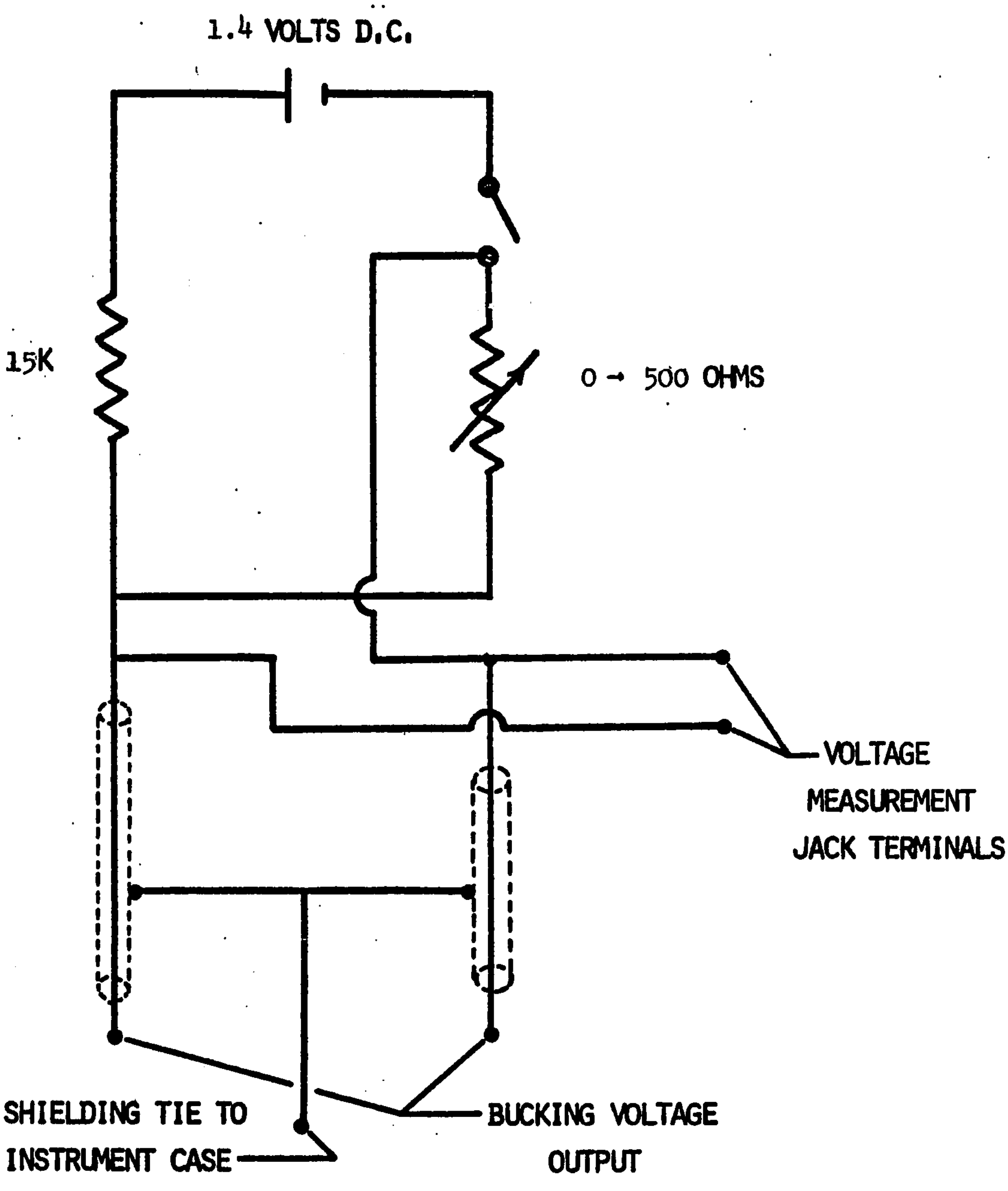

FIGURE (8) CIRCUIT DIAGRAM FOR ONE CHANNEL OF THE FOUR-CHANNEL BUCKING VOLTAGE SYSTEM

CHAPTER III

EXPERIMENTAL PROCEDURE

The loop was assembled and pressure checked for leaks at 4500 psig with water as the system fluid by utilizing a hydraulic pump to achieve that pressure. After all leaks had been stopped, the system was allowed to remain at that pressure. After 24 hours, the pressure had dropped approximately 600 psi. This was judged as sufficiently leak free since the inlet bleed valve was known to leak slightly at that high pressure.

After leak checking, the loop was drained of water and a Freon-12 cylinder was connected to the inlet process fluid line. The entire system was then evacuated utilizing a vacuum pump. After the system had been evacuated, Freon-12 was introduced into the system until the pressure in the loop and in the Freon-12 cylinder had equalized. The cooling water was then turned on and allowed to circulate through the heat exchangers. The pressure was lowered in the loop and additional fluid was allowed into the system. To further charge the system, the Freon-12 cylinder was heated in order that the fluid be distilled into the loop. This heating continued until the pressure in the loop reached 180 psig (later the same technique was utilized for charging the system with Freon-114 and CO_2 - Freon-114 was distilled in the loop until the pressure in the loop rose to 90 psig and CO_2 was pressurized to 1250 psig). These pressures assured that sufficient liquid was in the loop.

The accumulator was then charged with nitrogen gas to a pre-determined pressure for the particular test to be run. This pressure depended on the thermodynamic region in which the loop was operated in for that particular run. Subsequent operation with the accumulator in the system showed the following:

(1) The accumulator tended to damp the oscillations encountered; however, it was much more effective for the slower oscillations than for the acoustic-type oscillations.

(2) When trying to reach a certain thermodynamic operating region, the accumulator valve was sometimes kept closed. If the accumulator valve was left closed, very high amplitude oscillations such as those shown in Figure (17) were often encountered and attempts to get out of this region were very difficult. This situation often occurred just as the system was approaching a sustained oscillation. The power level for this condition was just high enough for the system to attain an oscillatory mode and then damp out.

(3) The accumulator was essential in the constant pressure runs. For these runs, the loop was filled and the accumulator nitrogen side was pressurized to the desired operating pressure. The loop was then heated slowly and the thermodynamic operating region was reached as the fluid was bled from the system to the accumulator while maintaining a constant loop pressure.

After filling the loop and integrating the accumulator into the fluid circuit, the Barton differential pressure gauge was bled to insure that only liquid occupied the line.

Various techniques were utilized to establish loop operation in a particular thermodynamic region. The most common method was to first establish a relatively high flow rate in the loop by turning on the power and operating with the heat exchangers at maximum cooling water flow. This established a density head and a flow resulted. After the fluid had attained a sufficient flow rate, the danger of heater section burnout was reduced. After the establishment of this flow rate, the oscillations were approached by bracketing the $\rho h(T)$ maximum with the bulk inlet and the bulk outlet (heater section) fluid temperatures. The cooling water flow rate and the power were then adjusted simultaneously until the $\rho h(T)$ maximum was isolated between these two bulk temperatures.

Various other techniques of locating these oscillations were utilized. One method was to slowly bring the loop pressure up by slowly heating the fluid. In this way the flow oscillations spontaneously resulted without operating the loop in any specific manner.

Control of loop operation was possible by adjusting the amount of power into the heater section, adjusting the amount of cooling water flow, and utilization of the accumulator to control system pressure.

After each series of test runs, the system was taken apart and cleaned. During operation one had to be careful not to allow the heater section wall temperature to achieve too high a value (approximately 600 to 700 F for the Freons). If the loop was allowed to overheat, a chemical reaction would occur and a residue would be deposited on the heater section walls. This deposit would severely reduce fluid flow rates and the loop would have to be disassembled and cleaned thoroughly.

CHAPTER IV

ANALYTICAL TREATMENT

A. Establishment of the General Equations

In order to be able to avert the oscillation problem which exists in the type of fluid flow systems with heat addition encountered in this investigation, it becomes necessary to accurately predict the envelope of these instabilities. An accurate prediction depends on how closely the mathematical model describes the physical situation.

Figure (9) gives a schematic representation of the physical situation. The fluid flows in a cylindrical pipe due to a pressure difference between the entrance and exit of the pipe. This one-dimensional flow of fluid is considered as flowing through three separate regions. The regions considered are:

(1) Upstream adiabatic section.

(2) Center heated section.

(3) Downstream adiabatic section.

This closely approximates the physical situation since the upstream portion and the downstream portion are insulated. One could consider a fourth region following the downstream adiabatic section, the cooler section. However, it is not really necessary to consider this section as long as it is possible to specify the conditions entering the upstream

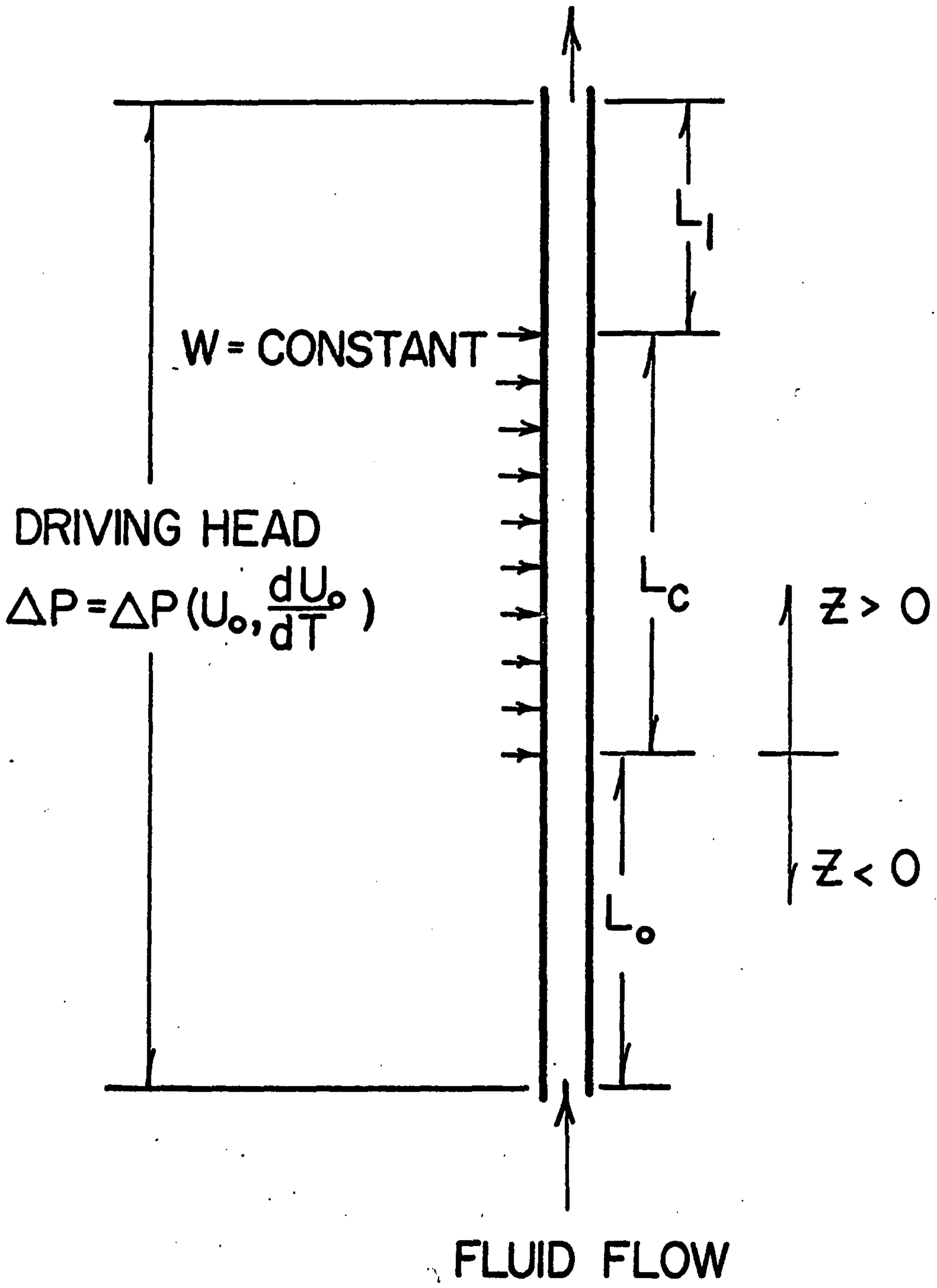

FIGURE (9) FLOW MODEL SCHEMATIC

adiabatic section and those leaving the downstream adiabatic section. This section would become necessary, for example, if integration around the loop were employed in the mathematical model. As shown in Figure (9) Z has been considered as the coordinate direction along the length of the pipe with which the various properties (R, H, etc.) vary. L_i are the various lengths of the three sections of the pipe. $U_o(T)$ is the entrance velocity into the upstream adiabatic section. W is the constant volumetric heat flux over the heated section of the pipe.

With these definitions and with the aid of Figure (9), the mathematical model is formulated. As defined above, the problem consists of the determination of four functions of distance, Z, and time, T. These functions are:

(1) Density - R = R(Z,T)

(2) Enthalpy - H = H(Z,T)

(3) Pressure - P = P(Z,T)

(4) Velocity - U = U(Z,T)

Determination of these four quantities as functions of distance and time would give a perfect definition of the fluid flow system. In order to determine these four unknown functions, four equations are necessary. The four equations that are applicable are:

(1) Conservation of mass

(2) Conservation of momentum

(3) Conservation of energy

(4) Equation of state

The conservation equations (1 - 3 above) can be found derived in most fluid mechanics texts and in Bird, Stewart, and Lightfoot[2] in particular. However, it is necessary to make several simplifying assumptions to reduce the complexity of the equations. In this analysis, the following assumptions were made:

(1) Radial variations of thermodynamic properties and velocity are neglected.

(2) Kinetic and potential energy terms are neglected.

(3) Heat transfer by conduction along the Z axis is neglected.

(4) Shear forces are neglected.

(5) The effect of pressure changes with time are neglected.

With these assumptions, the conservation equations can be written as follows:

(1) <u>Conservation of Mass</u>

$$\frac{\partial R}{\partial T} + \frac{\partial (RU)}{\partial Z} = 0 \tag{1}$$

(2) <u>Conservation of Energy</u>

$$R\frac{\partial H}{\partial T} + RU\frac{\partial H}{\partial Z} = W \tag{2}$$

(3) <u>Conservation of Momentum</u>

$$\frac{\partial P}{\partial Z} + R\frac{\partial U}{\partial T} + RU\frac{\partial U}{\partial Z} + RG + \frac{FRU^2}{2D} = 0 \tag{3}$$

Having developed the conservation equations, it becomes necessary to develop an equation of state. The installation of an accumulator in the physical system provides justification for using a simplified equation of state. The accumulator provides a relatively constant pressure throughout the system due to a discharge of fluid into the system when system pressure becomes less than a pre-set value and a removal of fluid when system pressure becomes greater than this pre-set value. The assumption of an absolutely constant pressure is valid strictly only for the low frequency oscillations. However, the accumulator was able to keep the system pressure constant until the oscillations occur and the value of the system parameters just prior to the oscillations were the ones utilized in predicting the instability envelope. Therefore, an equation of state will be utilized in which the density is a function of the enthalpy only since a constant pressure system is assumed; i.e.

$$R = R(H) \tag{4}$$

A typical plot of density as a function of enthalpy along an isobar is shown in Figure (10) for water at the critical pressure. Representations for substances other than water and for other supercritical pressures are similar (cf. Figures (11 - 14)). In order to develop an analytical expression for R(H), it is convenient to move the enthalpy zero reference from saturated liquid at 32F to the zero point shown in Figure (15). This is the point where the liquid becomes saturated for a sub-critical fluid. By changing this arbitrary reference point, the equation of state can be approximated by a single function in each region ($H \leq 0$ and $H \geq 0$). The equation of state shown in Figure (10) was approximated in the two regions by the following expressions:

$$\begin{aligned} R &= R_o + (-4H)^{1/2} \qquad && \text{for} \quad H \leq 0 \\ R &= \frac{R_o H_c}{H + H_c} && \text{for} \quad H \geq 0 \end{aligned} \tag{5}$$

where

$$R_o = R \text{ @ } H = 0$$

$$H_c = H \text{ @ } R = R_o/2$$

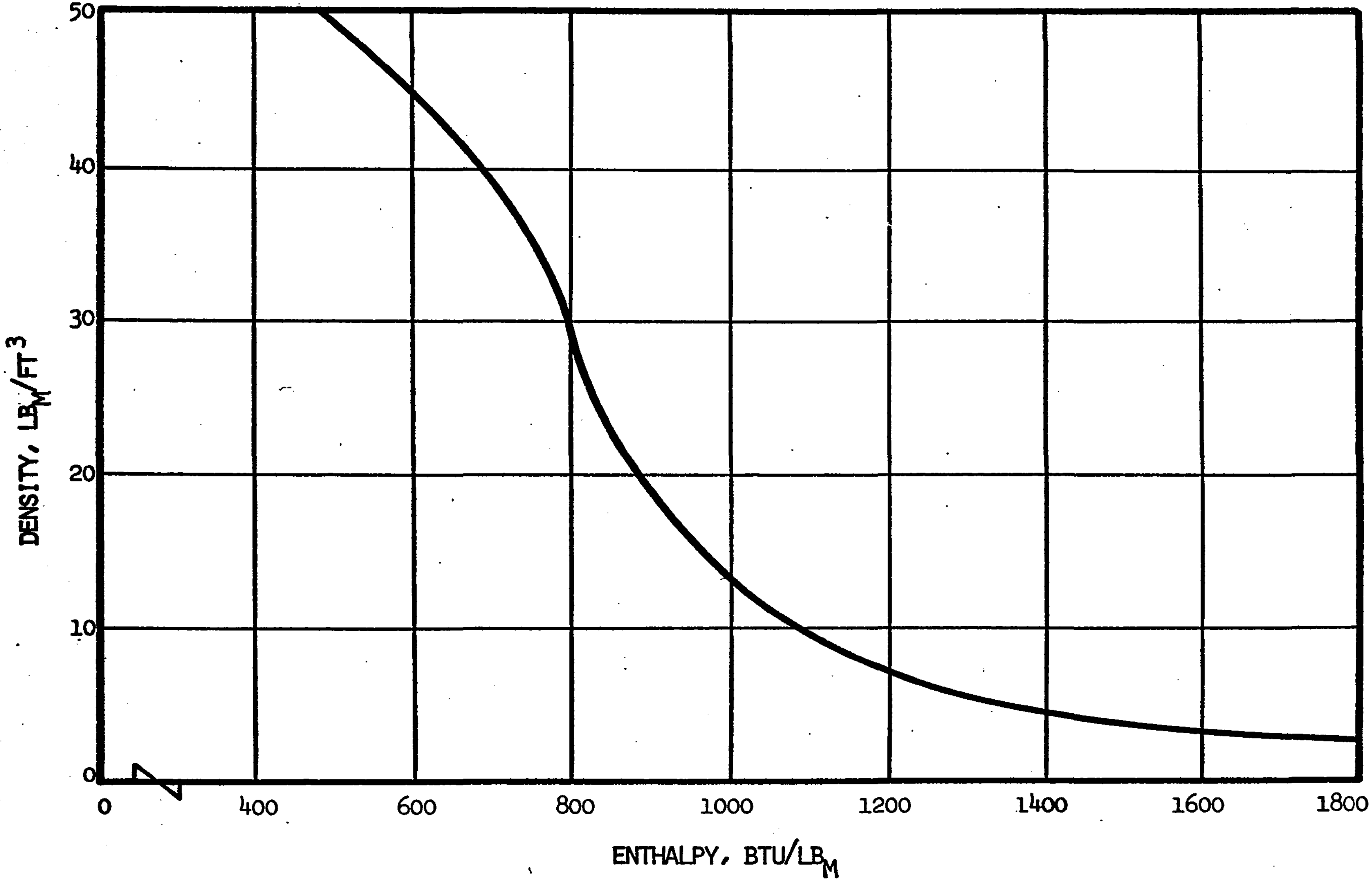

FIGURE (10) $\rho = \rho(h)$ FOR H_2O AT 3206.2 PSIA

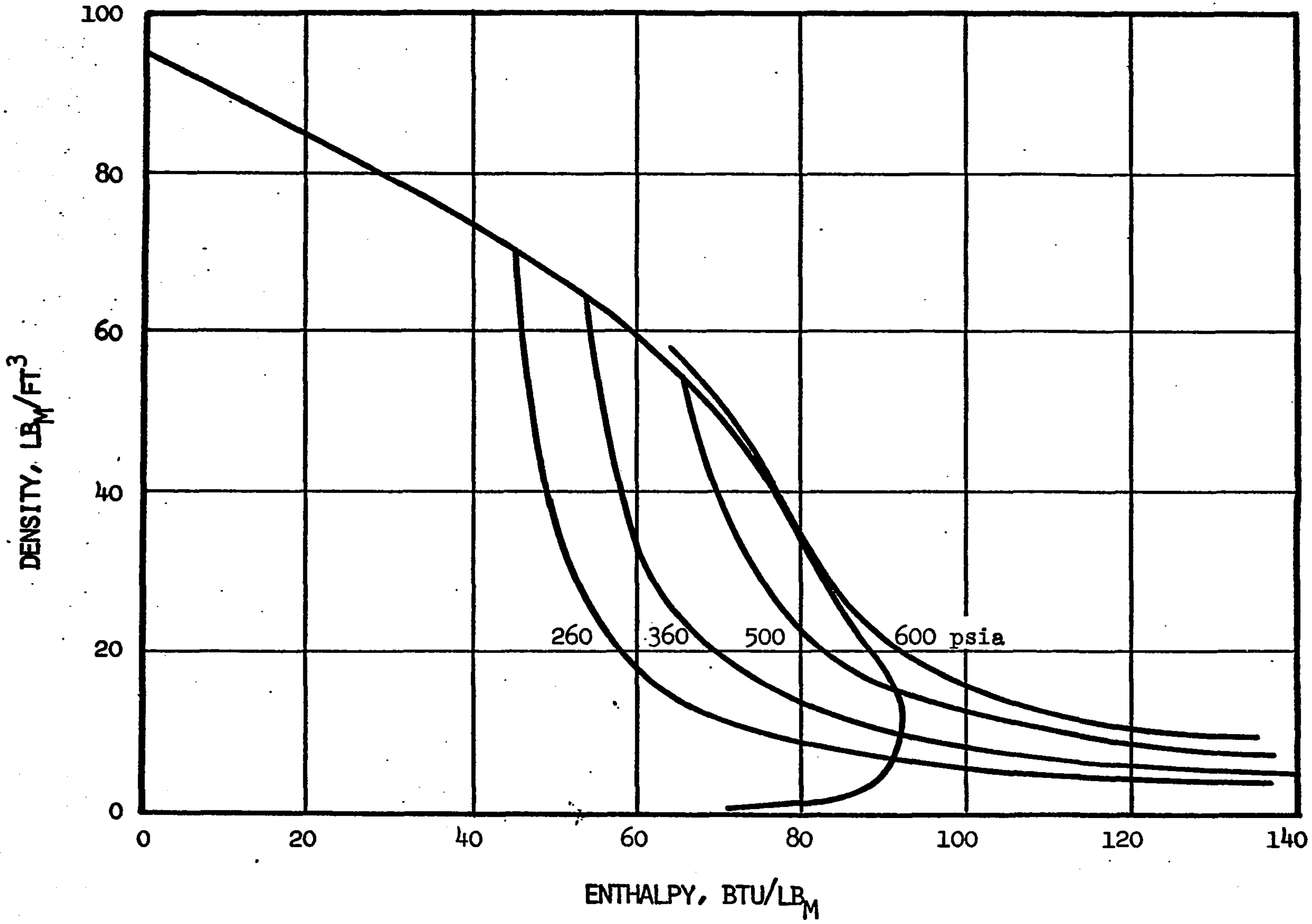

FIGURE (11) $\rho = \rho(h)$ FOR FREON-12 ALONG ISOBARS

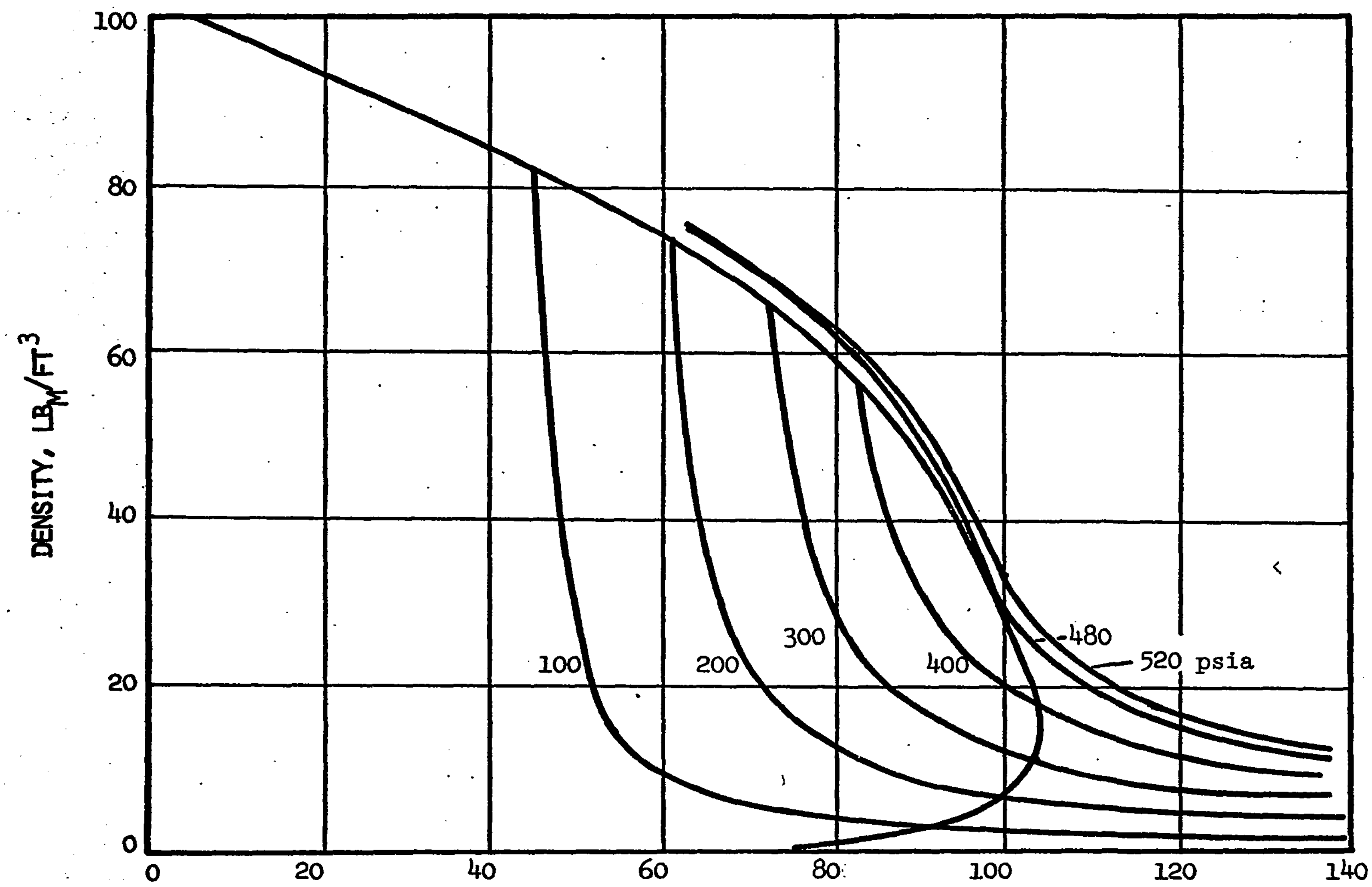

FIGURE (12) $\rho = \rho(h)$ FOR FREON-114 ALONG ISOBARS

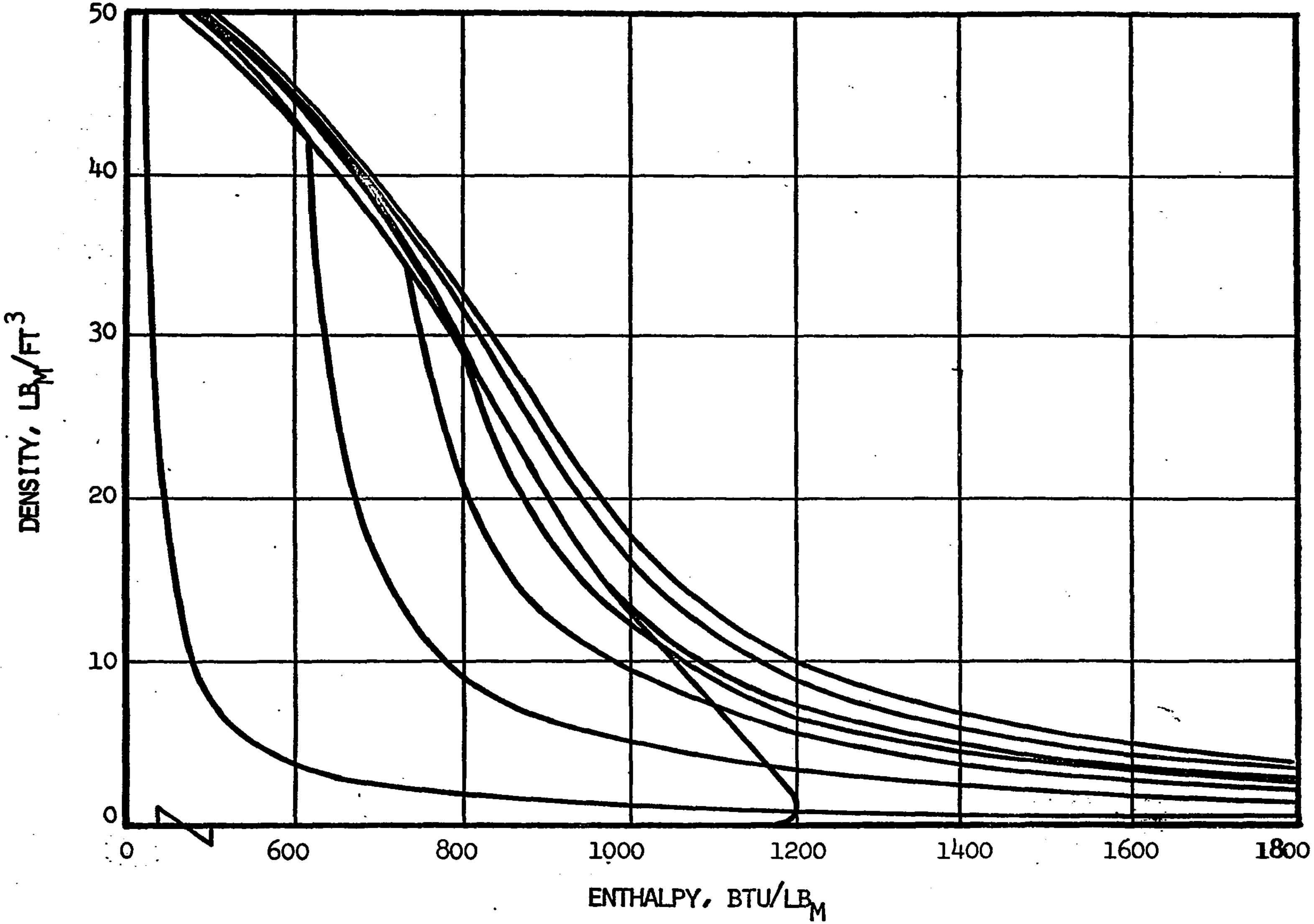

FIGURE (13) $\rho = \rho(h)$ FOR H_2O ALONG ISOBARS

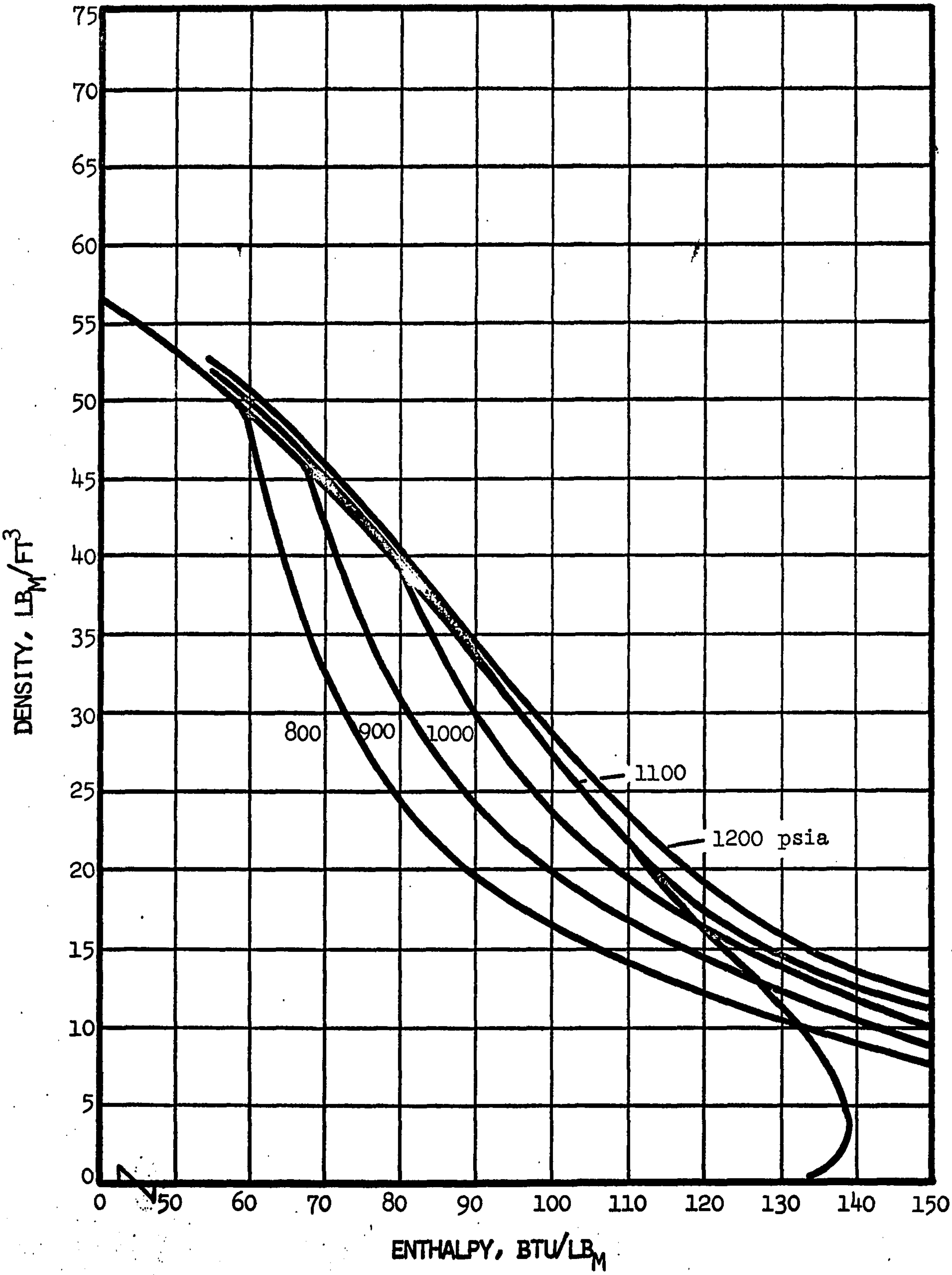

FIGURE (14) $\rho = \rho(h)$ FOR CO_2 ALONG ISOBARS

Equations (1), (2), (3), and (5) should now allow for the solution of the four unknowns. Since these four equations must be solved simultaneously, an attempt to combine these equations gives the following.

Since

$$R = R(H)$$

$$\frac{\partial R}{\partial T} = \frac{dR}{dH}\,\frac{\partial H}{\partial T}$$

$$\frac{\partial R}{\partial Z} = \frac{dR}{dH}\,\frac{\partial H}{\partial Z}$$

Substituting these relations into Equation (1),

$$\frac{dR}{dH}\frac{\partial H}{\partial T} + R\,\frac{\partial U}{\partial Z} + U\,\frac{dR}{dH}\frac{\partial H}{\partial Z} = 0$$

and

$$\frac{dR}{dH}\left[\frac{\partial H}{\partial T} + U\,\frac{\partial H}{\partial Z}\right] = -R\,\frac{\partial U}{\partial Z} \tag{6}$$

Substituting the energy equation (2) into (6) gives

$$\frac{dR}{dH}\left[\,\frac{W}{R}\,\right] = -R\,\frac{\partial U}{\partial Z}$$

and

$$\frac{\partial U}{\partial Z} = W\,\frac{d}{dH}\left[\,\frac{1}{R}\,\right] \tag{7}$$

Utilizing the equation of state (5), the derivative on the right side of (7) can be determined.

<u>For $H \leq 0$</u>

$$\frac{d}{dH}\left[\,\frac{1}{R}\,\right] = \frac{d}{dH}\left[\frac{1}{R_o + (-4H)^{1/2}}\right]$$

$$= \frac{1}{(-H)^{1/2}\left[R_o + (-4H)^{1/2}\right]^2}$$

For $H \geq 0$

$$\frac{d}{dH}\left[\frac{1}{R}\right] = \frac{1}{R_o H_c} \tag{8}$$

Simplifying the notation, let $\frac{d}{dH}\left[\frac{1}{R}\right] = f(H)$ where $f(H)$ is given by Equation (8). Therefore (7) becomes

$$\frac{\partial U}{\partial Z} = Wf(H) \tag{9}$$

Finally, Equation (9) can be substituted into the conservation of momentum equation to obtain

$$\frac{\partial P}{\partial Z} + R\frac{\partial U}{\partial T} + RU\,Wf(H) + RG + \frac{FRU^2}{2D} = 0 \tag{10}$$

Little simplification was obtained from this and the set of Equations (1), (2), (5), and (10) must still be solved.

This set of equations is a set of mixed partial derivatives and cannot be solved analytically without further simplifications. Therefore, it is necessary that a closer look at the physical aspects of the problem be taken in order to make some simplifying assumptions.

One method of solution of this problem based on the assumption of an oscillatory flow would be a small perturbation technique. Various investigators have employed this technique in two-phase instability studies with various degrees of success. Boure[7] presents a very excellent theoretical model in what he calls the "single-phase model". He utilizes this theoretical model to predict flow instabilities in the two-phase region.

The fundamental idea that this model stresses is what Boure calls the "density effect". Since this effect is identical to the occurrence of a maximum in the density-enthalpy product in Walker and Harden[29] (this effect occurs since the density decreases faster than the enthalpy increases in this region thereby giving rise to a maximum in the density-enthalpy product), the model is quite applicable to the present study with only slight modifications.

The fundamental idea in Boure's model is the representation of the equation of state which leads to the so-called density effect. Figure (16) shows the equation of state for water in the two-phase region at a constant pressure of 400 psia. This is a representative pressure that might be considered in applying this model to a two-phase flow problem. Figure (15) as well as Figure (16) shows the idealized equation of state to be used in this analysis. This equation is written as follows:

$$
\begin{aligned}
R &= R_o & H &\leq 0 \\
R &= \frac{R_o H_c}{H + H_c} & H &\geq 0
\end{aligned}
\tag{11}
$$

Here it can be seen that the density in the compressed liquid region has been idealized as a constant R_o.

Comparison of the density-enthalpy relationships for water along an isobar for a subcritical and a supercritical pressure shows that they are quite similar under certain conditions. If slip and local boiling (cf. Garlid et al[12]) are taken into account, the density-enthalpy relationship is given as shown in Figure (16). This representation compared to a supercritical isobar for water as shown in Figure (10) shows a striking similarity. Therefore, utilization of the simplified equation of state should give results in the critical and supercritical thermodynamic regions comparable to those obtained in the two-phase region.

Utilizing the equation of state (11) in Equation (8) gives

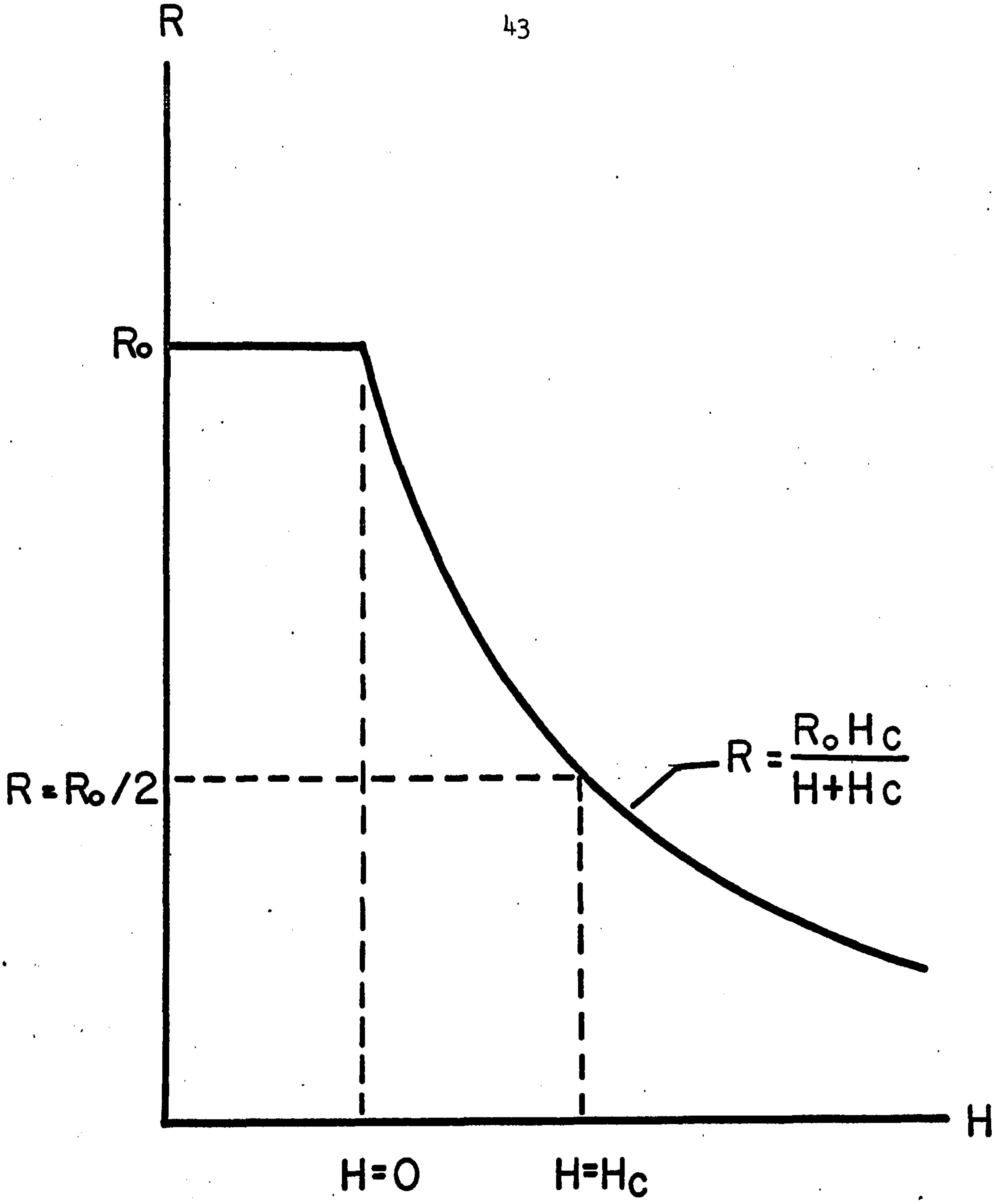

FIGURE (15) MODEL EQUATION OF STATE

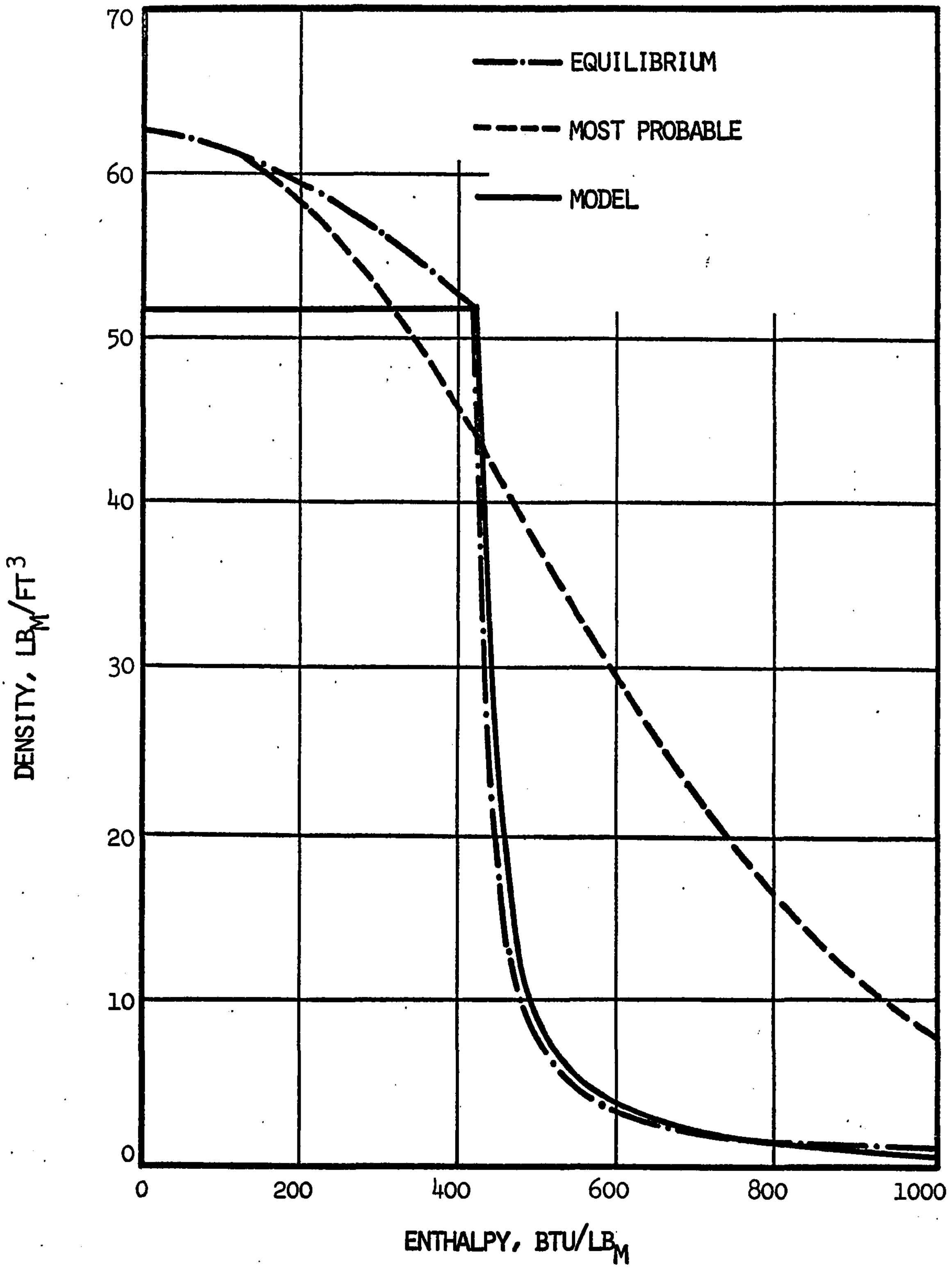

FIGURE (16) EQUATION OF STATE FOR WATER AT 400 PSIA

$$\frac{d}{dH}\left[\frac{1}{R}\right] = \frac{d}{dH}\left[\frac{1}{R_o}\right] = 0 \qquad H \leq 0$$

$$\frac{d}{dH}\left[\frac{1}{R}\right] = \frac{1}{R_o H_c} \qquad H \geq 0 \tag{12}$$

Substituting (12) into (7) gives

$$\frac{\partial U}{\partial Z} = 0 \qquad H \leq 0$$

and (13)

$$\frac{\partial U}{\partial Z} = \frac{W}{R_o H_c} \qquad H \geq 0$$

Checking the dimensions of Equation (13) shows that this expression has units of the reciprocal of time, therefore, a dimensional time parameter is defined as

$$\frac{1}{\Theta} \equiv W \frac{d}{dH}\left[\frac{1}{R}\right] \tag{14}$$

Note that in the adiabatic sections and in the heated sections for $H \leq 0$, the time parameter just defined approaches ∞. In the heated section for $H \geq 0$, this parameter becomes Θ_c where Θ_c is defined as

$$\Theta_c \equiv \frac{H_c R_o}{W} \tag{15}$$

Therefore, with these definitions, the system of equations to be solved can be written as follows:

(i) Continuity

$$\frac{\partial U}{\partial Z} = \frac{1}{\Theta} \tag{16}$$

(ii) Energy

$$R\frac{\partial H}{\partial T} + RU\frac{\partial H}{\partial Z} = W \tag{2}$$

(iii) Momentum

$$\Delta P = -\int_{\text{Entrance}}^{\text{Exit}} \frac{\partial P}{\partial Z} dZ = \int_{\text{Entrance}}^{\text{Exit}} \left[\frac{\partial U}{\partial T} + \frac{U}{\Theta} + G + \frac{FU^2}{2D}\right] RdZ \tag{17}$$

(iv) State

$$R = R_o \qquad H \le 0$$
$$R = \frac{H_c R_o}{H + H_c} \qquad H \ge 0 \tag{11}$$

along with the definition

$$\frac{1}{\Theta} = W \frac{d}{dH}\left[\frac{1}{R}\right] \tag{14}$$

and since the fluid enters the pipe in the compressed liquid region,

$$H_{entrance} = -H_o \tag{18}$$

B. Dimensional Analysis

The following dimensional parameters have been introduced in the preceding section.

(i) Geometric parameters

1) D - hydraulic diameter

2) F - friction coefficient

3) L_i - lengths of the sections of the pipe

(ii) Physical properties

1) R_o - density

2) H_c - enthalpy

(iii) Acceleration of gravity - G

(iv) Operating parameters

1) U_o - Entrance velocity

2) $-H_o$ - Entering enthalpy

3) W - Volumetric heat flux

Therefore, it can be seen that there are 11 parameters that were utilized in the dimensional equations. The number of parameters could be reduced by non-dimensionalizing. In order to non-dimensionalize, three basic independent parameters and their characteristic values were chosen. These quantities were chosen on the basis of their importance in the system of equations. Two quantities which are important are time with the characteristic value Θ_c and length with the characteristic value L_c (length of the heated section). The third parameter is not easy to choose. Both enthalpy and density are very important parameters, but density was chosen with a characteristic value of R_o since enthalpy can be eliminated between the continuity and energy equations for $H \geq 0$, i.e., from Equation (1)

$$\frac{\partial R}{\partial T} + U\frac{\partial R}{\partial Z} = -R\frac{\partial U}{\partial Z}$$

$$\frac{1}{R}\left[\frac{\partial R}{\partial T} + U\frac{\partial R}{\partial Z}\right] = -\frac{\partial U}{\partial Z}$$

Substituting from Equation (16)

$$\frac{1}{R}\left[\frac{\partial R}{\partial T} + U\frac{\partial R}{\partial Z}\right] = -\frac{1}{\Theta}$$

for $H \geq 0$, $\Theta = \Theta_c$ and

$$\frac{1}{R}\left[\frac{\partial R}{\partial T} + U\frac{\partial R}{\partial Z}\right] = -\frac{1}{\Theta_c} \qquad H \geq 0 \tag{19}$$

Therefore, the three independent quantities and their characteristic values are

(i) Length - L_c

(ii) Density - R_o

(iii) Time - Θ_c

Utilizing these quantities, the non-dimensional parameters become

(1) Reduced Length

$$\ell_i = \frac{L_i}{L_c} \qquad \text{where } i = 0 \text{ or } 1$$

(2) Reduced Coordinate

$$z = \frac{Z}{L_c}$$

(3) Reduced Time

$$t = \frac{T}{\Theta_c} = \frac{TW}{H_c R_o}$$

(4) Reduced Density

$$\rho = \frac{R}{R_o}$$

(5) Reduced Velocity

$$u = \frac{U\Theta_c}{L_c}$$

(6) Reduced Gravity

$$g = \frac{G\Theta_c^{\ 2}}{L_c} = \frac{G(H_c R_o)^2}{W^2 L_c}$$

(7) Reduced Friction

$$f = \frac{FL_c}{2D}$$

(8) Reduced Pressure Difference

$$\Delta p = \frac{\Delta P\ \Theta_c^{\ 2}}{R_o L_c^{\ 2}} = \frac{\Delta P\ R_o H_c^{\ 2}}{W^2 L_c^{\ 2}}$$

(9) Reduced Volumetric Heat Flux

$$w = \frac{W\ \Theta_c^{\ 3}}{R_o L_c^{\ 2}} = \frac{R_o^{\ 2} H_c^{\ 3}}{W^2 L_c^{\ 2}}$$

(10) Reduced Enthalpy

$$h = \frac{H\ \Theta_c^{\ 2}}{L_c^{\ 2}} = H\ \frac{(H_c R_o)^2}{W^2 L_c^{\ 2}}$$

(11) Reduced Time Parameter

$$\theta = \frac{\Theta}{\Theta_c}$$

(12) Reduced Frequency

$$\omega = \Omega \Theta_c$$

With the aid of these non-dimensional parameters, the non-dimensional equations which determine the three unknowns u, ρ, and h can be written. Using these definitions, the non-dimensional form of Equation (14) becomes

$$\frac{1}{\theta} = w \frac{d}{dh} \left[\frac{1}{\rho} \right] \tag{20}$$

From Equation (11), the non-dimensional equation of state is determined as being

$$\begin{aligned} \rho &= 1 \qquad \text{for } h \le 0 \\ \rho &= \frac{h_c}{h + h_c} \qquad \text{for } h \ge 0 \end{aligned} \tag{21}$$

Substituting Equation (21) into (20) it can be seen that θ takes on two values depending on the enthalpy:

<u>for h ≤ 0</u>

$$\frac{1}{\theta} = w \frac{d}{dh} \left[1 \right] = 0$$

therefore, $\theta \to \infty$ (22)

<u>for h ≥ 0</u>

$$\frac{1}{\theta} = w \frac{d}{dh} \left[\frac{h + h_c}{h_c} \right] = \frac{w}{h_c} = 1$$

therefore, $\theta = 1$

Hence, it is seen that the non-dimensional model equations may be written for two non-dimensional times, $\theta = 1$ and $\theta \to \infty$.

Therefore, the continuity equation can be written for the two zones (non-dimensional time). From Equation (16)

$$\frac{\partial U}{\partial Z} = \frac{1}{\Theta}$$

Utilizing the non-dimensional quantities, (16) becomes

$$\frac{\partial u}{\partial z} = \frac{1}{\theta} \tag{23}$$

for the two zones

$$\theta = 1, \qquad \frac{\partial u}{\partial z} = 1 \tag{24}$$

$$\theta \to \infty, \qquad \frac{\partial u}{\partial z} = 0 \tag{25}$$

The energy equation is easily deduced utilizing the non-dimensional quantities. Equation (2) becomes

$$\rho \frac{\partial h}{\partial t} + \rho u \frac{\partial h}{\partial z} = w \tag{26}$$

In the zone where θ is finite ($\theta = 1$), it is more convenient to utilize the alternative form of the energy equation given by Equation (19). In non-dimensional form, this equation becomes

$$\frac{1}{\rho}\left[\frac{\partial \rho}{\partial t} + u\frac{\partial \rho}{\partial z}\right] = -1$$

hence, for the two zones, it is found that

$$\begin{aligned} \theta = 1, \qquad & \frac{1}{\rho}\left[\frac{\partial \rho}{\partial t} + u\frac{\partial \rho}{\partial z}\right] = -1 \\ \theta \to \infty, \qquad & \rho \frac{\partial h}{\partial t} + \rho u \frac{\partial h}{\partial z} = w \end{aligned} \tag{27}$$

Likewise, the momentum equation can be written in non-dimensional form. Equation (17) becomes

$$\Delta p = \int_{-\ell_o}^{1+\ell_1} \left[\frac{\partial u}{\partial t} + \frac{u}{\theta} + g + fu^2\right] \rho dz \tag{28}$$

From Equation (18) the non-dimensional entry condition becomes

$$h - -h_o \tag{29}$$

Table 1, consisting of equations (20) through (29), was constructed in order that one could visualize more clearly the pertinent equations in the two zones.

Zone Where $\theta = 1$ $\{h > 0\}$	Zone Where $\theta \to \infty$ $\left\{\begin{matrix} h < 0 \text{ (Compressed Liquid)} \\ h > 0 \ (w \to \infty) \end{matrix}\right\}$
Continuity: $\frac{\partial u}{\partial z} = 1$ (24)	$\frac{\partial u}{\partial z} = 0$ (25)
Energy: $\frac{1}{\rho}\left\{\frac{\partial \rho}{\partial t} + u\frac{\partial \rho}{\partial z}\right\} = -1$ (27)	$\rho\frac{\partial h}{\partial t} + \rho u \frac{\partial h}{\partial z} = w$ (26)
State: $h \geq 0$ $\rho = \frac{h_c}{h + h_c}$ (21)	$\rho = \frac{h_c}{h + h_c}$ (21)
$h \leq 0$ Impossible in this zone	$\rho = 1$
Momentum: $$\Delta p = \int_{-\ell_0}^{1+\ell_1} \left\{\frac{\partial u}{\partial t} + \frac{u}{\theta} + g + fu^2\right\} \rho \, dz \qquad (28)$$	
Entrance Condition: $$h = -h_o \qquad (29)$$	

Table 1. System of Equations for the Two Zones

C. Partial Reduction of the System of Equations

The system of equations for the upstream adiabatic zone are relatively simple.

(1) Upstream Adiabatic Zone. For this zone, $w = 0$ and $\theta \to \infty$. From Equation (25)

$$\frac{\partial u}{\partial z} = 0$$

which gives

$$u = u(t) \qquad (30)$$

and Equation (30) can be written

$$u = u_o(t) \tag{31}$$

where the o index refers to $z = 0$.

From Equation (26), it is found by utilizing Lagrangian variables that

$$\frac{\partial h}{\partial t} + u\,\frac{\partial h}{\partial z} = \frac{Dh}{Dt} = \frac{w}{\rho} = 0 \tag{32}$$

since an adiabatic section is being considered. Hence,

$$h = -h_o \tag{29}$$

Equation (21) gives $\rho = 1$ in this section.

Finally, for the upstream adiabatic section, the following equations are valid:

$$\boxed{\begin{aligned} u &= u_o(t) \\ \rho &= 1 \\ h &= -h_o \end{aligned}} \tag{33}$$

(2) <u>Heated Zone With $h \leq 0$</u>. In this section, $w > 0$ and $\theta \to \infty$. Integration of Equation (25) gives $u = u_o(t)$ as in the previous zone. Equation (26) gives

$$\frac{\partial h}{\partial t} + u\,\frac{\partial h}{\partial z} = \frac{Dh}{Dt} = \frac{w}{\rho} = w \tag{34}$$

Utilizing Lagrangian variables (following the particle) in the integration gives

$$h = wt + \text{constant} \tag{35}$$

Let τ be defined as the instant when the particle attains zero enthalpy (becomes saturated). Then $h = 0$ @ $t = \tau$ and the constant of integration in Equation (35) can be evaluated, i.e.,

$$h = w(t - \tau) \tag{36}$$

Equation (36) immediately leads to the evaluation of t_o the instant the particle passes the origin z = 0 by substituting in the last expression,

$$-h_o = w(t_o - \tau)$$

or

$$t_o = \tau - \frac{h_o}{w} \tag{37}$$

Utilizing Equation (37), a relation can be established between z, t, and τ

$$z = \int_{t_o}^{t} u_o(x)dx$$

or

$$z = \int_{\tau - \frac{h_o}{w}}^{t} u_o(x)dx \tag{38}$$

where x is a dummy variable of integration.

Now the length of the zone for which $h \leq 0$ can be calculated. If this length is defined as λ, it can be seen from this definition and the definition of τ above that λ is the value of the integral in Equation (38) for $t = \tau$. Hence,

$$\lambda(t) = \int_{t - \frac{h_o}{w}}^{t} u_o(x)dx \tag{39}$$

Looking at the quantity $\frac{h_o}{w}$ for a moment, it can be seen that if the non-dimensional definitions of w and h are recalled, this quantity in dimensional form is

$$\frac{H_o}{H_c}$$

where H_o represents the subcooling in two-phase flow.

By analogy with the definition of subcooling in two-phase flow, this ratio will be called the non-dimensional subcooling. Hence, for critical and supercritical flow it will be assumed that a quantity analogous to subcooling in two-phase flow exists and this quantity is defined by

$$s \equiv \frac{h_o}{w} \tag{40}$$

Therefore, Equation (39) becomes

$$\lambda(t) = \int_{\tau - s}^{t} u_o(x)dx \tag{41}$$

and likewise Equation (38) becomes

$$z(t,\tau) = \int_{\tau - s}^{t} u_o(x)dx \tag{42}$$

It is intuitively obvious and has been shown in Appendix V that for this region ($\rho = 1$) the flow is always stable for $\lambda \geq 1$ since the fluid would be in the subcooled or saturated thermodynamic region at all points inside the pipe. For this reason, the limits on the analysis will be that for which $\lambda < 1$.

The formulas relative to this zone (31), (36), (41), and (42) are reiterated below.

$$\boxed{\begin{gathered} u = u_o(t) \\ \rho = 1 \\ h = w(t - \tau) \\ \lambda(t) = \int_{t-s}^{t} u_o(x)dx \\ z(t,\tau) = \int_{\tau-s}^{t} u_o(x)dx \\ \lambda < 1 \\ \tau - s \leq t \leq \tau \end{gathered}} \tag{43}$$

(3) Heated Zone With $h \geq 0$. In this zone $\theta = 1$ and $w > 0$. From Equation (24)

$$\frac{\partial u}{\partial z} = 1$$

Integrating

$$u = z + f(t)$$

Since $u = u(t)$ for $z(0)$

$$u = u(t) + z \tag{44}$$

Now, from Equation (43) at the instant t for which $z = \lambda(t)$

$$u = u_o(t)$$

Hence,

$$u\left[\lambda(t), t\right] = u(t) + \lambda(t) = u_o(t)$$

where

$$u(t) = u_o(t) - \lambda(t) \tag{45}$$

Substituting Equation (45) into (44) gives

$$u(z,t) = u_o(t) + z - \lambda(t) \tag{46}$$

Integration of the energy equation (27) gives

$$\frac{1}{\rho}\left[\frac{\partial \rho}{\partial t} + u\,\frac{\partial \rho}{\partial z}\right] = \frac{D(\ell n \rho)}{Dt} = -1$$

and

$$\rho = e^{-t + \text{constant}}$$

The constant of integration can be evaluated from the condition that $\rho = 1$ for $t = \tau$. Therefore,

$$\rho = e^{-(t-\tau)} \quad \text{for } t \geq \tau \tag{47}$$

A relation between z, t, and τ similar to Equation (38) can be found in this particular zone by the integration of Equation (46) where

$$\frac{Dz}{Dt} = u(z,t) = u_o(t) + z - \lambda(t) \tag{46}$$

For the moment take t and τ as the independent variables that define the Lagrangian particle. The presence of z in the right hand member of Equation (46) suggests putting

$$z(t,\tau) = y(t,\tau)\ e^{t} \tag{47}$$

$\frac{Dz}{Dt}$ is the derivative according to the particle, given at constant τ,

$$\frac{Dz}{Dt} = \frac{\partial z}{\partial t} = \frac{\partial y}{\partial t}\ e^{t} + ye^{t}$$

where

$$\frac{\partial y}{\partial t} = e^{-t}\ \frac{Dz}{Dt} - y$$

From Equation (47)

$$\frac{\partial y}{\partial t} = e^{-t}\left[\frac{Dz}{Dt} - z\right] \tag{48}$$

Substituting for $\frac{Dz}{Dt}$ from Equation (46)

$$\frac{\partial y}{\partial t} = e^{-t}\left[u_o(t) - \lambda(t)\right] \tag{49}$$

Integrating Equation (49)

$$y = \int_{\tau}^{t} e^{-t}\left[u_o(t) - \lambda(t)\right] dt + f(\tau) \tag{50}$$

$f(\tau)$ is evaluated from the condition

$$z(t,\tau) = \lambda(\tau) \quad \text{for} \quad t = \tau$$

Hence,

$$e^{-\tau}\ \lambda(\tau) = \int_{\tau}^{\tau} e^{-t}\left[u_o(t) - \lambda(t)\right] dt + f(\tau)$$

and

$$f(\tau) = e^{-\tau}\ \lambda(\tau) \tag{51}$$

Therefore, Equations (50) and (51) give

$$y(t,\tau) = \lambda(\tau)\ e^{-\tau} + \int_{\tau}^{t} e^{-x}\left[u_o(x) - \lambda(x)\right] dx \tag{52}$$

and utilizing Equation (47)

$$z(t,\tau) = \lambda(\tau)\, e^{t-\tau} + e^{t} \int_{\tau}^{t} e^{-x} \left[u_o(x) - \lambda(x)\right] dx. \qquad (53)$$

The time t_1 when the particle is discharged from the heated zone into the adiabatic downstream zone is of interest in connection with this zone. This is given by Equation (53) for z = 1. Hence,

$$1 = \lambda(\tau)\, e^{t_1-\tau} + e^{t_1} \int_{\tau}^{t_1} e^{-x} \left[u_o(x) - \lambda(x)\right] dx \qquad (54)$$

The equations pertinent to this particular zone, Equations (21), (46), (47), (53), and (54), are reiterated below.

$$\boxed{\begin{gathered} u = u_o(t) - \lambda(t) + z \\ \rho = \frac{h_c}{h + h_c} \\ \rho = e^{-(t-\tau)} \\ z(t,\tau) = \lambda(\tau)\, e^{t-\tau} + e^{t} \int_{\tau}^{t} e^{-x} \left[u_o(x) - \lambda(x)\right] dx \\ \tau \le t \le t_1(\tau) \\ 1 = \lambda(\tau)\, e^{t_1-\tau} + e^{t_1} \int_{\tau}^{t_1} e^{-x} \left[u_o(x) - \lambda(x)\right] dx \end{gathered}} \qquad (55)$$

(4) <u>Downstream Adiabatic Zone</u>. In this zone w = 0 and $\theta \to \infty$. Integration of Equation (25) gives $u = u(t)$ and since $z = 1$ at the exit of the heated section, (55) gives

$$u = u(t) = u_o(t) - \lambda(t) + 1 \qquad (56)$$

The energy equation (26) gives

$$\frac{\partial h}{\partial t} + u \frac{\partial h}{\partial z} = \frac{Dh}{Dt} = \frac{w}{\rho} = 0$$

Again according to the particle, this expression gives h = constant. According to Equation (55)

$$\rho = \rho(\tau) = e^{-(t_1-\tau)} = \text{constant} \tag{57}$$

As before, the relation between t, z, and τ can be determined for this zone by the integration of Equation (56):

$$\frac{Dz}{Dt} = u = u_o(t) - \lambda(t) + 1$$

$$z = \int_{t_1}^{t} \left[u_o(t) - \lambda(t) + 1\right] dt + \text{constant} \tag{58}$$

The constant of integration can be evaluated from the condition z = 1 for $t = t_1$

$$1 = \int_{t_1}^{t_1} \left[u_o(t) - \lambda(t) + 1\right] dt + \text{constant}$$

therefore,

$$\text{constant} = 1$$

and Equation (58) gives

$$z(t,\tau) = 1 + \int_{t_1}^{t} \left[u_o(x) - \lambda(x) + 1\right] dx \tag{59}$$

The formulas relative to this zone are (21), (56), (57), and (59).

$$\boxed{\begin{gathered} u = u_o(t) - \lambda(t) + 1 \\ \rho = \frac{h_c}{h + h_c} \\ \rho = e^{-(t_1-\tau)} \\ z(t,\tau) = 1 + \int_{t_1}^{t} \left[u_o(x) - \lambda(x) + 1\right] dx \\ t_1 \le t \le \text{instant of discharge from pipe} \end{gathered}} \tag{60}$$

The sets of integrated equations (33), (43), (55), and (60) have replaced those of Equations (24 - 29). The remaining equation to be considered is the momentum equation (28) which will provide a look at the dynamics of the problem. The above mentioned sets of equations have allowed the reduction of the number of unknowns from four (velocity, density, pressure, and enthalpy) to two (entrance velocity and density).

D. Establishment of the Oscillation Mechanism Equation

The mechanism is now examined for which the model will be susceptible to produce sustained oscillations. The mathematical model has been built around the so-called density effect; in fact, the regions other than the variable density part of the heated zone have been added only to bring the mathematical model closer to physical reality since the fluid flow almost always behaves in these regions. Although these zones modify the characteristics of the model by their effect on damping and inertia for example, they do not modify the actual oscillation mechanism. Therefore, it is proper that this study is begun by studying the case of a single variable density heated zone. Following this, the upstream adiabatic and downstream adiabatic lengths will be added and finally a study will be made of the much more complicated case of the complete model as described in section C.

From the definition of a single, variable density, heated zone, the following is concluded:

$$\ell_o = \ell_1 = s = 0 \tag{61}$$

Physically this corresponds to the entrance of the fluid into the pipe at the saturation temperature for two-phase flow and at an analogous condition for a supercritical fluid. It is also evident that for this zone

$$\theta = 1$$

and

$$\lambda \equiv 0 \tag{62}$$

For this region, the set of Equation (55) is valid and after taking Equation (62) into account becomes

$$\boxed{\begin{gathered} u = u_o(t) + z \\ \rho = e^{-(t-\tau)} \\ z(t,\tau) = e^{t} \int_{\tau}^{t} e^{-x} u_o(x)\, dx \\ 1 = e^{t_1} \int_{\tau}^{t_1} e^{-x} u_o(x)\, dx \\ \tau \le t \le t_1(\tau) \end{gathered}} \tag{63}$$

The dynamics of the problem are considered by looking at the momentum equation (28). Taking Equation (61) and (62) into account gives

$$\Delta p = \int_0^1 \left[\frac{\partial u}{\partial t} + u + g + fu^2\right] \rho\, dz \tag{64}$$

Before substitution of Equation (63) into (64), it is convenient to define the following quantities:

$$\begin{gathered} \int_0^1 \rho\, dz \equiv \xi(t) \\ \int_0^1 \rho z\, dz \equiv \eta(t) \\ \int_0^1 \rho z^2 dz \equiv \zeta(t) \end{gathered} \tag{65}$$

Utilizing Equation (65), the momentum equation becomes

$$\Delta p = \left[\frac{du_o}{dt} + u_o + g + fu_o^2\right] \xi + (1 + 2fu_o)\, \eta + f\zeta \tag{66}$$

Since this investigation is concerned with periodic solutions, one is led to put

$$u_o(t) = u_\infty + v(t) \tag{67}$$

where u_∞ is the steady state velocity at the entrance. For now, the only restriction placed on $v(t)$ is that $v(t) \geq -u_\infty$. This condition states that the flow cannot reverse itself. This condition is not restrictive since this investigation is concerned with the instability thresholds.

Now by defining ξ_o, η_o, ζ_o as steady state quantities analogous to ξ, η, ζ, the steady state pressure drop can be obtained by letting $u = u_\infty$ and substituting into Equation (64). Upon making this substitution, the following expression is obtained:

$$\Delta p = (u_\infty + g + fu_\infty^{\ 2})\ \xi_o + (1 + 2fu_\infty)\ \eta_o + f\zeta_o \tag{68}$$

Since the steady state pressure drop is approximately equal to the transient pressure drop, Δp from Equation (66) is equated to Δp from Equation (68). Elimination of Δp between these two equations gives an equation in v:

$$\left[\frac{dv}{dt} + v + fv(2u_\infty + v)\right] \xi + \left[u_\infty + g + fu_\infty^{\ 2}\right] (\xi - \xi_o)$$

$$+ 2fv\eta + (1 + 2fu_\infty)(\eta - \eta_o) + f(\zeta - \zeta_o) = 0$$

or by rearranging

$$-\frac{dv}{dt} = fv(2u_\infty + v) + v + 2fv\frac{\eta}{\xi} + (u_\infty + g + fu_\infty^{\ 2})\frac{\xi - \xi_o}{\xi}$$

$$+ (1 + 2fu_\infty)\ \frac{\eta - \eta_o}{\xi} + (f)\ \frac{\zeta - \zeta_o}{\xi} \tag{69}$$

The problem is therefore reduced to the solution of Equation (69) taking into account Equations (63), (65), and (67).

An analytical solution to Equation (69) is, in general, impossible but inferences can be drawn from it. For example, one necessary condition that (69) possess an oscillatory solution is that for some period of time, v and $\frac{dv}{dt}$ be of the same sign. This can be seen by looking at the quantity

$$v \frac{dv}{dt}$$

if v and $\frac{dv}{dt}$ are of opposite sign

$$v \frac{dv}{dt} < 0$$

and

$$\frac{d(v^2)}{dt} < 0$$

therefore, the absolute value of v can only decrease. In order to obtain an oscillatory solution, it is necessary (at least over certain time intervals) that this product increase. Therefore, it is necessary for v and $\frac{dv}{dt}$ to be of the same sign over some time interval. However, this condition is not sufficient and the number of important terms in Equation (69) preclude the possibility of finding a simple stability criteria. Therefore, the problem of studying numerically the set of equations mentioned above ((63), (65), (67), and (69)) will be considered. A small perturbation analysis approach to the problem seems feasible in the light that the oscillatory mechanism is being studied. Although it should be realized that large perturbations are present in the physical system, it is valid to predict the instability thresholds on the basis of small perturbations since they eventually lead to the large perturbations.

Therefore, Equation (69) is linearized by suppressing the second order terms. Upon doing this, the following expression is obtained:

$$- \frac{dv}{dt} = 2fu_\infty v + v + 2f \frac{\eta_o}{\xi_o} v + (u_\infty + g + fu_\infty^2) \frac{\xi - \xi_o}{\xi_o} + (1 + 2fu_\infty) \frac{\eta - \eta_o}{\xi_o} + (f) \frac{\zeta - \zeta_o}{\xi_o} \tag{70}$$

Equation (70) is a first order linear differential equation and because of the nature of ξ, η, and ζ as functions of t, the solution of this equation can be written as a linear form of particular solutions in e^{ct}, i.e.,

$$\sum_i v_{o_i} e^{c_i t}$$

where v_{o_i} is small compared with u_∞ and c is a complex number. Therefore, the system of equations with

$$u_o = u_\infty + v_o e^{ct} \tag{71}$$

will be studied.

The linearization above must be considered as a physical hypothesis and the eventual comparison of experimental results with the results of the solution of the linearized equations will indicate whether or not this hypothesis is valid.

Next, it is necessary to investigate the case of a pipe heated over part of its length for zero subcooling (s = 0). This is identical to the case studied above with the upstream and downstream adiabatic sections added.

(i) Upstream Adiabatic Zone. For this zone, the set of Equations (33) are valid and substitution into the momentum Equation (28) gives

$$\Delta p_{U.A.S.} = \int_{-\ell_o}^{o} \left[\frac{\partial u}{\partial t} + \frac{u}{\theta} + g + fu^2\right] \rho dz =$$

$$\left[\frac{du_o}{dt} + g + fu_o^2\right] \ell_o \tag{72}$$

(ii) Heated Section. The momentum equation for this zone has already been established. From Equation (66)

$$\Delta p_{H.S.} = \left[\frac{du_o}{dt} + u_o + g + fu_o^2\right] \xi + (1 + 2fu_o)\,\eta + f\zeta \qquad (66)$$

(iii) Downstream Adiabatic Zone. For this zone, the set of Equations (60) are valid and substitution of (60) into the momentum equation (28) gives

$$\Delta p_{D.A.S.} = \int_1^{1+\ell_1} \left[\frac{\partial u}{\partial t} + \frac{u}{\theta} + g + fu^2\right] \rho\, dz =$$

$$\left[\frac{du_o}{dt} + g + f(u_o + 1)^2\right] \xi_1 \qquad (73)$$

where $\xi_1(t)$ is defined as

$$\xi_1(t) \equiv \int_1^{1+\ell_1} \rho\, dz \qquad (74)$$

Now by assuming that the velocity consists of a steady state and a transient component, we utilize Equation (67)

$$u_o(t) = u_\infty + v(t) \qquad (67)$$

by substituting it into Equation (72) where we obtain

$$\Delta p_{U.A.S.} = \left[\frac{dv}{dt} + g + fu_\infty^2 + 2fu_\infty v + fv^2\right] \ell_o \qquad (75)$$

Substitution of Equation (67) into (73) gives

$$\Delta p_{D.A.S.} = \left[\frac{dv}{dt} + g + f(u_\infty^2 + 2u_\infty v + 2u_\infty + v^2 + 2v + 1)\right] \xi_1 \qquad (76)$$

At steady state, Equation (75) becomes

$$\Delta p_{\substack{ss\\U.A.S.}} = \left[g + fu_\infty^2\right] \ell_o \qquad (77)$$

and at steady state, Equation (76) becomes

$$\Delta p_{\substack{ss\\D.A.S.}} = \left[g + f(u_\infty^2 + 2u_\infty + 1)\right] \xi_{10} \qquad (78)$$

where ξ_{10} is defined as the steady state value of $\xi_1(t)$.

For the heated section the steady state value of Δp has already been determined and is given by Equation (68),

$$\Delta p_{\substack{ss \\ H.S.}} = \left[u_\infty + g + fu_\infty^2\right] \xi_o + \left[1 + 2fu_\infty\right] \eta_o + f\zeta_o \tag{68}$$

The total steady state pressure drop across the pipe is equal to the sum of the steady state pressure drops across the three sections given by Equations (68), (77), and (78). Hence,

$$\Delta p_{ss} = (g + fu_\infty^2) \left[\ell_o + \xi_o + \xi_{10}\right] + u_\infty \xi_o + (1 + 2fu_\infty)\, \eta_o$$
$$+ f\zeta_o + \left[f(2u_\infty + 1)\right] \xi_{10} \tag{79}$$

For the heated section Equation (67) is substituted into (66) to obtain the transient pressure drop.

$$\Delta p_{H.S.} = \left[\frac{dv}{dt} + u_\infty + v + g + f(u_\infty + v)^2\right] \xi + \left[1 + 2f(u_\infty + v)\right] \eta$$
$$+ f\zeta \tag{80}$$

The total pressure drop across the pipe considering the transient portion is found by adding Equations (75), (76), and (80) to obtain

$$\Delta p = \left[\frac{dv}{dt} + g + fu_\infty^2 + 2fu_\infty v + fv^2\right] \ell_o + \left[\frac{dv}{dt} + g + fu_\infty^2 +\right.$$
$$\left. 2fu_\infty v + 2fu_\infty + fv^2 + 2fv + f\right] \xi_1 + \left[\frac{dv}{dt} + u_\infty + v + g\right.$$
$$\left. + fu_\infty^2 + 2fu_\infty v + fv^2\right] \xi + \left[1 + 2fu_\infty + 2fv\right] \eta$$
$$+ f\zeta \tag{81}$$

As before, Δp can be eliminated between Equations (79) and (81) to give

$$\left[\frac{dv}{dt} + fv(2u_\infty + v)\right](\ell_o + \xi + \xi_1) + \left[g + fu_\infty^2\right](\ell_o + \xi + \xi_1) + v\xi$$

$$+ u_\infty \xi + 2fv\eta + (1 + 2fu_\infty)\,\eta + f\zeta + 2fv\xi_1 + \left[f(2u_\infty + 1)\right]\xi_1$$

$$= \left[g + fu_\infty^{\,2}\right](\ell_o + \xi_o + \xi_{10}) + u_\infty \xi_o + \left[1 + 2fu_\infty\right]\eta_o + f\zeta_o$$

$$+ \left[f(2u_\infty + 1)\right]\xi_{10} \tag{82}$$

After simplification and rearrangement, Equation (82) becomes

$$- \frac{dv}{dt} = f(2u_\infty + v)v + (v)\,\frac{\xi}{\ell_o + \xi + \xi_1} + 2fv\,\frac{\eta + \xi_1}{\ell_o + \xi + \xi_1} +$$

$$(u_\infty + g + fu_\infty^{\,2})\,\frac{\xi - \xi_o}{\ell_o + \xi + \xi_1} + (1 + 2fu_\infty)\,\frac{\eta - \eta_o}{\ell_o + \xi + \xi_1} +$$

$$f\,\frac{\zeta - \zeta_o}{\ell_o + \xi + \xi_1} + \left[g + f(u_\infty + 1)^2\right]\frac{\xi_1 - \xi_{10}}{\ell_o + \xi + \xi_1} \tag{83}$$

After linearization of Equation (83) as was done for the simpler case of a heated section only, the following expression results:

$$- \frac{dv}{dt} = 2fu_\infty v + v\,\frac{\xi_o}{\ell_o + \xi_o + \xi_{10}} + 2fv\,\frac{\eta_o + \xi_{10}}{\ell_o + \xi_o + \xi_{10}}$$

$$+ (u_\infty + g + fu_\infty^{\,2})\,\frac{\xi - \xi_o}{\ell_o + \xi_o + \xi_{10}} + (1 + 2fu_\infty)\,\frac{\eta - \eta_o}{\ell_o + \xi_o + \xi_{10}}$$

$$+ f\,\frac{\zeta - \zeta_o}{\ell_o + \xi_o + \xi_{10}} + \left[g + f(u_\infty + 1)^2\right]\frac{\xi_1 - \xi_{10}}{\ell_o + \xi_o + \xi_{10}} \tag{84}$$

Equation (84) could now be solved as in the preceding example. However, the much more complicated case where a moving boundary is introduced between the constant density heated zone and the variable density zone must be considered. Physically, this is the boiling boundary for two-phase flow.

Taking this into account, there are four zones to consider in the general case. The momentum equation for this general case has been derived in Appendix I. Equation (I-14) gives

$$- \frac{dv}{dt} = f(2u_\infty + v)v + v \frac{\xi}{\ell_o + \lambda + \xi + \xi_1} + 2fv \frac{\eta + \xi_1}{\ell_o + \lambda + \xi + \xi_1}$$

$$+ (u_\infty + g + fu_\infty^2) \frac{\xi - \xi_o}{\ell_o + \lambda + \xi + \xi_1} + (1 + 2fu_\infty) \frac{\eta - \eta_o}{\ell_o + \lambda + \xi + \xi_1}$$

$$+ f \frac{\zeta - \zeta_o}{\ell_o + \lambda + \xi + \xi_1}$$

$$+ \left[g + f(u_\infty + 1)^2\right] \frac{\xi_1 - \xi_{10}}{\ell_o + \lambda + \xi + \xi_1} - (\frac{d\lambda}{dt}) \frac{\xi + \xi_1}{\ell_o + \lambda + \xi + \xi_1}$$

$$- 2fv \frac{\lambda(\xi + \xi_1)}{\ell_o + \lambda + \xi + \xi_1} + (g + fu_\infty^2) \frac{\lambda - \lambda_o}{\ell_o + \lambda + \xi + \xi_1} - (1 + 2fu_\infty)$$

$$\frac{\lambda\xi - \lambda_o\xi_o}{\ell_o + \lambda + \xi + \xi_1} + f \frac{\lambda^2\xi - \lambda_o^2\xi_o}{\ell_o + \lambda + \xi + \xi_1} - 2f \frac{\lambda\eta - \lambda_o\eta_o}{\ell_o + \lambda + \xi + \xi_1} - 2f(u_\infty + 1)$$

$$\frac{\lambda\xi_1 - \lambda_o\xi_{10}}{\ell_o + \lambda + \xi + \xi_1} + f \frac{\lambda^2\xi_1 - \lambda_o^2\xi_{10}}{\ell_o + \lambda + \xi + \xi_1} \tag{85}$$

where it is noted in Equation (84) that

$$\xi(t) = \int_0^1 \rho\, dz \tag{65}$$

while in Equation (85)

$$\xi(t) = \int_{\lambda(t)}^1 \rho\, dz \tag{86}$$

Equation (85) can be simplified slightly by letting

$$\ell = \ell_o + \lambda + \xi + \xi_1 \tag{87}$$

Taking Equation (87) into account, (85) can be rewritten:

$$- \ell \frac{dv}{dt} = f\ell(2u_\infty + v)v + (v - \frac{d\lambda}{dt})\xi - \frac{d\lambda}{dt} \xi_1 + 2fv \Big[\eta - \lambda\xi$$

$$+ \xi_1(1 - \lambda)\Big] + u_\infty(\xi - \xi_o) + (g + fu_\infty^{\ 2})(\xi - \xi_o + \lambda - \lambda_o) + (1 + 2fu_\infty)$$

$$\Big[\eta - \lambda\xi - (\eta_o - \lambda_o\xi_o)\Big] + f\Big[(\zeta - 2\lambda\eta + \lambda^2\xi) - (\zeta_o - 2\lambda_o\eta_o$$

$$+ \lambda_o^{\ 2}\xi_o)\Big] + \Big[g + f(u_\infty + 1)^2\Big](\xi_1 - \xi_{10}) - 2f(u_\infty + 1)(\lambda\xi_1$$

$$- \lambda_o\xi_{10}) + f(\lambda^2\xi_1 - \lambda_o^{\ 2}\xi_{10}) \qquad (88)$$

The next step would logically be the linearization of Equation (88) as has been done in the two preceding simpler cases. However, it is necessary to look first at the general case shown above under steady state conditions.

E. Steady State Equations

In the preceding section, the study of small perturbations around a steady state entrance velocity, u_∞, has been established. Since the model equations have been established in detail, it is possible to study the simple case of the steady state regime.

The momentum equation which has played a fundamental role in the preceding section is established in Appendix I (I-12) and is written:

$$\Delta p = (g + fu_\infty^{\ 2})(\ell_o + \lambda_o) + (u_\infty + g + fu_\infty^{\ 2})\ \xi_o +$$

$$(1 + 2fu_\infty)(\eta_o - \lambda_o\xi_o) + f(\zeta_o - 2\lambda_o\eta_o + \lambda_o^{\ 2}\xi_o) +$$

$$g\ \xi_{10} + f(u_\infty + 1 - \lambda_o)^2\ \xi_{10} \qquad (89)$$

It is necessary to write λ_o, ξ_o, η_o, ζ_o, and ξ_{10} as functions of the model parameters. This is accomplished in Appendix II. Below are reiterated the most important equations from this appendix.

$$\lambda_o = u_\infty s \qquad \text{with} \qquad u_\infty s < 1$$

$$\xi_o = u_\infty k \qquad \text{with} \qquad k = \ell n\, m$$
$$m = 1 - s + \frac{1}{u_\infty} \qquad \text{with} \qquad m > 1,\ k > 1 \tag{90}$$
$$\xi_{10} = \frac{\ell_1}{m}$$

The form of Δp, which is linear in g and f, is established by recalling (II-14) and (II-16) from Appendix II.

From (II-14)

$$\eta_o - \lambda_o \xi_o = u_\infty(1 - \lambda_o - \xi_o) \tag{91}$$

and from (II-16)

$$\zeta_o - 2\lambda_o\eta_o + \lambda_o^2\xi_o = u_\infty\left[\frac{(1 - \lambda_o)^2}{2} - u_\infty(1 - \lambda_o - \xi_o)\right] \tag{92}$$

Substitution of Equations (91) and (92) into (89) gives, after rearrangement

$$\Delta p = g(\ell_o + \lambda_o + \xi_o + \xi_{10}) + u_\infty(1 - \lambda_o) + f$$
$$\left[\frac{u_\infty}{2}(1 - \lambda_o)^2 + u_\infty^2(1 + \ell_o) + (u_\infty + 1 - \lambda_o)^2\,\xi_{10}\right] \tag{93}$$

The criterion that the channel cannot operate under steady state conditions when the slope of the pressure drop - flow rate is negative is now imposed, i.e., the condition imposed is that

$$\frac{\partial(\Delta p)}{\partial u_\infty} > 0 \tag{94}$$

The calculation of $\frac{\partial(\Delta p)}{\partial u_\infty}$ has been made in Appendix II and (II-27) gives, after a slight rearrangement

$$\frac{\partial(\Delta p)}{\partial u_\infty} = g\left[s + k - \frac{1}{mu_\infty} + \frac{\ell_1}{(mu_\infty)^2}\right] + 1 - 2\lambda_o +$$
$$f\left[\frac{1}{2} + \ell_1 + 2u_\infty(\ell_o + 1 + \ell_1) - 2\lambda_o(1 + \ell_1) + \frac{3}{2}\lambda_o^2\right] \tag{95}$$

It can be seen that the condition $\frac{\partial(\Delta p)}{\partial u_\infty} > 0$ implies the point of operation must lie inside a certain range limited by a hypersurface (S) derived from the condition $\frac{\partial(\Delta p)}{\partial u_\infty} = 0$, i.e.

$$g\left[s + k - \frac{1}{mu_\infty} + \frac{\ell_1}{(mu_\infty)^2}\right] + 1 - 2\lambda_o + f\left[\frac{1}{2} + \ell_1 + 2u_\infty\right.$$

$$\left.(\ell_o + 1 + \ell_1) - 2\lambda_o(1 + \ell_1) + \frac{3}{2}\lambda_o^2\right] = 0 \qquad (96)$$

It follows that this equation is represented in terms of six independent parameters (g, f, u_∞, ℓ_o, ℓ_1, s), i.e., in six-dimensional space. This equation can be reduced to an equation representable in three-space by setting three parameters equal to a constant. Any three could be chosen; however, ℓ_o, ℓ_1, and s were chosen. Therefore, the surface is given by $u_\infty(g,f)$, a simple surface since Equation (96) is a linear form in g and f; the intersection of the surface with a plane u_∞ = constant is a straight line. Note that the study of this surface is limited to the region

$$0 < u_\infty < \frac{1}{s}$$

$$f \geq 0$$

These conditions have already been established (see especially Equation (90)).

Knowing the surface (S) for which $\frac{\partial(\Delta p)}{\partial u_\infty} = 0$ in the (g, f, u_∞) space will give the domain of possible operation.

Equation (96) can be rearranged in order to see that the generatrix of the function u_∞ has for its projection in the (g, f) plane an equation of a straight line, i.e.,

$$f = \frac{-\left[s + k - \frac{1}{mu_\infty} + \frac{\ell_1}{(mu_\infty)^2}\right] g + 2u_\infty s - 1}{\frac{1}{2} + \ell_1 + 2u_\infty(\ell_o + 1 + \ell_1) - 2u_\infty s(1 + \ell_1) + \frac{3}{2} u_\infty^{\ 2} s^2} \tag{97}$$

Having established the condition $\frac{\partial(\Delta p)}{\partial u_\infty} > 0$, it will be assumed that this condition is fulfilled and the next section is devoted to a study of small perturbations about the steady state regime.

F. Small Perturbation Analysis

Given the expression for the velocity defined by Equation (71)

$$u_o = u_\infty + v_o e^{ct} \tag{71}$$

where v_o is an infinitesimal of the first order compared to u_∞ and c is a complex constant, an equation in c will be derived. After linearization and division by v_o which must appear as a factor because of this linearization, an equation in c will be obtained whose roots are given by Equation (71). This equation will give a determination of the transient behavior of the system.

For a group of parameters (g, f, u_∞, ℓ_o, ℓ_1, s) satisfying the steady state criterion of the preceding section and the linearized equations of this section, there are many possible cases:

(i) If the equation in c possesses only roots with the real part negative, every general solution

$$u_o = u_\infty + \sum_i v_{o_i} e^{c_i t}$$

approaches u_∞ for $t \to \infty$, i.e., the small perturbations are damped.

(ii) If the equation in c possesses only roots with the real part negative or zero, at least on being zero, every general solution tends toward a periodic solution when $t \rightarrow \infty$.

(iii) If the equation in c possesses at least one root with the real part positive, every general solution presents an increasing amplitude with time. When this amplitude is no longer small in comparison to u_∞, the linearization is no longer valid. The prediction of whether the amplitude increases indefinitely or whether it will be limited by the non-linear terms cannot be made. However, it is certain that the system is not stable.

If the possibility that at least one of the roots of the equation in c is a discontinuous function of the model parameters is ruled out, the passage from case (i) to case (iii) where the real part of the roots change from a negative to a positive sign can only occur by becoming zero.

If all the roots of the equation in c have a negative real part and a change in the system parameters causes one of the real parts to become zero, two cases are possible:

(a) The system is passing from a stable domain where all the roots have a negative real part to a domain where at least one root has a positive real part, i.e., one is at an instability threshold defined in the six-dimensional $(g, f, u_\infty, \ell_o, \ell_1, s)$ space.

(b) The trajectory of the root considered is tangent to the imaginary axis. One is at a point where the system effectively possesses a periodic solution, for its solution is stable at all neighboring points.

The possibility (b) above is a very special case with a small probability and therefore it will not be considered further except in very special cases. In these cases it is necessary to investigate the stability at neighboring points to determine whether or not all neighboring points are stable.

Therefore, an instability threshold can be defined as follows:

For the system represented by a point in the six-dimensional (g, f, u_∞, ℓ_o, ℓ_1, s) space, there is a correspondence between the desired instability thresholds and the roots of the equation in c with the real part zero, iff

(1) A domain can be found in the vicinity of that point where the system is stable, i.e., where it has roots of the equation in c with the real part negative.

(2) The equation in c allows in the neighborhood of this point neither roots with the real part positive and infinitely large nor with discontinuous functions of the parameters.

With this definition of the instability threshold, it is necessary to return to the "equation in c" as it has been called above. This equation is (88).

$$(\ell_o + \lambda + \xi + \xi_1)\frac{dv}{dt} + f(\ell_o + \lambda + \xi + \xi_1)(2u_\infty + v)\,v +$$

$$(v - \frac{d\lambda}{dt})\,\xi - \frac{d\lambda}{dt}\,\xi_1 + 2fv\left[\eta - \lambda\xi + \xi_1(1 - \lambda)\right] + u_\infty(\xi - \xi_o)$$

$$+ (g + fu_\infty^2)(\xi - \xi_o + \lambda - \lambda_o) + (1 + 2fu_\infty)\left[\eta - \lambda\xi - (\eta_o - \lambda_o\xi_o)\right]$$

$$+ f\left[(\zeta - 2\lambda\eta + \lambda^2\xi) - (\zeta_o - 2\lambda_o\eta_o + \lambda_o^2\xi_o)\right] + \left[g + \right.$$

$$\left. f(u_\infty + 1)^2\right](\xi_1 - \xi_{10}) - 2f(u_\infty + 1)(\lambda\xi_1 - \lambda_o\xi_{10}) +$$

$$f(\lambda^2\xi_1 - \lambda_o^2\xi_{10}) = 0 \qquad (88)$$

Looking at Equation (88) it can be seen that it is necessary to express λ, $\frac{d\lambda}{dt}$, ξ, η, ζ, and ξ_1 as functions of the model parameters plus v_o and c. Equation (88) is linearized and then it is possible to proceed as before. This calculation is made in Appendix III for $c \neq 0$, $c \neq 1$, and $c \neq 2$. These restrictions do not affect the generality since $c = 0$ corresponds to the steady state solution in the previous section and $c = 1$ and $c = 2$ are particular cases which are not of great interest in this study (solution with the real part positive).

The equation in c is derived in Appendix III and is written

$$B_1 g + B_2 f u_\infty + B_3 = 0 \tag{98}$$

where

$$B_1 = - \frac{E_s E_y m^{-c}}{c(1 - c)} + \frac{E_s E_y m^{-1}}{c^2(1 - c)} - \frac{(E_s + E_y)m^{-1}}{c^2} + \frac{(1 - c)m^{-1}}{c^2} + \frac{1}{c} \tag{99}$$

$$B_2 = - m^2 u_\infty \frac{E_s E_y m^{-c}}{c(1 - c)} + m u_\infty \frac{E_s E_y}{c^2(1 - c)} + 2m^2 u_\infty \frac{E_s m^{-c}}{c(1 - c)(2 - c)} - \frac{E_s}{1 - c}\left[\frac{u_\infty}{2 - c} + 1 - u_\infty s + \frac{m u_\infty}{c^2}\right] + \frac{E_s}{c}(1 - u_\infty s + 2\ell_1) - \frac{m u_\infty E_y}{c^2} - \frac{1}{c}(1 - u_\infty s + 2\ell_1) + \frac{m u_\infty}{c^2} + 2(\ell_o + 1 + \ell_1) \tag{100}$$

$$B_3 = m u_\infty \frac{E_s m^{-c}}{(1 - c)^2} + E_s\left[\frac{u_\infty}{c} - \frac{u_\infty k c}{1 - c} - \frac{u_\infty}{(1 - c)^2} + \frac{\ell_1}{m}\right] + (\ell_o + u_\infty s + u_\infty k + \frac{\ell_1}{m})\, c - \frac{u_\infty}{c} - \frac{\ell_1}{m} \tag{101}$$

and from (II-10), (III-1), and (III-23)

$$m = 1 - s + \frac{1}{u_\infty}$$
$$k = \ln m \tag{II-10}$$

$$E_s = e^{-cs} \tag{III-1}$$

$$y = \frac{\ell_1}{mu_\infty}$$
$$E_y = e^{-cy} \tag{III-23}$$

For the instability thresholds, the equation in c is solved with the real part equal to zero. Therefore, we take

$$c = r + i\omega \tag{102}$$

and examine the equation in c for $r = 0$.

This will give a hypersurface (Σ) which is a function of the model parameters and will be defined by the expression

$$\Phi(g,\ f,\ u_\infty,\ \ell_o,\ \ell_1,\ s,\ r = 0) = 0 \tag{103}$$

Knowing the surface (Σ) and the stability domain (S), it is possible to deduce the threshold surface.

Therefore, by taking $c = i\omega$ in the equation in c (98), two equations in ω are obtained by separating the real part from the imaginary part. This is accomplished in Appendix IV. ω is the frequency of a possible "pure oscillating" system, i.e., one that is neither damped nor amplified. It is assumed that $\omega > 0$ to meet the physical requirements of the problem and this does not restrict the generality of the solution. The system of equations in ω is written:

$$\begin{aligned} a_1 g + a_2 u_\infty f + a_3 &= 0 \\ b_1 g + b_2 u_\infty f + b_3 &= 0 \end{aligned} \tag{104}$$

where

$$a_1 = -\frac{1}{1+\omega^2}\left[\cos(K+S+Y) - \frac{\sin(K+S+Y)}{\omega}\right] - \frac{1}{m\omega^2(1+\omega^2)}$$

$$\left[\cos(S+Y) + \omega\sin(S+Y)\right] + \frac{\cos S + \cos Y - 1}{m\omega^2} \tag{105}$$

$$b_1 = \frac{1}{\omega(1+\omega^2)}\left[\cos(K+S+Y) + \omega\sin(K+S+Y)\right] -$$

$$\frac{1}{m\omega(1+\omega^2)}\left[\cos(S+Y) - \frac{\sin(S+Y)}{\omega}\right] - \frac{\sin S + \sin Y}{m\omega^2}$$

$$+ \frac{1}{\omega}\left[\frac{1}{m} - 1\right] \tag{106}$$

$$a_2 = -\frac{m^2u_\infty}{1+\omega^2}\left[\cos(K+S+Y) - \frac{\sin(K+S+Y)}{\omega}\right] - \frac{mu_\infty}{\omega^2(1+\omega^2)}$$

$$\left[\cos(S+Y) + \omega\sin(S+Y)\right] + \frac{2m^2u_\infty}{(1+\omega^2)(4+\omega^2)}\left[3\cos(K+S)\right.$$

$$\left.+ (\omega - \frac{2}{\omega})\sin(K+S)\right] - \frac{\cos S}{1+\omega^2}\left[\frac{(2-\omega^2)u_\infty}{4+\omega^2} + 1 - u_\infty s\right.$$

$$\left.- \frac{mu_\infty}{\omega^2}\right] - \sin S\left[\frac{3\omega u_\infty}{(1+\omega^2)(4+\omega^2)} + \frac{\omega(1-u_\infty s)}{1+\omega^2} - \frac{mu_\infty}{\omega(1+\omega^2)}\right.$$

$$\left.+ \frac{1 - u_\infty s + 2\ell_1}{\omega}\right] - \frac{mu_\infty}{\omega^2}(1 - \cos Y) + 2(\ell_o + 1 + \ell_1) \tag{107}$$

$$b_2 = \frac{m^2u_\infty}{\omega(1+\omega^2)}\left[\cos(K+S+Y) + \omega\sin(K+S+Y)\right] - \frac{mu_\infty}{\omega(1+\omega^2)}\left[\cos(S+Y)\right.$$

$$\left.- \frac{\sin(S+Y)}{\omega}\right] + \frac{2m^2u_\infty}{(1+\omega^2)(4+\omega^2)}\left[(\omega - \frac{2}{\omega})\cos(K+S) - 3\sin(K+S)\right]$$

$$- \cos S\left[\frac{3\omega u_\infty}{(1+\omega^2)(4+\omega^2)} + \frac{\omega(1-u_\infty s)}{1+\omega^2} - \frac{mu_\infty}{\omega(1+\omega^2)} + \frac{1 - u_\infty s + 2\ell_1}{\omega}\right] +$$

$$\frac{\sin S}{1+\omega^2}\left[\frac{(2-\omega^2)u_\infty}{4+\omega^2} + 1 - u_\infty s - \frac{mu_\infty}{\omega^2}\right] - \frac{mu_\infty \sin Y}{\omega^2} + \frac{1 - u_\infty s + 2\ell_1}{\omega} \tag{108}$$

$$a_3 = \frac{mu_\infty}{(1+\omega^2)^2}\Big[(1-\omega^2)\cos(K+S) + 2\omega\sin(K+S)\Big] + \cos S\left[\frac{u_\infty k\omega^2}{1+\omega^2}\right.$$
$$\left. - \frac{u_\infty(1-\omega^2)}{(1+\omega^2)^2} + \frac{\ell_1}{m}\right] - \sin S\left[\frac{u_\infty}{\omega} + \frac{u_\infty k\omega}{1+\omega^2} + \frac{2u_\infty \omega}{(1+\omega^2)^2}\right] - \frac{\ell_1}{m} \tag{109}$$

$$b_3 = \frac{mu_\infty}{(1+\omega^2)^2}\Big[2\omega\cos(K+S) - (1-\omega^2)\sin(K+S)\Big] - \cos S\left[\frac{u_\infty}{\omega} + \frac{u_\infty k\omega}{1+\omega^2}\right.$$
$$\left. + \frac{2u_\infty\omega}{(1+\omega^2)^2}\right] - \sin S\left[\frac{u_\infty k\omega^2}{1+\omega^2} - \frac{u_\infty(1-\omega^2)}{(1+\omega^2)^2} + \frac{\ell_1}{m}\right] + (\ell_o + u_\infty s + u_\infty k$$
$$+ \frac{\ell_1}{m})\,\omega + \frac{u_\infty}{\omega} \tag{110}$$

and from (IV-3)

$$K = \omega k = \omega\, \ell n(1 - s + \frac{1}{u_\infty})$$
$$S = \omega s \tag{IV-3}$$
$$Y = \omega y = \frac{\omega\ell_1}{1 + (1-s)u_\infty}$$

The equation of the surface (Σ) could now be obtained by eliminating ω between the two equations in (104). However, ω does not occur directly in (104) but occurs in the transcendental forms of

$$K + S + Y = \omega(k + s + y)$$
$$S + Y = \omega(s + y)$$
$$K + S = \omega(k + s)$$

$$S = \omega s$$

$$Y = \omega y \qquad (111)$$

So it is seen that this elimination becomes impossible and it is necessary to define the surface (Σ) as defined parametrically by Equation (104). Notice that this system is linear in g and f and this will be useful when considering the numerical solution.

It is reiterated that for the small perturbations, the system can be represented by a point in the six-dimensional (g, f, u_∞, ℓ_0, ℓ_1, s) space of the model parameters and can be either stable or unstable. The stability is determined by the position of the representative point in relation to a threshold surface about which the system oscillates indefinitely. This threshold surface is a portion of the more important surface (Σ) defined by a system of equations acting as the frequency parameter ω of a pure oscillatory solution. Knowing (Σ) and a domain where the system is stable, this domain can be extended until the surface (Σ) is reached or the surface (S), which marks off the impossible domain studied in the previous section, is reached. In this way, the stability envelope can be determined for the physical system.

CHAPTER V

EXPERIMENTAL RESULTS

The experimental portion of this investigation was carried out primarily to obtain data to compare with the theoretical predictions of the instability thresholds. However, various experimental results were obtained which did not relate directly to the theoretical predictions of the model.

The first experimental observation made concerned the varying degree of difficulty of adjusting the loop operating parameters to a position such that oscillations would occur. Loop tests utilizing four different heat transfer fluids showed that instabilities were most readily found for Freon-114. Next came Freon-12 followed by H_2O and finally CO_2. This is verified in the literature by the fact that although extensive critical region studies had been made utilizing CO_2, no oscillations had been reported before the work of Walker and Harden[29].

The reason for these results can be seen in Figures (11 - 14). Note that at critical pressure $\left|\frac{d\rho}{dh}\right|$ is largest for Freon-114, next largest for Freon-12, followed by H_2O and finally CO_2. Since the behavior of $\rho(h)$ has been shown to be the fundamental cause of the oscillations, this observation provides agreement between theory and experiment.

The utility of the $(\rho h)_{max}$ concept for determining experimental instability points was again shown in this study. These experimental instability points were found much easier by making use of this concept. This method was utilized to locate experimental instability points regardless of whether operation was at subcritical or supercritical pressures.

Previous investigators[8,10,24] have considered (one author pursued this line of thinking) the possibility that a time-varying transfer of heat to the fluid in the heater section was the triggering mechanism for the sustained oscillations encountered. Since it is known from previous investigations (cf. Holman[17]) that convective heat transfer coefficients increase greatly in the critical region, it may be necessary to consider the heat capacity of the heater section walls. Considering this, it can be seen that the electrical power input into the heater section is divided into two parts,

$$W = Q_{fluid} + Q_{wall} \tag{112}$$

where

$$Q_{fluid} = \bar{h}A(T_{wall} - T_{fluid}) \tag{113}$$

and

$$Q_{wall} = mc_p \frac{\partial T}{\partial t} \tag{114}$$

From these equations, it can be seen that if the wall temperature of the heater section varied with time, it would be very important to account for this in the model since this mechanism would act as a "forcing function".

Since the model utilized in this study made no provision for a time-varying wall temperature, this was one of the first goals of the

The [illegible] determining experimental instability [illegible]. These experimental instability [illegible] making use of this concept. This [illegible] experimental instability points regardless [illegible] critical or supercritical pressures

Previous [illegible] the author pursued this line of thinking [illegible] a time-varying transfer of heat to the fluid [illegible] triggering mechanism for the sustained [illegible] it is known from previous investigations [illegible] convective heat transfer coefficients increase great[illegible] region, it may be necessary to consider [illegible] section walls. Considering this, [illegible] power input into the heater section is divided [illegible]

$$[illegible] \tag{112}$$

where

$$[illegible] \tag{113}$$

and

$$[illegible] \tag{114}$$

From these equations [illegible] wall temperature of the heater section [illegible] very important to account for this [illegible] would act as a "forcing function".

Since the model [illegible] provision for a time-varying wall temperature [illegible] first goals of the

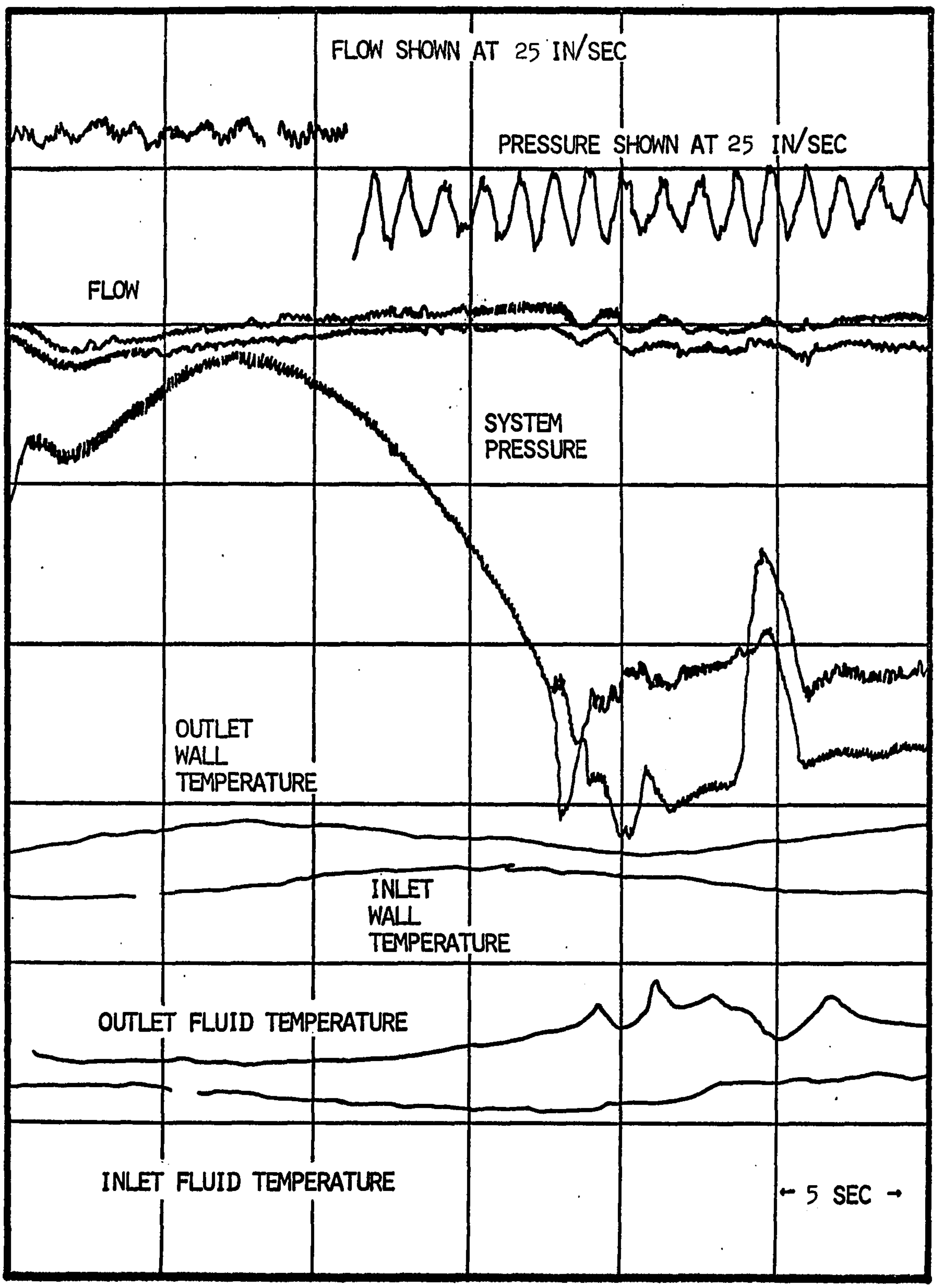

FIGURE (17) EXTREME PRESSURE OSCILLATION WHEN ACCUMULATOR WAS OUT OF THE CIRCUIT experimental part of this investigation.

Experimental results from this investigation showed that there was no appreciable oscillation of heater section wall temperature. Results did show that there was a significant wall temperature drop when the loop was operated near the critical region. However, this drop occurred as the critical region was approached and there was no ensuing oscillatory wall temperature even though pressure and flow was oscillatory. These results can be seen in Figure (17). These results were in agreement with Harden[15] and since flow oscillations were found without oscillatory wall temperatures, it was concluded that this was not the triggering mechanism for the oscillations. Confidence in the model was strengthened by this observation. Fluctuating wall temperatures were noted in this investigation but they occurred only under certain operating conditions and as stated above were not a necessary condition for an oscillatory behavior.

An investigation of the oscillatory frequencies measured experimentally suggested that these frequencies were related to the natural frequencies of various modes of vibration of the loop. Therefore, the undamped natural frequencies for several of these modes were calculated and are found in Appendix VI.

Experimental results showed that the loop oscillation frequencies fell primarily into three frequency ranges:

(a) 0.2 - 0.3 cps

(b) 30.0 - 45.0 cps

(c) 575.0 - 625.0 cps

Although the heating rate, pressure, and other operating parameters did affect the oscillation frequencies, it appears that the definite ranges found above indicate that the loop tends to operate at certain frequencies characteristic of the natural frequencies of certain of its vibrational modes. These three modes are as follows:

(a) Oscillating Manometer - When the loop was idealized as an oscillating manometer, it was found that the calculated natural frequency was not a function of the fluid density, but only of the length of the loop (when $\rho_L >> \rho_V$). This calculation showed the natural frequency to be 0.276 cps. This corresponds closely to the experimental frequency range found in (a) above.

(b) Acoustic Oscillations - The second group of experimental frequencies in (b) above were found to be related to a pressure wave traveling around the loop. The calculated frequency for an acoustic oscillation was found from the relation $f = \frac{a}{\lambda}$ where a is the velocity of sound in the fluid medium and λ is the length of the loop. Acoustic velocities can be calculated for supercritical fluids from the definition $a^2 = \left(\frac{\partial p}{\partial \rho}\right)_s$, whenever thermodynamic data is available. The sonic velocity for water was determined in this manner and is shown in Figure (18) for critical pressure (3206.2 psia). Similar data for Freon-114 can be found in Cornelius[10]. The calculated value for a typical Freon-114 run was 44.2 cps and the experimental value was 42.5 cps.

(c) Longitudinal Pipe Vibration - The third mode of vibration was apparently a longitudinal pipe vibration. Experimental values varied in the 575-625 cps range while the calculated value

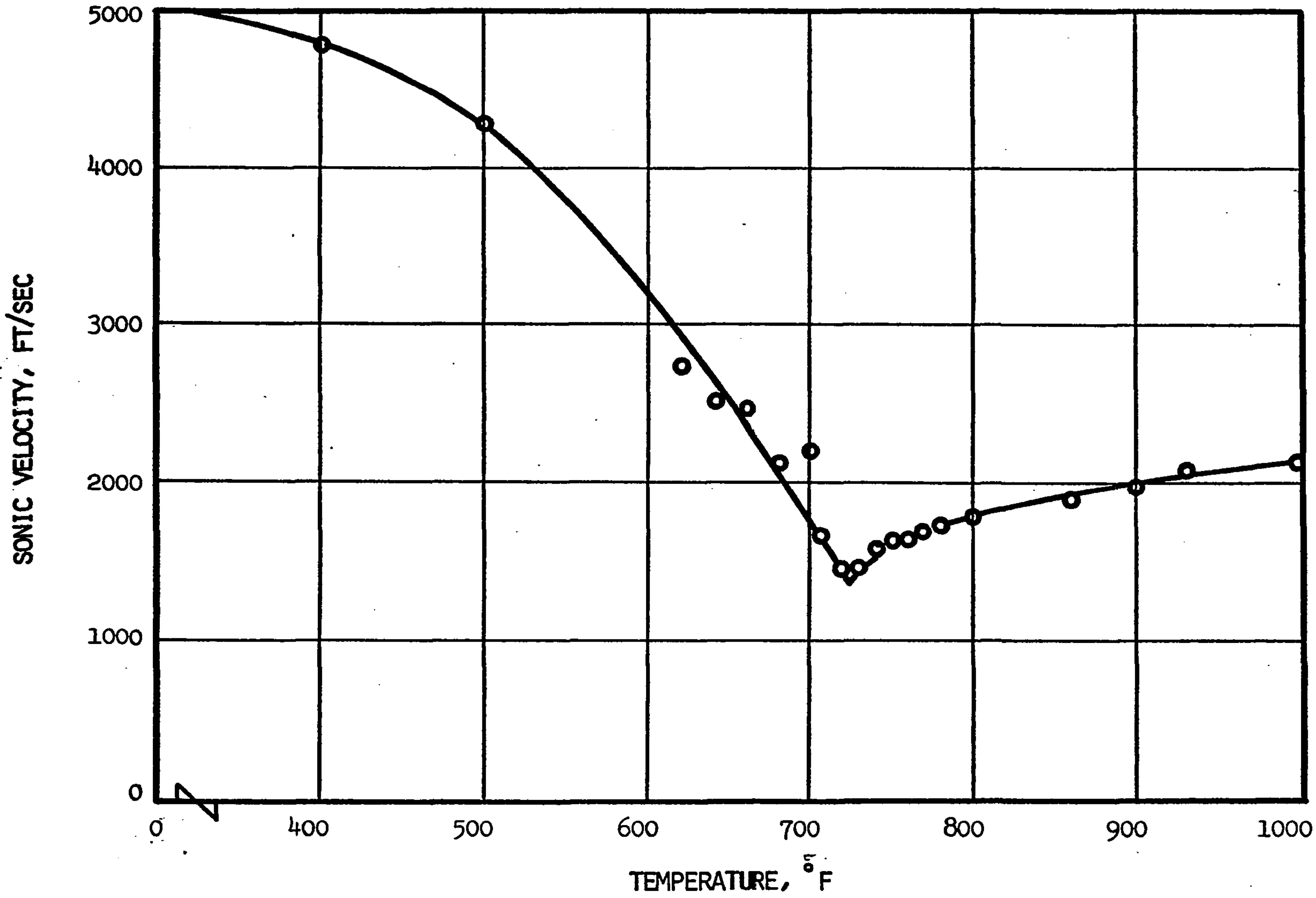

FIGURE (18) SONIC VELOCITY IN H_2O AT P_{CR} (3206.2 PSIA) lies in the $376 < f_n < 1404$ cps range. It is logical to assume the natural frequency should more closely approach that of a cantilever rather than a circular ring. Hence, one would expect the calculated natural frequency to be closer to the 376 cps value.

Other frequencies were calculated for the various modes and some coupling could have occurred. For example, the calculation for the natural frequency of bending vibrations was in the $0.072 < f_n < 0.457$ cps range. Therefore, it is possible that this mode could have affected the experimental values found in (a) above.

The natural frequency of one other mode was calculated in Appendix VI. This mode was the radial vibration in a pressurized pipe. The calculated natural frequency was 21,500 cps. No experimental values were found in this range since the instrumentation was limited to 1000 cps.

One of the results of this study was found not to be in agreement with the results of Garlid et al[12]. Their results showed that the frequency of oscillations at high pressure were approximately 30 times higher than those at low pressure which, according to them, was in agreement with experiment. In one series of tests with Freon-114 as the heat transfer fluid, the results of this series of tests in the present investigation revealed that as the system pressure varied from 109 - 340 psig, the experimentally measured frequency varied from 0.254 - 0.276 cps.

Further, the conclusion by Quandt[24] that flow oscillations become less prevalent at higher pressures for two-phase flow was not substantiated by this investigation.

Subcooling was found to be an important parameter in this study. This parameter was important since it was utilized to describe the thermodynamic state of the fluid. Oscillations were found to occur at all values of subcooling that could be attained in the loop. Oscillations were also found when both the heater section inlet and outlet bulk temperatures corresponded to a fluid in the subcooled liquid state. However, local boiling was occurring even though the bulk temperature was in the subcooled liquid region.

The acoustic oscillations encountered during this investigation occurred primarily in the critical and supercritical thermodynamic regions. However, they were also observed at subcritical pressures. Figures (19 - 21) show an oscillation of this type at three different chart speeds.

Audible vibrations were also encountered in this investigation. Figure (22) shows a trace of one of these vibrations when audible noises were present. From this figure it can be seen that this is an example of a "beat frequency". This particular waveform occurs because two slightly different frequencies were impressed on the system. It also can be shown (cf. Wylie[6]) that the pressure function shown here is almost exactly the product of a sine and a cosine, i.e.,

$$P = \left\{A \sin(\epsilon t)\right\} \cos \omega t \tag{115}$$

where

$$A = \text{Amplitude of the wave}$$

$$\frac{\epsilon}{2\pi} = 9.1 \text{ cps}$$

$$\frac{\omega}{2\pi} = 179.0 \text{ cps}$$

Notice in Equation (115) that the waveform contains a variable amplitude. This type waveform is said to be amplitude modulated thereby giving rise to the noise heard.

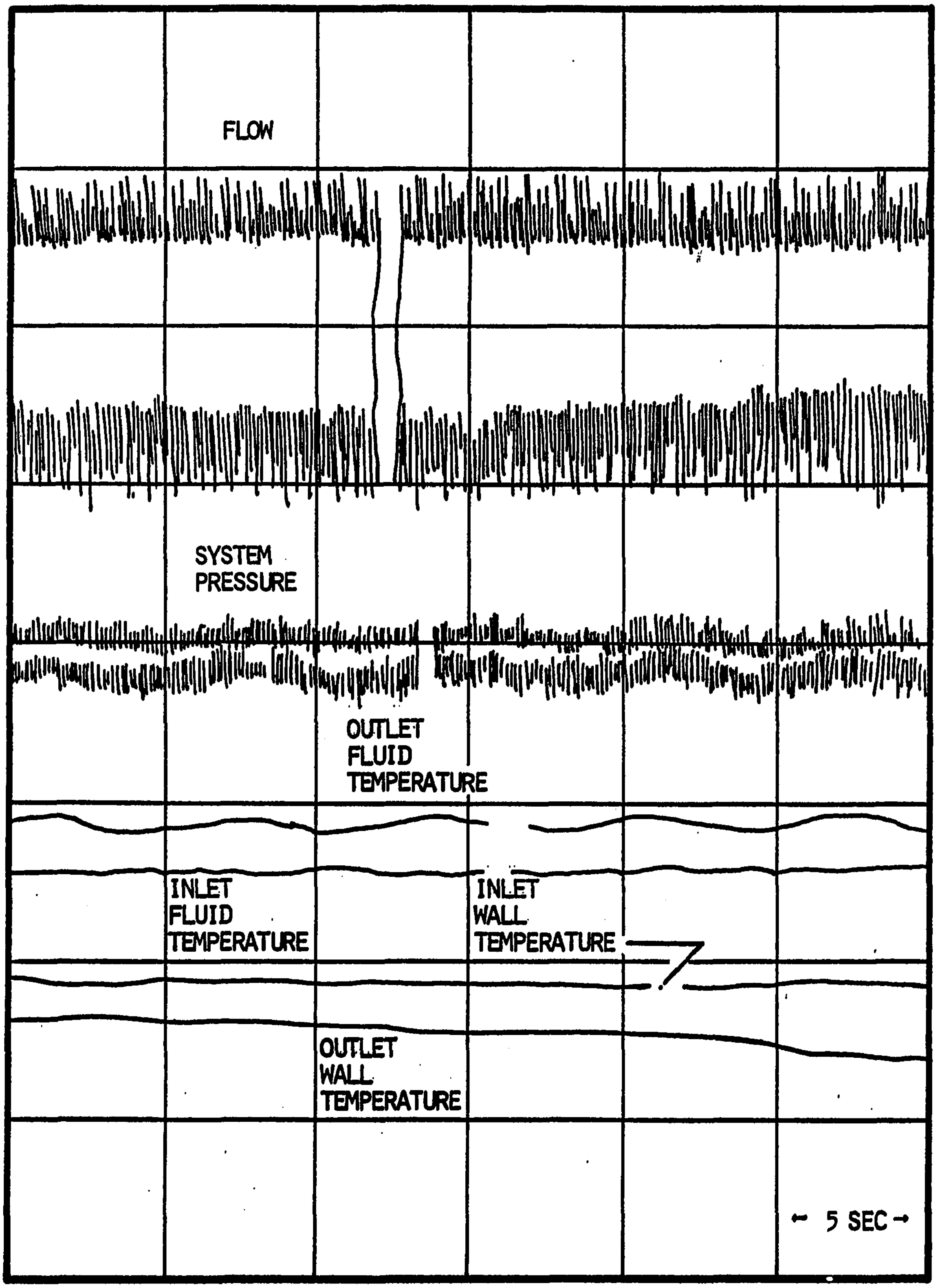

FIGURE (19) SUBCRITICAL ACOUSTIC OSCILLATION WITH FREON-114 AT 335 PSIA

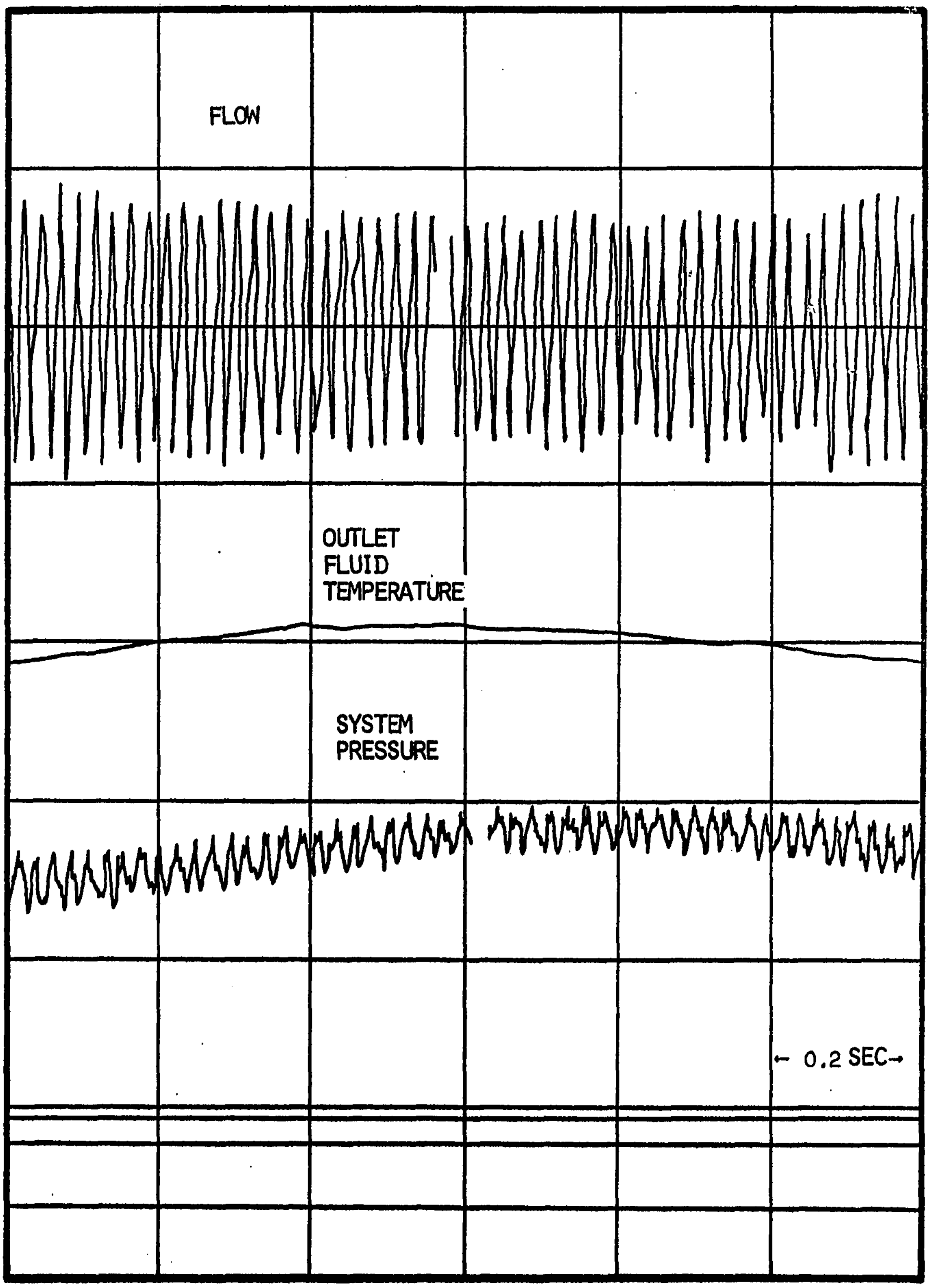

FIGURE (20) SUBCRITICAL ACOUSTIC OSCILLATION
WITH FREON-114 AT 335 PSIA

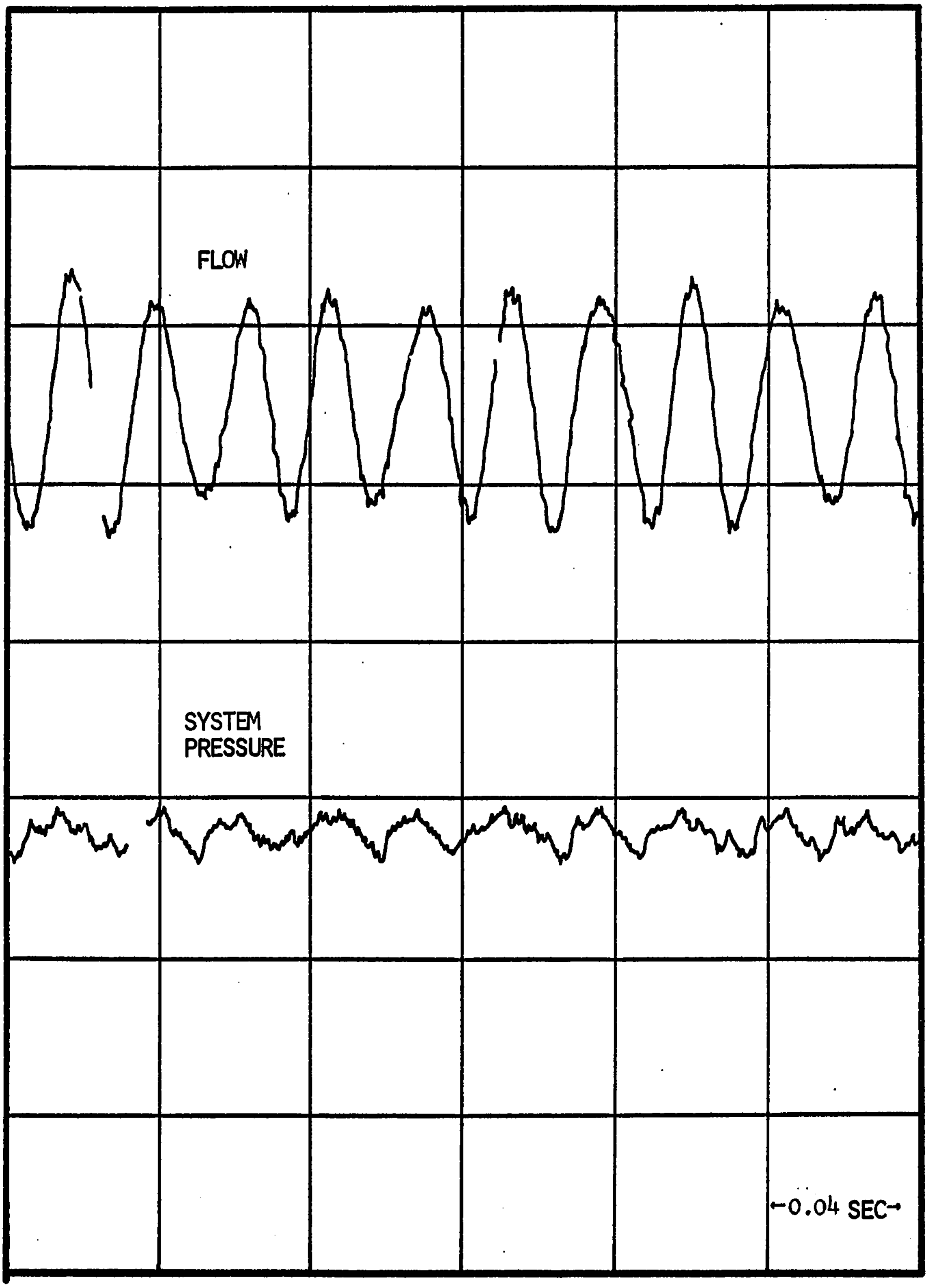

FIGURE (21) SUBCRITICAL ACOUSTIC OSCILLATION WITH FREON-114 AT 335 PSIA

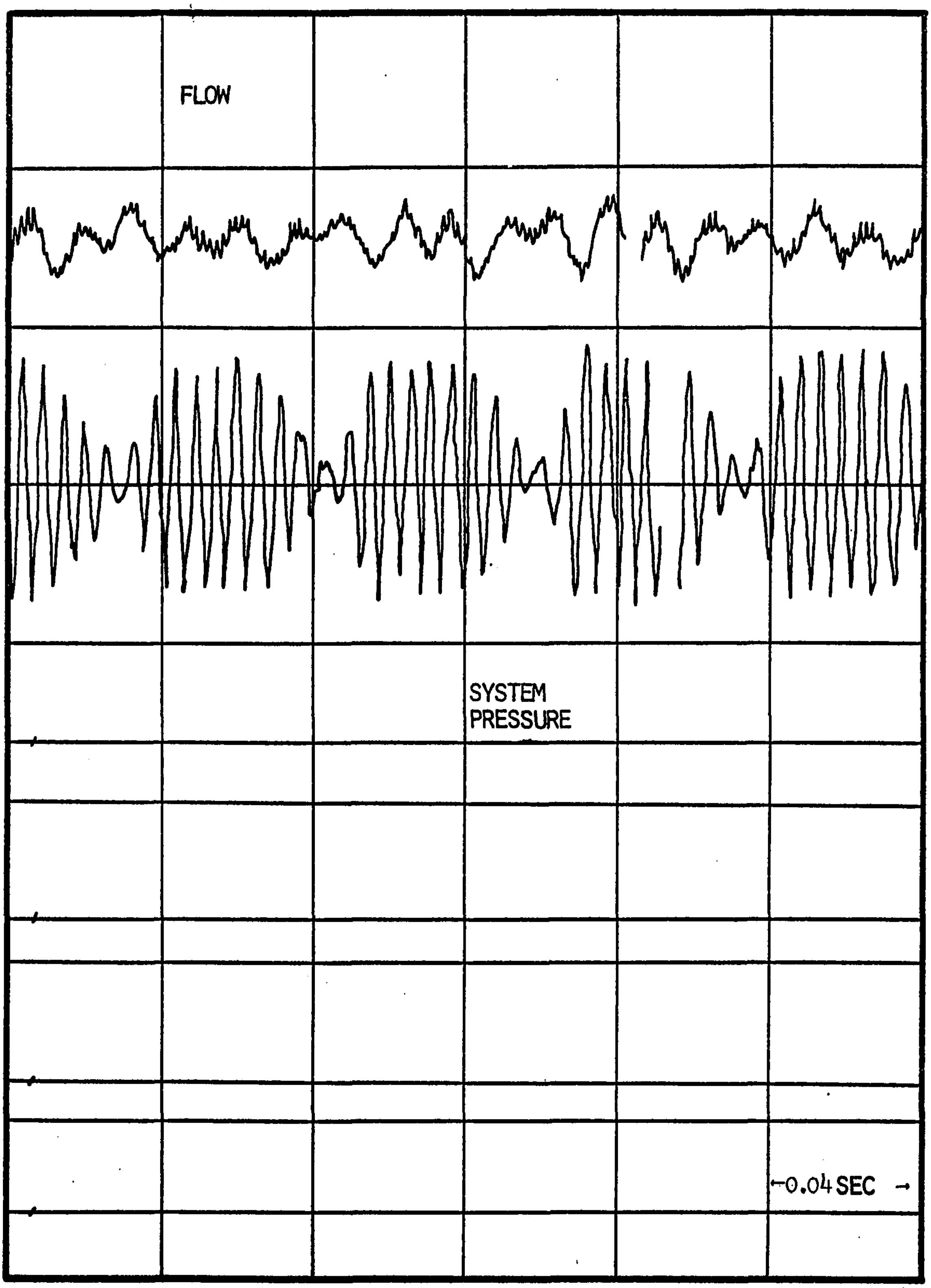

FIGURE (22) BEATING OSCILLATION (AUDIBLE NOISE)

CHAPTER VI

COMPARISON OF ANALYTICAL AND EXPERIMENTAL RESULTS

In order to compare the instability envelope determined by solving the set of equations in ω (104) numerically to obtain the hypersurface $(\Sigma) = \Sigma(g, f, u_\infty, \ell_o, \ell_1, s)$ with the experimental results, it was necessary to represent the surface (Σ) in three space. This was accomplished by setting each of the parameters ℓ_o, ℓ_1, and f equal to a constant. It was possible to set ℓ_o and ℓ_1 equal to a constant since the geometry of the experimental apparatus was not changed during the set of experimental runs. It was possible to set f equal to a constant since this was an inherent assumption in the derivation of the momentum equation (3). Making these simplifications, the surface (Σ) is given by

$$(\Sigma) = (u_\infty, g, s) \tag{116}$$

The surface (Σ) given by Equation (116) was then solved for numerically over a range of u_∞, g, s, and the non-dimensional frequency ω which was comparable to that observed in similar physical systems and comparable to that noted in the experimental portion of this investigation. That portion of the surface (Σ) where steady state operation is possible was then delineated by utilizing Equation (94) to give the instability threshold surface. The results of the numerical solution for the surface (S) where steady state operation is possible is shown in Figures (42 - 44).

It was determined that the best representation of the surface (Σ) would be in the u_∞-g plane with s as a parameter. The u_∞-g plane is called the "plane of operation" and is used to represent the surface (Σ) since it is the most convenient representation to use during the operation of the experimental apparatus. In the two extreme cases, the instability threshold can be approached at a constant power level and a varying entrance velocity or vice versa. In the first case, g would be a constant while u_∞ varied. In the second case, the power W can be eliminated between the definitions for u_∞ and g to give

$$u_\infty^{\;2} = c_1 g \tag{117}$$

where c_1 is a constant.

Therefore, approaching the instability threshold at constant power, W would be given on the operating plane by a vertical line parallel to the u_∞ axis. In the other extreme case, approaching the instability threshold at a constant entrance velocity U_∞ would be given on the operating plane by a parabola given by Equation (117). This parabola changes with the value of the entrance velocity U_∞ and approaches the u_∞ axis as U_∞ increases.

In the operation of the natural-circulation loop, the instability threshold is approached along a path shown on the operating plane somewhere between these two limiting cases since the power W and entrance velocity U_∞ change simultaneously. The approach to the instability threshold would appear as shown in Figure (23).

The results of the simultaneous numerical solution of the equations in ω (104) are shown in Figures (25 - 37) as s varies from 0.0 to 10.0 for f and g as μ_{max} varies from 10^{-3} to 3.5. The parameter μ_{max} is given by

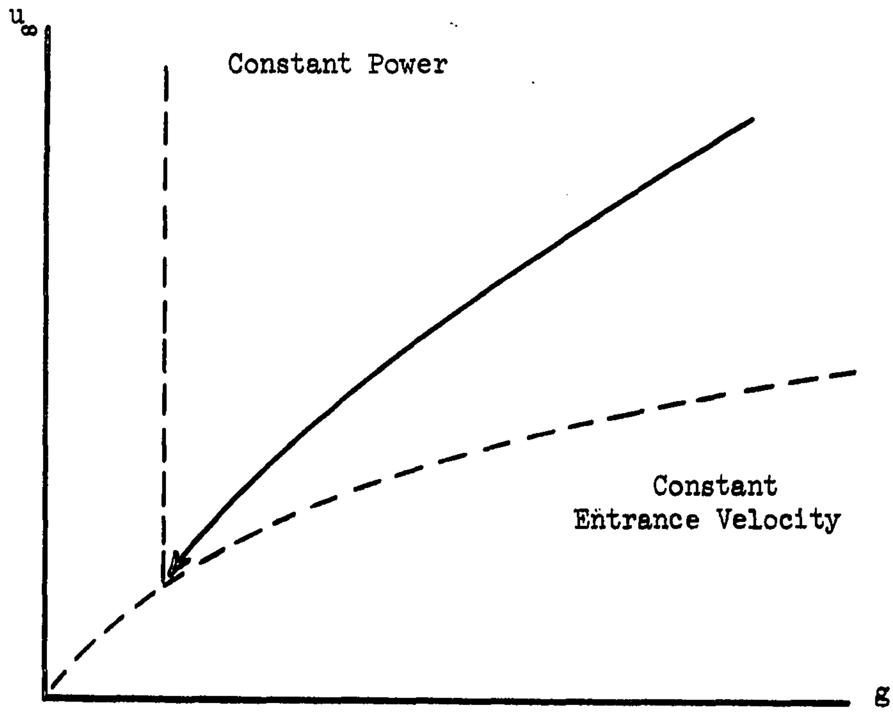

Figure (23) Approach to the Instability Threshold
Shown on the Operating Plane

$$\mu_{max} = \frac{\omega(s + k + z)}{2\pi} \tag{118}$$

and would become useful when utilized to present a constant frequency representation of the threshold surface.

The value of f was then calculated for the range of parameters of interest in this investigation and found to be 0.973. Utilizing this value, these curves were transformed to a single representation of the threshold surface shown on the operating plane in Figure (24). This

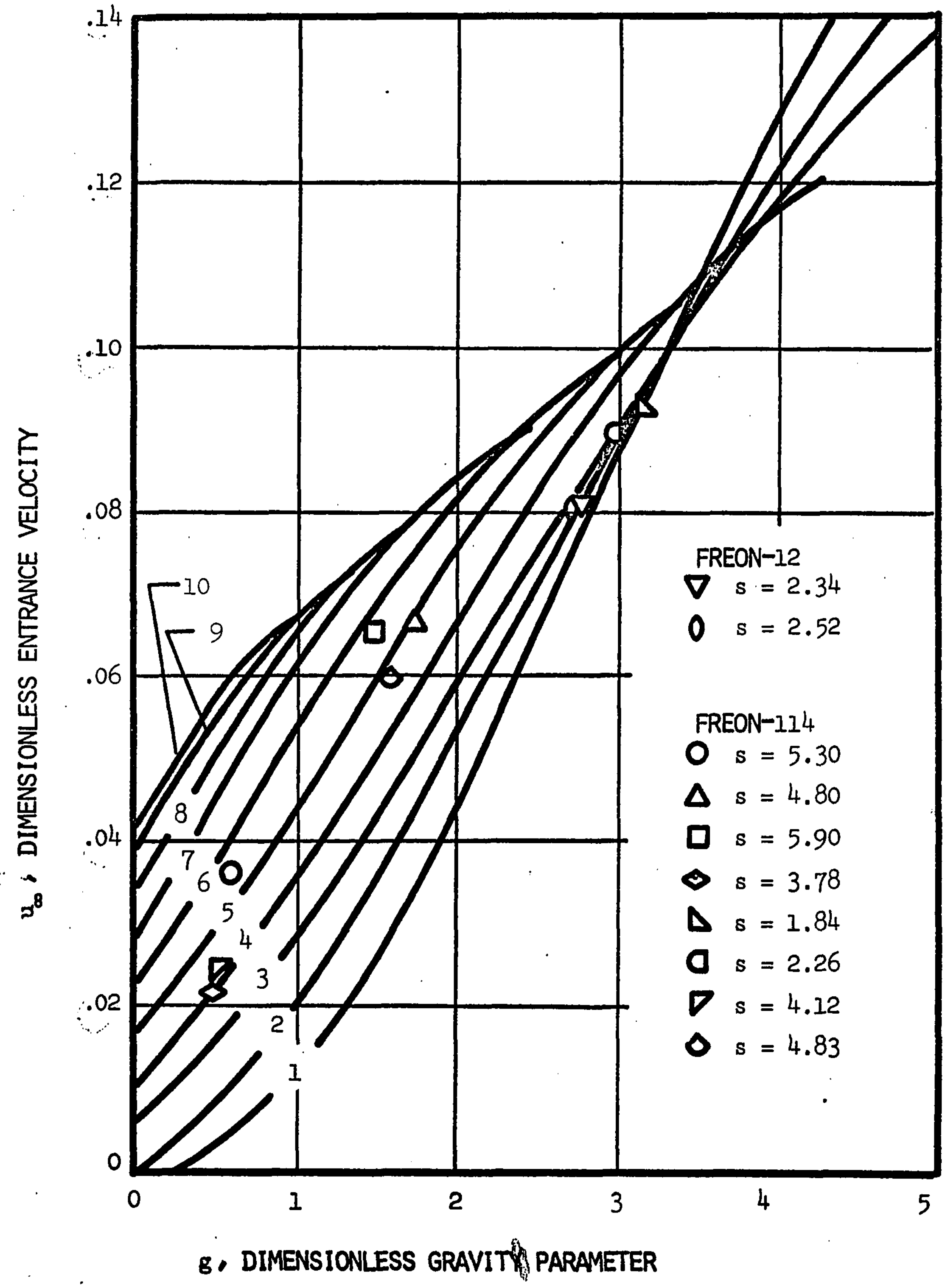

FIGURE (24) INSTABILITY THRESHOLD ALONG LINES OF CONSTANT S

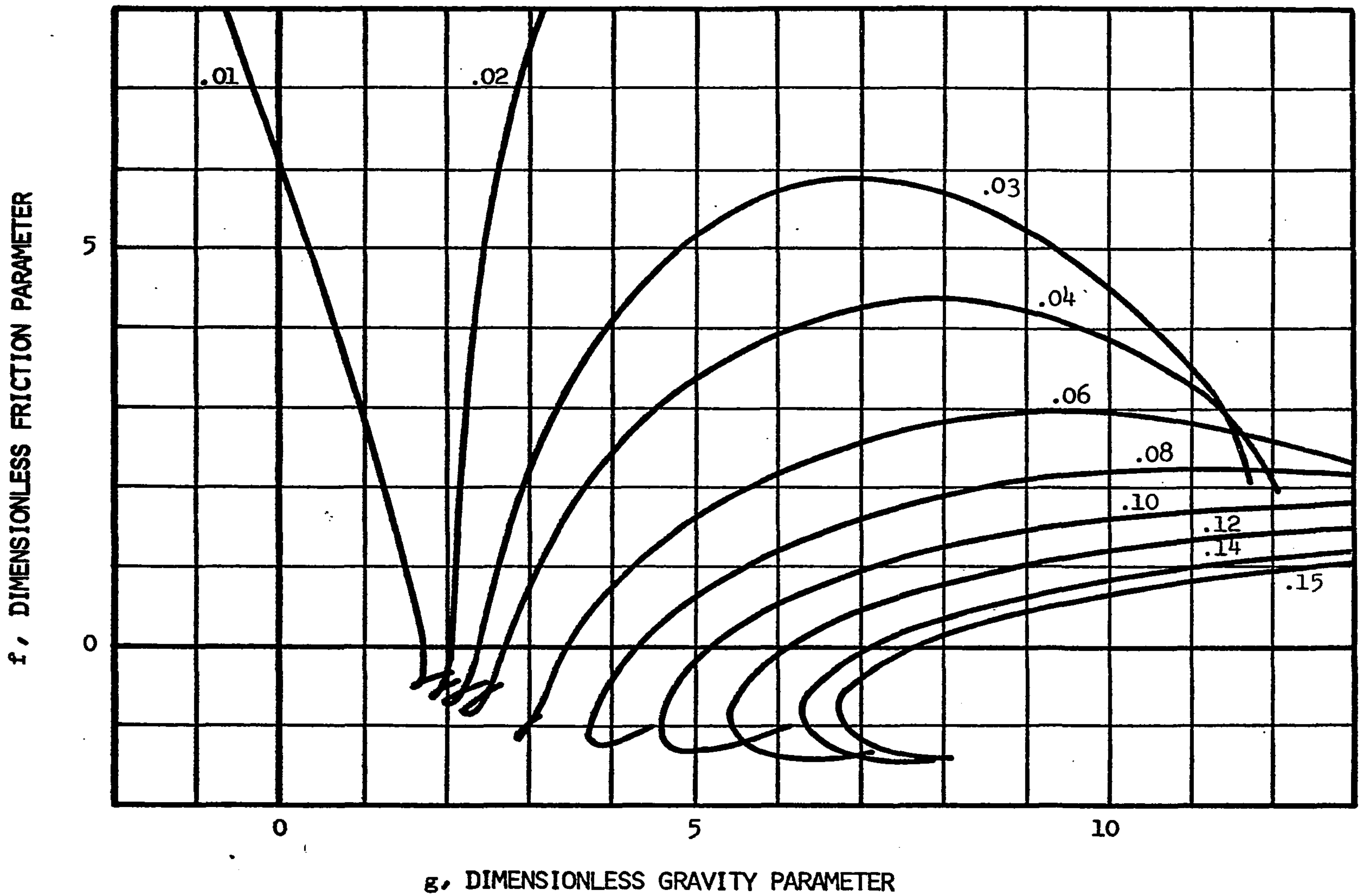

FIGURE (25) $f = f(g)$ FOR $S = 0.0$ WITH PARAMETER u_∞

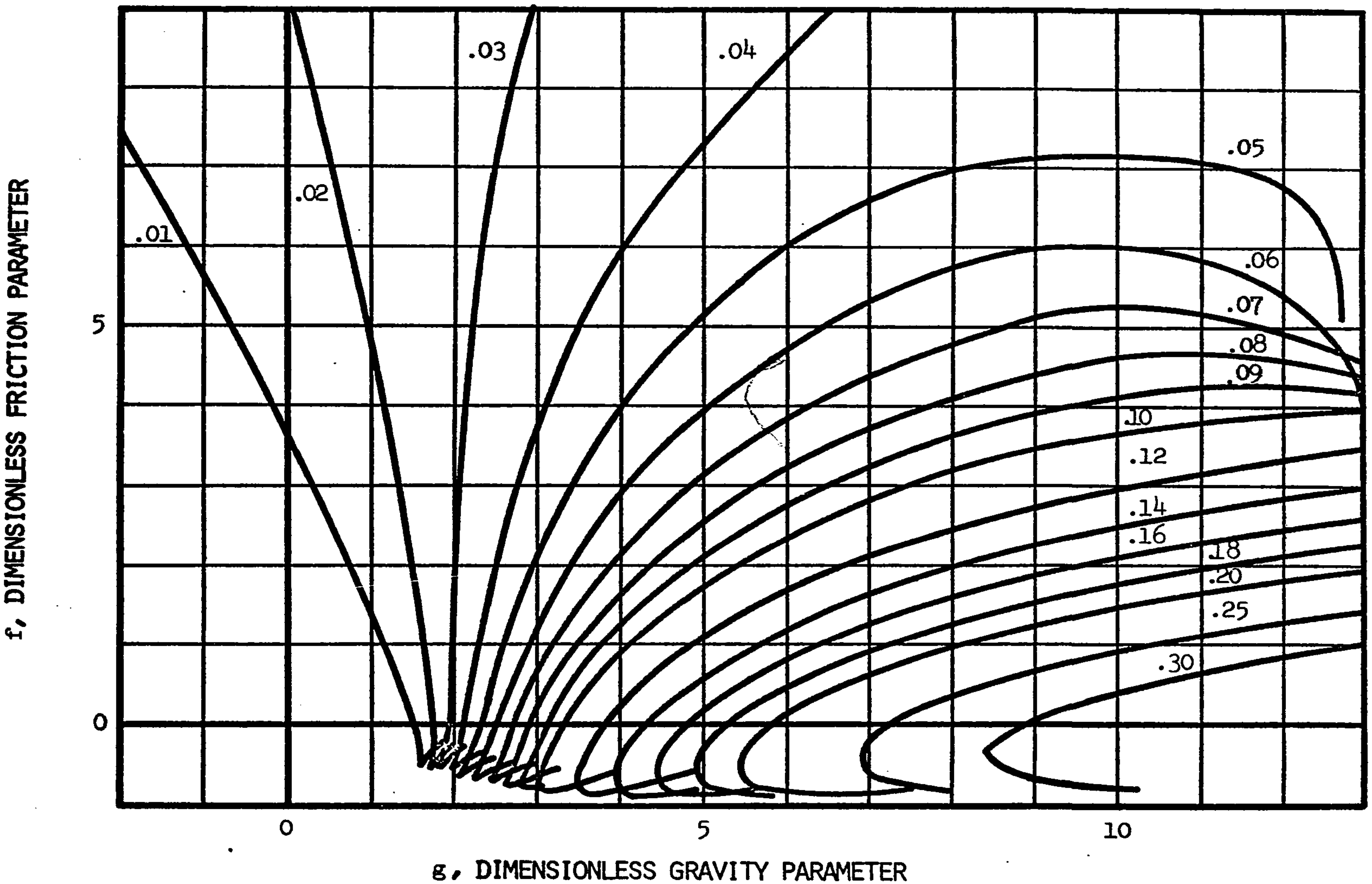

FIGURE (26) $f = f(g)$ FOR $S = 0.5$ WITH PARAMETER u_∞

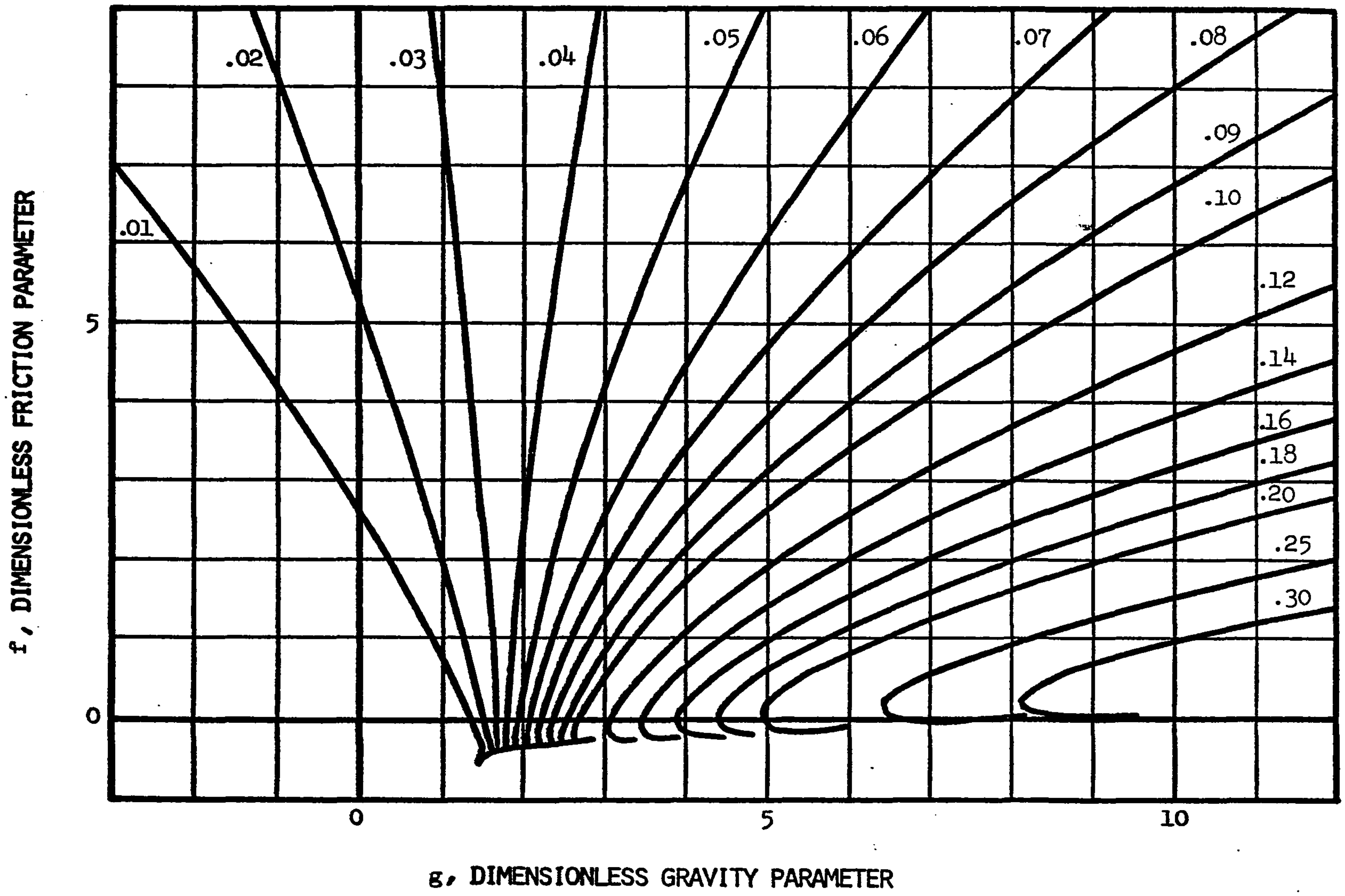

FIGURE (27) $f = f(g)$ FOR $S = 1.0$ WITH PARAMETER u_∞

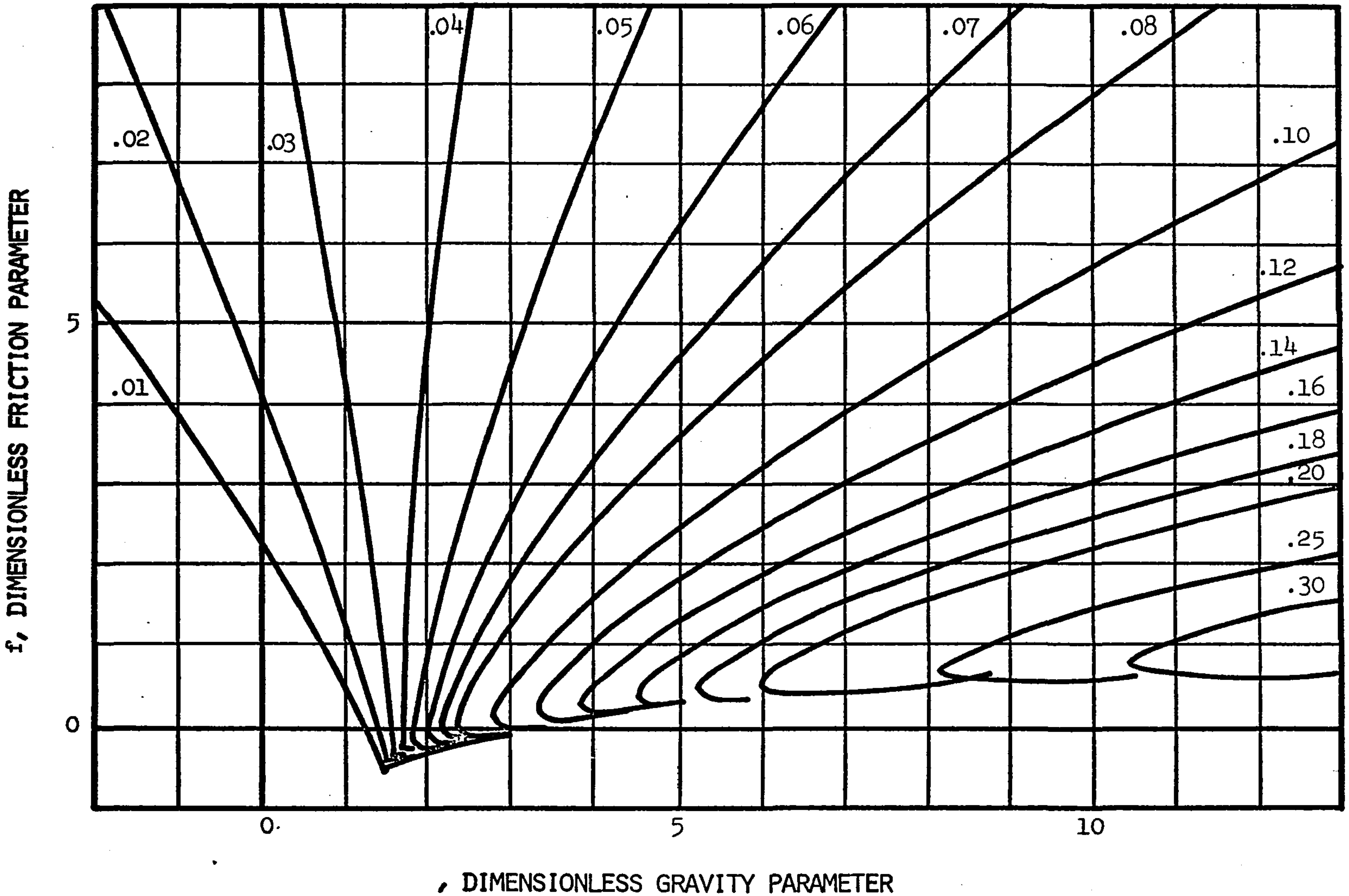

FIGURE (28) $f = f(g)$ FOR $S = 1.5$ WITH PARAMETER u_∞

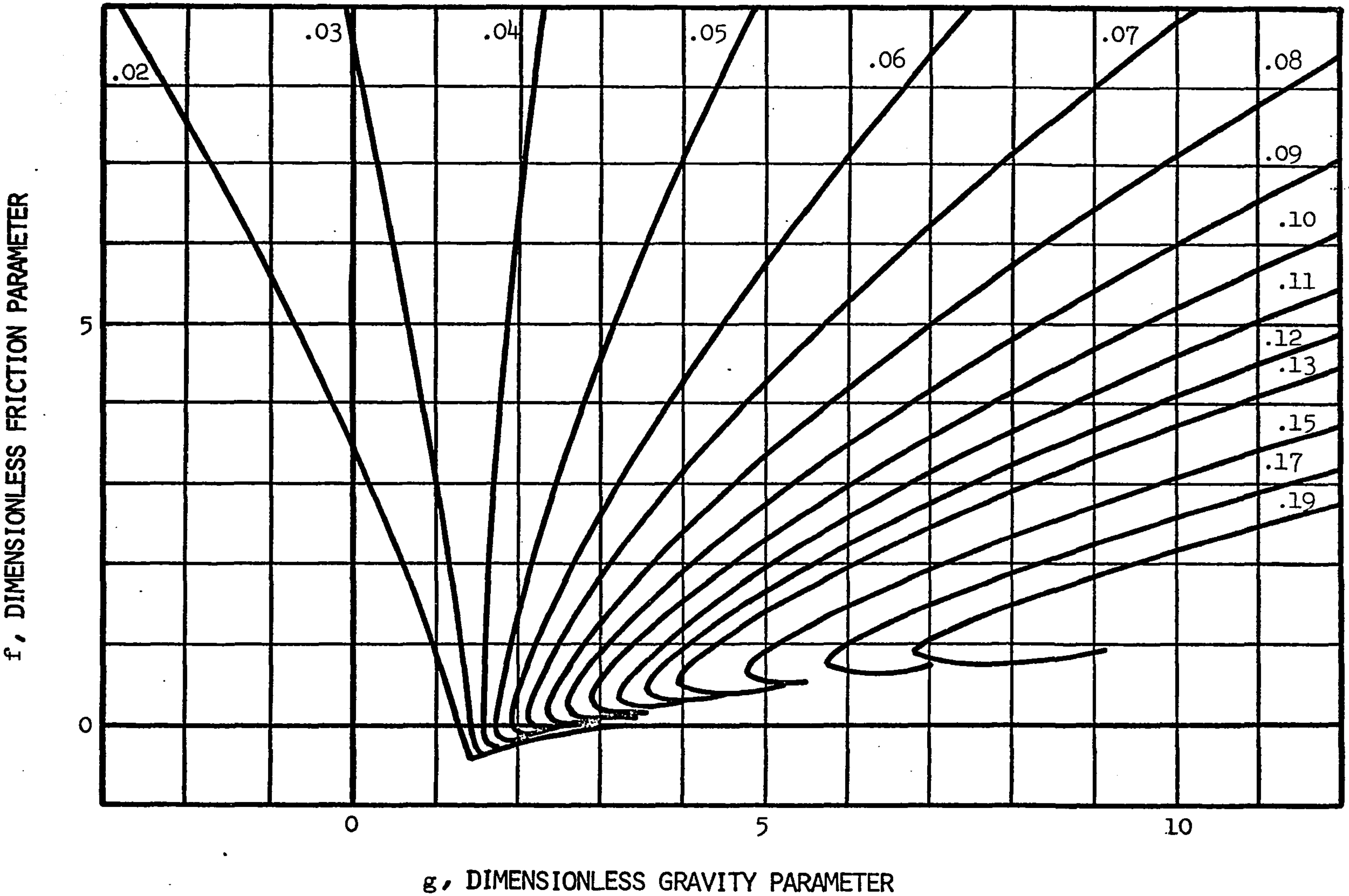

FIGURE (29) $f = f(g)$ FOR $S = 2.0$ WITH PARAMETER u_∞

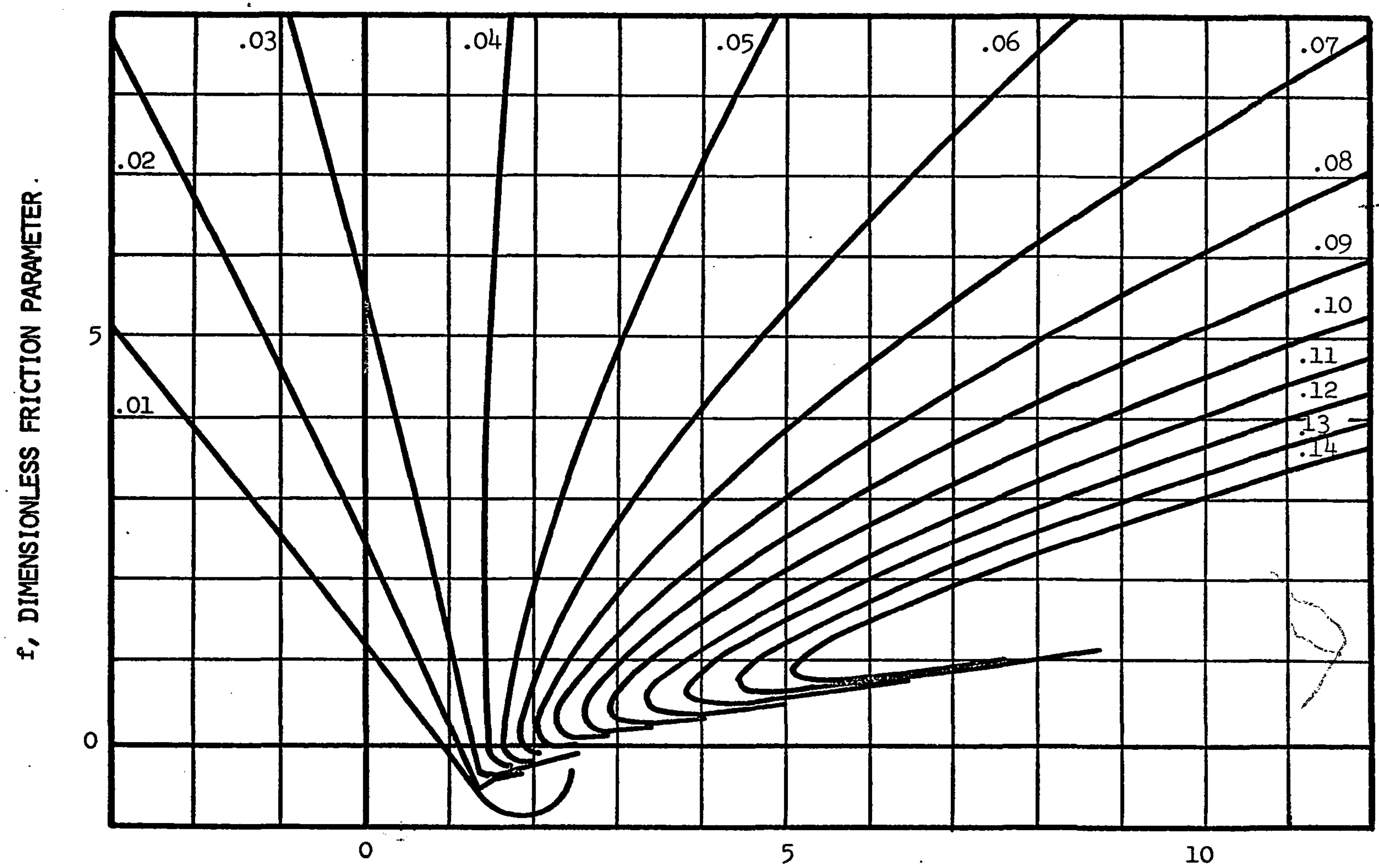

FIGURE (30) $f = f(g)$ FOR $S = 3.0$ WITH PARAMETER u_∞

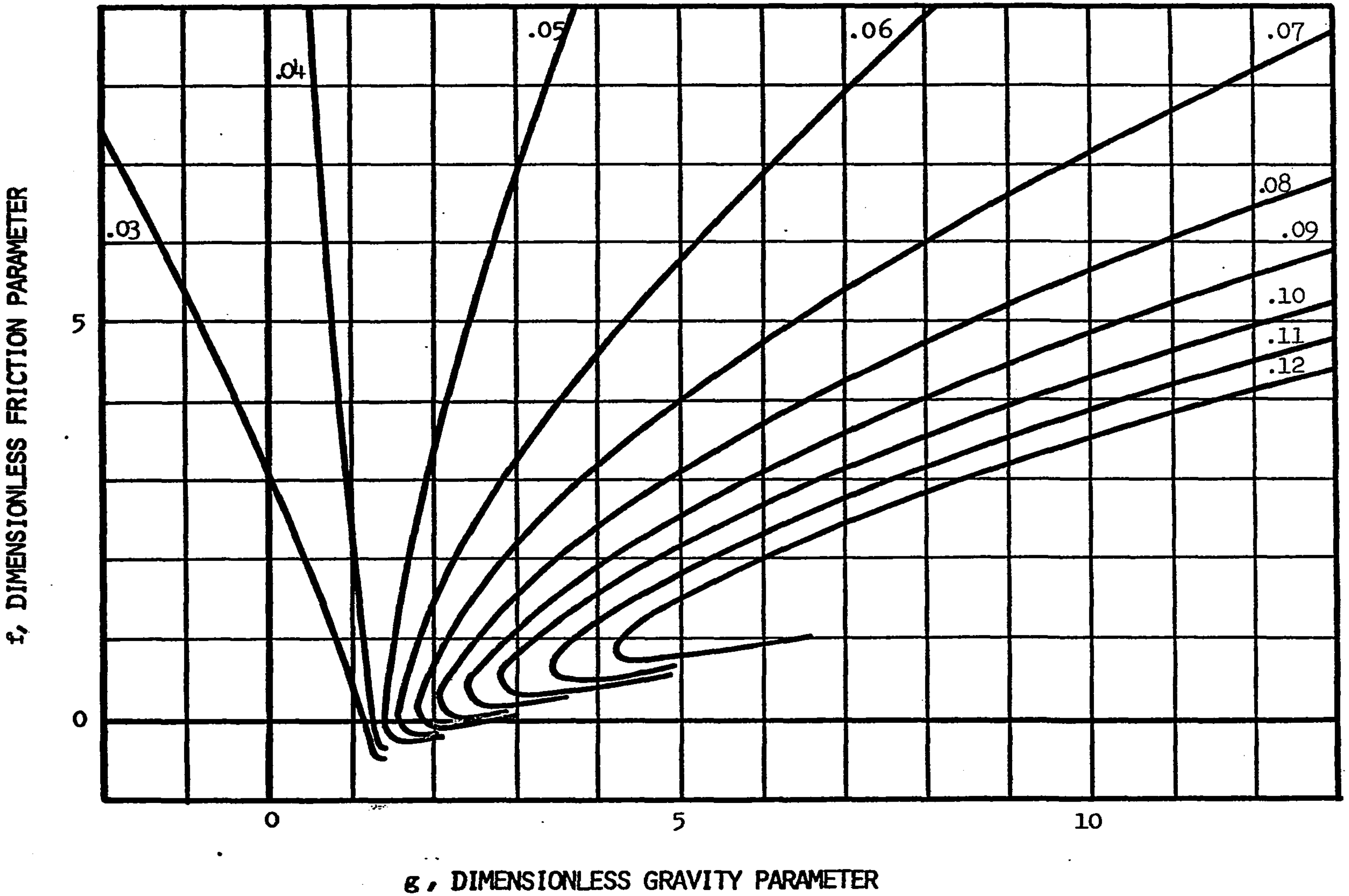

FIGURE (31) $f = f(g)$ FOR $S = 4.0$ WITH PARAMETER u_∞

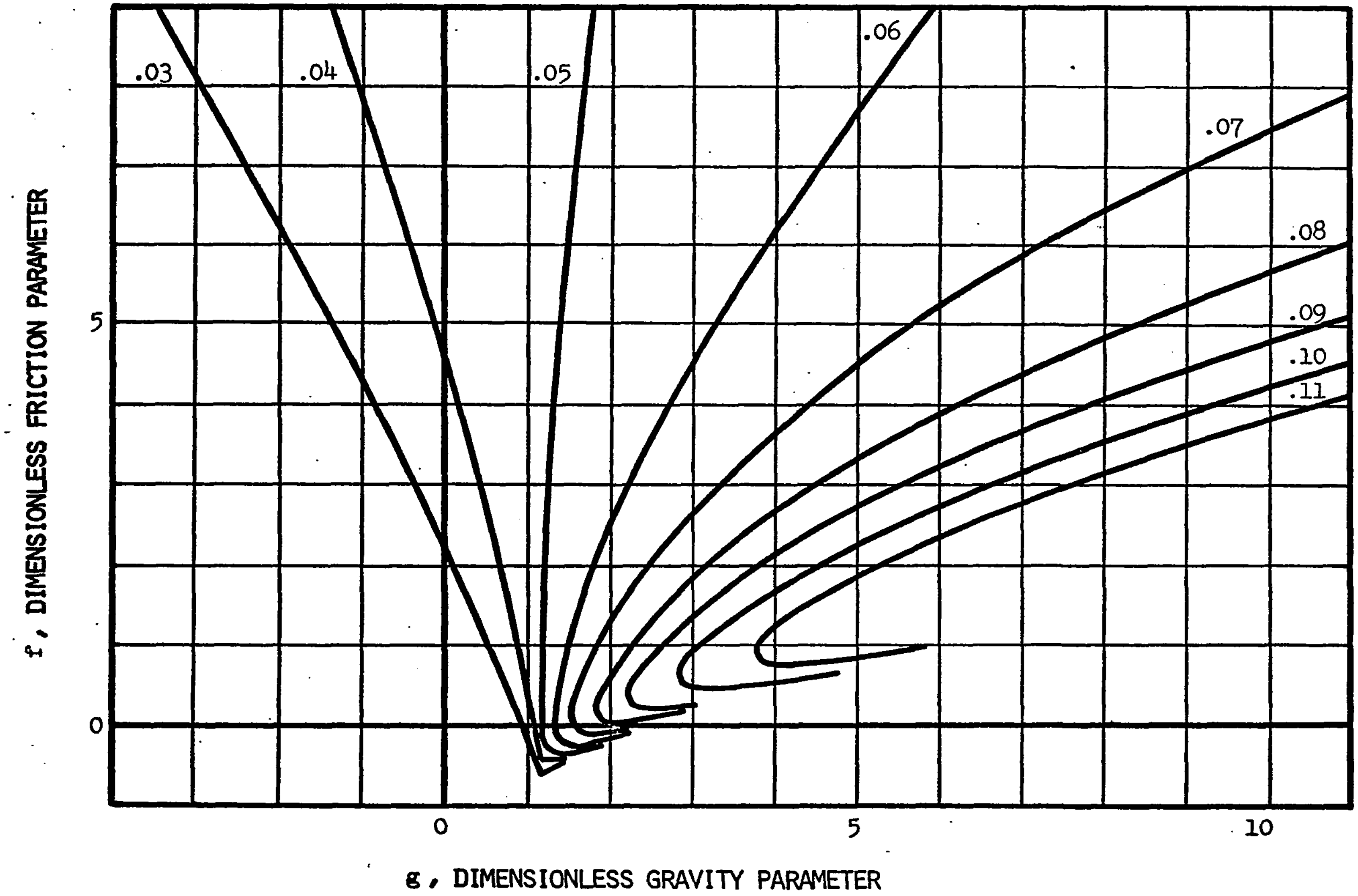

FIGURE (32) $f = f(g)$ FOR $S = 5.0$ WITH PARAMETER u_∞

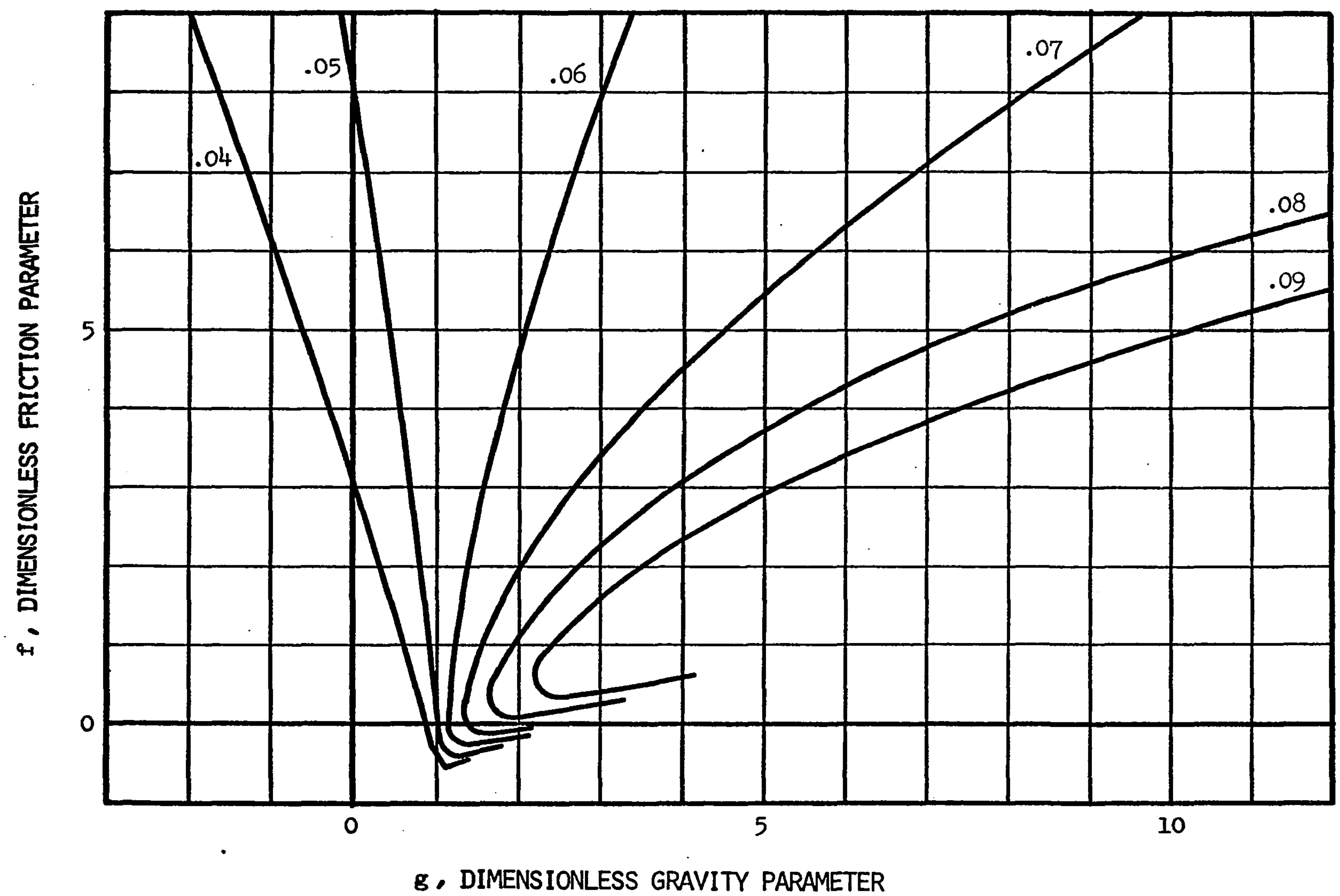

FIGURE (33) $f = f(g)$ FOR $S = 6.0$ WITH PARAMETER u_∞

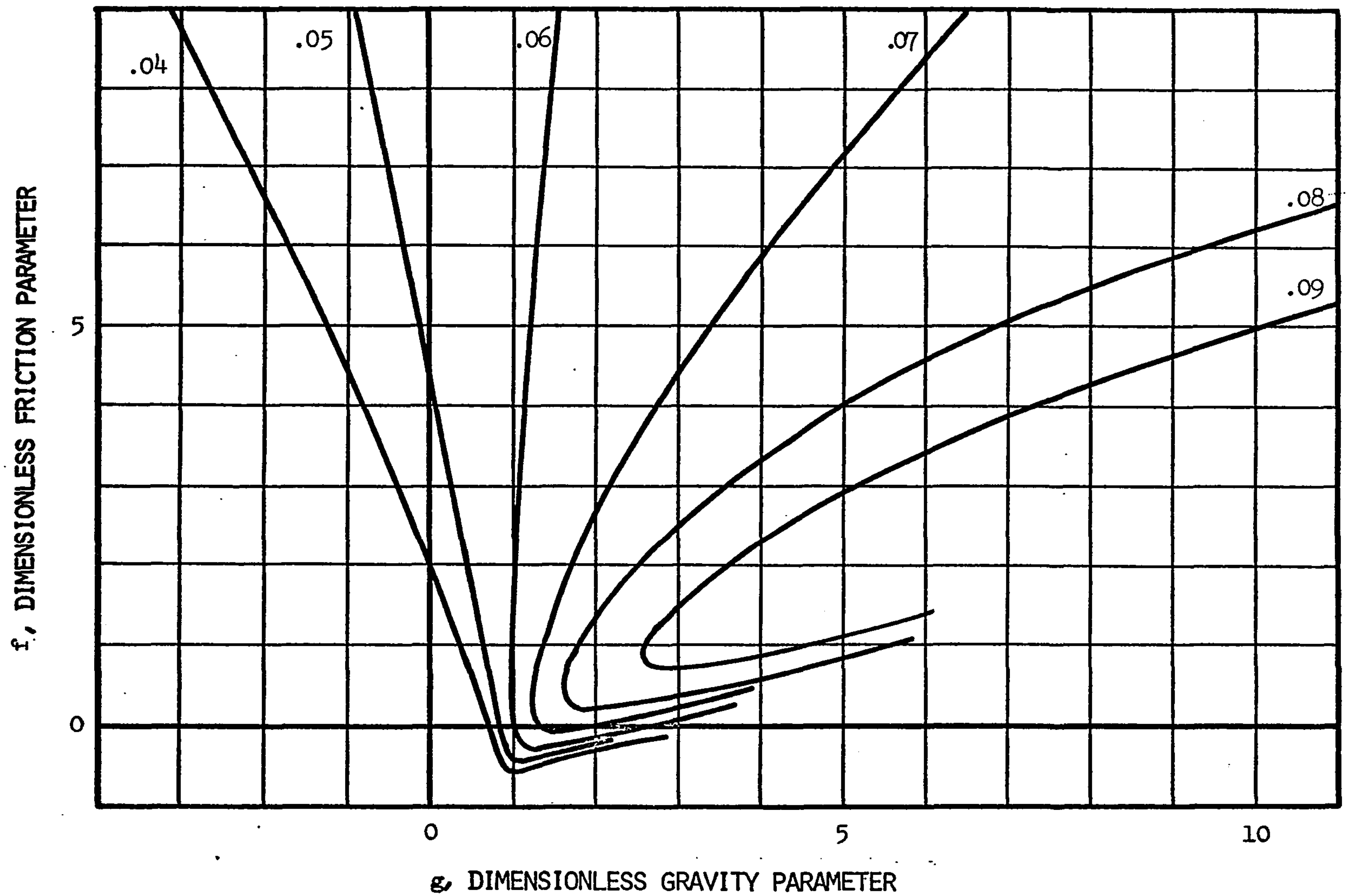

FIGURE (34) $f = f(g)$ FOR $S = 7.0$ WITH PARAMETER u_∞

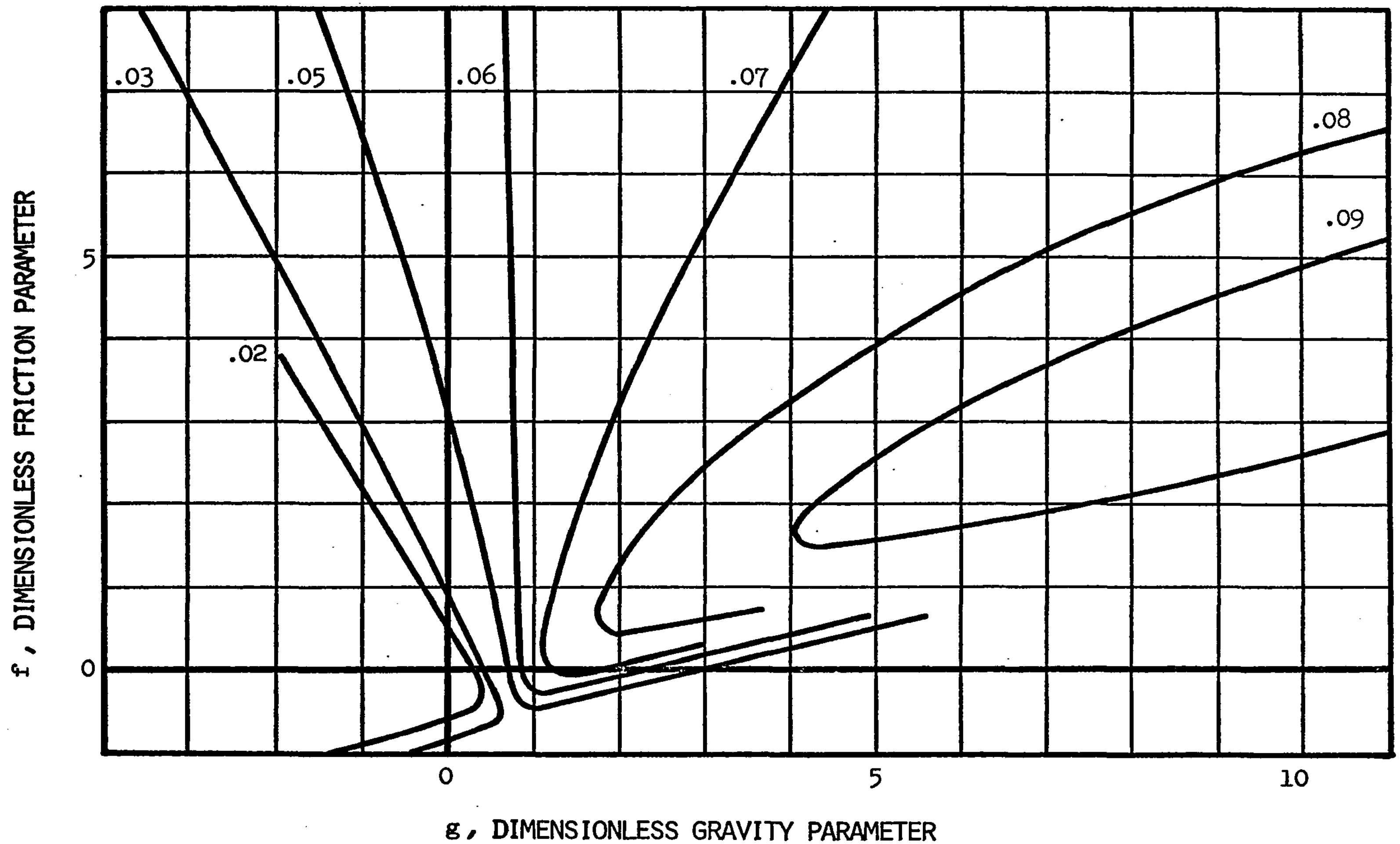

FIGURE (35) $f = f(g)$ FOR $S = 8.0$ WITH PARAMETER u_∞

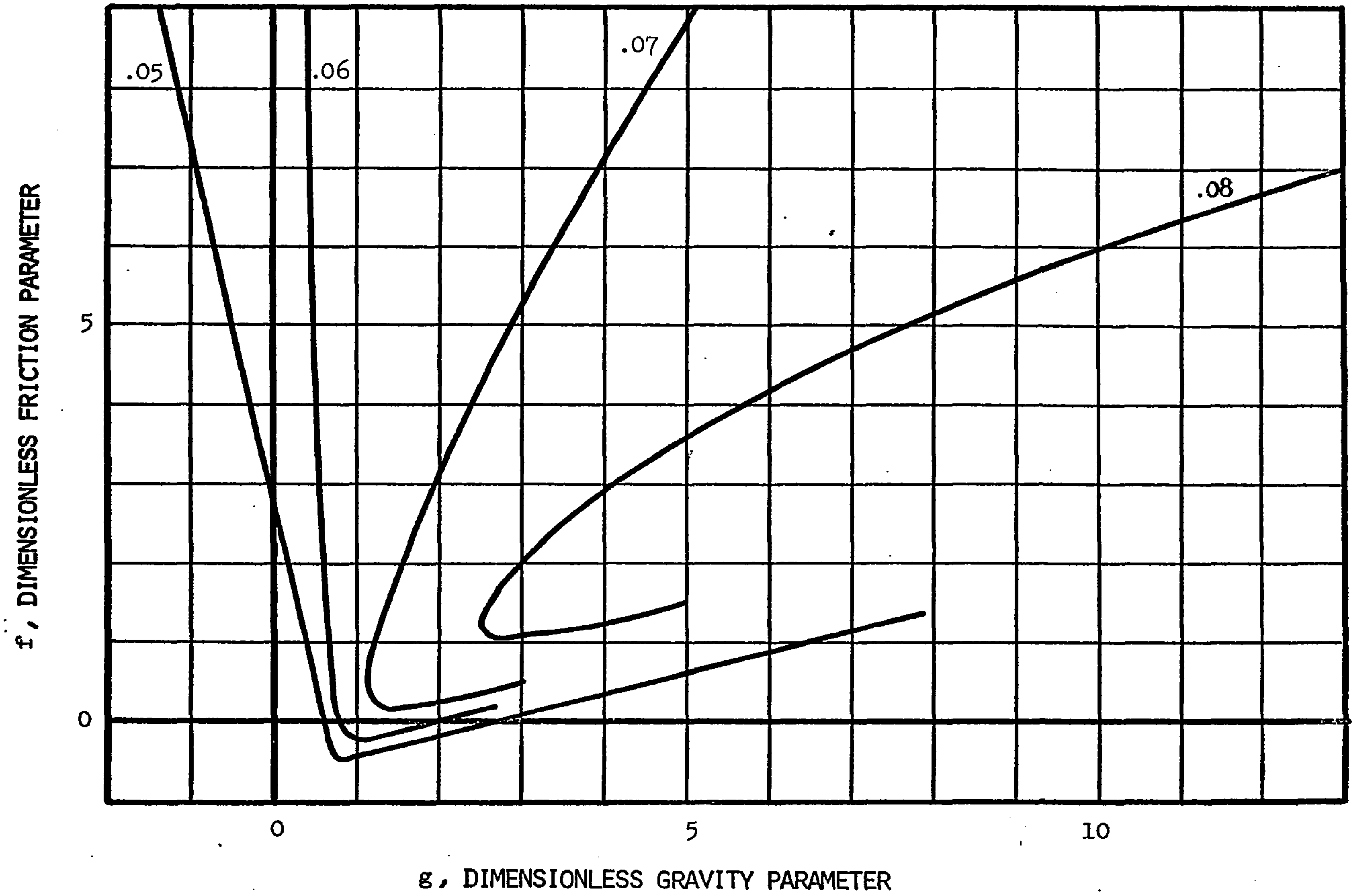

FIGURE (36) $f = f(g)$ FOR $S = 9.0$ WITH PARAMETER u_∞

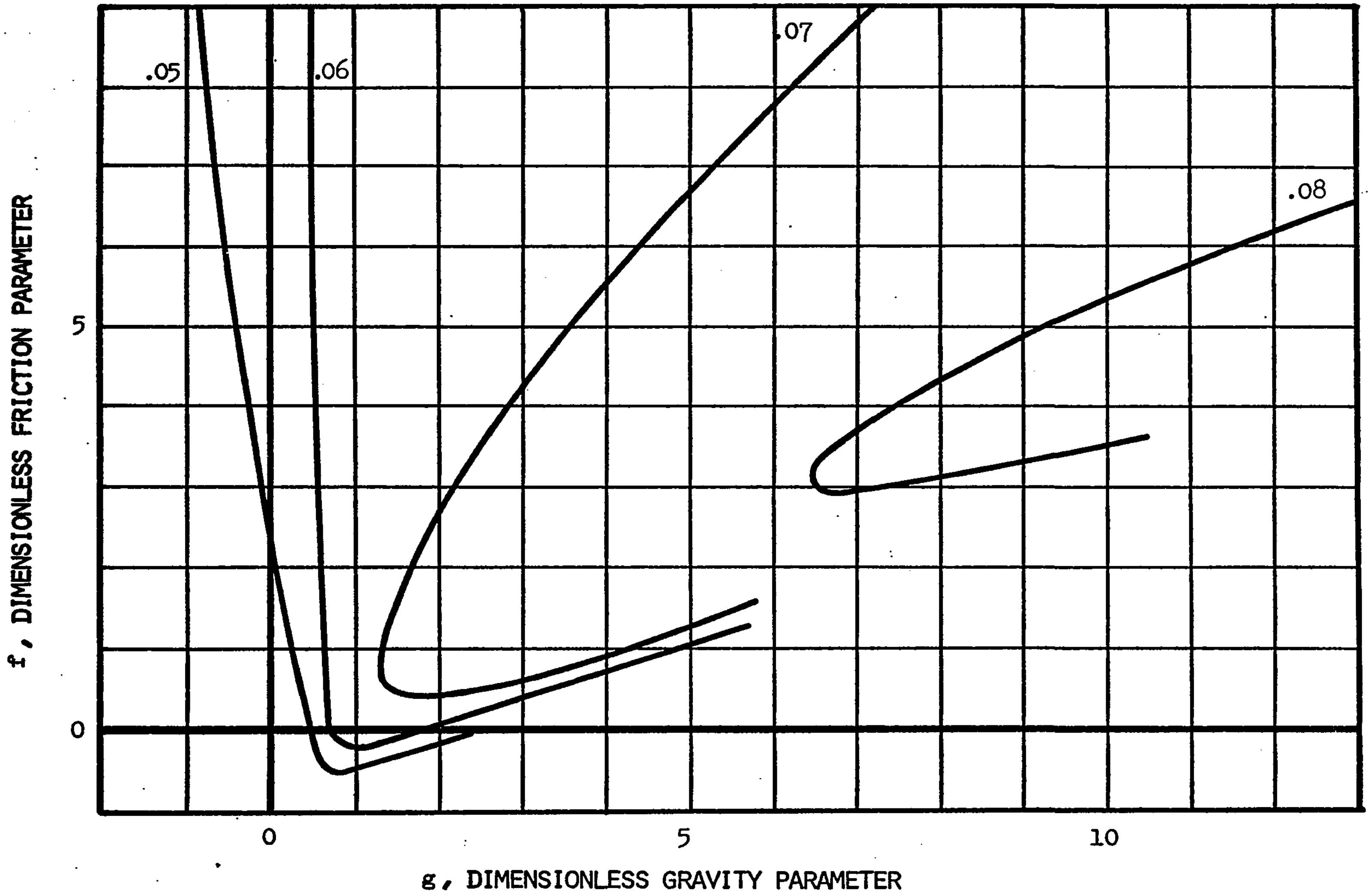

FIGURE (37) $f = f(g)$ FOR $S = 10.0$ WITH PARAMETER u_∞

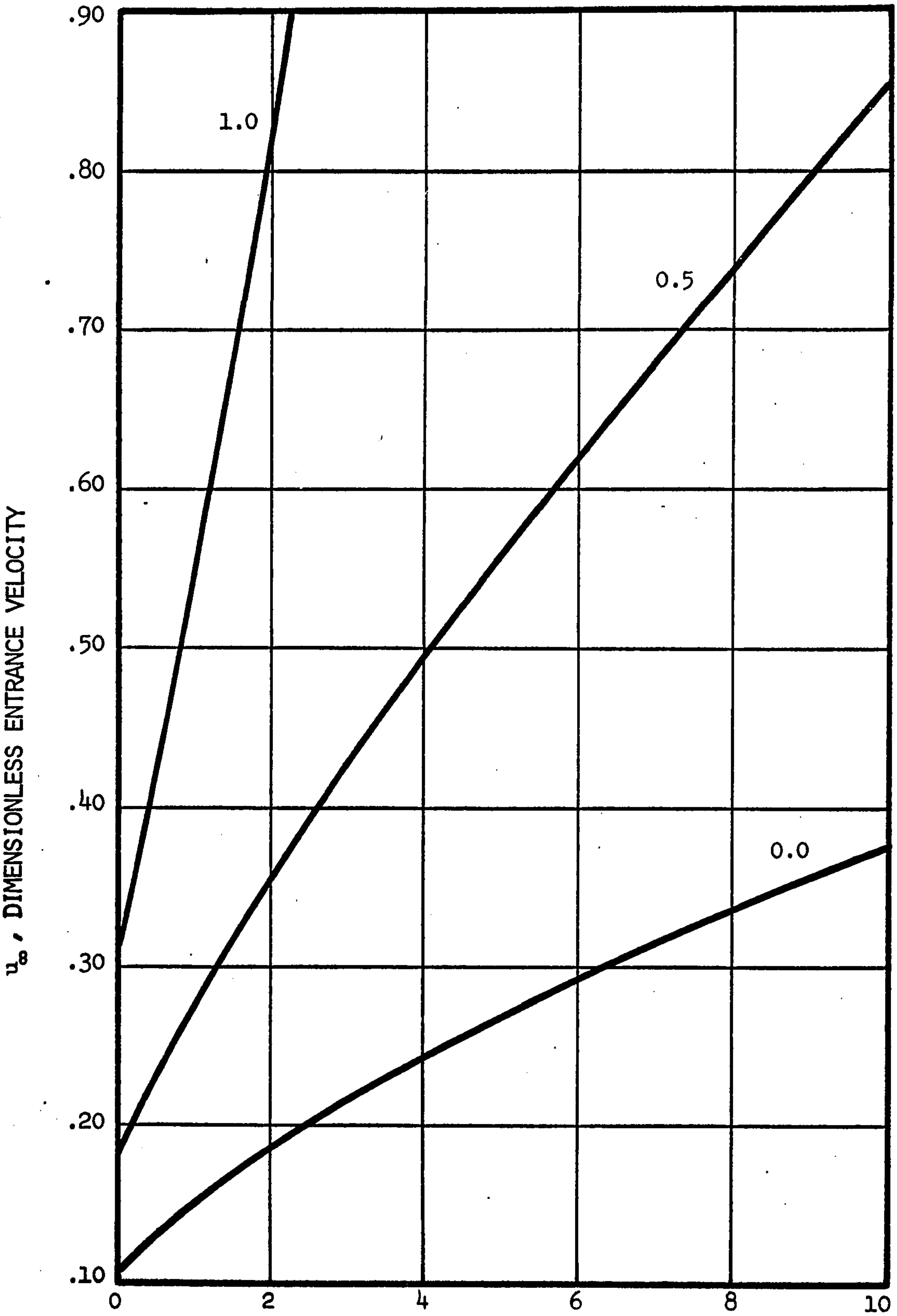

FIGURE (38) INSTABILITY THRESHOLDS WITH PARAMETER S AT LOW FREQUENCY

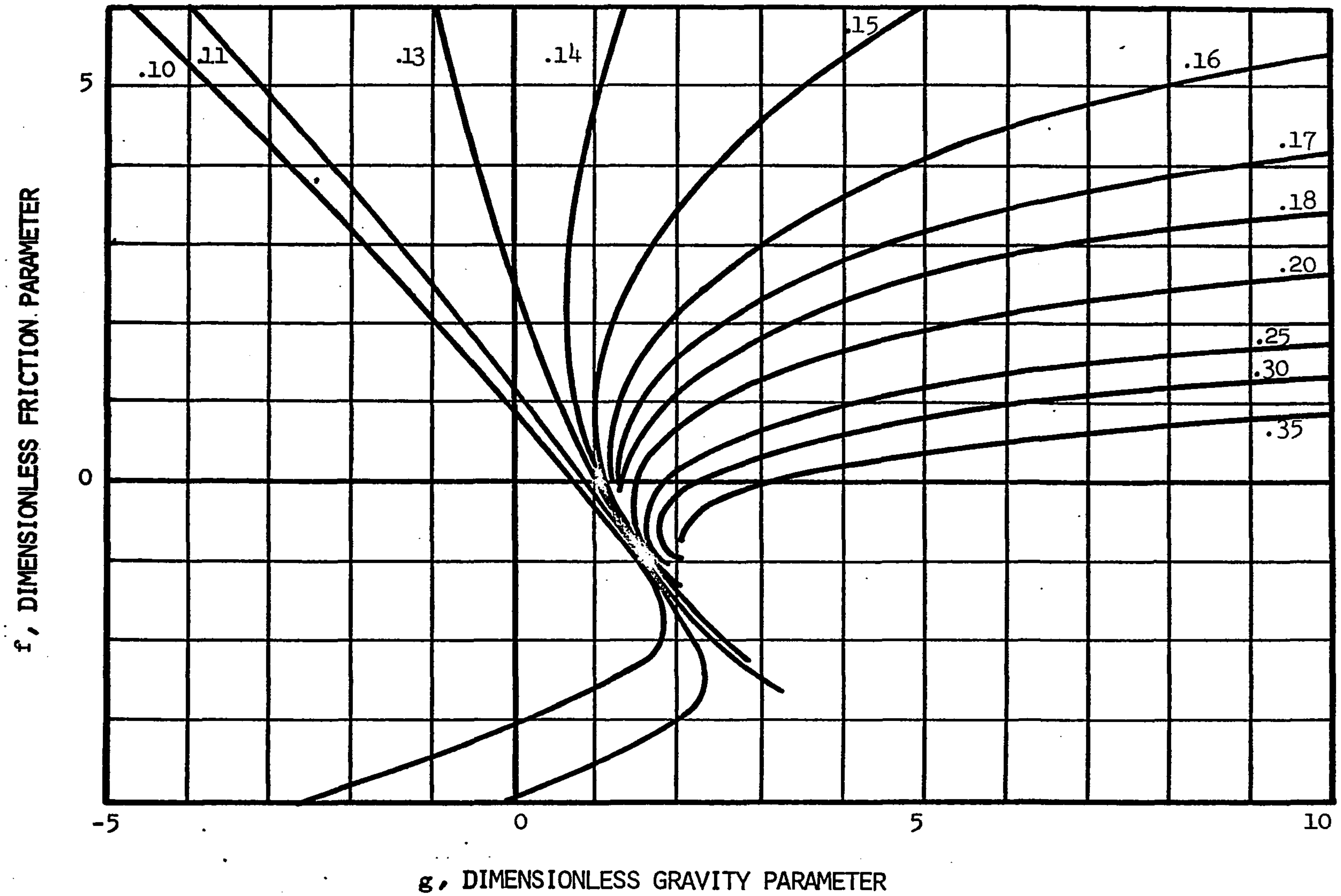

FIGURE (39) $f = f(g)$ FOR $S = 0.0$ WITH PARAMETER u_∞
(LOW FREQUENCY)

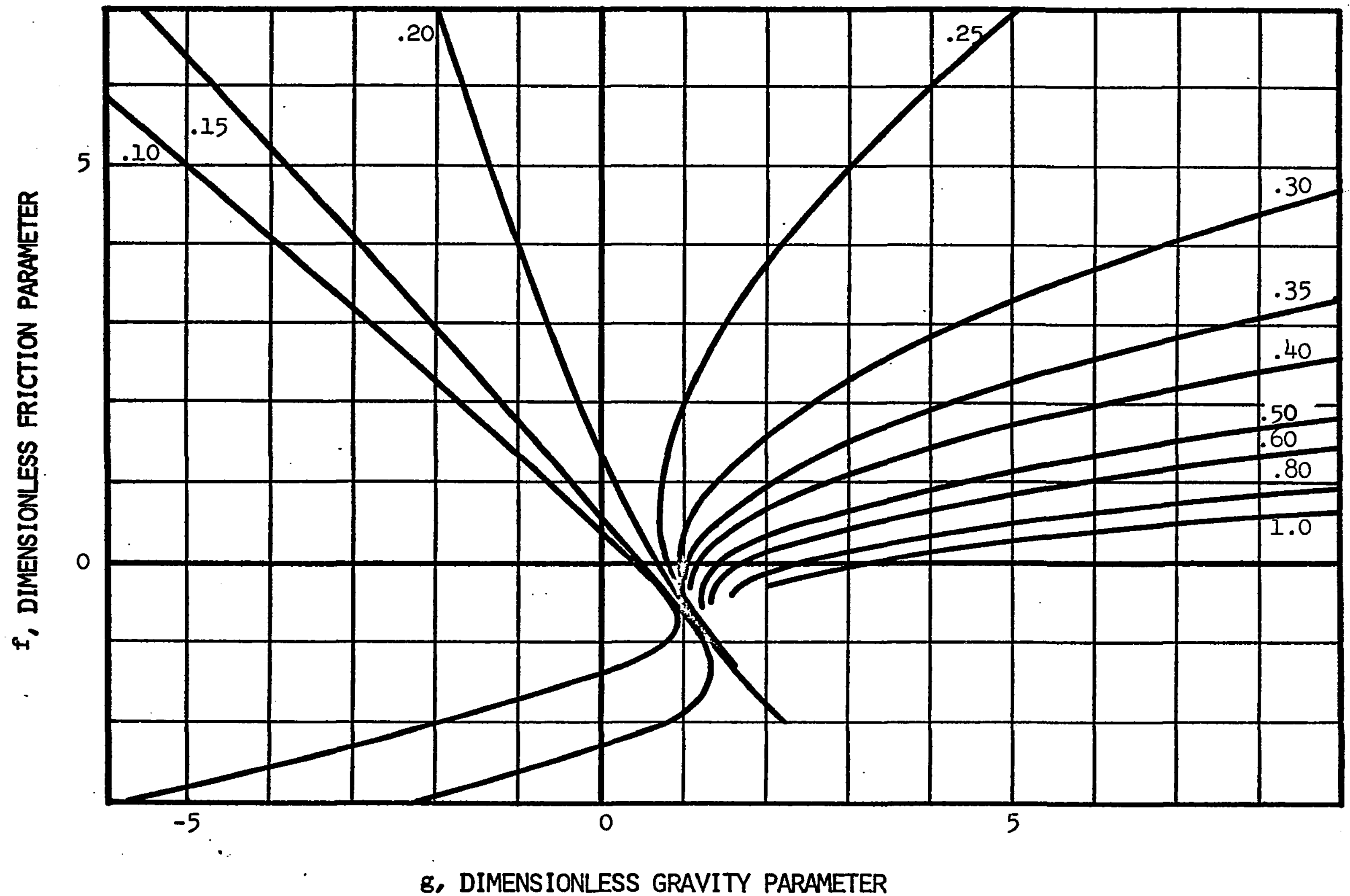

FIGURE (40) $f = f(g)$ FOR $S = 0.5$ WITH PARAMETER u_∞
(LOW FREQUENCY)

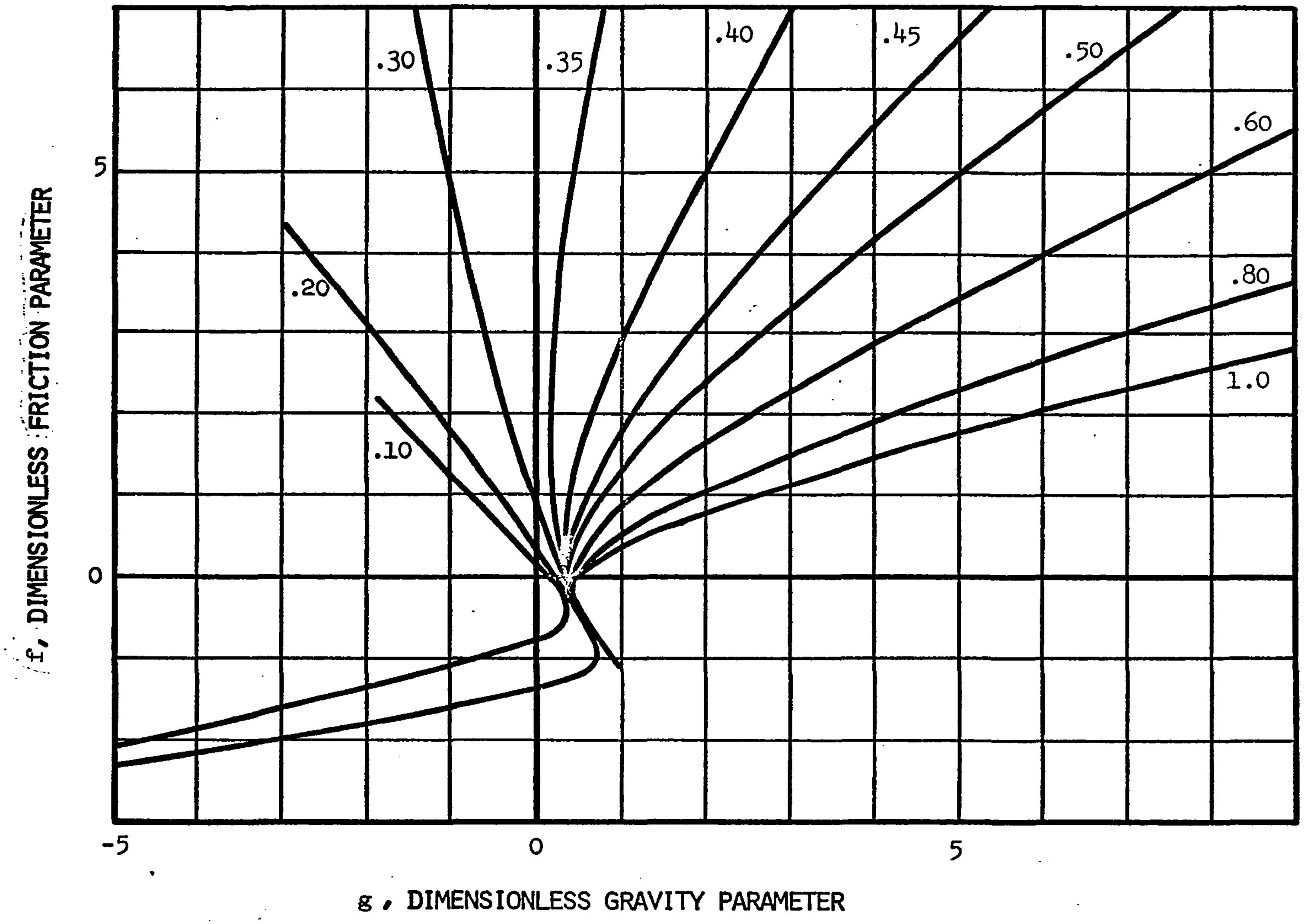

FIGURE (41) $f = f(g)$ FOR $S = 1.0$ WITH PARAMETER u_∞
(LOW FREQUENCY)

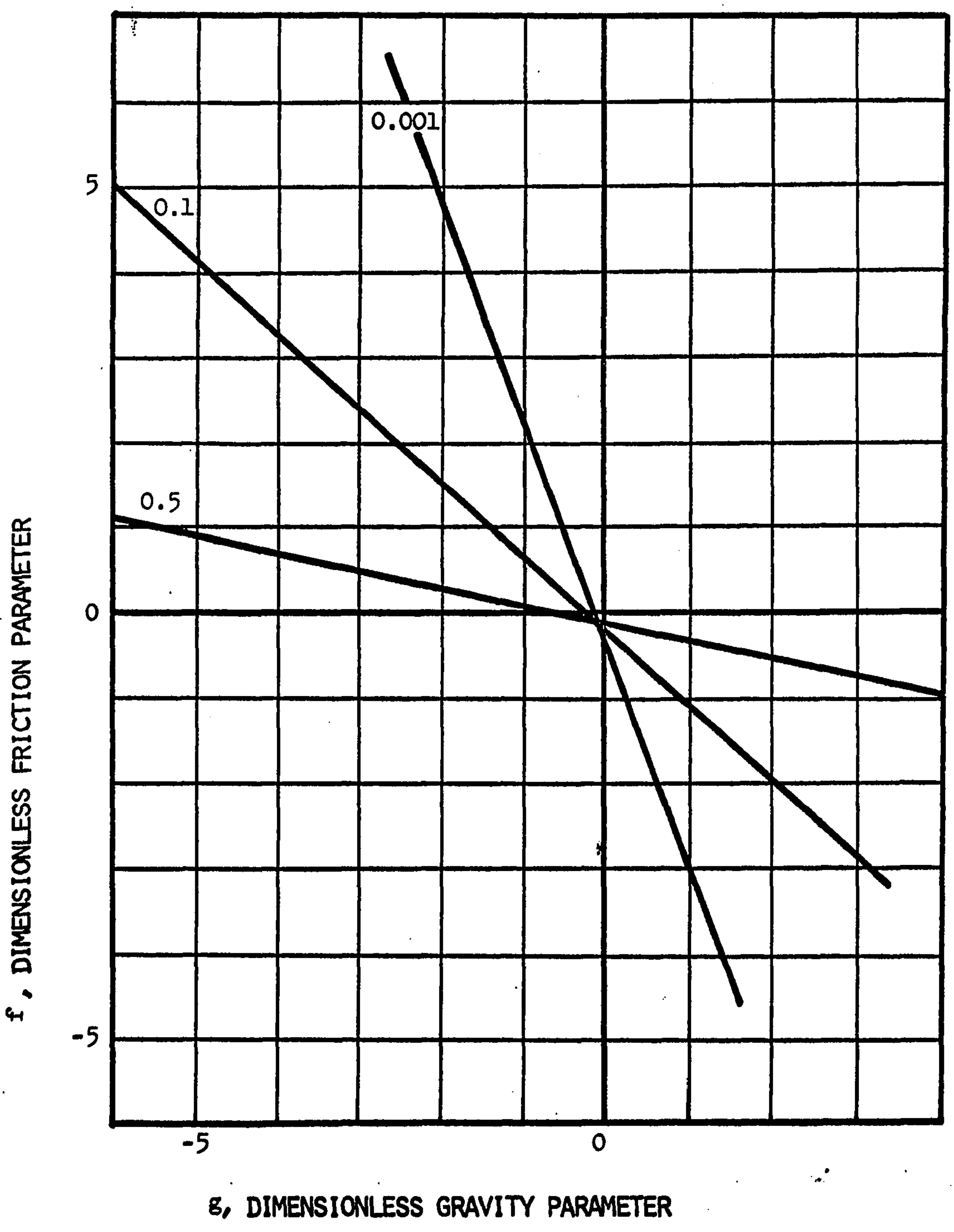

FIGURE (42) $f = f(g)$ FOR $S = 0.0$ WITH PARAMETER u_∞ AT STEADY STATE

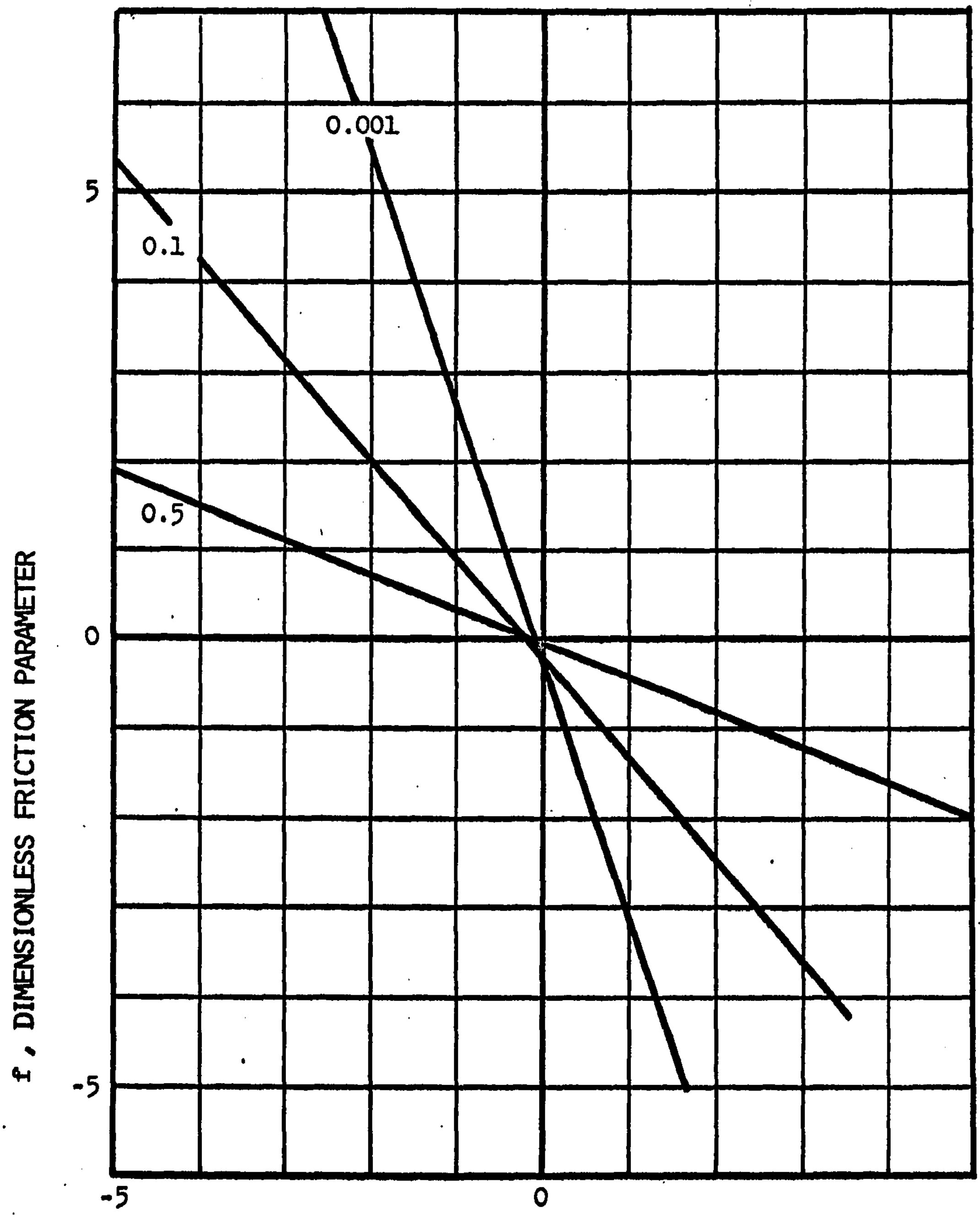

FIGURE (43) $f = f(g)$ FOR $S = 0.5$ WITH PARAMETER u_∞
AT STEADY STATE

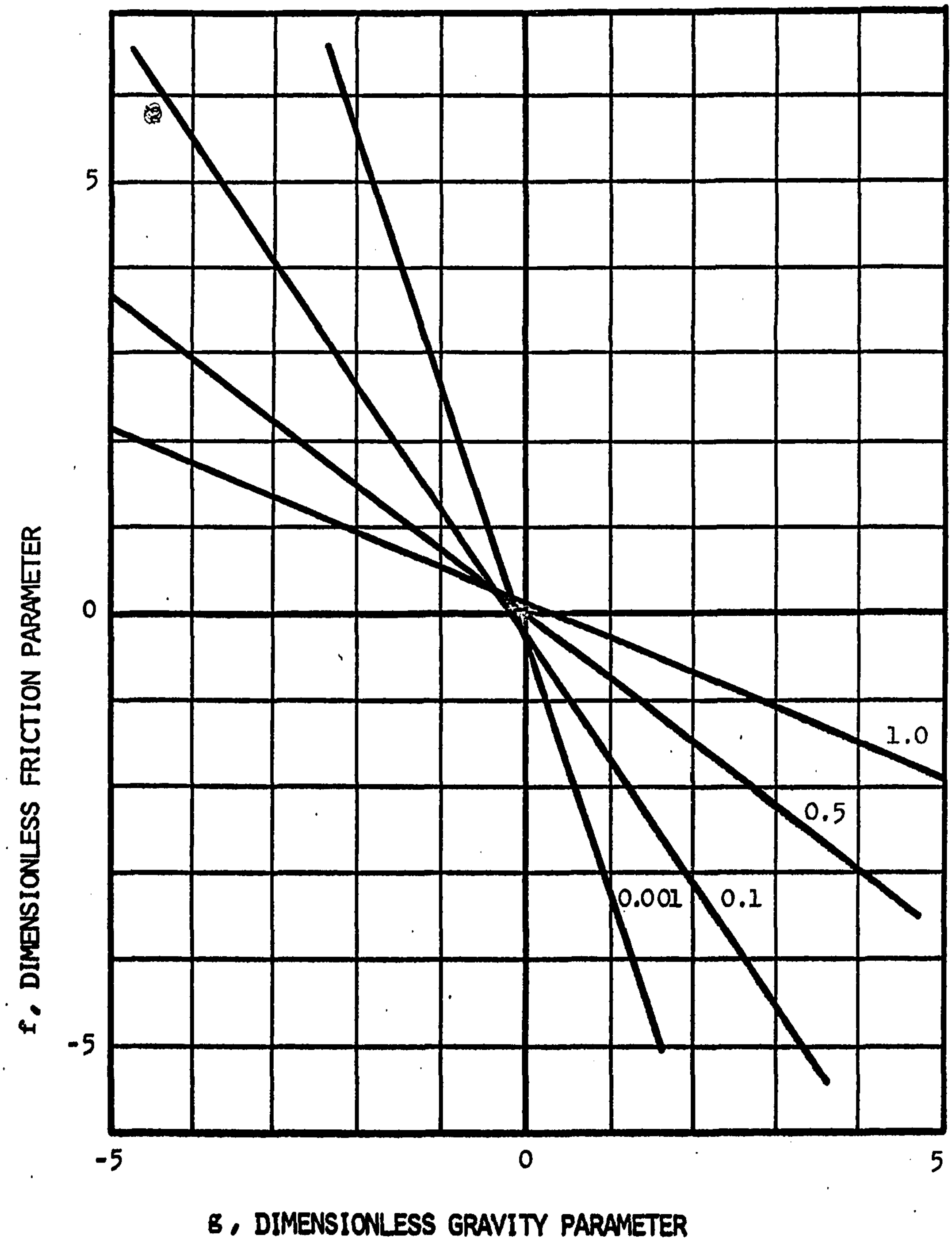

FIGURE (44) $f = f(g)$ FOR $S = 1.0$ WITH PARAMETER u_∞ AT STEADY STATE was accomplished by determining the value of g for the intersection of the line given by f = 0.973 and the u_∞ = constant curves. This was carried out for each value of the subcooling from 0.0 to 10.0 as shown in Figure (24). Also shown on this figure are several instability points taken during various random runs made with Freon-12 and Freon-114 as the heat transfer fluid. In this figure, the stable region for a constant subcooling s is above and to the left of that constant subcooling line while the unstable region is to the right and below the line. The regions of stability and instability were in agreement with experimental runs made in this investigation and can also be shown analytically. The analytical study of this is made in Appendix X. It should be noted from Figure (24) that the higher the subcooling, the less area on the plane of operation which corresponds to the stability region.

Figures (39 - 41) were obtained in the same manner as Figures (25 - 37) except that the frequency range for these solutions was lower than that for Figures (25 - 37). It should also be noted that the non-dimensional subcooling range is less (0.0 to 1.0). The results of these figures are shown on the operating plane in Figure (38). This shows that there are various "levels" of instability which can be represented on the operating plane depending on the frequency. The instability threshold represented in Figure (38) did not compare with any experimental instability points found in this investigation. It was not possible to reach u_∞ values shown in Figure (38) in the natural-circulation loop utilized in this investigation.

A series of runs were made and the experimental instability points were determined for the natural-circulation loop from experimental data taken during constant pressure runs with Freon-114 as the heat transfer fluid. These runs were convenient to make since the hydraulic accumulator was utilized to maintain a constant pressure until the instability point was reached. These experimental instability points are compared to the threshold surface given by Equation (116) by plotting $u_\infty = u_\infty(g)$ with s as a parameter for a constant pressure condition. Since the subcooling s varies during a constant pressure run, the analytical representation of the threshold surface is given at discrete values of s for which a numerical solution was obtained. This comparison was made for two subcritical pressures (310 and 400 psia) in Figures (45) and (46). This comparison was also made for five supercritical pressures (480 to 575 psia) in Figures (47 - 51). Note that the 480 and 495 psia runs are shown on the same Figure (47). This was necessary because of the relatively few data points taken at these pressures and since the theoretical curves are nearly coincident at these pressures. It should be noted from these figures that the agreement between experiment and theory at the higher pressures (575 psia) is not as good as at the lower pressures. This is due to the fact that the representation of the equation of state is not as accurate at the higher pressures. Also note that the agreement obtained for subcritical and supercritical pressures is quite similar. Therefore, this model is quite applicable to critical and supercritical fluids as long as the pressure is low enough that the representation of the equation of state remains in good accord with the model equation of state.

A series of runs were also made and the experimental instability

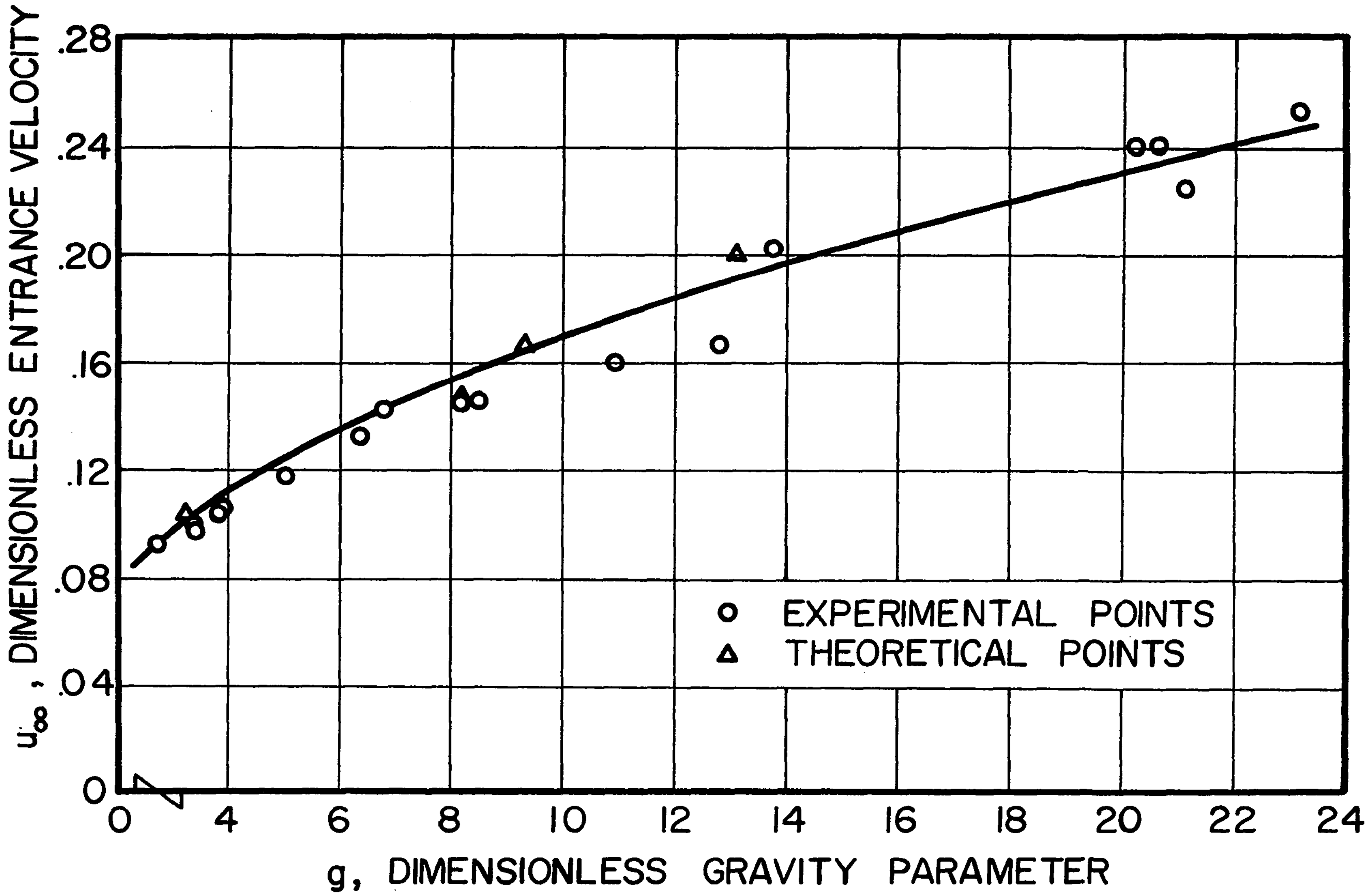

FIGURE (45) COMPARISON OF THEORETICAL AND EXPERIMENTAL RESULTS WITH FREON-114 AT 310 PSIA

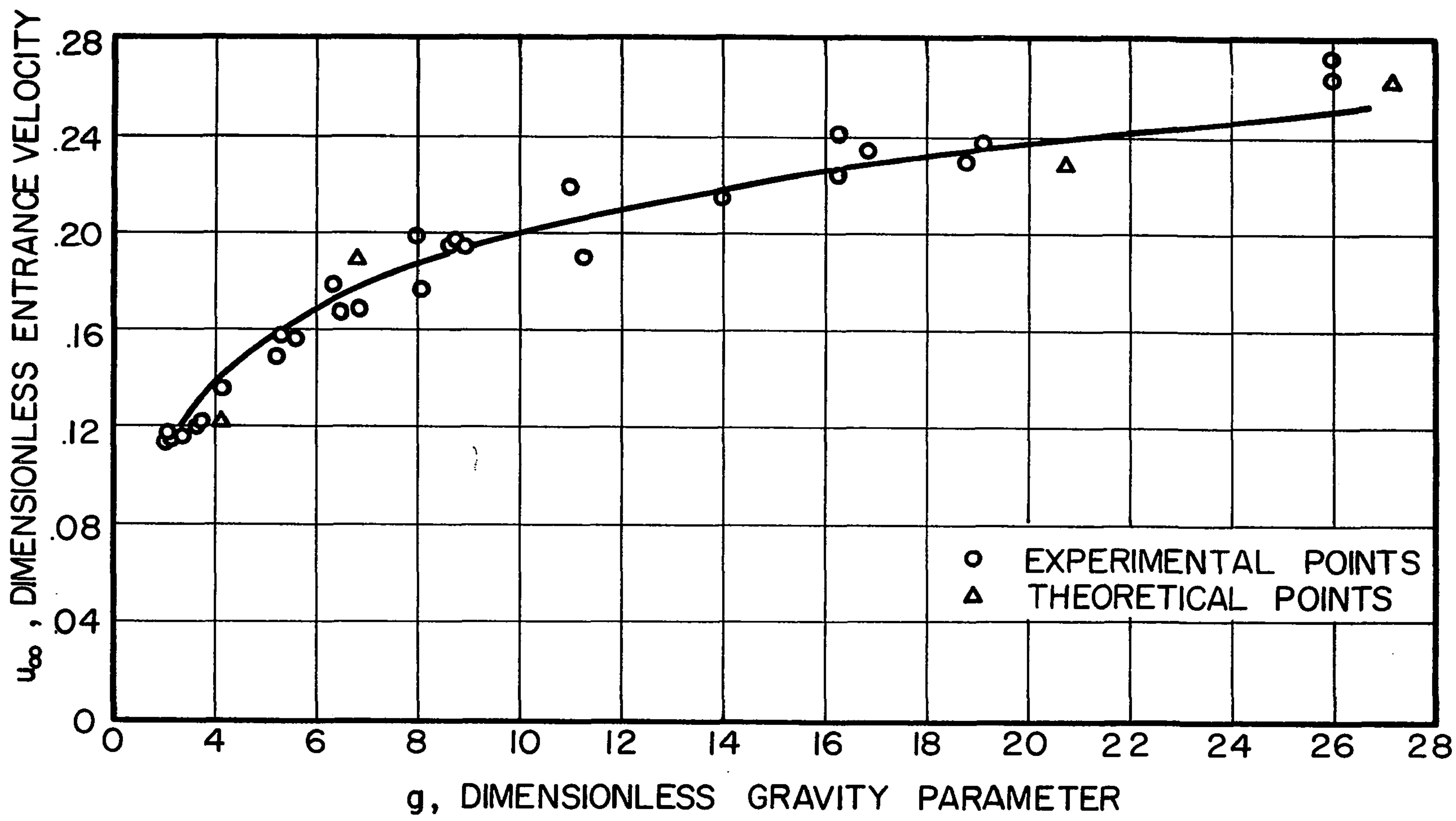

FIGURE (46) COMPARISON OF THEORETICAL AND EXPERIMENTAL RESULTS WITH FREON-114 AT 400 PSIA

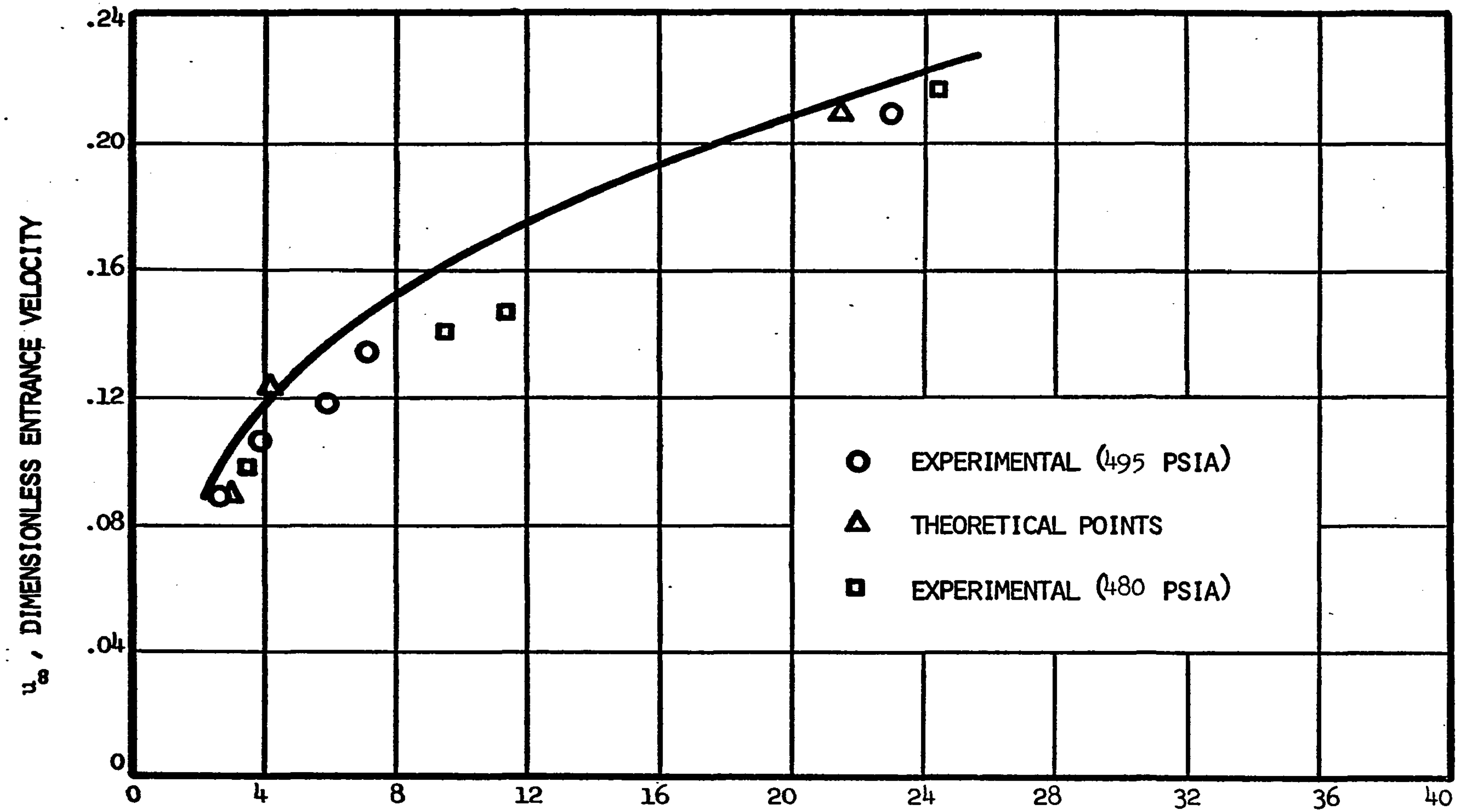

g, DIMENSIONLESS GRAVITY PARAMETER

FIGURE (47) COMPARISON OF THEORETICAL AND EXPERIMENTAL RESULTS WITH FREON-114 AT 480 AND 495 PSIA

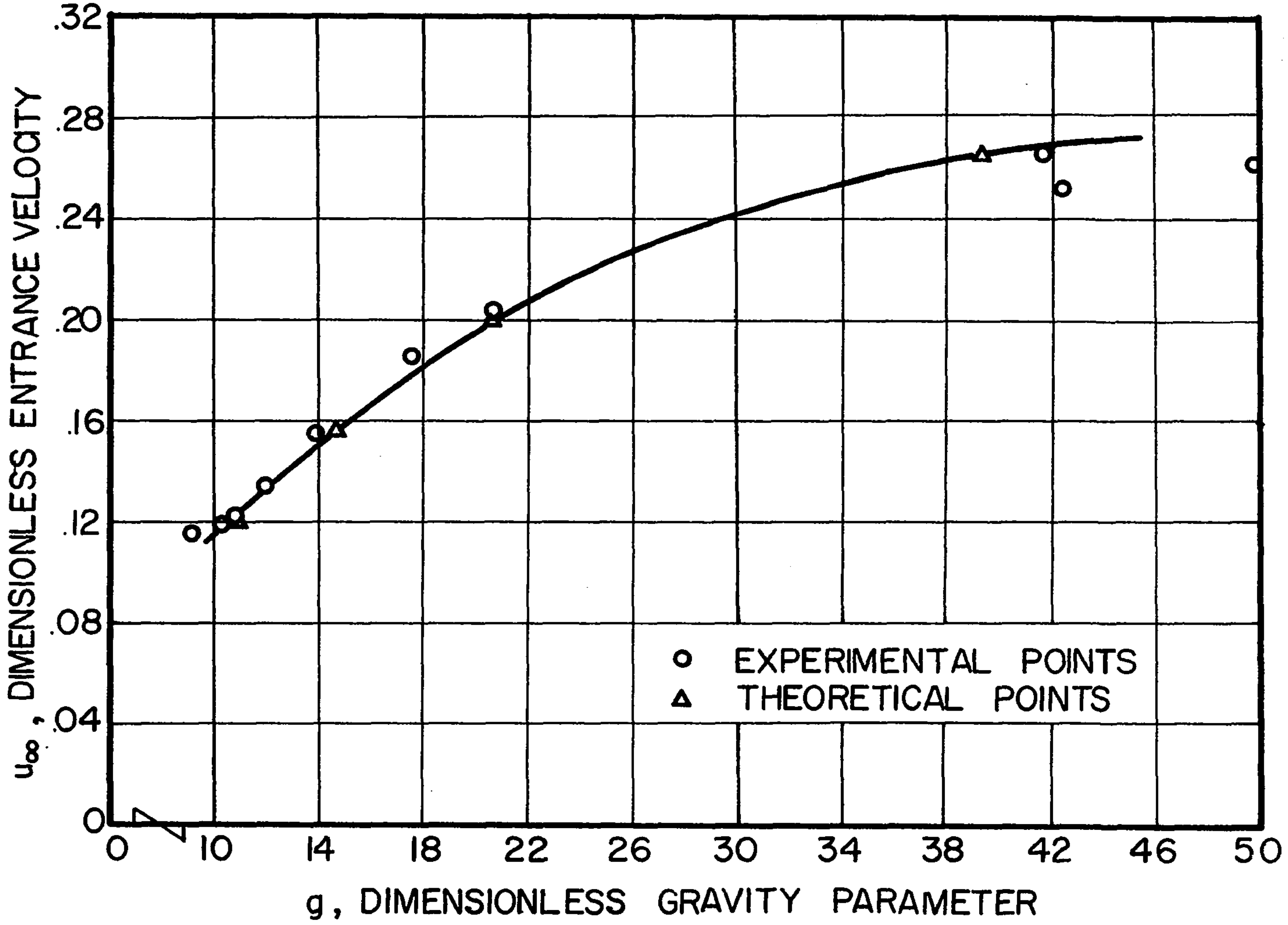

FIGURE (48) COMPARISON OF THEORETICAL AND EXPERIMENTAL RESULTS WITH FREON-114 AT 520 PSIA

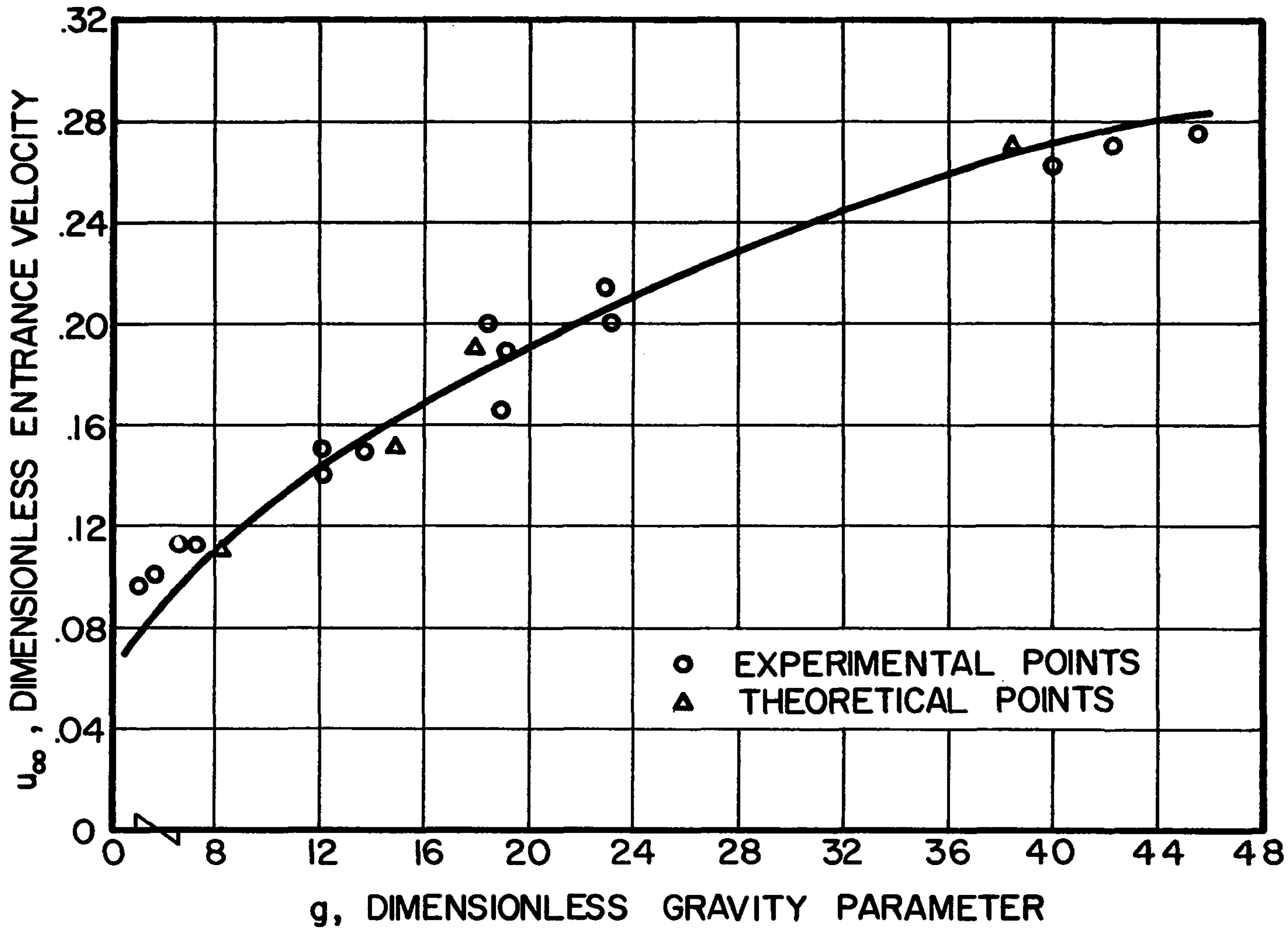

FIGURE (49) COMPARISON OF THEORETICAL AND EXPERIMENTAL RESULTS WITH FREON-114 AT 525 PSIA

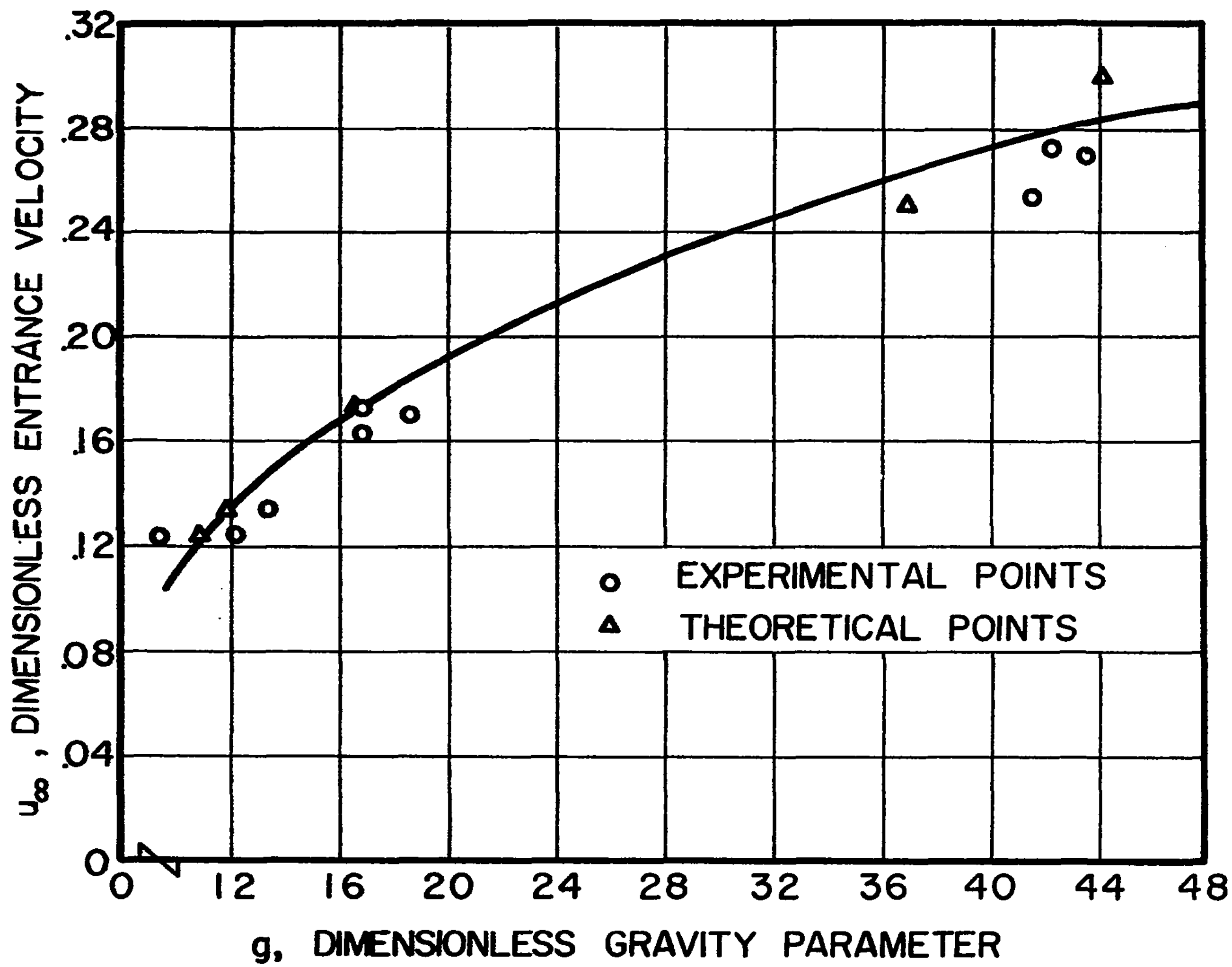

FIGURE (50) COMPARISON OF THEORETICAL AND EXPERIMENTAL RESULTS WITH FREON-114 AT 555 PSIA

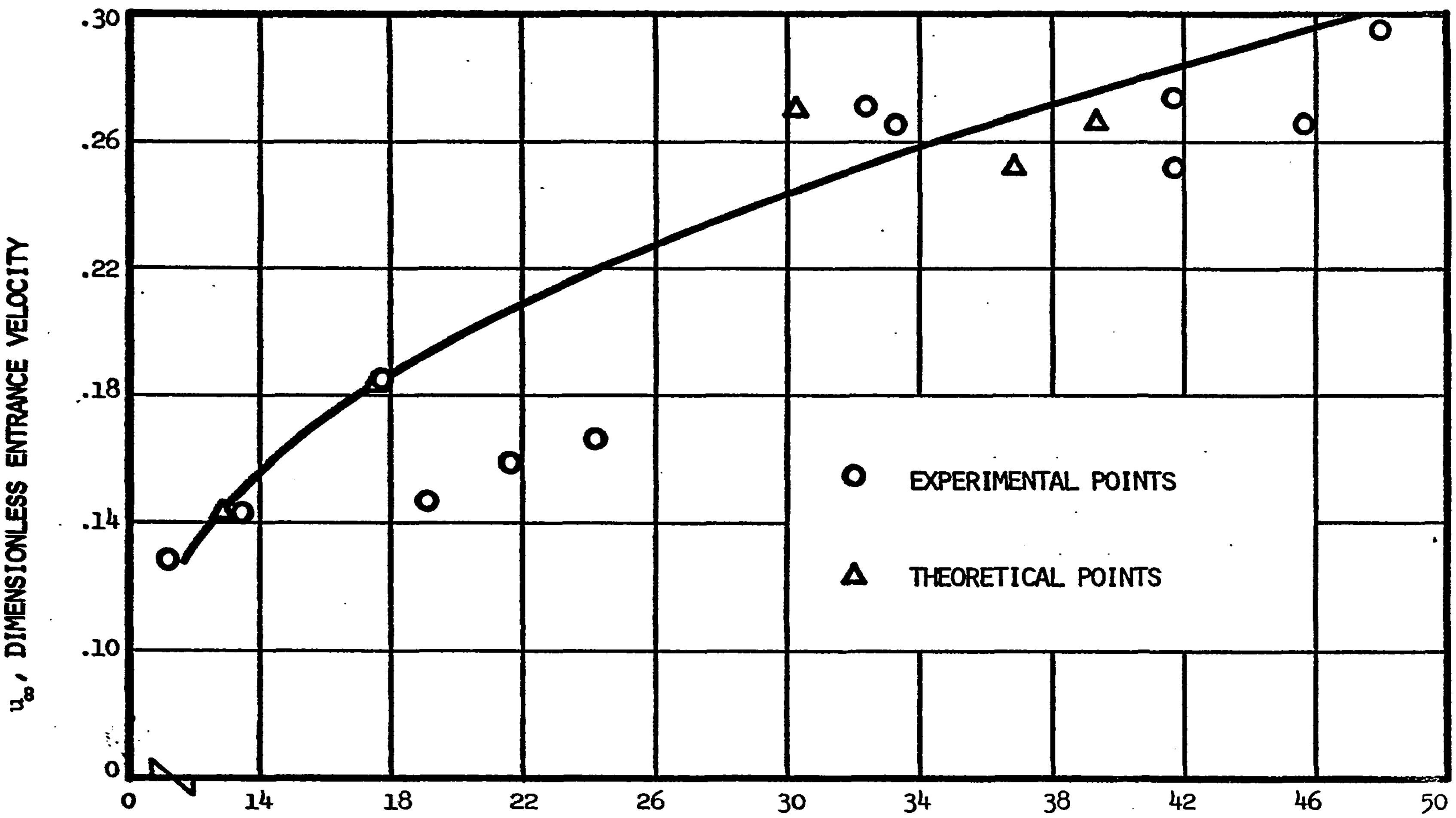

g, DIMENSIONLESS GRAVITY PARAMETER

FIGURE (51) COMPARISON OF THEORETICAL AND EXPERIMENTAL RESULTS WITH FREON-114 AT 575 PSIA

points were determined for the natural-circulation loop from experimental data taken during constant pressure runs with H_2O as the heat transfer fluid. The results obtained utilizing this fluid were similar to those obtained utilizing Freon-114. A comparison of theoretical and experimental results for two subcritical pressures (1740 and 2215 psia) in Figures (52) and (53) shows good agreement.

Unfortunately, experimental data was not obtained for water at supercritical pressures. However, this author can see no reason why this data should not be in agreement with subcritical data just as the Freon-114 data was.

Originally, it was planned to take experimental data for one other fluid (CO_2). However, it was not possible to take this data since the desired subcooling could not be attained in the natural-circulation loop without extensive modification.

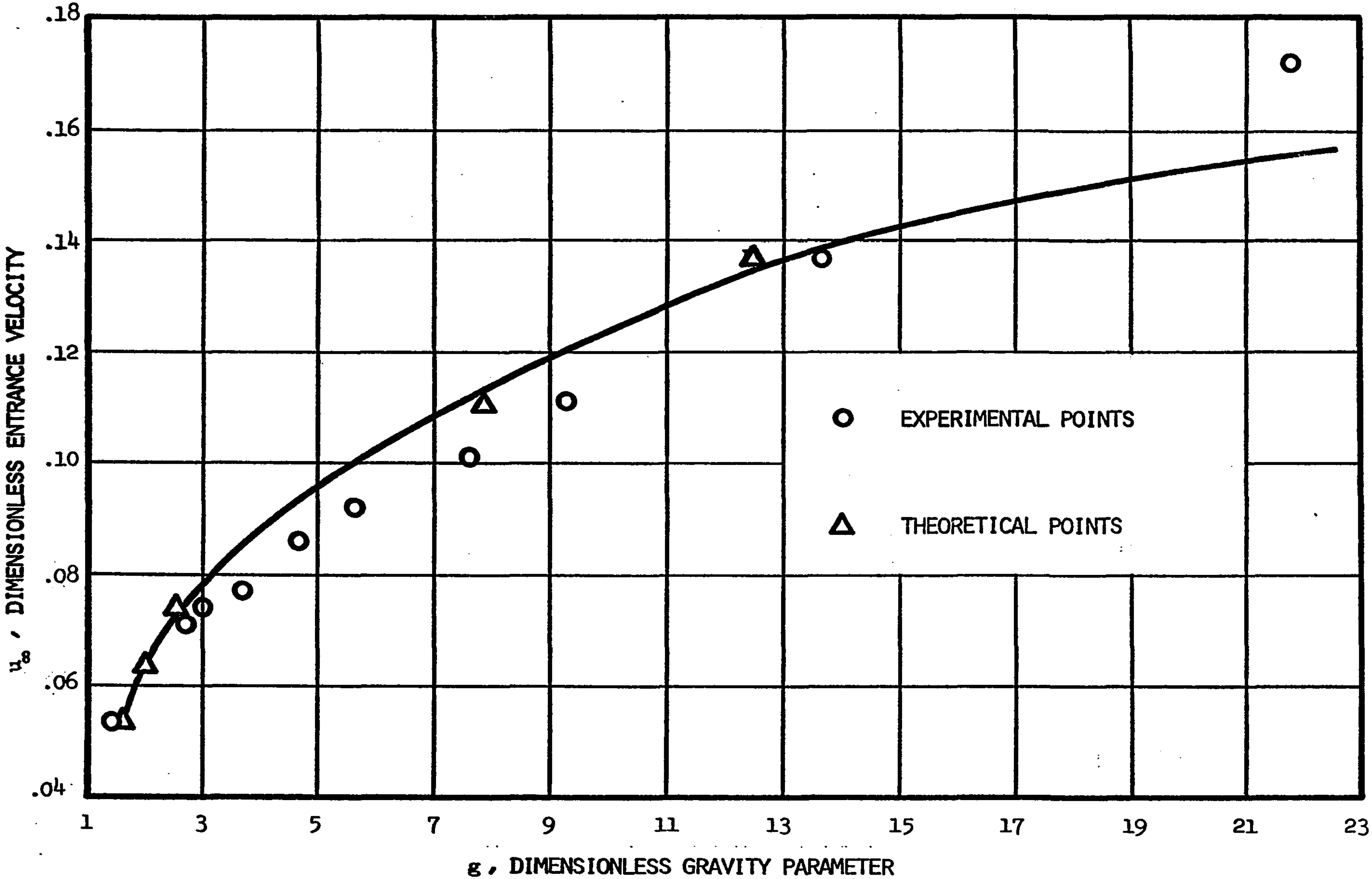

FIGURE (52) COMPARISON OF THEORETICAL AND EXPERIMENTAL RESULTS WITH WATER AT 1740 PSIA

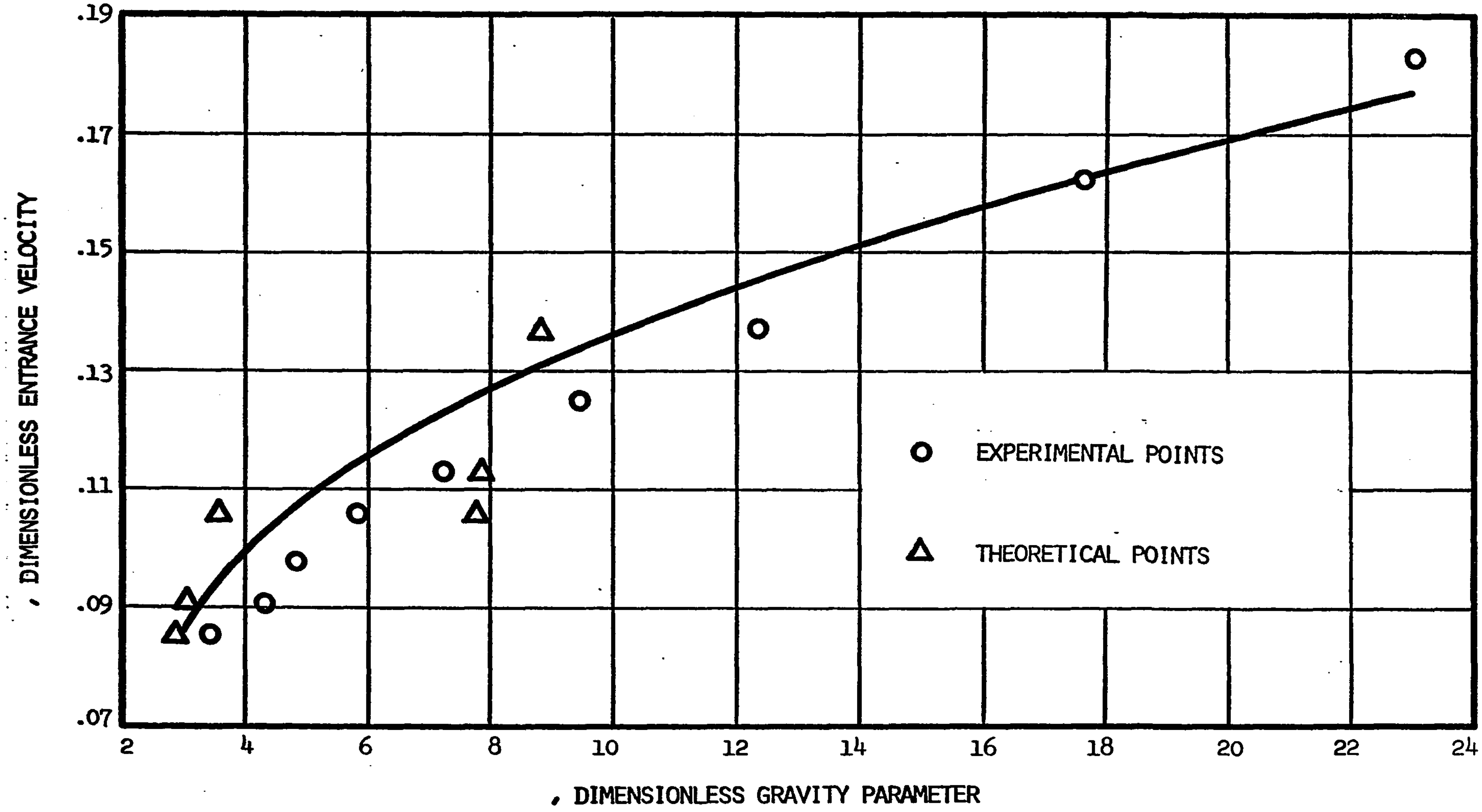

FIGURE (53) COMPARISON OF THEORETICAL AND EXPERIMENTAL RESULTS WITH WATER AT 2215 PSIA

CHAPTER VII

CONCLUSIONS

The "density effect" model was utilized to predict pressure and flow oscillations in a natural-circulation loop at both subcritical and supercritical pressures. Three different fluids were successfully utilized as the heat transfer fluid in the experimental apparatus.

The following conclusions were reached on the basis of this investigation:

(1) The density effect model will accurately predict the instability threshold of a natural-circulation loop.

(2) Heater section wall temperature oscillations are not the triggering mechanism for the pressure and flow oscillations since these oscillations were observed without accompanying fluctuations of heater section wall temperature.

(3) The energy density maximum, $(\rho h)_{max}$, theory of Harden is of great utility in determining experimentally the pressure and flow oscillations in a natural-circulation loop.

(4) The frequencies of oscillation of the natural-circulation loop are related to the natural frequency of the various modes of vibration of the loop.

(5) The density effect model applies to the critical region as

well as to the subcritical thermodynamic region and gives comparable results for the two regions.

BIBLIOGRAPHY

Books

1. ASHRAE Guide and Data Book; Fundamentals and Equipment. New York: 1961.

2. Bird, R. B., W. E. Stewart, and E. N. Lightfoot. Transport Phenomena. New York: John Wiley and Sons, 1960.

3. Cole, E. B. The Theory of Vibrations for Engineers. Third Edition, New York: Macmillan Co. p. 134, 1957.

4. Timoshenko, S. Vibration Problems in Engineering. Third Edition, New York: D. Van Nostrand Co. pp. 337-338, 332, 426, 1955.

5. Tong, L. S. Boiling Heat Transfer and Two-Phase Flow. New York: John Wiley and Sons, 1965.

6. Wylie, C. R., Jr. Advanced Engineering Mathematics. Second Edition, New York: McGraw-Hill Book Co. pp. 212-213, 1960.

Articles

7. Boure, J. "Contribution a l'etude theorique des oscillations dans les canaux chauffants a ebullition," These Docteur-Ingenieur-Centre D'etudes Nucleaires et Universite de Grenoble, France, Juin, 1965.

8. Boure, J. "The Oscillatory Behavior of Heated Channels," Rapport CEA 3049, Grenoble, France, 1966.

9. Bringer, R. P. and J. M. Smith. "Heat Transfer in the Critical Region," AIChE Journal, 3, pp. 49-55, 1957.

10. Cornelius, A. J. "An Investigation of Instabilities Encountered During Heat Transfer to a Supercritical Fluid," Argonne National Laboratory Report ANL-7032, April, 1965.

11. Cornelius, A. J. and J. D. Parker. "Heat Transfer Instabilities Near the Thermodynamic Critical Point," Proceedings of the 1965 Heat Transfer and Fluid Mechanics Institute, Stanford University Press, pp. 317-329, 1965.

12. Garlid, K., N. R. Amundson, and H. S. Isbin. "A Theoretical Study of the Transient Operation and Stability of Two-Phase Natural-Circulation Loops," Argonne National Laboratory Report ANL-6381, June, 1961.

13. Gouse, S. W. and C. D. Andrysiak. "Flow Oscillations in a Closed Loop With Transparent, Parallel, Vertical, Heated Channels," MIT Report 8973-2, June, 1963.

14. Gouse, S. W. and C. D. Andrysiak. "Some Observations on Two-Phase Flow Oscillations," Multi-Phase Flow Symposium, ASME Winter Annual Meeting, Philadelphia, Pennsylvania, November 17-22, 1963.

15. Harden, D. G. "Transient Behavior of a Natural-Circulation Loop Operating Near the Thermodynamic Critical Point," Argonne National Laboratory Report ANL-6710, May, 1963.

16. Hines, W. S. and H. Wolf. "Pressure Oscillations Associated with Heat Transfer to Hydrocarbon Fluids at Supercritical Pressures and Temperatures," ARS Journal, 32, pp. 361-366, March, 1962.

17. Holman, J. P. and J. H. Boggs. "Heat Transfer to Freon-12 Near the Critical State in a Natural-Circulation Loop, " Journal of Heat Transfer, 82, pp. 221-226, August, 1960.

18. Hsu, Yih-Yun and J. M. Smith. "The Effect of Density Variation on Heat Transfer in the Critical Region," Journal of Heat Transfer, 83, pp. 176-182, May, 1961.

19. Jain, K. C. "Self-Sustained Hydrodynamic Oscillations in a Natural-Circulation Two-Phase-Flow Boiling Loop," Argonne National Laboratory Report ANL-7073, August, 1965.

20. Koppel, L. B. and J. M. Smith. "Turbulent Heat Transfer in the Critical Region," Proceedings of the 1961 International Heat Transfer Conference, Part III, pp. 585-590, August, 1961.

21. Maulbetsch, J. S. and P. Griffith. "A Study of System-Induced Instabilities in Forced-Convection Flows With Sub-Cooled Boiling," MIT Report 5382-35, April, 1965.

22. Meyer, J. E. "Numerical Techniques for Boiling Flow Stability Analyses," Journal of Heat Transfer, 87, pp. 311-312, May, 1965.

23. McCarthy, J. R. and H. Wolf. "The Heat Transfer Characteristics of Gaseous Hydrogen and Helium," Rocketdyne Research Report RR-60-12, December, 1960.

24. Quandt, E. R. "Analysis and Measurements of Flow Oscillations," Chemical Engineering Progress, Symposium Series, 57, No. 32, pp. 111-126, 1961.

25. Schmidt, E., E. Eckert, and U. Grigull. "Heat Transfer by Liquids Near the Critical State," AAF Translation No. 527, Wright Field, Dayton, Ohio, February, 1946.

26. Van Putte, D. A. and R. J. Grosh. "Heat Transfer to Water in the Near-Critical Region," Technical Report No. 4, Purdue University, August, 1960.

27. Van Wie, N. H. and R. A. Ebel. "Some Thermodynamic Properties of Freon-114," Oak Ridge National Laboratory Report K-1430, Vol. I and II, September, 1959.

28. Walker, B. J. "An Experimental Study of a Natural-Circulation Loop Operating Near the Thermodynamic Critical Point," Master of Engineering Thesis, University of Oklahoma, June, 1964.

29. Walker, B. J. and D. G. Harden. "Heat-Driven Pressure and Flow Transients in the Supercritical Thermodynamic Region," ASME Paper No. 64-WA/HT-37, 1964.

30. Wallis, G. B. and J. H. Heasley. "Oscillations in Two-Phase Flow Systems," Journal of Heat Transfer, 83, pp. 363-369, 1961.

31. Wissler, E. H., H. S. Isbin, and N. R. Amundson. "Oscillatory Behavior of a Two-Phase Natural-Circulation Loop," AIChE Journal, 2, pp. 157-162, June, 1956.

APPENDIX I

THE GENERAL MOMENTUM EQUATION

This equation is given by (28)

$$\Delta p = \int_{-\ell_o}^{1+\ell_1} \left[\frac{\partial u}{\partial t} + \frac{u}{\theta} + g + fu^2\right] \rho\, dz \qquad \text{(I-1)}$$

and it will be utilized to calculate the pressure drop in each zone.

(1) Upstream Adiabatic Zone. This equation has already been established in (72).

$$\Delta p_{U.A.S.} = \left[\frac{du_o}{dt} + g + fu_o^2\right] \ell_o \qquad \text{(I-2)}$$

(2) Constant Density Heated Zone. For this zone, the set of equations (43) are valid and

$$u = u_o(\bar{t}) \qquad \rho = 1$$
$$\lambda(t) = \int_{t-s}^{t} u_o(x)dx \qquad \theta \to \infty \qquad \text{(I-3)}$$

Applying these relations to the heated section where the density is constant, i.e., from 0 to $\lambda(t)$, substitution of (I-3) into (I-1) gives

$$\Delta p_{U.H.S.} = \int_0^{\lambda} \left[\frac{du_o}{dt} + g + fu_o^2\right] dz$$

Integrating

$$= \left[\frac{du_o}{dt} + g + fu_o^2\right] \int_0^{\lambda} dz$$

and

$$\Delta p_{U.H.S.} = \left[\frac{du_o}{dt} + g + fu_o^2\right] \lambda \qquad \text{(I-4)}$$

(3) Variable Density Heated Zone. For this zone, the set of equations (55) are valid and

$$\begin{aligned} \rho &= \rho(z,t) \qquad \theta = 1 \\ u &= u_o(t) - \lambda(t) + z \end{aligned} \qquad \text{(I-5)}$$

Substituting (I-5) into (I-1) gives

$$\Delta p_{D.H.S.} = \int_{\lambda(t)}^{1} \left[\frac{du_o}{dt} - \frac{d\lambda}{dt} + u_o - \lambda + z + g + f(u_o - \lambda + z)^2\right] \rho\, dz$$

$$= \left\{\left[\frac{du_o}{dt} + u_o + g + fu_o^2\right] - \left[\frac{d\lambda}{dt} + \lambda(1 + 2fu_o) - f\lambda^2\right]\right\}$$

$$\int_{\lambda(t)}^{1} \rho\, dz + \left\{(1 + 2fu_o) - 2f\lambda\right\} \int_{\lambda(t)}^{1} \rho z\, dz + f \int_{\lambda(t)}^{1} \rho z^2 dz$$

The following quantities are defined:

$$\begin{aligned} \int_{\lambda(t)}^{1} \rho\, dz &\equiv \xi(t) \\ \int_{\lambda(t)}^{1} \rho z\, dz &\equiv \eta(t) \\ \int_{\lambda(t)}^{1} \rho z^2 dz &\equiv \zeta(t) \end{aligned} \qquad \text{(I-6)}$$

Utilizing these definitions (I-6)

$$\Delta p_{D.H.S.} = \left[\frac{du_o}{dt} + u_o + g + fu_o^2\right] \xi - \left[\frac{d\lambda}{dt} + \lambda(1 + 2fu_o) - f\lambda^2\right] \xi$$

$$+ \left[1 + 2fu_o\right] \eta - \left[2f\lambda\right] \eta + \left[f\right] \zeta \qquad \text{(I-7)}$$

(4) Downstream Adiabatic Zone. For this zone, the set of equations (60) are valid and

$$u = u_o - \lambda + 1 \qquad \rho = \rho(z,t)$$
$$\theta \to \infty \tag{I-8}$$

Substituting (I-8) into (I-1) gives

$$\Delta p_{D.A.S.} = \int_{1}^{1+\ell_1} \left[\frac{du_o}{dt} - \frac{d\lambda}{dt} + g + f(u_o - \lambda + 1)^2\right] \rho\, dz$$

By defining

$$\int_{1}^{1+\ell_1} \rho\, dz \equiv \xi_1(t) \tag{I-9}$$

the following expression is obtained

$$\Delta p_{D.A.S.} = \left[\frac{du_o}{dt} + g + f(u_o + 1)^2\right] \xi_1 - \left[\frac{d\lambda}{dt} + 2f(u_o + 1)\,\lambda - f\lambda^2\right] \xi_1 \tag{I-10}$$

Now by utilizing a steady state and a transient component of the velocity $u_o(t)$

$$u_o(t) = u_\infty + v(t) \tag{67}$$

as was given in (67), the total pressure drop throughout the four sections is obtained by adding (I-2), (I-4), (I-7), and (I-10).

$$\Delta p = \left[\frac{dv}{dt} + g + f(u_\infty + v)^2\right]\ell_o + \left[\frac{dv}{dt} + g + f(u_\infty + v)^2\right] \lambda + \left[\frac{dv}{dt} + u_\infty\right.$$
$$\left. + v + g + f(u_\infty + v)^2\right] \xi - \left[\frac{d\lambda}{dt} + \lambda(1 + 2f\left\{u_\infty + v\right\}) - f\lambda^2\right] \xi +$$
$$\left[1 + 2f(u_\infty + v)\right] \eta - 2f\lambda\eta + f\zeta + \left[\frac{dv}{dt} + g + f(u_\infty + v + 1)^2\right] \xi_1$$
$$- \left[\frac{d\lambda}{dt} + 2f\lambda(u_\infty + v + 1) - f\lambda^2\right] \xi_1 \tag{I-11}$$

At steady state, $v \to 0$ in the above equation and $\lambda \to \lambda_o$, $\xi \to \xi_o$, $\eta \to \eta_o$, $\zeta \to \zeta_o$, and $\xi_1 \to \xi_{10}$. With these substitutions, the following expression results:

$$\Delta p_{ss} = \left[g + fu_\infty^{\,2}\right](\ell_o + \lambda_o) + \left[u_\infty + g + fu_\infty^{\,2}\right]\xi_o + \left[1 + 2fu_\infty\right]\eta_o$$
$$+ f\zeta_o + \left[g + f(u_\infty + 1)^2\right]\xi_{10} - \left[1 + 2fu_\infty\right]\lambda_o\xi_o + f\lambda_o^{\,2}\xi_o$$
$$- 2f\lambda_o\eta_o - 2f(u_\infty + 1)\,\lambda_o\xi_{10} + f\lambda_o^{\,2}\xi_{10} \qquad \text{(I-12)}$$

The pressure drops (I-11) and (I-12) are equated to obtain

$$\left[\frac{dv}{dt} + fv(2u_\infty + v)\right](\ell_o + \lambda + \xi + \xi_1) + \left[g + fu_\infty^{\,2}\right]\lambda + v\xi + \left[u_\infty + g + fu_\infty^{\,2}\right]\xi$$
$$+ 2fv\eta + \left[1 + 2fu_\infty\right]\eta + f\zeta + 2fv\xi_1 + \left[g + f(u_\infty + 1)^2\right]\xi_1 - \frac{d\lambda}{dt}(\xi + \xi_1)$$
$$- 2fv\lambda\xi - (1 + 2fu_\infty)\,\lambda\xi + \left[f\right]\lambda^2\xi - 2f\lambda\eta - 2fv\lambda\xi_1 - 2f(u_\infty + 1)\,\lambda\xi_1 +$$
$$\left[f\right]\lambda^2\xi_1 = \left[g + fu_\infty^{\,2}\right]\lambda_o + \left[u_\infty + g + fu_\infty^{\,2}\right]\xi_o + \left[1 + 2fu_\infty\right]\eta_o + f\zeta_o +$$
$$\left[g + f(u_\infty + 1)^2\right]\xi_{10} - \left[1 + 2fu_\infty\right]\lambda_o\xi_o + \left[f\right]\lambda_o^{\,2}\xi_o - \left[2f\right]\lambda_o\eta_o -$$
$$\left[2f(u_\infty + 1)\right]\lambda_o\xi_{10} + \left[f\right]\lambda_o^{\,2}\xi_{10} \qquad \text{(I-13)}$$

By rearranging (I-13), the following expression is obtained:

$$-\frac{dv}{dt} = fv(2u_\infty + v) + \frac{v\xi}{\ell_o + \lambda + \xi + \xi_1} + 2fv\,\frac{\eta + \xi_1}{\ell_o + \lambda + \xi + \xi_1} +$$
$$(u_\infty + g + fu_\infty^{\,2})\,\frac{\xi - \xi_o}{\ell_o + \lambda + \xi + \xi_1} + (1 + 2fu_\infty)\,\frac{\eta - \eta_o}{\ell_o + \lambda + \xi + \xi_1}$$
$$+ f\,\frac{\zeta - \zeta_o}{\ell_o + \lambda + \xi + \xi_1} + \left[g + f(u_\infty + 1)^2\right]\frac{\xi_1 - \xi_{10}}{\ell_o + \lambda + \xi + \xi_1} - \frac{d\lambda}{dt}\,\frac{\xi + \xi_1}{\ell_o + \lambda + \xi + \xi_1}$$
$$- 2fv\,\frac{\lambda(\xi + \xi_1)}{\ell_o + \lambda + \xi + \xi_1} + (g + fu_\infty^{\,2})\,\frac{\lambda - \lambda_o}{\ell_o + \lambda + \xi + \xi_1} - (1 + 2fu_\infty)$$

$$\frac{\lambda\xi - \lambda_o\xi_o}{\ell_o + \lambda + \xi + \xi_1} + f\,\frac{\lambda^2\xi - \lambda_o^{2}\xi_o}{\ell_o + \lambda + \xi + \xi_1} - 2f\,\frac{\lambda\eta - \lambda_o\eta_o}{\ell_o + \lambda + \xi + \xi_1} - 2f(u_\infty + 1)$$

$$\frac{\lambda\xi_1 - \lambda_o\xi_{10}}{\ell_o + \lambda + \xi + \xi_1} + f\,\frac{\lambda^2\xi_1 - \lambda_o^{2}\xi_{10}}{\ell_o + \lambda + \xi + \xi_1} \tag{I-14}$$

APPENDIX II

STEADY STATE REGIME

(1) Expression For λ_o. From the set of equations (43)

$$\lambda(t) = \int_{t-s}^{t} u_o(x)\,dx \tag{II-1}$$

At steady state, $u_o = u_\infty$; therefore, (II-1) gives

$$\lambda_o(t) = \int_{t-s}^{t} u_\infty\,dx$$

and

$$\lambda_o = u_\infty s \tag{II-2}$$

This imposes an important condition on u_∞ since (43) requires

$$\lambda < 1$$

therefore, (II-2) imposes the condition

$$u_\infty s < 1 \tag{II-3}$$

since it is necessary that $\lambda_o < 1$. If this is not the case, the density will be constant throughout the heated section and an oscillatory solution is impossible as shown in Appendix V.

(2) Expression For ξ_o. From the definition (I-6)

$$\xi(t) = \int_{\lambda(t)}^{1} \rho\,dz \tag{II-4}$$

For the region between $\lambda(t)$ and 1, the set of equations (55) are valid and

$$\rho = e^{-(t - \tau)} \tag{II-5}$$

together with

$$z(t,\tau) = \lambda(\tau)e^{t-\tau} + e^{t} \int_{\tau}^{t} e^{-x} \left[u_o(x) - \lambda(x)\right] dx \tag{II-5}$$

For the steady state regime,

$$z(t,\tau) = \lambda_o e^{t-\tau} + e^{t} \int_{\tau}^{t} e^{-x} \left[u_\infty - \lambda_o\right] dx$$

$$= \lambda_o e^{t-\tau} + (u_\infty - \lambda_o)e^{t} \left[-e^{-x}\right] \Big|_{\tau}^{t}$$

and

$$z(t,\tau) = u_\infty e^{t-\tau} - u_\infty + \lambda_o$$

Substituting from (II-2)

$$z(t,\tau) = u_\infty(e^{t-\tau} + s - 1) \tag{II-6}$$

Taking into account the expression for ρ from (II-5),

$$\frac{1}{\rho} = 1 - s + \frac{z}{u_\infty} \tag{II-7}$$

From (II-4), the following expression is deduced,

$$\xi_o = \int_{\lambda_o}^{1} \rho \, dz \tag{II-8}$$

therefore, from (II-2), (II-7), and (II-8) it is found that

$$\xi_o = \int_{u_\infty s}^{1} \frac{dz}{1 - s + \frac{z}{u_\infty}}$$

$$= u_\infty \ell n(1 - s + \frac{z}{u_\infty}) \Big|_{u_\infty s}^{1}$$

and

$$\xi_o = u_\infty \ell n(1 - s + \frac{1}{u_\infty}) \tag{II-9}$$

This expression can be simplified by letting

$$m \equiv 1 - s + \frac{1}{u_\infty}$$
$$k \equiv \ln m \tag{II-10}$$

According to (II-3),

$$s < \frac{1}{u_\infty}$$

therefore, (II-10) shows

$$m > 1$$
$$k > 0 \tag{II-11}$$

Finally, with the definitions (II-10), Equation (II-9) gives

$$\xi_o = u_\infty k \tag{II-12}$$

(3) Expression For η_o. From the definition of η (I-6),

$$\eta_o = \int_{\lambda_o}^{1} \rho z dz$$

therefore,

$$\eta_o = \int_{\lambda_o}^{1} \frac{zdz}{1 - s + \frac{z}{u_\infty}}$$

Integrating

$$\eta_o = u_\infty^2 \left[1 - s + \frac{x}{u_\infty} - (1 - s) \ln(1 - s + \frac{x}{u_\infty})\right] \Bigg|_{u_\infty s}^{1}$$

$$= u_\infty \left[1 - \lambda_o - (1 - s) \left\{u_\infty \ln(1 - s + \frac{1}{u_\infty})\right\}\right]$$

and

$$\eta_o = u_\infty \left[1 - \lambda_o - (1 - s) \xi_o\right] \tag{II-13}$$

Solving for the expression given in Equation (91),

$$\eta_o - \lambda_o \xi_o = u_\infty (1 - \lambda_o - \xi_o) \tag{II-14}$$

since $\lambda_o = u_\infty s$.

(4) Expression For ζ_o. From the definition of ζ (I-6),

$$\zeta_o = \int_{\lambda_o}^{1} \rho z^2 dz$$

therefore,

$$\zeta_o = \int_{\lambda_o}^{1} \frac{z^2 dz}{1 - s + \frac{z}{u_\infty}}$$

$$= \int_{\lambda_o}^{1} u_\infty z dz + u_\infty (s - 1) \int_{\lambda_o}^{1} \frac{z dz}{1 - s + \frac{z}{u_\infty}}$$

and

$$\zeta_o = \frac{u_\infty}{2} z^2 \Bigg|_{\lambda_o}^{1} - u_\infty (1 - s) \int_{\lambda_o}^{1} \frac{z dz}{1 - s + \frac{z}{u_\infty}}$$

where the second integral is equal to η_o as seen in section (3); therefore,

$$\zeta_o = u_\infty \left\{ \left(\frac{1 - \lambda_o^2}{2}\right) - (1 - s)\, \eta_o \right\} \tag{II-15}$$

Solving for the expression given in Equation (92),

$$\zeta_o - 2\lambda_o \eta_o + \lambda_o^2 \xi_o = \zeta_o - \lambda_o \eta_o - \lambda_o (\eta_o - \lambda_o \xi_o)$$

Expanding the right side by substitution for ζ_o from (II-15) gives

$$= u_\infty \left(\frac{1 - \lambda_o^2}{2}\right) - u_\infty \eta_o - \lambda_o (\eta_o - \lambda_o \xi_o)$$

Substituting from (II-14)

$$= u_\infty \left[\left(\frac{1 - \lambda_o^2}{2}\right) - \eta_o \right] - \lambda_o u_\infty (1 - \lambda_o - \xi_o)$$

$$= u_\infty \left[\frac{1}{2} (1 - \lambda_o^2 - 2\lambda_o + 2\lambda_o^2) - (\eta_o - \lambda_o \xi_o) \right]$$

Again by substituting from (II-14),

$$\zeta_o - 2\lambda_o\eta_o + \lambda_o^2\xi_o = u_\infty\left[\frac{(1-\lambda_o)^2}{2} - u_\infty(1-\lambda_o-\xi_o)\right] \quad \text{(II-16)}$$

(5) Expression For ξ_{10}. From the definition of ξ_1 (I-9),

$$\xi_{10} = \int_1^{1+\ell_1} \rho\, dz$$

The density for this region can be found by substituting $z = 1$ into (II-7) to give

$$\xi_{10} = \int_1^{1+\ell_1} \frac{dz}{1 - s + \frac{1}{u_\infty}}$$

and

$$\xi_{10} = \frac{\ell_1}{1 - s + \frac{1}{u_\infty}} \quad \text{(II-17)}$$

From (II-10) it can be seen that

$$\xi_{10} = \frac{\ell_1}{m} \quad \text{(II-18)}$$

(6) Steady State Criterion Calculations. The expression for Δp is given by Equation (93):

$$\Delta p = g(\ell_o + \lambda_o + \xi_o + \xi_{10}) + u_\infty(1-\lambda_o) + f\left[\frac{u_\infty}{2}(1-\lambda_o)^2 + u_\infty^2(1+\ell_o) + (u_\infty + 1 - \lambda_o)^2\xi_{10}\right] \quad \text{(II-19)}$$

Multiplying (II-10) by u_∞,

$$u_\infty + 1 - \lambda_o = mu_\infty \quad \text{(II-20)}$$

Utilizing (II-18) and (II-20) in (II-19), the following expression is obtained:

$$\Delta p = g(\ell_o + \lambda_o + \xi_o + \xi_{10}) + u_\infty(1 - \lambda_o) + fu_\infty^2(\ell_o + 1)$$

$$+ f\frac{u_\infty}{2}(1 - \lambda_o)^2 + f\ell_1 m u_\infty^2 \qquad \text{(II-21)}$$

Differentiating

$$\frac{\partial(\Delta p)}{\partial u_\infty} = g\left[\frac{\partial\lambda_o}{\partial u_\infty} + \frac{\partial\xi_o}{\partial u_\infty} + \frac{\partial\xi_{10}}{\partial u_\infty}\right] + u_\infty\left(-\frac{\partial\lambda_o}{\partial u_\infty}\right) + (1 - \lambda_o)$$

$$+ (\ell_o + 1)\, 2u_\infty f - fu_\infty(1 - \lambda_o)\frac{\partial\lambda_o}{\partial u_\infty} + (1 - \lambda_o^2)\frac{f}{2}$$

$$+ 2f\ell_1 m u_\infty + u_\infty^2 f\ell_1 \frac{\partial m}{\partial u_\infty} \qquad \text{(II-22)}$$

The first derivatives appearing in (II-22) are calculated as follows: from (II-2)

$$\lambda_o = u_\infty s$$

$$\frac{\partial\lambda_o}{\partial u_\infty} = s \qquad \text{(II-23)}$$

from (II-10)

$$m = 1 - s + \frac{1}{u_\infty}$$

$$\frac{\partial m}{\partial u_\infty} = -\frac{1}{u_\infty^2} \qquad \text{(II-24)}$$

from (II-10) and (II-12)

$$\xi_o = u_\infty k = u_\infty \ell n\, m$$

$$\frac{\partial\xi_o}{\partial u_\infty} = (u_\infty)\left(\frac{1}{m}\right)\frac{\partial m}{\partial u_\infty} + \ell n\, m$$

and from (II-24)

$$\frac{\partial\xi_o}{\partial u_\infty} = k - \frac{1}{m u_\infty} \qquad \text{(II-25)}$$

From (II-18)

$$\frac{\partial \xi_{10}}{\partial u_\infty} = \ell_1 \frac{\partial(\frac{1}{m})}{\partial u_\infty} = \ell_1 \frac{\partial}{\partial u_\infty} \left\{\frac{1}{1 - s + \frac{1}{u_\infty}}\right\}$$

$$= \frac{-\ell_1(-\frac{1}{u_\infty^2})}{(1 - s + \frac{1}{u_\infty})^2}$$

and

$$\frac{\partial \xi_{10}}{\partial u_\infty} = \frac{\ell_1}{(mu_\infty)^2} \qquad \text{(II-26)}$$

Substitution of the derivatives (II-23) through (II-26) into (II-22) gives, after simplification,

$$\frac{\partial(\Delta p)}{\partial u_\infty} = g\left[s + k - \frac{1}{mu_\infty} + \frac{\ell_1}{(mu_\infty)^2}\right] + (1 - 2\lambda_o) + 2fu_\infty$$

$$\left[\ell_o + 1 + \ell_1(1 - s)\right] + \frac{f}{2}(1 - \lambda_o)(1 - 3\lambda_o) + f\ell_1 \qquad \text{(II-27)}$$

APPENDIX III

THE GENERAL EQUATION IN C

The equation in c is the form taken by Equation (88),

$$
\begin{aligned}
&(\ell_o + \lambda + \xi + \xi_1)\frac{dv}{dt} + f(\ell_o + \lambda + \xi + \xi_1)(2u_\infty + v)v + \left(v - \frac{d\lambda}{dt}\right)\xi \\
&- \frac{d\lambda}{dt}\xi_1 + 2fv\left[\eta - \lambda\xi + \xi_1(1 - \lambda)\right] + u_\infty(\xi - \xi_o) + (g + fu_\infty{}^2) \\
&(\xi + \lambda - \xi_o - \lambda_o) + (1 + 2fu_\infty)\left[\eta - \lambda\xi - (\eta_o - \lambda_o\xi_o)\right] + f \\
&\left[(\zeta - 2\lambda\eta + \lambda^2\xi) - (\zeta_o - 2\lambda_o\eta_o + \lambda_o{}^2\xi_o)\right] + \left[g + f(u_\infty + 1)^2\right](\xi_1 - \xi_{10}) \\
&- 2f(u_\infty + 1)(\lambda\xi_1 - \lambda_o\xi_{10}) + f(\lambda^2\xi_1 - \lambda_o{}^2\xi_{10}) = 0 \qquad (88)
\end{aligned}
$$

when the transient component of the velocity is taken as $v = v_o e^{ct}$ deduced from

$$u_o = u_\infty + v_o e^{ct} \qquad (71)$$

by neglecting second order terms.

It will be assumed that $c \neq 0$, $c \neq 1$, $c \neq 2$ so that a general equation can be developed. Otherwise some terms in the equation would approach zero thereby giving a special case of the general problem.

(1) <u>Expressions For λ and $\frac{d\lambda}{dt}$</u> . From Equation (43)

$$\lambda(t) = \int_{t-s}^{t} u_o(x)dx$$

Substituting for $u_o(x)$ from Equation (71)

$$\lambda(t) = \int_{t-s}^{t} \left[u_\infty + v_o e^{cx}\right] dx$$

$$= u_\infty x \Big|_{t-s}^{t} + \frac{v_o}{c} e^{cx} \Big|_{t-s}^{t}$$

and

$$\lambda(t) = \lambda_o + \frac{v_o e^{ct}}{c} \left\{1 - e^{-cs}\right\}$$

Adopting the notation

$$E_s \equiv e^{-cs} \qquad \text{(III-1)}$$

the following expression is obtained

$$\lambda(t) = \lambda_o + \frac{v_o e^{ct}}{c} (1 - E_s) \quad . \qquad \text{(III-2)}$$

Differentiating (III-2)

$$\frac{d\lambda}{dt} = v_o e^{ct} (1 - E_s) \qquad \text{(III-3)}$$

(2) <u>Expression For ξ</u>. By definition

$$\xi \equiv \int_{\lambda(t)}^{1} \rho \, dz \qquad \text{(I-6)}$$

ρ is a function of z and t and (55) gives

$$\rho = e^{-(t-\tau)}$$

$$z(t,\tau) = \lambda(\tau) e^{t-\tau} + e^{t} \int_{\tau}^{t} e^{-x} \left[u_o(x) - \lambda(x)\right] dx \qquad \text{(55)}$$

Evaluating the integral in Equation (55) by substituting for u_o from Equation (71) and λ from (III-2) gives

$$\int_{\tau}^{t} e^{-x} \left[u_o(x) - \lambda(x)\right] dx = \int_{\tau}^{t} e^{-x} \left[u_\infty + v_o e^{cx} - \lambda_o - \right.$$

$$\frac{v_o e^{cx}}{c} (1 - E_s)\Big] dx$$

and

$$= \int_{\tau}^{t} (u_\infty - \lambda_o)\, e^{-x}\, dx + v_o - \frac{v_o}{c} (1 - E_s) \int_{\tau}^{t} e^{(c-1)x}\, dx$$

finally,

$$= u_\infty (1 - s)(e^{-\tau} - e^{-t}) + \frac{v_o}{c-1} \left\{1 - \frac{(1 - E_s)}{c}\right\}$$

$$\left\{e^{(c-1)t} - e^{(c-1)\tau}\right\}$$

Substituting this into the expression for z (55)

$$z(t,\tau) = \left[\lambda_o + \frac{v_o e^{c\tau}}{c} (1 - E_s)\right] e^{t-\tau} + u_\infty (1 - s)(e^{t-\tau} - 1)$$

$$+ \frac{v_o}{c-1} \left[1 - \frac{(1 - E_s)}{c}\right] \left\{e^{-t(1-c)}\, e^{t} - e^{-\tau(1-c)}\, e^{t}\right\}$$

After algebraic manipulation, the following is obtained

$$z(t,\tau) = u_\infty (e^{t-\tau} + s - 1) + v_o e^{ct} \left[\frac{E_s e^{(1-c)(t-\tau)}}{1-c} + \frac{1}{c} - \frac{E_s}{c(1-c)}\right] \tag{III-4}$$

Now the desired expression $\rho(z,t)$ could be obtained by elimination of τ between the expression for the density

$$\rho = e^{-(t-\tau)} \tag{55}$$

and (III-4).

However, this elimination would not give ρ explicitly because of the different exponents. An approximate expression for $\rho(z,t)$ can be found by considering the following. Since the second member of the right side of (III-4) is an infinitesimal of the first order, the following expression can be written:

$$z(t,\tau) \approx u_\infty(e^{t-\tau} + s - 1)$$

Solving for $e^{t-\tau}$,

$$e^{t-\tau} = 1 - s + \frac{z}{u_\infty} + \text{first order terms}$$

Substituting for $e^{t-\tau}$ in the second member of the right side of (III-4) gives

$$z(t,\tau) = u_\infty(e^{t-\tau} + s - 1) + v_o e^{ct}\left[\frac{E_s}{1-c}\left(1 - s + \frac{z}{u_\infty}\right)^{1-c} + \frac{1}{c} - \frac{E_s}{c(1-c)}\right] + \text{second order terms} \qquad \text{(III-5)}$$

Discounting the second order terms in (III-5), $e^{t-\tau}$ can be eliminated between Equations (55) and (III-5) to obtain

$$\frac{1}{\rho} = \left(\frac{z}{u_\infty} - s + 1\right) - \frac{v_o e^{ct}}{u_\infty}\left[\frac{E_s}{1-c}\left\{1 - s + \frac{z}{u_\infty}\right\}^{1-c} + \frac{1}{c} - \frac{E_s}{c(1-c)}\right]$$

Dividing both sides by $(1 - s + \frac{z}{u_\infty})$ and raising both sides to the -1 power gives

$$\rho\left(1 - s + \frac{z}{u_\infty}\right) = \left\{1 - \frac{v_o e^{ct}}{u_\infty}\left[\frac{E_s}{1-c}\left(1 - s + \frac{z}{u_\infty}\right)^{-c} + \frac{\frac{1}{c} - \frac{E_s}{c(1-c)}}{1 - s + \frac{z}{u_\infty}}\right]\right\}^{-1}$$

Expanding the term in the $\{\ \}$ brackets in a series and neglecting higher order terms,

$$(1 - x)^{-1} = 1 + x + \ldots$$

therefore,

$$\rho\left(1 - s + \frac{z}{u_\infty}\right) = 1 + \frac{v_o e^{ct}}{u_\infty}\left[\frac{E_s}{1-c}\left(1 - s + \frac{z}{u_\infty}\right)^{-c} +\right.$$

$$\frac{\frac{1}{c} - \frac{E_s}{c(1-c)}}{1 - s + \frac{z}{u_\infty}} \Bigg]$$

whereby

$$\rho = \frac{1}{1 - s + \frac{z}{u_\infty}} + \frac{v_o e^{ct}}{u_\infty} \left[\frac{\frac{E_s}{1-c}}{(1 - s + \frac{z}{u_\infty})^{1+c}} + \frac{\frac{1}{c} - \frac{E_s}{c(1-c)}}{(1 - s + \frac{z}{u_\infty})^2} \right] \tag{III-6}$$

Upon knowing $\rho(z,t)$, ξ can be calculated. From (I-6)

$$\xi = \int_{\lambda(t)}^{1} \rho dz = u_\infty \ln(1 - s + \frac{z}{u_\infty}) + v_o e^{ct} \left[\frac{-E_s}{c(1-c)} (1 - s + \frac{z}{u_\infty})^{-c} - \right.$$

$$\left. - \left\{ \frac{1}{c} - \frac{E_s}{c(1-c)} \right\} \left\{ 1 - s + \frac{z}{u_\infty} \right\}^{-1} \right] \Bigg|_{\lambda(t)}^{1}$$

Utilizing the series approximation that

$$\ln(1 + x) \approx x$$

the following expression is obtained after simplification

$$\xi = \xi_o + v_o e^{ct} \left[\frac{-E_s m^{-c}}{c(1-c)} + \frac{E_s m^{-1}}{c(1-c)} + \frac{E_s}{c} - \frac{1}{cm} \right] \tag{III-7}$$

Utilizing the identity

$$\frac{E_s}{c} - \frac{1}{cm} = \frac{-(1 - E_s)}{c} - \frac{1}{c} (m^{-1} - 1)$$

gives the following expression for ξ

$$\xi = u_\infty k + v_o e^{ct} \left[\frac{-E_s}{1-c} \frac{(m^{-c} - m^{-1})}{c} - \frac{(1 - E_s)}{c} - \frac{1}{c} (m^{-1} - 1) \right] \tag{III-8}$$

(3) <u>Expression For η</u>. η is defined as

$$\eta \equiv \int_{\lambda(t)}^{1} \rho z dz \tag{I-6}$$

Utilizing the expression developed for ρ(III-6), the integral becomes

$$\eta = \int_{\lambda(t)}^{1} \frac{zdz}{1 - s + \frac{z}{u_\infty}} + \frac{v_o e^{ct}}{u_\infty} \int_{\lambda(t)}^{1} \left[\frac{\frac{E_s}{1-c}\, zdz}{(1 - s + \frac{z}{u_\infty})^{1+c}} \right.$$

$$+ \int_{\lambda(t)}^{1} \frac{\left[\frac{1}{c} - \frac{E_s}{c(1-c)}\right] zdz}{u_\infty (1 - s + \frac{z}{u_\infty})^2}$$

The first integral on the right side of the preceding equation can be broken into two integrals:

$$\int_{\lambda(t)}^{1} \frac{zdz}{1 - s + \frac{z}{u_\infty}} = u_\infty \int_{\lambda(t)}^{1} dz - u_\infty(1 - s) \int_{\lambda(t)}^{1} \frac{dz}{1 - s + \frac{z}{u_\infty}}$$

$$= u_\infty \left[z - u_\infty(1 - s)\, \ell n(1 - s + \frac{z}{u_\infty}) \right] \Bigg|_{\lambda(t)}^{1}$$

The second integral is evaluated as

$$\int_{\lambda(t)}^{1} \frac{zdz}{(1 - s + \frac{z}{u_\infty})^{1+c}} = u_\infty^2 \left[\frac{(1 - s + \frac{z}{u_\infty})^{1-c}}{1-c} + \frac{1 - s}{c} (1 - s + \frac{z}{u_\infty})^{-c} \right] \Bigg|_{\lambda(t)}^{1}$$

The third integral is evaluated as

$$\int_{\lambda(t)}^{1} \frac{zdz}{(1 - s + \frac{z}{u_\infty})^2} = u_\infty^2 \left[\ell n(1 - s + \frac{z}{u_\infty}) + \frac{1 - s}{1 - s + \frac{z}{u_\infty}} \right] \Bigg|_{\lambda(t)}^{1}$$

Limiting the evaluation of the integrals to the first order terms, simplification and addition of the three integrals above give, according to (I-6):

$$\eta = \eta_o + v_o e^{ct} u_\infty \left[\frac{E_s m^{1-c}}{(1-c)^2} + \frac{E_s m^{-c} (1 - s)}{c(1-c)} - \frac{E_s m^{-1} (1 - s)}{c(1-c)} \right.$$

$$- \frac{E_s k}{c(1-c)} + E_s \left\{ \frac{s}{c} - \frac{1}{(1-c)^2} \right\} + \frac{k}{c} + \frac{1}{c} \left\{ m^{-1}(1 - s) - 1 \right\} \Big] \qquad \text{(III-9)}$$

(III-9) can be written in a slightly different form so that

$$\eta = \eta_o + v_o e^{ct} u_\infty \left[\frac{E_s}{1-c} \left\{ \frac{m^{1-c} - 1}{1-c} + \frac{(1 - s)(m^{-c} - m^{-1})}{c} - \frac{k}{c} \right\} - \frac{s(1 - E_s)}{c} + \frac{1}{c} \left\{ k + (1 - s)(m^{-1} - 1) \right\} \right] \qquad \text{(III-10)}$$

(4) <u>Expression For $\eta - \lambda\xi$</u>. This is the expression that appears in Equation (88) and η does not appear directly. Therefore, this expression will be evaluated utilizing those individual terms found above. From (III-2) and (III-7):

$$\lambda\xi = \left[\lambda_o + \frac{v_o e^{ct}}{c} (1 - E_s) \right] \left[\xi_o + v_o e^{ct} \left\{ \frac{-E_s m^{-c}}{c(1-c)} + \frac{E_s m^{-1}}{c(1-c)} + \frac{E_s}{c} - \frac{1}{cm} \right\} \right]$$

Neglecting second order terms

$$\lambda\xi = \lambda_o \xi_o + v_o e^{ct} u_\infty \left[\frac{k(1 - E_s)}{c} - \frac{sE_s m^{-c}}{c(1-c)} + \frac{sE_s m^{-1}}{c(1-c)} + \frac{sE_s}{c} - \frac{s}{cm} \right]$$

Utilizing the expression for η (III-9),

$$\eta - \lambda\xi = \eta_o - \lambda_o \xi_o + v_o e^{ct} u_\infty \left[\frac{E_s m^{1-c}}{(1-c)^2} + \frac{E_s m^{-c}}{c(1-c)} - \frac{E_s m^{-1}}{c(1-c)} - \frac{E_s k}{1-c} - \frac{E_s}{(1-c)^2} - \frac{(m-1)}{cm} \right] \qquad \text{(III-11)}$$

This expression can be rearranged to give a slightly different form,

$$\eta - \lambda\xi = \eta_o - \lambda_o\xi_o + v_o e^{ct} u_\infty \left[\frac{E_s}{1-c}\left\{\frac{m^{1-c} - 1}{1-c} + \frac{m^{-c} - m^{-1}}{c} - \frac{k}{c}\right\} - \frac{k(1 - E_s)}{c} + \frac{1}{c}(k + m^{-1} - 1)\right] \quad \text{(III-12)}$$

(5) <u>Expression For ζ</u>. ζ is defined by

$$\zeta(t) \equiv \int_{\lambda(t)}^{1} \rho z^2 dz \quad \text{(I-6)}$$

Utilizing the expression for ρ (III-6)

$$\zeta(t) = \int_{\lambda(t)}^{1} \frac{z^2 dz}{1 - s + \frac{z}{u_\infty}} + \frac{v_o e^{ct}}{u_\infty}\left[\frac{E_s}{1-c}\int_{\lambda(t)}^{1} \frac{z^2 dz}{(1 - s + \frac{z}{u_\infty})^{1+c}} + \left\{\frac{1}{c} - \frac{E_s}{c(1-c)}\right\}\int_{\lambda(t)}^{1} \frac{z^2 dz}{(1 - s + \frac{z}{u_\infty})^2}\right. \quad \text{(III-13)}$$

The first integral in (III-13) can be simplified.

$$\int_{\lambda(t)}^{1} \frac{z^2 dz}{1 - s + \frac{z}{u_\infty}} = u_\infty \int_{\lambda(t)}^{1} z dz - u_\infty(1 - s)\int_{\lambda(t)}^{1} \frac{z dz}{1 - s + \frac{z}{u_\infty}}$$

The second integral above has already been determined in the process of deriving the expression for $\eta - \lambda\xi$ (III-11).

Therefore, the first integral in (III-13) gives

$$= u_\infty \left[\frac{z^2}{2} - (1 - s)^2 u_\infty^2 - (1 - s)u_\infty z + u_\infty^2(1 - s)^2 \ell n(1 - s + \frac{z}{u_\infty})\right]\Bigg|_{\lambda(t)}^{1}$$

and the second integral in (III-13) gives

$$\int_{\lambda(t)}^{1} \frac{z^2 dz}{(1 - s + \frac{z}{u_\infty})^{1+c}} = u_\infty^3 \left[\frac{1}{2-c}(1 - s + \frac{z}{u_\infty})^{2-c} - \frac{2(1 - s)}{1-c}\right.$$

$$\left.(1 - s + \frac{z}{u_\infty})^{1-c} - \frac{(1 - s)^2}{c}(1 - s + \frac{z}{u_\infty})^{-c}\right]\Bigg|_{\lambda(t)}^{1}$$

The third integral in (III-13) gives

$$\int_{\lambda(t)}^{1} \frac{z^2 dz}{(1 - s + \frac{z}{u_\infty})^2} = u_\infty^3 \Big[(1 - s + \frac{z}{u_\infty}) - 2(1 - s)\,\ell n(1 - s + \frac{z}{u_\infty})$$

$$\left. - \frac{(1 - s)^2}{1 - s + \frac{z}{u_\infty}}\right]\Bigg|_{\lambda(t)}^{1}$$

Again, by eliminating second order terms in the evaluation of the limits, ζ is found to be

$$\zeta = \zeta_o + v_o e^{ct} u_\infty \Big[\frac{E_s u_\infty}{1-c}\Big\{\frac{m^{2-c} - 1}{2 - c} - \frac{2(1 - s)(m^{1-c} - 1)}{1 - c}$$

$$- \frac{(1 - s)^2 (m^{-c} - m^{-1})}{c}\Big\} + \frac{E_s u_\infty}{1-c}\Big\{\frac{2k(1 - s)}{c}\Big\} - \frac{E_s(1 - u_\infty s)}{c(1 - c)}$$

$$- \frac{(1 - E_s)u_\infty s^2}{c} + \frac{1}{c}\Big\{1 - u_\infty s - 2u_\infty k(1 - s) - (1 - s)^2 u_\infty(m^{-1} - 1)\Big\}\Big]$$

(III-14)

(6) <u>Expression For $\zeta - 2\lambda\eta + \lambda^2\xi$</u>. ζ does not appear directly in Equation (88), but the expression above does. Therefore, $2\lambda\eta$ and $\lambda^2\xi$ are calculated utilizing Equations (II-2), (II-12), (II-13), (III-2), (III-7), and (III-9).

$$- 2\lambda\eta = -2\Big\{\lambda_o + \frac{v_o e^{ct}}{c}(1 - E_s)\Big\}\Big[\eta_o + v_o e^{ct} u_\infty \Big\{\frac{E_s m^{1-c}}{(1-c)^2}$$

$$+ \frac{(1 - s) E_s m^{-c}}{c(1-c)} - \frac{(1 - s) E_s m^{-1}}{c(1-c)} - \frac{E_s k}{c(1-c)} +$$

$$+ E_s\left(\frac{s}{c} - \frac{1}{(1-c)^2}\right) + \frac{1}{c}\left(k - 1 + (1 - s)m^{-1}\right)\Big\} \Big]$$

After simplification

$$-2\lambda\eta = -2\lambda_o\eta_o + v_o e^{ct} u_\infty \Big[\frac{E_s u_\infty}{1-c}\Big\{\frac{-2s(m^{1-c} - 1)}{1-c} - \frac{2s(1 - s)(m^{-c} - m^{-1})}{c} + \frac{2sk}{c}\Big\} + \frac{1 - E_s}{c}\Big\{2u_\infty k(1 - s) - 2 + 2u_\infty s + 2u_\infty s^2\Big\} + \frac{1}{c}\Big\{-2u_\infty sk - 2u_\infty s(1 - s)(m^{-1} - 1)\Big\}\Big] \tag{III-15}$$

The expression for $\lambda^2\xi$ is given by

$$\lambda^2\xi = \Big\{\lambda_o + \frac{v_o e^{ct}}{c}(1 - E_s)\Big\}^2 \Big\{\xi_o + v_o e^{ct}\Big[\frac{-E_s m^{-c}}{c(1-c)} + \frac{E_s m^{-1}}{c(1-c)} + \frac{E_s}{c} - \frac{1}{cm}\Big]\Big\}$$

After simplification

$$\lambda^2\xi = \lambda_o^2\xi_o + v_o e^{ct} u_\infty \Big\{\frac{-E_s u_\infty s^2}{1-c}\Big[\frac{m^{-c} - m^{-1}}{c}\Big] + \frac{1 - E_s}{c}\Big[2ku_\infty s - u_\infty s^2\Big] + \frac{1}{c}\Big[-u_\infty s^2(m^{-1} - 1)\Big]\Big\} \tag{III-16}$$

By adding (III-14), (III-15), and (III-16), it is found that

$$\zeta - 2\lambda\eta + \lambda^2\xi = \zeta_o - 2\lambda_o\eta_o + \lambda_o^2\xi_o + v_o e^{ct} u_\infty \Big\{\frac{E_s u_\infty}{1-c}\Big[\frac{m^{2-c} - 1}{2-c} - \frac{2(m^{1-c} - 1)}{1-c} - \frac{(m^{-c} - m^{-1})}{c} + \frac{2k}{c}\Big] - \frac{E_s}{1-c}\left(\frac{1 - u_\infty s}{c}\right) + \frac{2E_s}{c}(1 - u_\infty s - u_\infty k) - \frac{1}{c}\Big[1 - u_\infty s + u_\infty(m^{-1} - 1)\Big]\Big\} \tag{III-17}$$

By combining two terms, (III-17) becomes

$$\zeta - 2\lambda\eta + \lambda^2\xi = \zeta_o - 2\lambda_o\eta_o + \lambda_o^2\xi_o + v_o e^{ct}\, u_\infty \Big\{\frac{E_s u_\infty}{1-c}\Big[\frac{m^{2-c} - 1}{2-c}$$

$$- \frac{2(m^{1-c} - 1)}{1-c} - \frac{(m^{-c} - m^{-1})}{c}\Big] + \frac{2E_s u_\infty k}{1-c} - \frac{E_s}{1-c}\Big(\frac{1 - u_\infty s}{c}\Big)$$

$$+ \frac{2E_s}{c}(1 - u_\infty s) - \frac{1}{c}\Big[1 - u_\infty s + u_\infty(m^{-1} - 1)\Big]\Big\} \qquad \text{(III-18)}$$

(7) <u>Expression For ξ_1</u>. ξ_1 is defined by

$$\xi_1(t) \equiv \int_1^{1+\ell_1} \rho\, dz \qquad \text{(I-9)}$$

As in section (2) above, it is necessary to express ρ as $\rho(z,t)$. The expression for ρ in this zone can be found by putting $z = 1$ and $t = t_1$ in (III-6), hence

$$\rho = \frac{1}{1 - s + \frac{1}{u_\infty}} + \frac{v_o e^{ct_1}}{u_\infty}\left[\frac{\frac{E_s}{1-c}}{(1 - s + \frac{1}{u_\infty})^{1+c}} + \frac{\frac{1}{c} - \frac{E_s}{c(1-c)}}{(1 - s + \frac{1}{u_\infty})^2}\right]$$

and from the definition of m,

$$\rho = \frac{1}{m} + \frac{v_o e^{ct_1}}{u_\infty}\left[\frac{E_s}{1-c}\, m^{-(1+c)} + \left\{\frac{1}{c} - \frac{E_s}{c(1-c)}\right\} m^{-2}\right] \qquad \text{(III-19)}$$

For this region, the set of equations (60) are valid and

$$z(t,\tau) = 1 + \int_{t_1}^{t} \Big[u_o(x) - \lambda(x) + 1\Big]\, dx \qquad (60)$$

Integrating

$$z(t,t_1) = 1 + \int_{t_1}^{t} \Big[u_\infty + v_o e^{cx}\Big]\, dx - \int_{t_1}^{t} \Big[\lambda_o + \frac{v_o e^{cx}}{c}(1 - E_s)\Big]\, dx + \int_{t_1}^{t} dx$$

Evaluating this integral

$$z(t,t_1) = 1 + (u_\infty - \lambda_o + 1)(t-t_1) + \frac{v_o e^{ct}}{c}\left[1 - \frac{(1 - E_s)}{c}\right]\left[1 - e^{-c(t-t_1)}\right] \qquad \text{(III-20)}$$

By neglecting the higher order terms, (III-20) can be approximated by

$$z(t,t_1) \approx 1 + (u_\infty - \lambda_o + 1)(t-t_1)$$

Utilizing this approximation, t_1 can be evaluated as

$$t_1 = t - \frac{(z - 1)}{mu_\infty} \qquad \text{(III-21)}$$

Substituting (III-21) into (III-19) eliminates t_1 and gives $\rho = \rho(z,t)$.

$$\rho(z,t) = \frac{1}{m} + \frac{v_o e^{ct}}{u_\infty}\left\{\frac{E_s}{1-c}\, m^{-(1+c)} + \left[\frac{1}{c} - \frac{E_s}{c(1-c)}\right] m^{-2}\right\} e^{-\frac{c(z-1)}{mu_\infty}} \qquad \text{(III-22)}$$

This expression for ρ will now allow the calculation of ξ_1. Substituting (III-22) into (I-9),

$$\xi_1 = \int_1^{1+\ell_1} \frac{dz}{m} + \frac{v_o e^{ct}}{u_\infty}\left\{\frac{E_s}{1-c}\, m^{-(1+c)} + \left[\frac{1}{c} - \frac{E_s}{c(1-c)}\right] m^{-2}\right\} \int_1^{1+\ell_1} e^{-\frac{c(z-1)}{mu_\infty}}\, dz$$

Making a variable change by letting

$$x = z - 1$$

the second integral above becomes

$$= \int_0^{\ell_1} e^{-\frac{cx}{mu_\infty}}\, dx$$

$$= \frac{mu_\infty}{c}\left[1 - e^{-\frac{c\ell_1}{mu_\infty}}\right]$$

Introducing the notation

$$y \equiv \frac{\ell_1}{mu_\infty}$$

and (III-23)

$$E_y \equiv e^{-cy}$$

by analogy with the definition of E_s.

With this notation it is found that

$$\xi_1 = \xi_{10} + \frac{v_o e^{ct}}{c}\left\{\frac{E_s}{1-c} m^{-c} + \left[\frac{1}{c} - \frac{E_s}{c(1-c)}\right] m^{-1}\right\}(1 - E_y) \qquad \text{(III-24)}$$

(8) <u>Expression For $\lambda\xi_1$</u>. Utilizing the expression for λ (III-2) and the expression for ξ_1 (III-24),

$$\lambda\xi_1 = \left\{\lambda_o + \frac{v_o e^{ct}}{c}(1 - E_s)\right\}\left\{\xi_{10} + \frac{v_o e^{ct}}{c}\left[\frac{E_s m^{-c}}{1-c} + \frac{m^{-1}}{c} - \frac{E_s m^{-1}}{c(1-c)}\right]\left[1 - E_y\right]\right\}$$

Simplifying

$$\lambda\xi_1 = \lambda_o\xi_{10} + \frac{v_o e^{ct}}{c}\left[\frac{(1 - E_s)\ell_1}{m} + (1 - E_y)\, u_\infty s\left\{\frac{E_s m^{-c}}{1-c} - \frac{E_s m^{-1}}{c(1-c)} + \frac{1}{cm}\right\}\right] \qquad \text{(III-25)}$$

(9) <u>Expression For $\lambda^2\xi_1$</u>. The equations found in section (8) above are utilized to obtain (neglecting second order terms)

$$\lambda^2\xi_1 = \left\{\lambda_o^{\,2} + \frac{2u_\infty}{c}\, s\, v_o e^{ct}(1 - E_s)\right\}\left\{\xi_{10} + \frac{v_o e^{ct}}{c}\right.$$

$$\left[\frac{E_s m^{-c}}{1 - s} + \left(\frac{1}{c} - \frac{E_s}{c(1-c)}\right) m^{-1}\right] (1 - E_y)\Big\}$$

simplifying

$$\lambda^2 \xi_1 = \lambda_o^2 \xi_{10} + \frac{v_o e^{ct}\, u_\infty}{c} \Big[\frac{2s\ell_1(1 - E_s)}{m} + (1 - E_y)\, u_\infty s^2$$

$$\left\{\frac{E_s m^{-c}}{1-c} - \frac{E_s m^{-1}}{c(1-c)} + \frac{1}{cm}\right\} \Big] \qquad \text{(III-26)}$$

(10) Linearization of the Equation in C. The expressions have now been obtained for all terms in the equation in c (88). Note that all these terms contain $v_o e^{ct}$, thereby allowing us to divide through by this factor.

Before continuing on to the equation in c, it is convenient to introduce some new notation. The following is defined:

$$M_o \equiv \ell_o + \lambda_o + \xi_o + \xi_{10}$$

$$M_1 u_\infty \equiv \eta_o - \lambda_o \xi_o + \xi_{10}(1 - \lambda_o)$$

$$M_2 v_o e^{ct} \equiv \xi - \xi_o$$

$$M_3 v_o e^{ct} \equiv \xi + \lambda - (\xi_o + \lambda_o)$$

$$M_4 u_\infty v_o e^{ct} \equiv \eta - \lambda\xi - (\eta_o - \lambda_o \xi_o) \qquad \text{(III-27)}$$

$$M_5 u_\infty v_o e^{ct} \equiv \zeta - 2\lambda\eta + \lambda^2\xi - (\zeta_o - 2\lambda_o \eta_o + \lambda_o^2 \xi_o)$$

$$M_6 v_o e^{ct} \equiv \xi_1 - \xi_{10}$$

$$M_7 u_\infty v_o e^{ct} \equiv \lambda\xi_1 - \lambda_o \xi_{10}$$

$$M_8 u_\infty v_o e^{ct} \equiv \lambda^2 \xi_1 - \lambda_o^2 \xi_{10}$$

Now writing Equation (88) in the form

$$Au_\infty f + Bg + C = 0$$

gives

$$\Big[v(\ell_o + \lambda + \xi + \xi_1)(2u_\infty + v) + 2v\left\{\eta - \lambda\xi + \xi_1(1-\lambda)\right\} + u_\infty^2(\xi + \lambda - \xi_o - \lambda_o)$$

$$+ 2u_\infty\left\{\eta - \lambda\xi - (\eta_o - \lambda_o\xi_o)\right\} + \left\{(\zeta - 2\lambda\eta + \lambda^2\xi) - (\zeta_o - 2\lambda_o\eta_o + \lambda_o^2\xi_o)\right\}$$

$$+ (u_\infty + 1)^2 (\xi_1 - \xi_{10}) - 2(u_\infty + 1)(\lambda\xi_1 - \lambda_o\xi_{10}) + \lambda^2\xi_1 - \lambda_o^2\xi_{10} \Big] f$$

$$+ \Big[(\xi_1 - \xi_{10}) + (\xi + \lambda - \xi_o - \lambda_o)\Big] g + \Big[(\ell_o + \lambda + \xi + \xi_1) \frac{dv}{dt}$$

$$+ (v - \frac{d\lambda}{dt}) \xi - \frac{d\lambda}{dt} \xi_1 + u_\infty(\xi - \xi_o) + \left\{\eta - \lambda\xi - (\eta_o - \lambda_o\xi_o)\right\} \Big] = 0 \tag{III-28}$$

Equation (III-28) can now be linearized by neglecting terms of the second order. In order to do this, the following relationships which were developed earlier are utilized:

$$\begin{aligned} v &= v_o e^{ct} \\ \frac{dv}{dt} &= v_o c e^{ct} \\ \lambda &= \lambda_o + \frac{v_o e^{ct}}{c} (1 - E_s) \\ \frac{d\lambda}{dt} &= v_o e^{ct} (1 - E_s) \end{aligned} \tag{III-29}$$

The following terms are non-linear in (III-28) and must be linearized utilizing the equations (III-29):

(i) <u>Coefficients of f.</u>

$$v(\ell_o + \lambda + \xi + \xi_1)(2u_\infty + v) + 2v \left\{\eta - \lambda\xi + \xi_1(1 - \lambda)\right\}$$

After linearization this expression becomes

$$v_o e^{ct} \Big[(\ell_o + \lambda_o + \xi_o + \xi_{10})\, 2u_\infty + 2\left\{\eta_o - \lambda_o\xi_o + \xi_{10}(1 - \lambda_o)\right\}\Big] \tag{III-30}$$

(ii) Constant Coefficients.

$$\frac{dv}{dt}(\ell_o + \lambda + \xi + \xi_1) + (v - \frac{d\lambda}{dt})\,\xi - \frac{d\lambda}{dt}\,\xi_1$$

After linearization this expression becomes

$$v_o e^{ct}\left[(\ell_o + \lambda_o + \xi_o + \xi_{10})\,c + E_s(\xi_o + \xi_{10}) - \xi_{10}\right] \qquad \text{(III-31)}$$

Substitution of the linearized equations (III-30) and (III-31) into the equation in c (III-28) gives the linearized equation in c in the following form:

$$\Big[v_o e^{ct}(\ell_o + \lambda_o + \xi_o + \xi_{10})\,2u_\infty + 2v_o e^{ct}\left\{\eta_o - \lambda_o\xi_o + \xi_{10}(1 - \lambda_o)\right\} + u_\infty^2$$

$$(\xi + \lambda - \xi_o - \lambda_o) + 2u_\infty\left\{\eta - \lambda\xi - (\eta_o - \lambda_o\xi_o)\right\} + \left\{(\zeta - 2\lambda\eta + \lambda^2\xi) -\right.$$

$$\left.(\zeta_o - 2\lambda_o\eta_o + \lambda_o^2\xi_o)\right\} + (u_\infty + 1)^2\,(\xi_1 - \xi_{10}) - 2(u_\infty + 1)(\lambda\xi_1 - \lambda_o\xi_{10})\Big]\,f +$$

$$\Big[(\xi_1 - \xi_{10}) + (\xi + \lambda - \xi_o - \lambda_o)\Big]\,g + \Big[v_o e^{ct}(\ell_o + \lambda_o + \xi_o + \xi_{10})\,c +$$

$$v_o e^{ct}\left\{E_s(\xi_o + \xi_{10}) - \xi_{10}\right\} + u_\infty(\xi - \xi_o) + \left\{\eta - \lambda\xi - (\eta_o - \lambda_o\xi_o)\right\}\Big] = 0$$

$$\text{(III-32)}$$

Utilizing the notation defined in (III-27), the linearized equation (III-32) becomes, after dividing by $v_o e^{ct}$:

$$\Big[2M_o u_\infty + 2M_1 u_\infty + u_\infty^2 M_3 + 2u_\infty^2 M_4 + u_\infty M_5 + (u_\infty + 1)^2\,M_6 - 2(u_\infty + 1)u_\infty M_7$$

$$+ u_\infty M_8\Big]\,f + \Big[M_6 + M_3\Big]\,g + \Big[M_o c + E_s(\xi_o + \xi_{10}) - \xi_{10} + u_\infty M_2$$

$$+ u_\infty M_4\Big] = 0 \qquad \text{(III-33)}$$

Rearranging (III-33), the following is obtained:

$$\left[M_3 + M_6\right] g + \left[2M_o + 2M_1 + u_\infty M_3 + 2u_\infty M_4 + M_5 + \frac{(u_\infty + 1)^2}{u_\infty} M_6 \right.$$

$$\left. - 2(u_\infty + 1) M_7 + M_8\right] u_\infty f + \left[M_o c + E_s(\xi_o + \xi_{10}) - \xi_{10}\right.$$

$$\left. + u_\infty M_2 + u_\infty M_4 \right] = 0 \qquad \text{(III-34)}$$

(11) Expressions For The M_i. The M_i have been defined in (III-27) in terms of parameters which have been calculated in this Appendix. Therefore, equations from this Appendix and Appendix II will be utilized to calculate the expressions for the M_i.

A)

$$M_o \equiv \ell_o + \lambda_o + \xi_o + \xi_{10}$$

Substituting for λ_o, ξ_o, and ξ_{10},

$$M_o = \ell_o + u_\infty s + u_\infty k + \frac{\ell_1}{m} \qquad \text{(III-35)}$$

B)

$$M_1 \equiv \frac{1}{u_\infty}\left[\eta_o - \lambda_o \xi_o + \xi_{10}(1 - \lambda_o)\right]$$

Utilizing (II-14)

$$M_1 = 1 - u_\infty s - u_\infty k + (1 - u_\infty s) \frac{\ell_1}{m u_\infty} \qquad \text{(III-36)}$$

C)

$$M_2 v_o e^{ct} \equiv \xi - \xi_o$$

Utilizing (III-7)

$$M_2 = \frac{-E_s m^{-c}}{c(1-c)} + \frac{E_s}{c}\left(\frac{m^{-1}}{1-c} + 1\right) - \frac{m^{-1}}{c} \qquad \text{(III-37)}$$

D)

$$M_3 v_o e^{ct} \equiv \xi + \lambda - (\xi_o + \lambda_o)$$

Substituting for ξ and λ from (III-7) and (III-2),

$$M_3 = \frac{-E_s m^{-c}}{c(1-c)} + \frac{E_s m^{-1}}{c(1-c)} - \frac{(m^{-1} - 1)}{c} \tag{III-38}$$

E)

$$M_4 u_\infty v_o e^{ct} \equiv \eta - \lambda\xi - (\eta_o - \lambda_o \xi_o)$$

Utilizing (III-11)

$$M_4 = \frac{E_s m^{-c}}{1-c} \left(\frac{m}{1-c} + \frac{1}{c}\right) - \frac{E_s}{1-c} \left(\frac{m^{-1}}{c} + k + \frac{1}{1-c}\right) + \frac{m^{-1} - 1}{c} \tag{III-39}$$

F)

$$M_5 u_\infty v_o e^{ct} \equiv \zeta - 2\lambda\eta + \lambda^2\xi - (\zeta_o - 2\lambda_o\eta_o + \lambda_o{}^2\xi_o)$$

Utilizing (III-18)

$$M_5 = \frac{E_s m^{-c} u_\infty}{1-c} \left\{\frac{m^2}{2-c} - \frac{2m}{1-c} - \frac{1}{c}\right\} + \frac{E_s u_\infty}{1-c} \left\{\frac{-1}{2-c} + \frac{2}{1-c}\right.$$

$$\left. + \frac{m^{-1}}{c} + 2k\right\} + \frac{E_s(1 - u_\infty s)}{c(1-c)} (1 - 2c) - \frac{1}{c}\left\{1 - u_\infty s + u_\infty(m^{-1} - 1)\right\} \tag{III-40}$$

G)

$$M_6 v_o e^{ct} \equiv \xi_1 - \xi_{10}$$

Utilizing (III-24)

$$M_6 = \frac{-E_s E_y m^{-c}}{c(1-c)} + \frac{E_s E_y m^{-1}}{c^2(1-c)} + \frac{E_s m^{-c}}{c(1-c)} - \frac{E_s m^{-1}}{c^2(1-c)}$$

$$- \frac{E_y m^{-1}}{c^2} + \frac{m^{-1}}{c^2} \tag{III-41}$$

H)

$$M_7 u_\infty v_o e^{ct} \equiv \lambda\xi_1 - \lambda_o \xi_{10}$$

Utilizing (III-25)

$$M_7 = \frac{-E_s E_y m^{-c} s}{c(1-c)} + \frac{E_s E_y m^{-1} s}{c^2(1-c)} + \frac{E_s m^{-c} s}{c(1-c)} - \frac{E_s}{c}\left\{\frac{\ell_1}{m u_\infty}\right.$$

$$\left. + \frac{m^{-1} s}{c(1-c)}\right\} - \frac{E_y m^{-1} s}{c^2} + \frac{m^{-1} s}{c^2} + \frac{\ell_1}{c m u_\infty} \tag{III-42}$$

I) $$M_8 u_\infty v_o e^{ct} \equiv \lambda^2 \xi_1 - \lambda_o^2 \xi_{10}$$

Utilizing (III-26)

$$M_8 = \frac{-E_s E_y m^{-c} u_\infty s^2}{c(1-c)} + \frac{E_s E_y m^{-1} u_\infty s^2}{c^2(1-c)} + \frac{E_s m^{-c} u_\infty s^2}{c(1-c)}$$

$$- \frac{E_s}{c}\left\{\frac{2\ell_1 s}{m} + \frac{m^{-1} u_\infty s^2}{c(1-c)}\right\} - \frac{E_y m^{-1} u_\infty s^2}{c^2} + \frac{m^{-1} u_\infty s^2}{c^2} + \frac{2\ell_1 s}{cm} \tag{III-43}$$

In these M_i groupings c appears in four different ways: through c, E_s, E_y, and m^{-c}.

In calculating the coefficients of the equation in c, the coefficients will be grouped in relation to $E_s E_y m^{-c}$, $E_s E_y$, $E_s m^{-c}$, E_s, and E_y.

(12) Coefficient of g in the Equation in c. Utilizing (III-34) and introducing the notation

$$B_1 \equiv M_3 + M_6 \tag{III-44}$$

Adding (III-38) and (III-41)

$$B_1 = \frac{-E_s E_y m^{-c}}{c(1-c)} + \frac{E_s E_y m^{-1}}{c^2(1-c)} - \frac{E_s m^{-1}}{c^2} - \frac{E_y m^{-1}}{c^2} + \frac{1}{c} + \frac{1-c}{mc^2} \tag{III-45}$$

(13) Coefficient of f in the Equation in c. The coefficient of f is much more complicated than the coefficient of g; therefore, use is made of the grouping mentioned above. Utilizing (III-34) and the notation above, B_2 becomes

$$B_2 \equiv 2(M_o + M_1) + u_\infty M_3 + 2u_\infty M_4 + M_5 + (u_\infty + 1)^2 \frac{M_6}{u_\infty} - 2(u_\infty + 1)\, M_7 + M_8 \tag{III-46}$$

(A) Terms in $E_s E_y m^{-c}$. The term $E_s E_y m^{-c}$ appears in M_6, M_7, and M_8 as

$$\frac{-E_s E_y m^{-c}}{c(1-c)} \left\{ \frac{(u_\infty + 1)^2}{u_\infty} - 2(u_\infty + 1)s + u_\infty s^2 \right\}$$

Simplifying, this term becomes

$$- m^2 u_\infty \frac{E_s E_y m^{-c}}{c(1-c)} \qquad \text{(III-47)}$$

(B) Terms in $E_s E_y$. This term is calculated as in (A),

$$\frac{E_s E_y m^{-1}}{c^2(1-c)} \left[\frac{(u_\infty + 1)^2}{u_\infty} - 2(u_\infty + 1) + u_\infty s^2 \right]$$

This coefficient is identical to that calculated in (A); therefore, this term becomes

$$m u_\infty \frac{E_s E_y}{c^2(1-c)} \qquad \text{(III-48)}$$

(C) Terms in $E_s m^{-c}$. This term is included in M_3 through M_8.

$$\frac{E_s m^{-c}}{1-c} \left[\frac{-u_\infty}{c} + 2u_\infty \left(\frac{m}{1-c} + \frac{1}{c}\right) + u_\infty \left(\frac{m^2}{2-c} - \frac{2m}{1-c} - \frac{1}{c}\right) \right.$$

$$\left. + \left\{ \frac{(u_\infty + 1)^2}{c u_\infty} - 2(u_\infty + 1)\frac{s}{c} + \frac{u_\infty s^2}{c} \right\} \right]$$

The term in the $\{\ \}$ brackets is the same term as above except for the factor $\frac{1}{c}$; therefore, this term becomes

$$2m^2 u_\infty \frac{E_s m^{-c}}{c(1-c)(2-c)} \qquad \text{(III-49)}$$

(D) Terms in E_s. This term is included in M_3 through M_8

$$\frac{E_s}{1-c} \left\{ \frac{m^{-1} u_\infty}{c} - \frac{2u_\infty m^{-1}}{c} - 2u_\infty k - \frac{2u_\infty}{1-c} - \frac{u_\infty}{2-c} + \frac{2u_\infty}{1-c} \right.$$

$$\left. + \frac{u_\infty m^{-1}}{c} + 2u_\infty k \right\} + \frac{E_s(1 - u_\infty s)(1 - 2c)}{c(1-c)} - \frac{E_s m^{-1}}{c^2(1-c)} \left\{ \frac{(u_\infty + 1)^2}{u_\infty} \right.$$

$$- 2(u_\infty + 1)s + u_\infty s^2\Big\} + \frac{E_s}{c}\left[\frac{2(u_\infty + 1)\ell_1}{mu_\infty} - \frac{2\ell_1 s}{m}\right]$$

Again noting the second term in the $\{\ \}$ brackets has already been evaluated, the following expression is obtained:

$$\frac{-E_s}{1-c}\left[\frac{u_\infty}{2-c} + 1 - u_\infty s + \frac{mu_\infty}{c^2}\right] + \frac{E_s(1 - u_\infty s)}{c} + \frac{2\ell_1 E_s}{c} \qquad \text{(III-50)}$$

(E) Terms in E_y. These terms are included in M_6, M_7, and M_8.

$$\frac{-E_y m^{-1}}{c^2}\left\{\frac{(u_\infty + 1)^2}{u_\infty} - 2(u_\infty + 1)s + u_\infty s^2\right\}$$

As before, this term reduces to

$$- mu_\infty \frac{E_y}{c^2} \qquad \text{(III-51)}$$

(F) Terms in $\frac{1}{c}$. These terms are included in M_3 through M_8.

$$\frac{m^{-1} - 1}{c}(-u_\infty + 2u_\infty - u_\infty) - \frac{1}{c}(1 - u_\infty s) + \frac{m^{-1}}{c^2}\left\{\frac{(u_\infty + 1)^2}{u_\infty}\right.$$

$$\left. - 2(u_\infty + 1)s + u_\infty s^2\right\} - \frac{2\ell_1}{cmu_\infty}(u_\infty + 1 - u_\infty s)$$

This term reduces to

$$- \frac{1}{c}(1 - u_\infty s) + \frac{mu_\infty}{c^2} - \frac{2\ell_1}{c} \qquad \text{(III-52)}$$

(G) Terms Independent of c. These terms occur in M_1 and M_2.

$$2M_o + 2M_1 = 2(\ell_o + u_\infty s + u_\infty k + \frac{\ell_1}{m}) + 2\left\{1 - u_\infty s - u_\infty k + (1 - u_\infty s)\frac{\ell_1}{mu_\infty}\right\}$$

This term reduces to

$$2(\ell_o + 1 + \ell_1) \qquad \text{(III-53)}$$

Adding Equations (III-47) through (III-53) gives

$$B_2 = -m^2 u_\infty \frac{E_s E_y m^{-c}}{c(1-c)} + m u_\infty \frac{E_s E_y}{c^2(1-c)} + 2m^2 u_\infty \frac{E_s m^{-c}}{c(1-c)(2-c)}$$

$$-\frac{E_s}{(1-c)}\left\{\frac{u_\infty}{2-c} + 1 - u_\infty s + \frac{m u_\infty}{c^2}\right\} + \frac{E_s(1 - u_\infty s)}{c} +$$

$$\frac{2\ell_1 E_s}{c} - m u_\infty \frac{E_y}{c^2} - \frac{1}{c}(1 - u_\infty s) + \frac{m u_\infty}{c^2} - \frac{2\ell_1}{c} +$$

$$+ 2(\ell_o + 1 + \ell_1) \qquad \text{(III-54)}$$

(14) <u>Constant Coefficient</u>. Utilizing (III-34) and the notation

$$B_3 \equiv M_o c + E_s(\xi_o + \xi_{10}) - \xi_{10} + u_\infty M_2 + u_\infty M_4 \qquad \text{(III-55)}$$

From (II-12) and (II-18)

$$\xi_o + \xi_{10} = u_\infty k + \frac{\ell_1}{m}$$

Utilizing Equations (III-35), (III-37), (III-39), (III-27), and the above equation

$$B_3 = (\ell_o + u_\infty s + u_\infty k + \frac{\ell_1}{m}) + E_s(u_\infty k + \frac{\ell_1}{m}) - \frac{\ell_1}{m}$$

$$+ u_\infty \left\{\frac{-E_s m^{-c}}{c(1-c)} + \frac{E_s}{c}\left(\frac{m^{-1}}{1-c} + 1\right) - \frac{m^{-1}}{c} + \frac{E_s m^{-c}}{1-c}\right.$$

$$\left.\left(\frac{m}{1-c} + \frac{1}{c}\right) - \frac{E_s}{1-c}\left(\frac{m^{-1}}{c} + k + \frac{1}{1-c}\right) + \frac{m^{-1} - 1}{c}\right\}$$

This expression reduces to

$$B_3 = m u_\infty \frac{E_s m^{-c}}{(1-c)^2} + E_s\left[\frac{u_\infty}{c} - \frac{u_\infty kc}{1-c} - \frac{u_\infty}{(1-c)^2} + \frac{\ell_1}{m}\right]$$

$$+ (\ell_o + u_\infty s + u_\infty k + \frac{\ell_1}{m})c - \frac{u_\infty}{c} - \frac{\ell_1}{m} \qquad \text{(III-56)}$$

Therefore, the coefficients of the equation in c as given in

Equation (98) have been determined,

$$B_1 g + B_2 f u_\infty + B_3 = 0 \tag{98}$$

in Equations (III-45), (III-54), and (III-56) respectively.

APPENDIX IV

THE GENERAL EQUATIONS IN ω

The system of equations in ω of the surface (Σ) is the system deduced from the equation in c (98)

$$B_1 g + B_2 f u_\infty + B_3 = 0 \tag{98}$$

when c is taken as

$$c = i\omega$$

and when the real and the pure imaginary terms are separated.

The following definitions are made:

$$\begin{aligned} B_1(i\omega) &\equiv a_1 + ib_1 \\ B_2(i\omega) &\equiv a_2 + ib_2 \\ B_3(i\omega) &\equiv a_3 + ib_3 \end{aligned} \tag{IV-1}$$

Assuming $\omega \neq 0$, two equations occur as a result of the separation of the real and the imaginary parts, i.e.,

$$\begin{aligned} a_1 g + a_2 u_\infty f + a_3 &= 0 \\ b_1 g + b_2 u_\infty f + b_3 &= 0 \end{aligned} \tag{IV-2}$$

(1) Preliminary Calculations. From the equations (II-10)

$$k = \ell n\, m$$

therefore,

$$m^{-c} = e^{-kc}$$

since $c = i\omega$

$$m^{-c} = e^{-i\omega k} = \cos(\omega k) - i \sin(\omega k)$$

also

$$E_s \equiv e^{-cs} = e^{-i\omega s} = \cos(\omega s) - i \sin(\omega s)$$

$$E_y \equiv e^{-cy} = e^{-i\omega y} = \cos(\omega y) - i \sin(\omega y)$$

It is convenient to introduce the notation

$$\begin{aligned} \omega k &\equiv K \\ \omega y &\equiv Y \\ \omega s &\equiv S \end{aligned} \tag{IV-3}$$

With this notation the following calculations are made:

$$\begin{aligned} E_s E_y m^{-c} &= e^{-i(K+S+Y)} = \cos(K + S + Y) - i \sin(K + S + Y) \\ E_s E_y &= e^{-i(S+Y)} = \cos(S + Y) - i \sin(S + Y) \\ E_s m^{-c} &= e^{-i(K+S)} = \cos(K + S) - i \sin(K + S) \\ E_s &= e^{-iS} = \cos(S) - i \sin(S) \\ E_y &= e^{-iY} = \cos(Y) - i \sin(Y) \end{aligned} \tag{IV-4}$$

also

$$\frac{1}{c} = -\frac{i}{\omega}$$

$$\frac{1}{c^2} = -\frac{1}{\omega^2}$$

$$\frac{1}{1-c} = \frac{1 + i\omega}{1 + \omega^2}$$

$$\frac{1}{(1-c)^2} = \frac{(1 - \omega^2) + 2i\omega}{(1 + \omega^2)^2}$$

$$\frac{1}{2-c} = \frac{2 + i\omega}{4 + \omega^2}$$

$$\frac{1}{c(1-c)} = \frac{1}{1+\omega^2} - \frac{i}{\omega(1+\omega^2)}$$

$$\frac{1}{c^2(1-c)} = \frac{-1}{\omega^2(1+\omega^2)} - \frac{i}{\omega(1+\omega^2)} \qquad \text{(IV-5)}$$

$$\frac{1}{(1-c)(2-c)} = \frac{2-\omega^2}{(1+\omega^2)(4+\omega^2)} + \frac{3i\omega}{(1+\omega^2)(4+\omega^2)}$$

$$\frac{1}{c(1-c)(2-c)} = \frac{3}{(1+\omega^2)(4+\omega^2)} + \frac{i(\omega^2-2)}{\omega(1+\omega^2)(4+\omega^2)}$$

All of the complex terms of B_1, B_2, and B_3 are given in (IV-4) and (IV-5). Therefore, it is possible to write the equation in c in terms of the equation in ω.

(2) Expression for B_1. B_1 is given by (III-45)

$$B_1 = \frac{-E_s E_y m^{-c}}{c(1-c)} + \frac{E_s E_y m^{-1}}{c^2(1-c)} - \frac{E_s m^{-1}}{c^2} - \frac{E_y m^{-1}}{c^2} + \frac{1}{c} + \frac{1-c}{mc^2} \qquad \text{(III-45)}$$

Utilizing (IV-4) and (IV-5)

$$B_1 = \left[-\cos(K+S+Y) + i\sin(K+S+Y)\right]\left[\frac{1}{1+\omega^2} - \frac{i}{\omega(1+\omega^2)}\right]$$

$$+ \frac{\cos(S+Y) - i\sin(S+Y)}{m}\left[\frac{-1}{\omega^2(1+\omega^2)} - \frac{i}{\omega(1+\omega^2)}\right] +$$

$$\frac{\cos(S) + \cos(Y) - i(\sin S + \sin Y)}{m\omega^2} - \frac{1-i\omega}{m\omega^2} - \frac{i}{\omega} \qquad \text{(IV-6)}$$

Separating the real and imaginary parts of (IV-6) and recalling (IV-2),

$$a_1 = \frac{-1}{1+\omega^2}\left[\cos(K+S+Y) - \frac{\sin(K+S+Y)}{\omega}\right] - \frac{1}{m\omega^2(1+\omega^2)}$$

$$\left[\cos(S+Y) + \omega\sin(S+Y)\right] + \frac{\cos(S) + \cos(Y) - 1}{m\omega^2} \qquad \text{(IV-7)}$$

$$b_1 = \frac{1}{\omega(1+\omega^2)}\left[\cos(K+S+Y) + \omega\sin(K+S+Y)\right] - \frac{1}{m\omega(1+\omega^2)}$$

$$\left[\cos(S+Y) - \frac{\sin(S+Y)}{\omega}\right] - \frac{\sin(S)+\sin(Y)}{m\omega^2} + \frac{1}{\omega}\left(\frac{1}{m} - 1\right) \tag{IV-8}$$

(3) Expression for B_2. B_2 is given by (III-54)

$$B_2 = -m^2u_\infty \frac{E_sE_ym^{-c}}{c(1-c)} + mu_\infty \frac{E_sE_y}{c^2(1-c)} + 2m^2u_\infty \frac{E_sm^{-c}}{c(1-c)(2-c)}$$

$$- \frac{E_s}{1-c}\left\{\frac{u_\infty}{2-c} + 1 - u_\infty s + \frac{mu_\infty}{c^2}\right\} + \frac{E_s(1-u_\infty s)}{c} + \frac{2\ell_1E_s}{c}$$

$$- \frac{mu_\infty E_y}{c^2} - \frac{1}{c}(1-u_\infty s) + \frac{mu_\infty}{c^2} - \frac{2\ell_1}{c} + 2(\ell_o + 1 + \ell_1) \tag{III-54}$$

Utilizing (IV-4) and (IV-5)

$$B_2 = m^2u_\infty\left[-\cos(K+S+Y) + i\sin(K+S+Y)\right]\left[\frac{1}{1+\omega^2} - \frac{i}{\omega(1+\omega^2)}\right]$$

$$+ mu_\infty\left[\cos(S+Y) - i\sin(S+Y)\right]\left[\frac{-1}{\omega^2(1+\omega^2)} - \frac{i}{\omega(1+\omega^2)}\right]$$

$$+ 2m^2u_\infty\left[\cos(K+S) - i\sin(K+S)\right]\left[\frac{3}{(1+\omega^2)(4+\omega^2)} + \frac{i(\omega^2-2)}{\omega(1+\omega^2)(4+\omega^2)}\right]$$

$$+\left[-\cos(S) + i\sin(S)\right]\left[\frac{(2-\omega^2)u_\infty}{(1+\omega^2)(4+\omega^2)} + \frac{3i\omega u_\infty}{(1+\omega^2)(4+\omega^2)}\right.$$

$$\left. + \frac{(1-u_\infty s)(1+i\omega)}{1+\omega^2} - \frac{mu_\infty}{\omega^2(1+\omega^2)} - \frac{imu_\infty}{\omega(1+\omega^2)} + \frac{(1-u_\infty s+2\ell_1)i}{\omega}\right]$$

$$+ \frac{mu_\infty}{\omega^2}\left[\cos(Y) - i\sin(Y)\right] + \frac{(1-u_\infty s+2\ell_1)i}{\omega} - \frac{mu_\infty}{\omega^2} + 2(\ell_o + 1 + \ell_1) \tag{IV-9}$$

Separating the real and imaginary parts of (IV-9) and recalling (IV-2),

$$a_2 = -\frac{m^2 u_\infty}{(1+\omega^2)}\left[\cos(K+S+Y) - \frac{\sin(K+S+Y)}{\omega}\right] - \frac{mu_\infty}{\omega^2(1+\omega^2)}\left[\cos(S+Y) + \omega\sin(S+Y)\right] + \frac{2m^2 u_\infty}{(1+\omega^2)(4+\omega^2)}\left[3\cos(K+S) + \frac{\omega^2-2}{\omega}\sin(K+S)\right]$$

$$-\frac{\cos(S)}{1+\omega^2}\left[\frac{(2-\omega^2)u_\infty}{4+\omega^2} + 1 - u_\infty s - \frac{mu_\infty}{\omega^2}\right] - \sin(S)\left[\frac{3\omega u_\infty}{(1+\omega^2)(4+\omega^2)} + \frac{\omega(1-u_\infty s)}{1+\omega^2}\right.$$

$$\left.-\frac{mu_\infty}{\omega(1+\omega^2)} + \frac{1-u_\infty s+2\ell_1}{\omega}\right] - \frac{mu_\infty}{\omega^2}\left[1-\cos(Y)\right] + 2(\ell_o + 1 + \ell_1) \qquad \text{(IV-10)}$$

$$b_2 = \frac{m^2 u_\infty}{\omega(1+\omega^2)}\left[\cos(K+S+Y) + \omega\sin(K+S+Y)\right] - \frac{mu_\infty}{\omega(1+\omega^2)}\left[\cos(S+Y) - \frac{\sin(S+Y)}{\omega}\right] + \frac{2m^2 u_\infty}{(1+\omega^2)(4+\omega^2)}\left[\frac{\omega^2-2}{\omega}\cos(K+S) - 3\sin(K+S)\right] - \cos(S)$$

$$\left[\frac{3\omega u_\infty}{(1+\omega^2)(4+\omega^2)} + \frac{\omega(1-u_\infty s)}{1+\omega^2} - \frac{mu_\infty}{\omega(1+\omega^2)} + \frac{1-u_\infty s+2\ell_1}{\omega}\right] + \frac{\sin(S)}{1+\omega^2}$$

$$\left[\frac{(2-\omega^2)u_\infty}{4+\omega^2} + 1 - u_\infty s - \frac{mu_\infty}{\omega^2}\right] - \frac{mu_\infty}{\omega^2}\sin(Y) + \frac{1-u_\infty s+2\ell_1}{\omega} \qquad \text{(IV-11)}$$

(4) <u>Expression for B_3.</u> From (III-56)

$$B_3 = mu_\infty \frac{E_s m^{-c}}{(1-c)^2} + E_s\left[\frac{u_\infty}{c} - \frac{u_\infty kc}{1-c} - \frac{u_\infty}{(1-c)^2} + \frac{\ell_1}{m}\right]$$

$$+ (\ell_o + u_\infty s + u_\infty k + \frac{\ell_1}{m})c - \frac{u_\infty}{c} - \frac{\ell_1}{m} \qquad \text{(III-56)}$$

Utilizing (IV-4) and (IV-5),

$$B_3 = mu_\infty \left[\cos(K + S) - i \sin(K + S)\left\{\frac{1-\omega^2 + 2i\omega}{(1 + \omega^2)^2}\right\}\right] + \left[\cos(S) - i \sin(S)\right]$$

$$\left[\frac{-u_\infty i}{\omega} - \frac{u_\infty k\omega i(1 + i\omega)}{1 + \omega^2} - \frac{u_\infty(1 - \omega^2 + 2i\omega)}{(1 + \omega^2)^2} + \frac{\ell_1}{m}\right] + (\ell_o + u_\infty s$$

$$+ u_\infty k + \frac{\ell_1}{m})\ i\omega + \frac{u_\infty i}{\omega} - \frac{\ell_1}{m} \tag{IV-12}$$

Separating the real and imaginary parts of (IV-12) and recalling (IV-2)

$$a_3 = \frac{mu_\infty}{(1 + \omega^2)^2}\left[(1 - \omega^2)\cos(K + S) + 2\omega \sin(K + S)\right] + \cos(S)\left[\frac{u_\infty k\omega^2}{1 + \omega^2}\right.$$

$$\left. - \frac{u_\infty(1 - \omega^2)}{(1 + \omega^2)^2} + \frac{\ell_1}{m}\right] - \sin(S)\left[\frac{u_\infty}{\omega} + \frac{u_\infty k\omega}{1 + \omega^2} + \frac{2u_\infty\omega}{(1 + \omega^2)^2}\right] - \frac{\ell_1}{m}$$

$$\tag{IV-13}$$

$$b_3 = \frac{mu_\infty}{(1 + \omega^2)^2}\left[2\omega \cos(K + S) - (1 - \omega^2) \sin(K + S)\right] - \cos(S)\left[\frac{u_\infty}{\omega} + \frac{u_\infty k\omega}{1 + \omega^2}\right.$$

$$\left. + \frac{2u_\infty\omega}{(1 + \omega^2)^2}\right] - \sin(S)\left[\frac{u_\infty k\omega^2}{1 + \omega^2} - \frac{u_\infty(1 - \omega^2)}{(1 + \omega^2)^2} + \frac{\ell_1}{m}\right] + (\ell_o + u_\infty s + u_\infty k$$

$$+ \frac{\ell_1}{m})\ \omega + \frac{u_\infty}{\omega} \tag{IV-14}$$

Therefore, with these calculations the equation in c has been replaced by the set of equations in ω (IV-2) with the defining relations (IV-7) and (IV-8), (IV-10) and (IV-11), plus (IV-13) and (IV-14).

APPENDIX [illegible]

CONSTANT DENSITY FLOW

For constant density flow, the [illegible]

(16) for $\Theta \rightarrow \infty$.

Hence,

$$\frac{\partial U}{\partial Z} = 0$$

Therefore, U is a function of T only.

$$U = [illegible]$$

Applying the momentum equation (17),

$$\Delta P = \int_{\text{entrance}}^{\text{exit}} \left[\frac{\partial U}{\partial T} + G + \frac{FU^2}{2D}\right] dZ$$

and

$$\Delta P = R_o \left[\frac{dU}{dT} + G + \frac{FU^2}{2D}\right] [illegible] \qquad (A-1)$$

This equation can be written in the form

$$\frac{dU}{dT} = - aU^2 + b \qquad (A-2)$$

where a and b are positive constants.

By putting

$$U = U_o + V \qquad (A-3)$$

where

$$U_o = \text{steady state velocity}$$

APPENDIX V

CONSTANT DENSITY FLOW

For constant density flow, the continuity equation is given by (16) for $\Theta \to \infty$.

Hence,

$$\frac{\partial U}{\partial Z} = 0$$

Therefore, U is a function of T only.

$$U = U(T)$$

Applying the momentum equation (17),

$$\Delta P = \int_{\text{entrance}}^{\text{exit}} \left[\frac{\partial U}{\partial T} + G + \frac{FU^2}{2D}\right] R_o dZ$$

and

$$\Delta P = R_o \left[\frac{dU}{dT} + G + \frac{FU^2}{2D}\right] (L_o + L_c + L_1) \tag{V-1}$$

This equation can be written in the form

$$\frac{dU}{dT} = - aU^2 + b \tag{V-2}$$

where a and b are positive constants.

By putting

$$U = U_o + V \tag{V-3}$$

where

U_o = steady state velocity

$$V = \text{transient component of velocity}$$

then

$$\frac{dV}{dT} = - aU_o^{\ 2} + b - a(2U_o + V)V = - a(2U_o + V)V \qquad (V\text{-}4)$$

Taking an initial perturbation such that

$$|V(0)| < U_o$$

since the right hand member of (V-4) is of opposite sign to V, this equation gives

$$V \frac{dV}{dT} < 0 \qquad (V\text{-}5)$$

which says

$$\frac{d(V^2)}{dT} < 0 \qquad (V\text{-}6)$$

This says that V can only decrease in absolute value, therefore, the flow becomes stable in the sense that stability has been defined earlier in this investigation.

APPENDIX VI

UNDAMPED NATURAL FREQUENCIES OF THE LOOP

In order to determine what vibrating frequencies are important

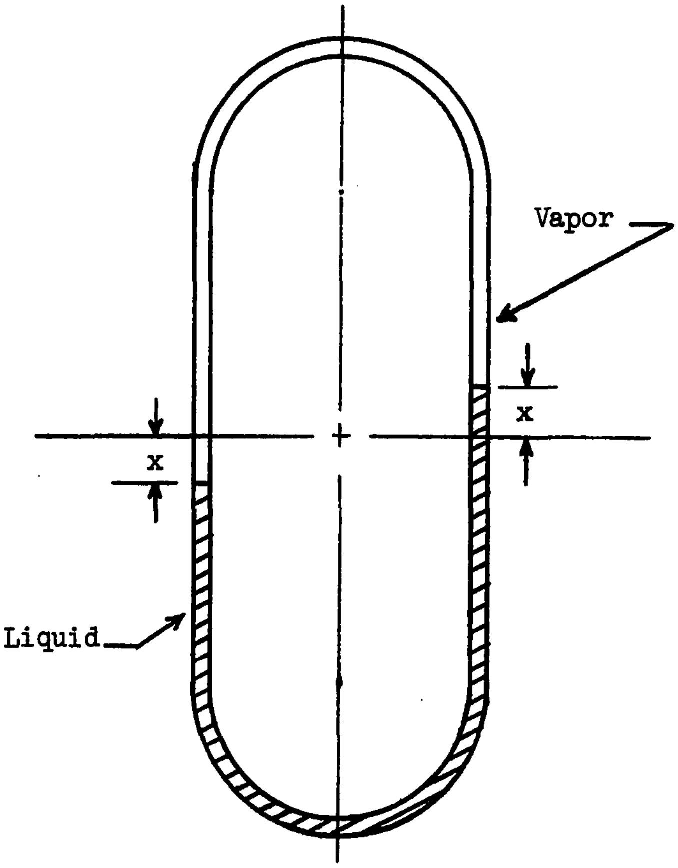

Figure (54) Loop Idealized as a U-Tube Manometer

in the operation of a natural-circulation loop, it is necessary to investigate the various modes of vibration that can occur and to compare these calculated natural frequencies with those found experimentally.

Since the loop is operated in a thermodynamic region where the density of the fluid in the portion of the loop from the heater section to the heat exchanger is much greater than the density of the fluid in the rest of the loop, the loop can be treated as a vertical U-tube manometer and the natural frequency of the manometer can be calculated. This will give, as a first approximation, the longitudinal natural frequency of the loop considering the loop fluid to be a solid body.

If, referring to Figure (54), the liquid is displaced a distance x from equilibrium, the potential energy of the system is changed (assuming no mixing of the liquid and the vapor) as follows:

$$\text{P.E.} = \frac{(\rho_L A x) g x}{g_c} - \frac{(\rho_V A x) g x}{g_c} \qquad \text{(VI-1)}$$

The kinetic energy of the system is given by

$$\text{K.E.} = \frac{1}{2g_c}\left[\frac{\rho_L + \rho_V}{2}\right] A\ell\left(\frac{dx}{dt}\right)^2 \qquad \text{(VI-2)}$$

where

ρ_L = Liquid density, lb_m/ft^3

ρ_V = Vapor density, lb_m/ft^3

A = Cross-sectional area of loop, ft^2

ℓ = One-half loop circumference, ft

In a conservative field,

$$\text{P.E.} + \text{K.E.} = \text{Constant}$$

Hence,

$$\frac{d}{dt}(\text{P.E.} + \text{K.E.}) = 0$$

Therefore,

$$\frac{d}{dt}\left[\frac{Ax^2 g}{g_c}(\rho_L - \rho_V) + \frac{1}{2g_c}\left\{\frac{\rho_L + \rho_V}{2}\right\} A\ell\left(\frac{dx}{dt}\right)^2\right] = 0$$

Differentiating and simplifying,

$$\frac{d^2x}{dt^2} + \frac{2g}{\ell} \frac{(\rho_L - \rho_V)}{(\rho_L + \rho_V)} x = 0 \qquad \text{(VI-3)}$$

From the solution of (VI-3), it is found that the natural frequency is

$$\omega_n = \sqrt{\frac{2g(\rho_L - \rho_V)}{\ell(\rho_L + \rho_V)}}$$

and

$$f_n = \frac{1}{2\pi}\sqrt{\frac{2g(\rho_L - \rho_V)}{\ell(\rho_L + \rho_V)}} \qquad \text{(VI-4)}$$

If $\rho_L >> \rho_V$,

$$f_n = \frac{1}{2\pi}\sqrt{\frac{2g}{\ell}} \qquad \text{(VI-5)}$$

Utilizing (VI-5), the natural frequency assuming $\rho_L >> \rho_V$ is

$$f_n = 0.276 \text{ cps}$$

Another mode of vibration would be the radial mode in a pressurized pipe as shown in Figure (55). The natural frequency for this mode is given by

$$\omega_n = \sqrt{\frac{K}{m}} \qquad \text{(VI-6)}$$

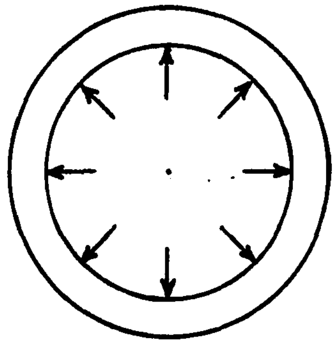

Figure (55) Radial Mode of Vibration

Now

$$K = \frac{p}{\delta}$$

and

$$\delta = R\varepsilon_h$$

$$= \frac{R}{E} (\sigma_h - \nu\sigma_a)$$

$$= \frac{R}{E} (\frac{pR}{t} - \nu \frac{pR}{2t})$$

$$\delta = \frac{pR^2}{Et} (1 - \frac{\nu}{2})$$

Therefore,

$$K = \frac{p}{\delta} = \frac{2\pi RpLEt}{pr^2(1- \frac{\nu}{2})}$$

$$K = \frac{2\pi EtL}{R(1- \frac{\nu}{2})} \tag{VI-7}$$

and

$$m = \frac{2\pi RtL\gamma}{g_c} \tag{VI-8}$$

Substituting (VI-7) and (VI-8) into (VI-6) gives

$$\omega_n = \sqrt{\frac{Eg_c}{R^2\gamma(1- \frac{\nu}{2})}} \tag{VI-9}$$

and

$$f_n = \frac{1}{2\pi} \sqrt{\frac{Eg_c}{R^2\gamma(1- \frac{\nu}{2})}} \tag{VI-10}$$

where

γ = Density, lb_m/ft^3

p = Pressure, psi

R = Pipe radius, in.

E = Young's modulus, psi

ν = Poisson's ratio

σ_h = Hoop stress

σ_a = Axial stress

Utilizing the properties of the loop, the radial natural frequency is found to be

$$f_n = 21{,}500 \text{ cps}$$

In order to investigate bending vibrations, the two limiting cases of hinged ends and fixed ends are considered.

For hinged ends, it is found[4]

$$\beta L = \pi \qquad \text{(VI-11)}$$

where

$$\beta = \left[\frac{\rho A \omega^2}{EI}\right]^{\frac{1}{4}} \qquad \text{(VI-12)}$$

ρ = Specific weight, $\frac{\gamma}{g}$

A = Material cross-section, in^2

I = Moment of inertia, $\frac{\pi}{64}(D_o^{\,4} - D_i^{\,4})$

L = One-half total length, in.

E = Young's modulus, psi

Utilizing the formulas (VI-11) and (VI-12) and the material properties,

$$f_n = 0.457 \text{ cps}$$

Now for fixed ends,

$$\beta = \frac{4.73}{L} \qquad \text{(VI-13)}$$

Utilizing (VI-12) and (VI-13) and the material properties, it is found that

$$f_n = 0.0722 \text{ cps}$$

The circulation loop would fall somewhere between these two limiting cases. Therefore, the natural frequency for the bending mode is

$$0.0722 < f_n < 0.457 \text{ cps}$$

The next mode to consider is the longitudinal vibration of the loop. To approximate this mode, it will first be assumed that the loop is a cantilever. Therefore, the longitudinal vibration of a uniform cantilever is given by[3]

$$f_n = \frac{1}{2\pi} \left(\frac{\pi}{2\ell}\right) \sqrt{\frac{EAg}{w}} \qquad \text{(VI-14)}$$

where

ℓ = One-half total loop length

w = Weight per unit length

Utilizing (VI-14), the longitudinal frequency is

$$f_n = 376 \text{ cps}$$

Now if the loop is considered as a circular ring, this case and the previous case will give the limiting cases for the longitudinal mode. Hence, the natural frequency of a pure radial vibration of the pipe is given by[4]

$$f_n = \frac{1}{2\pi R} \sqrt{\frac{Eg}{\gamma}}$$

Now if the entire loop is considered as a circular ring, the equivalent radius is

$$R = \frac{L}{2\pi}$$

where L is the circumference of the loop. Therefore,

$$f_n = \frac{1}{L}\sqrt{\frac{Eg}{\gamma}} \tag{VI-15}$$

Utilizing (VI-15)

$$f_n = 1404 \text{ cps}$$

Therefore, it can be seen that the actual frequency would lie between

$$376 < f_n < 1404 \text{ cps}$$

APPENDIX VII

CALIBRATION OF THE 1000 PSIG STATHAM ABSOLUTE PRESSURE TRANSDUCER

In order to determine the calibration factor, F, for the 1000 psig absolute pressure transducer used in this investigation, it was necessary to calibrate the transducer with a dead weight tester. This was done and the results are shown in Figure (56).

From the curve shown in Figure (56) the slope was found to be

$$20.4\ \mu\text{-volts/psi}$$

Utilizing the formula

$$E_g = FNE \tag{VII-1}$$

where

E_g = Transducer output voltage, mv

E = Excitation voltage, volts

N = Pressure signal, psi

F = Calibration factor, $\dfrac{\mu\text{-volts}}{\text{volt psi}}$

Equation (VII-1) gives E_g as a function of the pressure signal, N, where FE is the slope $\Delta E_g/\Delta N$. Therefore,

$$FE = 20.4\ \mu\text{-volts/psi}$$

and since the excitation voltage used in the calibration run was E = 5 volts, the calibration factor is

$$F = 4.08\ \mu\text{-volts/volt psi}$$

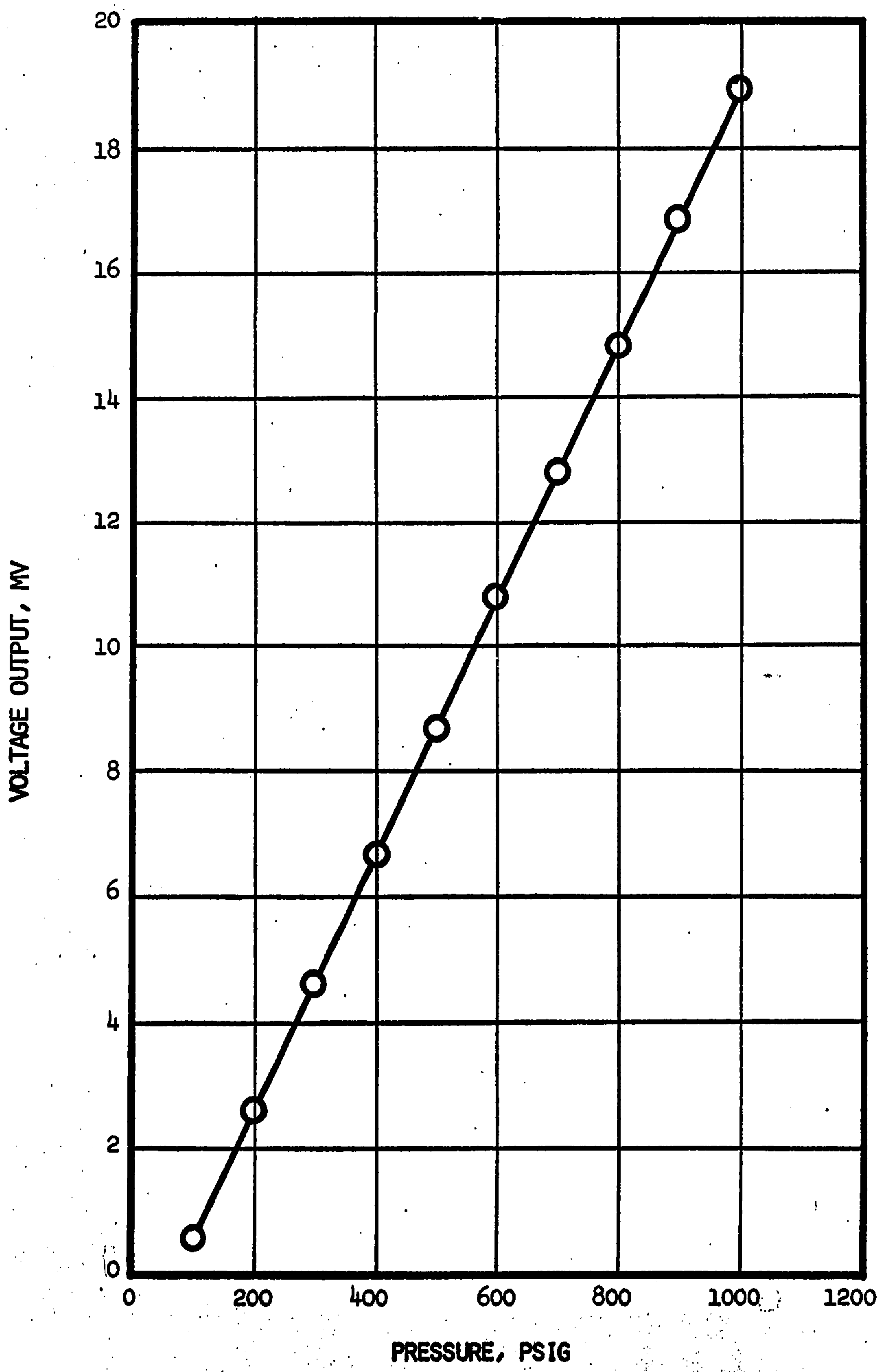

FIGURE (56) 1000 PSIG TRANSDUCER CALIBRATION CURVE

APPENDIX VIII

PRESSURE TRANSDUCER CHECKING AND CALIBRATION

Calibration of the pressure instrumentation was accomplished in two different ways. The first method was to calibrate the transducer with a dead weight tester as mentioned in the previous appendix. The second method was to calibrate the transducer with the bourdon tube pressure gauges.

The method of checking the transducer consisted of electrically simulating a pressure by keying a resistor across one arm of the transducer bridge. This causes a deflection in the output circuit which simulates the effect of resistance changes of the active bridge arms due to a pressure change in the loop. In this manner checking the output circuit can be made without the necessity of applying standardizing input pressures.

The effect of adding a calibrating resistor in parallel with an active bridge arm is shown in Figure (57).

The Honeywell carrier amplifier has the calibrating circuit shown in Figure (57) built into it. It contains five shunt resistors (300K, 150K, 75K, 30K, and 15K) which serve as calibrating resistors. These calibrating resistors can be shunted across R_{34} (- calibration positions) or across R_{31} (+ calibration positions). The five calibrating resistors will give five convenient calibration positions for the transducers.

Table (2) gives the value of the simulated psi signal for the three transducers used in this investigation. These values were calculated utilizing Equation (VIII-1) below. The values of R and F come from the transducer manufacturer for the differential pressure transducer and the 5000 psi transducer. These values for the 1000 psi transducer come from a calibration of the transducer, the results of which are contained in Appendix VII.

When the output resistance of the bridge is much less than the resistance of the calibrating resistor ($R << R_c$), the output change from the transducer is given by

$$N = \frac{(10^6)R}{N_a R_c F} \qquad \text{(VIII-1)}$$

where

N = Transducer output signal, psi

N_a = Number of active strain gauge arms (4)

R = Transducer output resistance, ohms (R_{23})

R_c = Calibrating resistor, ohms

F = Transducer calibration factor, $\frac{\mu\text{-volts}}{\text{volt psi}}$

Calibration Position	Calibrating Resistor (ohms)	PRESSURE TRANSDUCER OUTPUT		
		Pressure Transducer[+]		
		ΔP = 5 psid R = 357.6 F = 406.9	P = 1000 psig R = 350.0 F = 4.08	P = 5000 psig R = 353.2 F = 0.8376
± 1	300,000	0.732	71.6	351.4
± 2	150,000	1.464	143.2	702.8
± 3	75,000	2.929	286.4	1405.6
± 4	30,000	7.323*	716.0	3514.0
± 5	15,000	14.647*	1432.0*	7028.0*

[+] R in ohms, F in μ-volts/volt psi

* Calibration positions which exceed the pressure rating of the transducer

Table (2) Carrier Amplifier Calibration Values

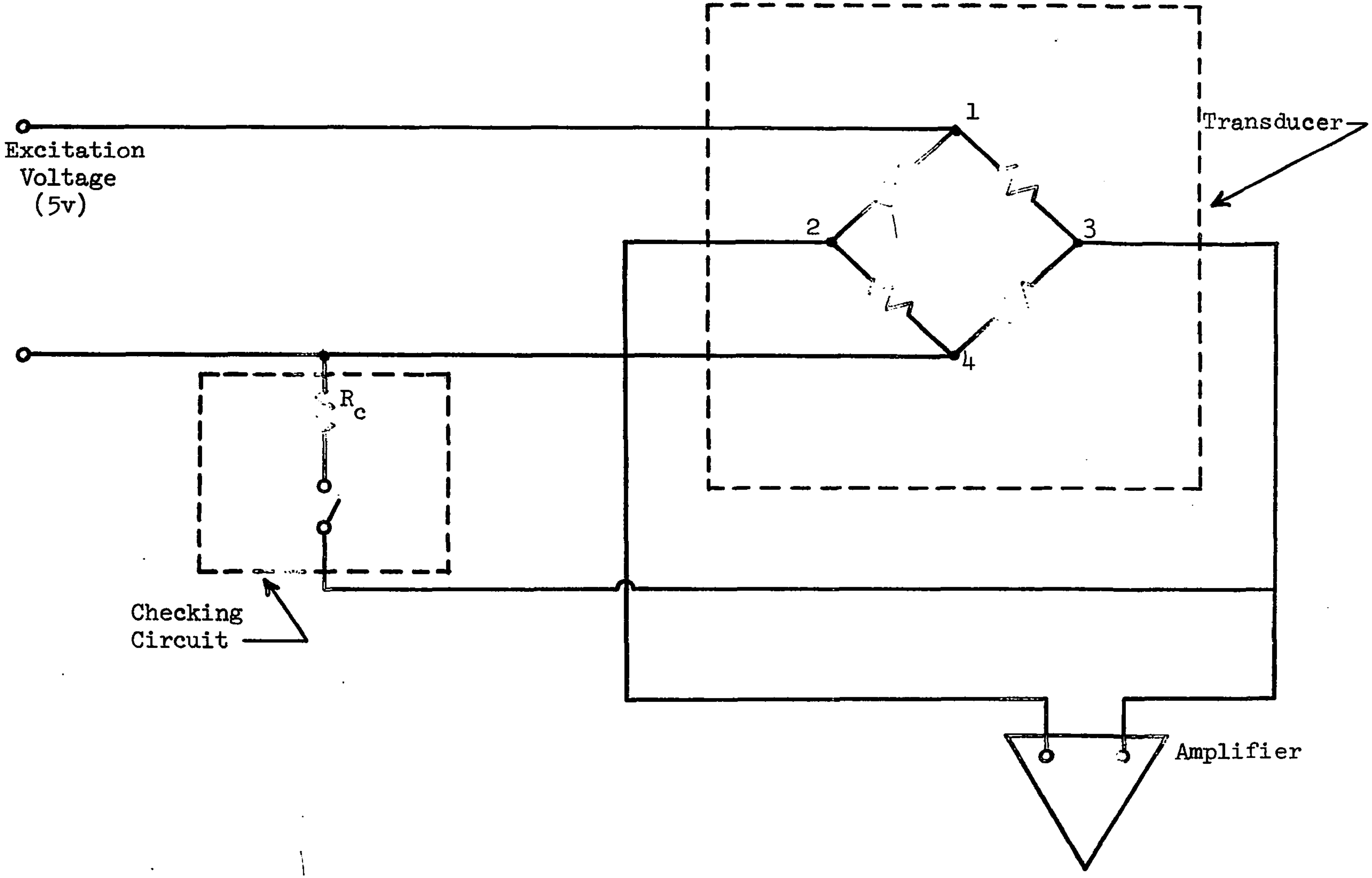

Figure (57) Pressure Transducer Checking Circuit

APPENDIX IX

COMPUTER PROGRAMS

The following gives the relationship of the Computer Program variable notation to the model parameter.

Model Parameter	Corresponding Program Notation
ℓ_o	XLO, XLO2, XLO3
ℓ_1	XL1, XL11, XL2, XL13
s	S
u_∞	U
m	XM
k	XK
N	XN
μ_{max}	XMUMAX
ω	W
u_1	U1
g	G
f	F
r	R

```
C     PROGRAM SIGMA
      READ 11, XL02,XL03,XL11,XL12,XL13
   11 FORMAT (5E12.3)
  302 READ 12,S
   12 FORMAT(E12.3)
      MC=0
      U=.001
  300 DO100 J=1,31
      MC=MC+1
      NC=0
      XMUMAX=.01
      IF(MC-1)75,75,76
   76 IF(MC-2)84,84,85
   84 U=.01
      GO TO 75
   85 IF(MC-21)77,77,78
   77 U=U+.01
      GO TO 75
   78 IF(MC-27)79,79,80
   79 U=U+.05
      GO TO 75
   80 IF(MC-28)81,81,82
   81 U=.6
```

```
      GO TO 75
   82 IF(MC-30)83,83,200
   83 U=U+.2
   75 XM=1.-S+1./U
      XK=LOGF(XM)
      U1=XM*U
      Y11=XL11/U1
      Y12=XL12/U1
      Y13=XL13/U1
      IF(Y11-Y12)1,1,2
    2 IF(Y11-Y13)7,3,4
    4 Z=Y11
      GO TO 10
    1 IF(Y12-Y13)7,5,6
    6 Z=Y12
      GO TO 10
    7 Z=Y13
      GO TO 10
    5 PRINT 8
    8 FORMAT(2X,1H , 11HY11=Y12=Y13//)
      GO TO 7
    3 PRINT 9
    9 FORMAT(2X, 1H , 7HY11=Y13//)
   10 XN=S+XK+Z
      DO100 I=1,61
      IF(NC-1)50,51,52
```

```
51 XMUMAX=.25
   GO TO 50
52 IF(NC-2)53,53,54
53 XMUMAX=.5
   GO TO 50
54 IF(NC-4)55,55,56
55 XMUMAX=XMUMAX+.05
   GO TO 50
56 IF(NC-26)57,57,58
57 XMUMAX=XMUMAX+.025
   GO TO 50
58 IF(NC-47)59,59,60
59 XMUMAX=XMUMAX+.05
   GO TO 50
60 IF(NC-60)61,61,300
61 XMUMAX=XMUMAX+.1
50 W=2.*3.1416*XMUMAX/XN
   R11=W*(S+XK+Y11)
   R12=W*(S+XK+Y12)
   R21=W*(S+Y11)
   R22=W*(S+Y12)
   R3=W*(S+XK)
   R4=W*S
   Y21=W*Y11
   Y22=W*Y12
   D1=1.+W*W
```

```
 D4=4.+W*W
 E21=U/D1*(U/D4*(2.-W*W)+1.-U*S-U1/(W*W))
 E22=U*(3.*W*U/(D1*D4)+W/D1*(1.-U*S)-U1/(W*D1)+(1.-U*S+2.*XL12)/W)
 E31=U*XK*W*W/D1-U/(D1*D1)*(1.-W*W)+XL13/XM
 E32=U/W+U*XK*W/D1+2.*U*W/(D1*D1)
 A1=-COSF(R11)/D1+SINF(R11)/(W*D1)-COSF(R21)/(XM*W*W*D1)-SINF(R21)/
1(XM*W*D1)+(COSF(R4)+COSF(Y21)-1.)/(XM*W*W)
 A20=-U1*U1*COSF(R12)/D1+U1*U1*SINF(R12)/(W*D1)-U*U1*COSF(R22)/
1(W*W*D1)-U*U1*SINF(R22)/(W*D1)+2.*U1*U1*(3.*COSF(R3)+(W-2./W)*SINF
2(R3))/(D1*D4)
 A21=-E21*COSF(R4)-E22*SINF(R4)-U*U1*(1.-COSF(Y22))/(W*W)+2.*U*
1(XL02+1.+XL12)
 A2=A20+A21
 A3=U1*((1.-W*W)*COSF(R3)+2.*W*SINF(R3))/(D1*D1)+E31*COSF(R4)-
1E32*SINF(R4)-XL13/XM
 B1=COSF(R11)/(W*D1)+SINF(R11)/D1-COSF(R21)/(XM*W*D1)+SINF(R21)/
1(XM*W*W*D1)-(SINF(R4)+SINF(Y21))/(XM*W*W)+1./W*(1./XM-1.)
 B20=U1*U1*COSF(R12)/(W*D1)+U1*U1*SINF(R12)/D1-U*U1*COSF(R22)/
1(W*D1)+U*U1*SINF(R22)/
2(W*W*D1)+2.*U1*U1*((W-2./W)*COSF(R3)-3.*SINF(R3))/(D1*D4)
 B21=-E22*COSF(R4)+E21*SINF(R4)-U*U1*SINF(Y22)/(W*W)+(1.-U*S+2.
1*XL12)*U/W
 B2=B20+B21
 B3=U1*(2.*W*COSF(R3)-(1.-W*W)*SINF(R3))/(D1*D1)-E32*COSF(R4)-
1E31*SINF(R4)+W*(XL03+U*S+U*XK+XL13/XM)+U/W
 G=(A2*B3-A3*B2)/(A1*B2-A2*B1)
```

```
      F=(A3*B1-A1*B3)/(A1*B2-A2*B1)
      NC=NC+1
      IF(NC-1)13,13,14
   13 PRINT15
   15 FORMAT(10X,19HDESCRIPTION OF CASE///)
   16 PRINT17,XL02,XL03,XL11,XL12,XL13
   17 FORMAT(2X,F6.3,5X,F6.3,5X,F6.3,5X,F6.3,5X,F6.3//)
   18 PRINT19,S,U
   19 FORMAT(2X,2HS=F10.3,5X,2HU=F10.3///)
   20 PRINT21
   21 FORMAT(5X,5HMUMAX,14X,1HW,14X,1HG,15X,1HF///)
   14 PRINT22,XMUMAX,W,G,F
   22 FORMAT(2X,E12.5,4X,E12.5,4X,E12.5,4X,E12.5/)
      IF(U-1./S)100,100,302
  100 CONTINUE
  200 STOP
      END
```

```
C    PROGRAM ROOT
     READ11,XL0,XL1
  11 FORMAT(2E12.3)
   1 READ12, S
  12 FORMAT(E12.3)
     R=-10.
     KC=0
     DO100 K=1,7
     U=.1
     KC=KC+1
     IF(KC-3)105,105,106
 105 R=R*.01
     GO TO 300
 106 IF(KC-4)107,107,108
 107 R=0.
     GO TO 300
 108 IF(KC-5)109,109,110
 109 R=.00001
     GO TO 300
 110 R=R*1.E+2
 300 XM=1.-S+1./U
     XK=LOGF(XM)
     U1=XM*U
     Y1=XL1/U1
     XN=S+XK+Y1
     NC=0
```

```
      XMUMAX=.01
   75 DO100 I=1,61
      IF(NC-1)50,51,52
   51 XMUMAX=.25
      GO TO 50
   52 IF(NC-2)53,53,54
   53 XMUMAX=.5
      GO TO 50
   54 IF(NC-4)55,55,56
   55 XMUMAX=XMUMAX+.05
      GO TO 50
   56 IF(NC-26)57,57,58
   57 XMUMAX=XMUMAX+.025
      GO TO 50
   58 IF(NC-47)59,59,60
   59 XMUMAX=XMUMAX+.05
      GO TO 50
   60 IF(NC-60)61,61,300
   61 XMUMAX=XMUMAX+,1
   50 W=2.*3.1416*XMUMAX/XN
      D1=(1.-R)*(1.-R)+W*W
      D2=2.*R*W*W
      D3=R*(1.-R)+W*W
      D4=(2.-R)*(2.-R)+W*W
      D5=R*R+W*W
      D6=R*R-W*W
```

```
 D7=3.*R*R-2.*R-W*W
 D8=1.-R
 D9=2.*R-1.
 D10=2.-R
 D11=W*W-2.
 D12=1.-U*S
 D13=(1.-R)*(1.-R)-W*W
 D14=R*(1.-R)-W*W
 R1=W*(S+XK+Y1)
 R2=W*(S+Y1)
 R3=W*(S+XK)
 R4=W*S
 Y2=W*Y1
 E1=EXPF(-R*(S+XK+Y1))
 E2=EXPF(-R*(S+Y1))
 E3=EXPF(-R*(S+XK))
 E4=EXPF(-R*S)
 E5=EXPF(-R*Y1)
 A1=-E1*(D3*COSF(R1)+W*D9*SINF(R1))/(D5*D1)+E2/XM*((D6*D8+D2)
1*COSF(R2)+W*D7*SINF(R2))/(D5*D5*D1)-E4/XM*(D6*COSF(R4)-2.*
2R*W*SINF(R4))/(D5*D5)-E5/XM*(D6*COSF(Y2)-2.*R*W*SINF(R4))
3/(D5*D5)+R/D5+1./XM*(D6*D8-D2)/(D5*D5)
 A2=U1*U1*E1*(-D3*COSF(R1)-W*D9*SINF(R1))/(D5*D1)+U*U1*E2
1*((D6*D8+D2)*COSF(R2)+W*D7*SINF(R2))/(D5*D5*D1)+2.*U1*U1*
2E3*((R*D8*D10+3.*W*W*D8)*COSF(R3)+W*(3.*R*D10+D11)*SINF(R3))
3/(D5*D1*D4)-U*U*E4*(D10*(D8*COSF(R4)+W*SINF(R4))+W*D8*SINF(R4)
```

```
4-W*W*COSF(R4))/(D1*D4)-U*E4*D12*(D8*COSF(R4)+W*SINF(R4))/
5D1-U*U1*E4*(D6*(D8*COSF(R4)+W*SINF(R4))+2.*R*W*(W*COSF(R4)
6-D8*SINF(R4))/(D1*D5*D5)-U*U1*E5*(D6*COSF(Y2)-2.*R*W*SINF(Y2
7))/(D5*D5)+U*E4*D12*(R*COSF(R4)-W*SINF(R4))/D5+2.*XL1*U*E4*
8(R*COSF(R4)-W*SINF(R4))/D5-R*D12*U/D5+U*U1*D6/(D5*D5)-2.*
9XL1*R*U/D5+2.*U*(XL0+1.+XL1)
 A3=U1*E3*(D13*COSF(R3)+2.*W*D8*SINF(R3))/(D1*D1)+U*E4*(R*
1COSF(R4)-W*SINF(R4))/D5-E4*U*XK*(D14*COSF(R4)+W*SINF(R4))/D1-U*E
24*(D13*COSF(R4)+2.*W*D8*SINF(R4))/(D1*D1)+E4*XL1*COSF(R4)/XM+
3R*(XL0+U*S+U*XK+XL1/XM)-R*U/D5-XL1/XM
 B1=-E1*(-D3*SINF(R1)+W*D9*COSF(R1))/(D5*D1)+E2/XM*(-D6*D8
1*SINF(R2)+W*D7*COSF(R2))/(D5*D5*D1)-E4/XM*(-D6*SINF(R4)-2.*R*W
2*COSF(R4))/(D5*D5)-E5/XM*(-D6*SINF(Y2)-2.*R*W*COSF(Y2))/
3(D5*D5)-W/D5-1./XM*(W*D6+2.*R*W*D8)/(D5*D5)
 B2=U1*U1*E1*(D3*SINF(R1)-W*D9*COSF(R1))/(D5*D1)+U*U1*E2*
1(-1.*(D6*D8+D2)*SINF(R2)+W*D7*COSF(R2))/(D5*D5*D1)+2.*U1*
2U1*E3*(-1.*(R*D8*D10+3.*W*W*D8)*SINF(R3)+W*(3.*R*D10+D11)
3*COSF(R3))/(D5*D1*D4)-U*U*E4*(D10*(WCOSF(R4)-D8*SINF(R4))
4+W*(D8*COSF(R4)+W*SINF(R4)))/(D1*D4)-U*D12*E4*(W*COSF(R4)-D8*
5SINF(R4))/D1-U*U1*E4*(D6*(W*COSF(R4)-D8*SINF(R4))-2.*R*W*
6(D8*COSF(R4)+W*SINF(R4)))/(D1*D5*D5)-U*E4*D12*(R*SINF(R4)
7+W*COSF(R4))/D5-2.*XL1*U*E4*(R*SINF(R4)+W*COSF(R4))/D5+U*U1
8*E5*(D6*SINF(Y2)+2.*R*W*COSF(Y2))/(D5*D5)+U*W*D12/D5-2.*U*U1
9*R*W/(D5*D5)+2.*XL1*U*W/D5
 B3=U1*E3*(-D13*SINF(R3)+2.*W*D8*COSF(R3))/(D1*D1)-U*E4*
1(R*SINF(R4)+W*COSF(R4))/D5-U*XK*E4*(-D14*SINF(R4)+W*COSF(R4))/
```

```
     2D1-U*E4*(-D13*SINF(R4)+2.*W*D8*COSF(R4))/(D1*D1)-E4*XL1*
     3SINF(R4)/XM+W*(XL0+U*S+U*XK+XL1/XM)+U*W/D5
      G=(A2*B3-A3*B2)/(A1*B2-A2*B1)
      F=(A3*B1-A1*B3)/(A1*B2-A2*B1)
      NC=NC+1
      IF(NC-1)13,13,14
   13 PRINT 15
   15 FORMAT(10X, 19HDESCRIPTION OF CASE///)
   16 PRINT 17,XL0,XL1
   17 FORMAT(2X,3HL0=F5.3,5X,3HL1=F5.3//)
   18 PRINT19,S,U,R
   19 FORMAT(2X, 2HS=F10.3,5X,2HU=F10.3,5X,2HR=F10.3///)
   20 PRINT 21
   21 FORMAT(5X, 5HMUMAX,14X,1HW,14X,1HG,15X,1HF///)
   14 PRINT 22,XMUMAX,W,G,F
   22 FORMAT(2X,E12.5,4X,E12.5,4X,E12.5,4X,E12.5/)
  100 CONTINUE
      GO TO 1
  200 STOP
      END
```

```
C   PROGRAM STEADY STATE
    READ1,XLO2,XL11,XL12
  1 FORMAT(3E12.3)
  5 READ2, S
  2 FORMAT(E12.3)
    N=0
    DO 11 I=1,32
    IF(N-1)4,6,12
  4 U=.001
    GO TO 10
  6 U=.01
    GO TO 10
 12 IF(N-20)13,13,14
 13 U=U+.01
    GO TO 10
 14 IF(N-26)15,15,16
 15 U=U+.05
    GO TO 10
 16 U=U+.1
 10 XM=1.-S+1./U
    XK=LOGF(XM)
    Y11=XL11/(XM*U)
    E1=S+XK+(Y11-1.)/(XM*U)
    E2=.5+XL12+2.*U*(XLO2+1.+XL12)-2.*U*S*(1.+XL12)+1.5*U*U*S*S
    E3=1.-2.*U*S
    GO=-E3/E1
```

```
      G1=-(E3+E2)/E1
      G5=-(5.*E2+E3)/E1
      PRINT3,G0,G1,G5
    3 FORMAT(2X,3HG0=E12.5,4X,3HG1=E12.5,4X,3HG5=E12.5/)
      N=N+1
   11 CONTINUE
      GO TO 5
      STOP
      END
```

APPENDIX X

EXAMINATION OF POINTS NEAR THE INSTABILITY THRESHOLDS

In this derivation, the instability thresholds have been defined utilizing the condition that r be equal to zero. However, it is also necessary to be able to locate on the threshold map the regions for which r = - (damped oscillations) and r = + (amplified oscillations) in order to show which of the regions are stable and which are unstable. From the experimental portion of this investigation, it was found that the regions of higher entrance velocity were the stable regions. However, this can also be shown analytically for the region of interest in this investigation.

This requires a look at the equations for which r = 0. If the possibility of solutions going to infinity is discounted, the "equation in c" gives solutions which go from r = - through r = 0, then to r = + as an instability threshold is passed through. It can be seen that r = - corresponds to a damped oscillation and r = + corresponds to an amplified oscillation in Equation (71)

$$u_o = u_\infty + v_o e^{ct} \qquad (71)$$

where

$$c = r + i\omega \qquad (102)$$

In order to investigate the regions near the instability thresholds, it is necessary to consider the equation in c and to proceed as in Appendix IV with

$$c = r + i\omega \tag{102}$$

It is necessary to develop the following expressions in order to proceed from the equation in c to the equations in ω.

From (II-10)

$$k = \ln m$$

therefore,

$$m^{-c} = e^{-kc} = e^{-k(r+i\omega)}$$

and

$$m^{-c} = e^{-kr}\left[\cos(\omega k) - i\,\sin(\omega k)\right] \tag{X-1}$$

Also,

$$E_s = e^{-cs} = e^{-rs}\,e^{-i\omega s}$$

From the definitions (III-1) and (III-23)

$$E_s = e^{-rs}\left[\cos(S) - i\,\sin(S)\right] \tag{X-2}$$

Likewise,

$$E_y = e^{-cy} = e^{-ry}\,e^{-i\omega y}$$

$$E_y = e^{-ry}\left[\cos(Y) - i\,\sin(Y)\right] \tag{X-3}$$

Combinations of (X-1), (X-2), and (X-3) give

$$E_sE_ym^{-c} = e^{-r(s+k+y)}\left[\cos(S + K + Y) - i\,\sin(S + K + Y)\right] \tag{X-4}$$

$$E_sE_y = e^{-r(s+y)}\left[\cos(S + Y) - i\,\sin(S + Y)\right] \tag{X-5}$$

$$E_sm^{-c} = e^{-r(s+k)}\left[\cos(S + K) - i\,\sin(S + K)\right] \tag{X-6}$$

The following identities appear in the equation in c and are useful in simplifying this equation. Utilizing the definition of c, it is found that

$$\frac{1}{c} = \frac{r - i\omega}{r^2 + \omega^2}$$

$$\frac{1}{c^2} = \frac{(r^2 - \omega^2) - 2i\omega r}{(r^2 + \omega^2)^2}$$

$$\frac{1}{1-c} = \frac{(1 - r) + i\omega}{(1 - r)^2 + \omega^2}$$

$$\frac{1}{(1-c)^2} = \frac{\left[(1 - r)^2 - \omega^2\right] + (1 - r)\ 2i\omega}{\left[(1 - r)^2 + \omega^2\right]^2}$$

$$\frac{1}{2-c} = \frac{(2 - r) + i\omega}{(2 - r)^2 + \omega^2}$$

$$\frac{1}{c(1-c)} = \frac{\left[r(1 - r) + \omega^2\right] + i\omega(2r - 1)}{(r^2 + \omega^2)\left[(1 - r)^2 + \omega^2\right]} \qquad \text{(X-7)}$$

$$\frac{1}{c^2(1-c)} = \frac{\left[(r^2 - \omega^2)(1 - r) + 2\omega^2 r\right] + i\omega(3r^2 - 2r - \omega^2)}{(r^2 + \omega^2)^2\left[(1 - r)^2 + \omega^2\right]}$$

$$\frac{1}{(1-c)(2-c)} = \frac{\left[(1 - r)(2 - r) - \omega^2\right] + i\omega(3 - 2r)}{\left[(1 - r)^2 + \omega^2\right]\left[(2 - r)^2 + \omega^2\right]}$$

$$\frac{1}{c(1-c)(2-c)} = \frac{\left[r(1 - r)(2 - r) + 3\omega^2(1 - r)\right] + i\omega\left[3r(2 - r) + (\omega^2 - 2)\right]}{(r^2 + \omega^2)\left[(1 - r)^2 + \omega^2\right]\left[(2 - r)^2 + \omega^2\right]}$$

$$\frac{c}{1-c} = \frac{\left[r(1 - r) - \omega^2\right] + i\omega}{(1 - r)^2 + \omega^2}$$

Utilizing the Equation (X-1) through (X-7), it is possible to determine the expression for B_1. Substituting into (III-45) gives:

$$B_1 = -e^{-r(s+k+y)}\left[\cos(S+K+Y) - i\sin(S+K+Y)\right]$$

$$\left[\frac{\left\{r(1-r)+\omega^2\right\}+i\left\{\omega(2r-1)\right\}}{(r^2+\omega^2)\left\{(1-r)^2+\omega^2\right\}}\right] + \frac{e^{-r(s+y)}}{m}\left[\cos(S+Y) - i\sin(S+Y)\right]$$

$$\left[\frac{\left\{(r^2-\omega^2)(1-r)+2\omega^2 r\right\}+i\left\{\omega(3r^2-2r-\omega^2)\right\}}{(r^2+\omega^2)^2\left\{(1-r)^2+\omega^2\right\}}\right] - \frac{e^{-rs}}{m}$$

$$\left[\cos(S) - i\sin(S)\right]\left[\frac{(r^2-\omega^2)-2ir\omega}{(r^2+\omega^2)^2}\right] - \frac{e^{-ry}}{m}\left[\cos(Y) - i\sin(Y)\right]$$

$$\left[\frac{(r^2-\omega^2)-2ir\omega}{(r^2+\omega^2)^2}\right] + \frac{r-i\omega}{r^2+\omega^2} + \frac{(1-r)-i\omega}{m}\left[\frac{(r^2-\omega^2)-2ir\omega}{(r^2+\omega^2)^2}\right] \tag{X-8}$$

Separating B_1 into its real and imaginary parts,

$$B_1 = a_1 + ib_1$$

it is found that

$$a_1 = -e^{-r(s+k+y)}\left[\frac{\cos(S+K+Y)\left\{r(1-r)+\omega^2\right\}+\omega(2r-1)\sin(S+K+Y)}{(r^2+\omega^2)\left\{(1-r)^2+\omega^2\right\}}\right]$$

$$+\frac{e^{-r(s+y)}}{m}\left[\frac{\cos(S+Y)\left\{(r^2-\omega^2)(1-r)+2\omega^2 r\right\}+\omega(3r^2-2r-\omega^2)\sin(S+Y)}{(r^2+\omega^2)^2\left\{(1-r)^2+\omega^2\right\}}\right]$$

$$- \frac{e^{-rs}}{m}\left[\frac{\cos(S)(r^2 - \omega^2) - 2r\omega \sin(S)}{(r^2 + \omega^2)^2}\right] - \frac{e^{-ry}}{m}\left[\frac{\cos(Y)(r^2 - \omega^2) - 2r\omega \sin(S)}{(r^2 + \omega^2)^2}\right]$$

$$+ \frac{r}{r^2 + \omega^2} + \frac{1}{m}\left[\frac{(1 - r)(r^2 - \omega^2) - 2r\omega^2}{(r^2 + \omega^2)^2}\right] \qquad \text{(X-9)}$$

$$b_1 = -e^{-r(s+k+y)}\left[\frac{-\left\{r(1 - r) + \omega^2\right\} \sin(S + K + Y) + \omega(2r - 1)\cos(S + K + Y)}{(r^2 + \omega^2)\left\{(1 - r)^2 + \omega^2\right\}}\right]$$

$$+ \frac{e^{-r(s+y)}}{m}\left[\frac{-\left\{(r^2 - \omega^2)(1 - r)\sin(S + Y) + \omega(3r^2 - 2r - \omega^2)\cos(S + Y)\right\}}{(r^2 + \omega^2)^2\left\{(1 - r)^2 + \omega^2\right\}}\right]$$

$$- \frac{e^{-rs}}{m}\left[\frac{-(r^2 - \omega^2) \sin(S) - 2r\omega \cos(S)}{(r^2 + \omega^2)^2}\right]$$

$$- \frac{e^{-ry}}{m}\left[\frac{-(r^2 - \omega^2) \sin(Y) - 2r\omega \cos(Y)}{(r^2 + \omega^2)^2}\right] - \frac{\omega}{r^2 + \omega^2}$$

$$- \frac{1}{m}\left[\frac{\omega(r^2 - \omega^2) + 2r\omega (1 - r)}{(r^2 + \omega^2)^2}\right] \qquad \text{(X-10)}$$

Again Equations (X-1) through (X-7) are utilized to determine the expression for B_2. Substituting into (III-54) gives

$$B_2 = m^2 u_\infty e^{-r(s+k+y)}\left[-\cos(S + K + Y) + i \sin(S + K + Y)\right]$$

$$\left[\frac{\left\{r(1 - r) + \omega^2\right\} + i\left\{\omega(2r - 1)\right\}}{(r^2 + \omega^2)\left\{(1 - r)^2 + \omega^2\right\}}\right] + m u_\infty e^{-r(s+y)}\left[\cos(S + Y) - i \sin(S + Y)\right]$$

$$\left[\frac{\left\{(r^2 - \omega^2)(1 - r) + 2\omega^2 r\right\} + i\left\{\omega(3r^2 - 2r - \omega^2)\right\}}{(r^2 + \omega^2)^2\left\{(1 - r)^2 + \omega^2\right\}}\right] + 2m^2 u_\infty e^{-r(s+k)}$$

$$\left[\cos(S + K) - i\sin(S + K)\right]$$

$$\left[\frac{\left\{r(1 - r)(2 - r) + 3\omega^2(1 - r)\right\} + i\left\{\omega\left[3r(2 - r) + (\omega^2 - 2)\right]\right\}}{(r^2 + \omega^2)\left\{(1 - r)^2 + \omega^2\right\}\left\{(2 - r)^2 + \omega^2\right\}}\right]$$

$$- e^{-rs}\left[\cos(S) - i\sin(S)\right]\left[\frac{(1 - r) + i\omega}{(1 - r)^2 + \omega^2}\right]\left[u_\infty\left\{\frac{(2 - r) + i\omega}{(2 - r)^2 + \omega^2}\right\}\right.$$

$$\left. + 1 - u_\infty s + mu_\infty\left\{\frac{(r^2 - \omega^2) - 2ir\omega}{(r^2 + \omega^2)^2}\right\}\right] + e^{-rs}\left[\cos(S) - i\sin(S)\right]$$

$$\left[1 - u_\infty s\right]\left[\frac{r - i\omega}{r^2 + \omega^2}\right] + 2\ell_1 e^{-rs}\left[\cos(S) - i\sin(S)\right]\left[\frac{r - i\omega}{r^2 + \omega^2}\right]$$

$$- mu_\infty e^{-ry}\left[\cos(Y) - i\sin(Y)\right]\left[\frac{(r^2 - \omega^2) - 2ir\omega}{(r^2 + \omega^2)^2}\right] - (1 - u_\infty s)\left[\frac{r - i\omega}{r^2 + \omega^2}\right]$$

$$+ mu_\infty\left[\frac{(r^2 - \omega^2) - 2ir\omega}{(r^2 + \omega^2)^2}\right] - 2\ell_1\left[\frac{r - i\omega}{r^2 + \omega^2}\right] + 2(\ell_o + 1 + \ell_1) \qquad \text{(X-11)}$$

Separating B_2 into its real and imaginary parts

$$B_2 = a_2 + ib_2$$

it is found that

$$a_2 = m^2 u_\infty e^{-r(s+k+y)} \left[\frac{-\cos(S+K+Y)\left\{r(1-r)+\omega^2\right\} - \omega(2r-1)\sin(S+K+Y)}{(r^2+\omega^2)\left\{(1-r)^2+\omega^2\right\}} \right]$$

$$+ m u_\infty e^{-r(s+y)} \left[\frac{\left\{(r^2-\omega^2)(1-r)+2\omega^2 r\right\}\cos(S+Y) + \omega(3r^2-2r-\omega^2)\sin(S+Y)}{(r^2+\omega^2)^2\left\{(1-r)^2+\omega^2\right\}} \right]$$

$$+ 2m^2 u_\infty e^{-r(s+k)} \left[\frac{\left\{r(1-r)(2-r)+3\omega^2(1-r)\right\}\cos(S+K) + \omega\left\{3r(2-r)+(\omega^2-2)\right\}\sin(S+K)}{(r^2+\omega^2)\left\{(1-r)^2+\omega^2\right\}\left\{(2-r)^2+\omega^2\right\}} \right]$$

$$- e^{-rs} u_\infty \left[\frac{(2-r)\left\{(1-r)\cos(S)+\omega\sin(S)\right\} + \omega(1-r)\sin(S) - \omega^2\cos(S)}{\left\{(1-r)^2+\omega^2\right\}\left\{(2-r)^2+\omega^2\right\}} \right]$$

$$- e^{-rs}(1-u_\infty s) \left[\frac{\left\{(1-r)\cos(S)+\omega\sin(S)\right\}}{(1-r)^2+\omega^2} \right]$$

$$- m u_\infty e^{-rs} \left[\frac{(r^2-\omega^2)\left\{(1-r)\cos(S)+\omega\sin(S)\right\} + 2r\omega\left\{\omega\cos(S)-(1-r)\sin(S)\right\}}{\left\{(1-r)^2+\omega^2\right\}(r^2+\omega^2)^2} \right]$$

$$+ e^{-rs}(1-u_\infty s)\left[\frac{r\cos(S)-\omega\sin(S)}{r^2+\omega^2}\right] + 2\ell_1 e^{-rs}\left[\frac{r\cos(S)-\omega\sin(S)}{r^2+\omega^2}\right]$$

$$- m u_\infty e^{-ry}\left[\frac{(r^2-\omega^2)\cos(Y)-2r\omega\sin(Y)}{(r^2+\omega^2)^2}\right] - \frac{(1-u_\infty s)r}{r^2+\omega^2} + m u_\infty\left[\frac{r^2-\omega^2}{(r^2+\omega^2)^2}\right]$$

$$- \frac{2\ell_1 r}{r^2+\omega^2} + 2(\ell_o + 1 + \ell_1) \qquad \text{(X-12)}$$

$$b_2 = m^2 u_\infty e^{-r(s+k+y)} \left[\frac{\left\{r(1-r)+\omega^2\right\}\sin(S+K+Y) - \omega(2r-1)\cos(S+K+Y)}{(r^2+\omega^2)\left\{(1-r)^2+\omega^2\right\}} \right]$$

$$+ mu_\infty e^{-r(s+y)}\left[\frac{-\{(r^2 - \omega^2)(1 - r) + 2\omega^2 r\} \sin(S + Y) + \omega(3r^2 - 2r - \omega^2)\cos(S+Y)}{(r^2 + \omega^2)^2 \{(1 - r)^2 + \omega^2\}}\right]$$

$$+ 2m^2 u_\infty e^{-r(s+k)}\left[\frac{-\{r(1-r)(2-r) + 3\omega^2(1-r)\} \sin(S+K) + \omega\{3r(2-r) + \omega^2 - 2\} \cos(S+K)}{(r^2 + \omega^2)\{(1 - r)^2 + \omega^2\}\{(2 - r)^2 + \omega^2\}}\right]$$

$$- e^{-rs} u_\infty \left[\frac{(2-r)\{\omega \cos(S) - (1 - r) \sin(S)\} + \omega\{(1-r) \cos(S) + \omega \sin(S)\}}{\{(1 - r)^2 + \omega^2\}\{(2 - r)^2 + \omega^2\}}\right]$$

$$- e^{-rs}(1 - u_\infty s)\left[\frac{\omega \cos S - (1 - r) \sin S}{(1 - r)^2 + \omega^2}\right]$$

$$- mu_\infty e^{-rs}\left[\frac{(r^2 - \omega^2)\{\omega \cos(S) - (1-r) \sin(S)\} - 2r\omega\{(1-r) \cos(S) + \omega \sin(S)\}}{\{(1 - r)^2 + \omega^2\}(r^2 + \omega^2)^2}\right]$$

$$- e^{-rs}(1 - u_\infty s)\left[\frac{r \sin(S) + \omega \cos(S)}{r^2 + \omega^2}\right] - 2\ell_1 e^{-rs}\left[\frac{r \sin(S) + \omega \cos(S)}{r^2 + \omega^2}\right]$$

$$+ mu_\infty e^{-ry}\left[\frac{(r^2 - \omega^2) \sin(Y) + 2r\omega \cos(Y)}{(r^2 + \omega^2)^2}\right] + (1 - u_\infty s)\frac{\omega}{r^2 + \omega^2}$$

$$- \frac{2mu_\infty r\omega}{(r^2 + \omega^2)^2} + \frac{2\ell_1 \omega}{r^2 + \omega^2} \qquad \text{(X-13)}$$

B_3 is determined as above utilizing (X-1) through (X-7). Substituting into (III-56) gives

$$B_3 = mu_\infty e^{-r(s+k)}\left[\cos(S + K) - i \sin(S + K)\right]\left[\frac{\{(1-r)^2 - \omega^2\} + (1-r)2i\omega}{\{(1 - r)^2 + \omega^2\}^2}\right]$$

$$+ e^{-rs}\left[\cos(S) - i\sin(S)\right]\left[u_\infty\left\{\frac{r - i\omega}{r^2 + \omega^2}\right\} - u_\infty k\left\{\frac{\left[r(1-r) - \omega^2\right] + i\omega}{(1 - r)^2 + \omega^2}\right\}\right.$$

$$\left. - u_\infty\left\{\frac{\left[(1 - r)^2 - \omega^2\right] + (1 - r)2i\omega}{\left[(1 - r)^2 + \omega^2\right]^2}\right\} + \frac{\ell_1}{m}\right] + (\ell_o + u_\infty s + u_\infty k + \frac{\ell_1}{m})$$

$$(r + i\omega) - u_\infty\left\{\frac{r - i\omega}{r^2 + \omega^2}\right\} - \frac{\ell_1}{m} \qquad \text{(X-14)}$$

Separating B_3 into real and imaginary parts,

$$B_3 = a_3 + ib_3$$

it is found that

$$a_3 = mu_\infty e^{-r(s+k)}\left[\frac{\left\{(1 - r)^2 - \omega^2\right\}\cos(S + K) + 2\omega(1 - r)\sin(S + K)}{\left\{(1 - r)^2 + \omega^2\right\}^2}\right]$$

$$+ e^{-rs}u_\infty\left[\frac{r\cos(S) - \omega\sin(S)}{r^2 + \omega^2}\right] - e^{-rs}u_\infty k\left[\frac{\left\{r(1-r) - \omega^2\right\}\cos(S) + \omega\sin(S)}{(1 - r)^2 + \omega^2}\right]$$

$$- e^{-rs}u_\infty\left[\frac{\left\{(1 - r)^2 - \omega^2\right\}\cos(S) + 2\omega(1 - r)\sin(S)}{\left\{(1 - r)^2 + \omega^2\right\}^2}\right] + \frac{e^{-rs}\,\ell_1\cos(S)}{m}$$

$$+ r(\ell_o + u_\infty s + u_\infty k + \frac{\ell_1}{m}) - \frac{ru_\infty}{r^2 + \omega^2} - \frac{\ell_1}{m} \qquad \text{(X-15)}$$

$$b_3 = mu_\infty e^{-r(s+k)}\left[\frac{-\left\{(1 - r)^2 - \omega^2\right\}\sin(S + K) + 2\omega(1 - r)\cos(S + K)}{\left\{(1 - r)^2 + \omega^2\right\}^2}\right]$$

$$- e^{-rs}u_\infty \left[\frac{r\sin(S) + \omega\cos(S)}{r^2+\omega^2}\right] - e^{-rs}u_\infty k\left[\frac{-\{r(1-r)-\omega^2\}\sin(S) + \omega\cos(S)}{(1-r)^2+\omega^2}\right]$$

$$- e^{-rs}u_\infty \left[\frac{-\{(1-r)^2-\omega^2\}\sin(S) + (1-r)2\omega\cos(S)}{\{(1-r)^2+\omega^2\}^2}\right] - \frac{e^{-rs}\,\ell_1\sin(S)}{m}$$

$$+ \omega(\ell_o + u_\infty s + u_\infty k + \frac{\ell_1}{m}) + \frac{u_\infty\omega}{r^2+\omega^2} \qquad \text{(X-16)}$$

Hence, the coefficients of the equations in ω have been found for $r \neq 0$. These equations were then solved utilizing the computer as was done for $r = 0$. Therefore, by solving them for $r \to 0$ allows the determination of the behavior between the levels of the instability threshold. This computer program is found in Appendix IX. Figure (58) shows the results of this investigation for $f > 0$ (which corresponds to physical reality), where g increases as r goes from negative to zero to positive values. Hence, plotting the same curve for a range of values, it is found that as shown in Figure (58) the region of stability ($r > 0$) and the region of instability ($r < 0$) is given as in Figure (59).

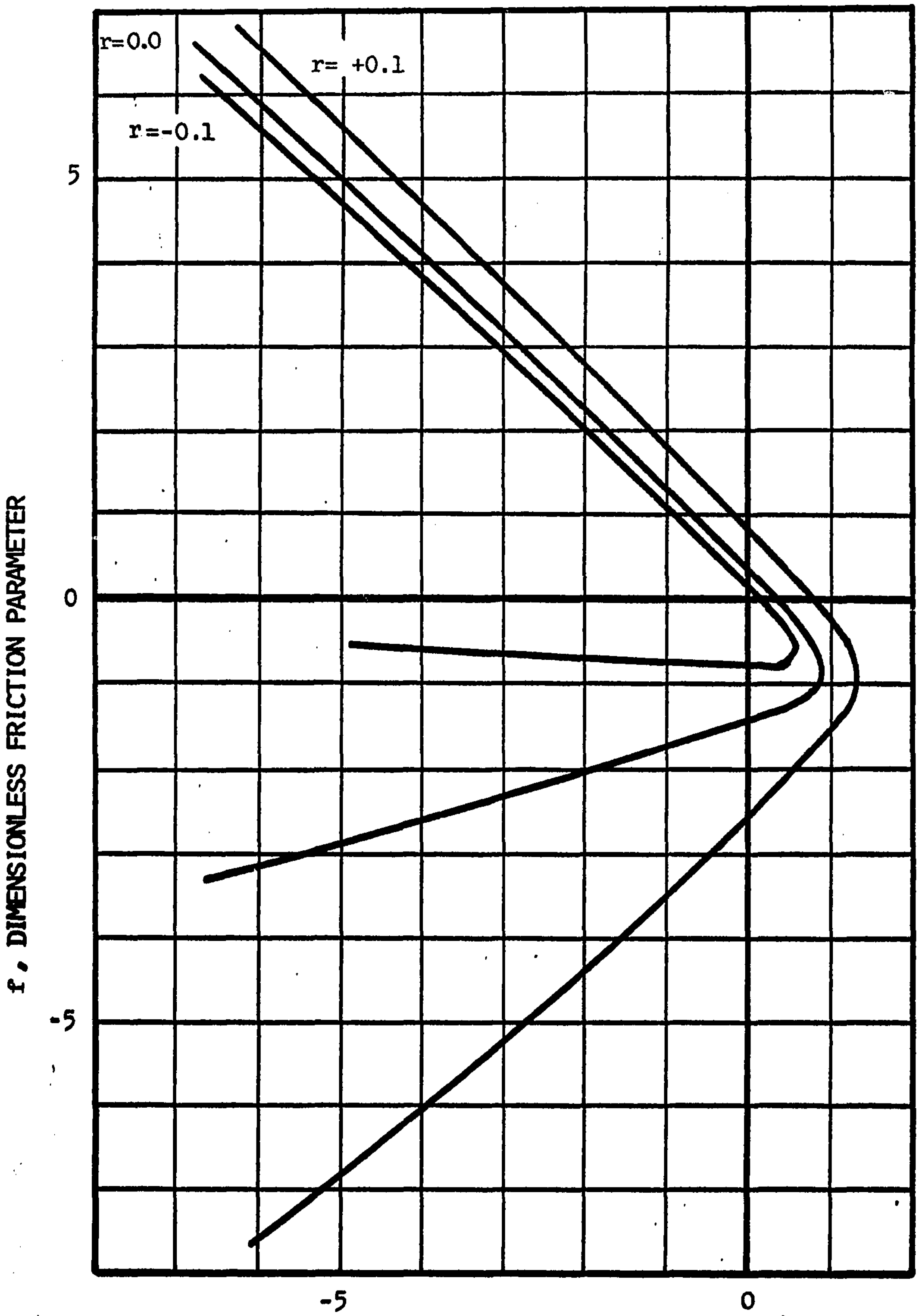

FIGURE (58) $f = f(g)$ FOR S = 0.5 WITH $u_\infty = 0.1$ AS r VARIES FROM NEGATIVE TO POSITIVE VALUES

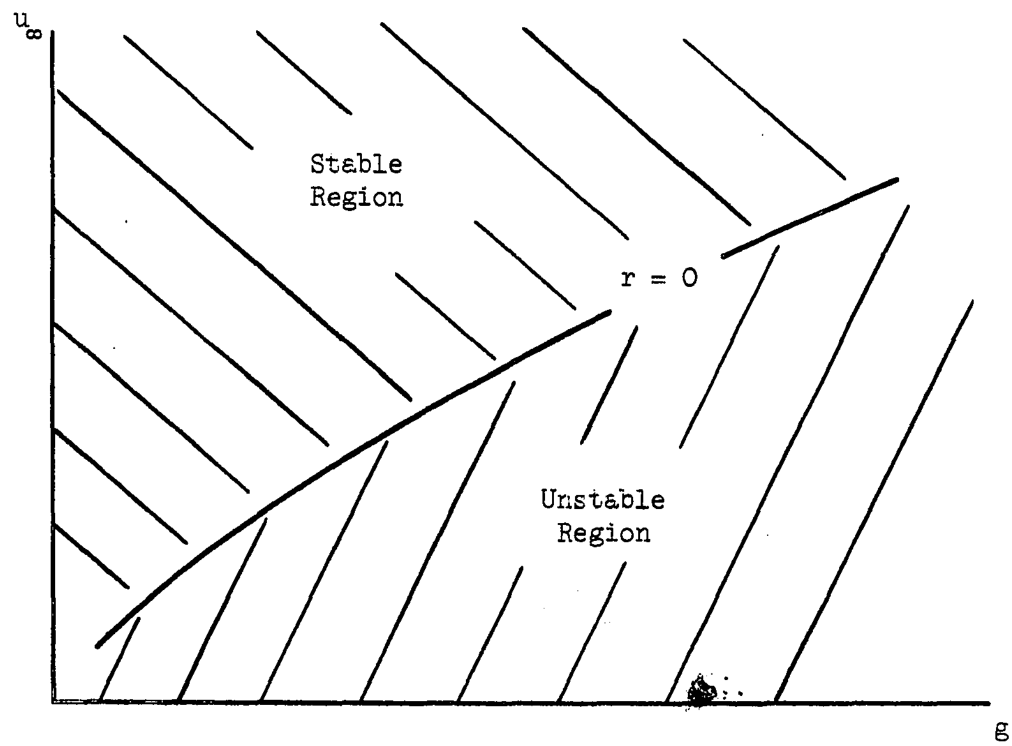

Figure (59) Stable and Unstable Regions of the Threshold Surface

APPENDIX XI

EXPERIMENTAL INSTABILITY POINT DATA

The following tables give the experimental instability point data which was shown in Figures (45 - 53).

TABLE 3a

EXPERIMENTAL INSTABILITY POINTS FOR CONSTANT PRESSURE TESTS

UTILIZING FREON-114 AS THE HEAT TRANSFER FLUID

F-114 Experimental Instability Points				
T_8 Inlet Temp ^oF	H_i Inlet Enthalpy Btu/lb_m	ρ Inlet Density lb_m/ft^3	H_o H_s-H_i	ΔP Flow In. H_2O
*P = 310 psia	H_s = 73 Btu/lb_m	R_o = 70 lb_m/ft^3	H_c = 6 Btu/lb_m	
194	56.51	76.11	16.49	4.00
196	57.07	75.79	15.93	4.00
198	57.62	75.47 -	15.38	4.1
173	50.78	79.25	22.22	4.4
162	47.82	80.78	25.18	4.1
148	44.11	82.64	28.89	4.2
147	43.57	82.90	29.43	4.3
195	57.29	75.95	15.71	3.4
192	55.96	76.42	17.04	4.25
184	53.76	77.64	19.24	3.4
183	53.49	78.29	19.51	3.75
173	50.78	79.25	22.22	4.10
157	46.49	81.46	26.51	4.25
153	45.42	81.93	27.58	4.30
152	45.16	82.12	27.84	4.75
189	55.13	76.88	17.87	3.1

185	54.04	77.49	18.96	3.6
P = 400 psia H_s = 83 Btu/lb_m R_o = 60 lb_m/ft^3 H_c = 10 Btu/lb_m				
216	62.69	72.40	20.31	3.85
200	58.18	75.14	24.72	5.45
196	57.07	75.79	25.93	6.25
173	50.78	79.25	32.22	5.85
168	49.43	79.96	33.57	6.05
170	49.97	79.68	33.03	5.85
170	49.97	79.68	33.03	6.10
218	63.26	72.04	19.74	4.40
220	63.83	71.67	19.17	5.95
223	64.70	71.11	18.30	3.80
214	62.12	72.76	20.88	4.0
214	62.12	72.76	20.88	4.5
217	62.98	72.22	20.02	4.4
216	62.69	72.40	20.31	5.8
219	63.50	71.86	19.50	6.0
225	65.27	70.73	17.73	6.0
200	58.18	75.14	24.82	6.1
209	60.70	73.64	22.30	7.0
225	65.27	70.73	17.73	6.5
197	57.34	75.62	25.66	5.9
198	57.62	75.47	25.38	6.6
193	56.24	76.26	26.76	6.1
186	54.31	77.34	28.69	6.4

177	51.82	78.68	31.18	5.9
175	51.32	78.97	31.68	6.6
170	49.97	79.68	33.03	6.25
220	63.83	71.67	19.17	3.60
225	65.27	70.73	17.73	4.75
213	61.90	72.94	21.10	4.25
P = 480 psia H_s = 80 Btu/lb_m R_o = 70 lb_m/ft^3 H_c = 16 Btu/lb_m				
260	75.96	62.61	4.04	2.40
255	74.34	64.0	5.66	2.50
210	60.98	73.46	19.02	3.75
262	76 62	62.03	3.38	2.20
P = 495 psia H_s = 80 Btu/lb_m R_o = 70 lb_m/ft^3 H_c = 16 Btu/lb_m				
245	71.20	66.49	8.80	2.40
218	63.26	72.04	16.70	3.40
203	58.46	74.65	21.50	3.40
198	57.62	75.47	22.40	4.20
191	55.68	76.57	24.30	4.00
P = 520 psia H_s = 80 Btu/lb_m R_o = 70 lb_m/ft^3 H_c = 16 Btu/lb_m				
228	66.15	70.14	13.85	2.00
228	66 15	70.14	13.85	2.25
214	62.12	72.76	17.88	2.75
205	59.58	74.30	20.42	2.75
169	49.69	79.81	30.31	2.25

163	48.09	80.92	31.91	2.25
195	56.79	75.95	23.21	2.50
162	47.82	80.78	32.18	2.10
162	47.82	80.78	32.18	2.10
230	66.73	69.74	13.27	1.85
P = 525 psia H_s = 80 Btu/lb_m R_o = 70 lb_m/ft^3 H_c = 16 Btu/lb_m				
254	74.02	64.26	5.98	2.00
252	73.39	64.78	6.61	2.10
264	77.30	61.42	2.70	2.00
257	75.00	63.45	5.00	2.00
270	79.39	59.43	0.61	2.10
211	61.25	73.28	18.75	2.00
267	78.33	60.43	1.67	2.55
206	59.86	74.15	20.14	2.25
206	59.86	74.15	20.14	2.25
220	63.83	71.67	16.16	2.50
196	57.07	75.79	22.93	2.45
195	56.79	75.95	23.21	2.50
198	57.62	75.47	22.38	2.55
197	57.34	75.63	22.66	2.55
257	74.98	63.45	5.02	2.40
P = 555 psia H_s = 85 Btu/lb_m R_o = 70 lb_m/ft^3 H_c = 16 Btu/lb_m				
178	52.13	78.53	27.87	2.40
262	76.63	62.03	3.37	1.95
246	71.52	66.26	8.48	2.20

232	67.32	69.33	12.68	2.00
202	58.74	74.82	21.26	2.40
203	59.01	74.65	20.99	2.50
197	57.34	75.94	22.66	2.25
170	49.97	79.68	30.03	2.00
165	48.61	80.37	31.39	1.90
P = 575 psia H_s = 85 Btu/lb_m R_o = 70 lb_m/ft^3 H_c = 16 Btu/lb_m				
153	45.42	81.99	34.58	1.60
151	44.89	82.25	35.11	1.75
233	67.61	69.13	12.39	2.00
252	73.39	64.78	6.61	2.20
238	69.10	68.07	10.90	2.00
249	72.44	65.53	7.56	2.25
250	72.76	65.29	7.24	2.60
263	76.96	61.72	3.04	2.65
210	60.98	73.46	19.02	2.70
180	52.67	78.24	27.33	2.25
169	49.70	79.82	30.30	2.20
157	46.49	81.46	33.51	1.75
153	45.43	81.99	34.57	1.80

*P = System Pressure H_s = Enthalpy Zero Point

TABLE 3b

EXPERIMENTAL INSTABILITY POINTS FOR CONSTANT PRESSURE TESTS

UTILIZING FREON-114 AS THE HEAT TRANSFER FLUID

F-114 Experimental Instability Points			
W Power KW	u_∞ Entrance Velocity	g Gravity Parameter	s Subcooling
*P = 310 psia H_s = 73 Btu/lb_m R_o = 70 lb_m/ft^3 H_c = 6 Btu/lb_m			
.713	.240	20.7	2.76
.675	.253	23.2	2.66
.720	.240	20.3	2.56
1.24	.142	6.85	3.70
1.44	.117	5.07	4.19
1.74	.096	3.48	4.82
1.65	.103	3.87	4.91
.705	.224	21.2	2.62
.874	.201	13.8	2.84
.98	.159	10.95	3.21
1.13	.144	8.25	3.26
1.28	.132	6.42	3.70
1.63	.104	3.96	4.42
1.74	.098	3.48	4.60
1.95	.092	2.77	4.64
.905	.166	12.85	2.98

1.11	.145	8.54	3.16
P = 400 psia H_s = 83 Btu/lb_m R_o = 60 lb_m/ft^3 H_c = 10 Btu/lb_m			
1.07	.229	18.8	2.03
1.63	.176	8.1	2.47
1.96	.156	5.6	2.59
2.43	.119	3.64	3.22
2.58	.114	3.24	3.36
2.52	.115	3.39	3.30
2.63	.112	3.11	3.30
1.13	.233	16.9	1.97
1.40	.219	10.97	1.92
.91	.271	26.0	1.83
1.06	.236	19.15	2.09
1.24	.214	14.0	2.09
1.39	.189	11.25	2.00
1.55	.194	8.95	2.03
1.58	.195	8.6	1.95
1.57	.197	8.73	1.77
1.82	.167	6.5	2.48
1.84	.178	6.35	2.23
1.64	.198	8.0	1.77
1.77	.168	6.87	2.57
2.01	.157	5.32	2.54
2.03	.148	5.22	2.68
2.27	.135	4.17	2.87
2.40	.122	3.73	3.12

2.64	.117	3.09	3.17
2.66	.112	3.04	3.30
0.91	.262	26.0	1.92
1.15	.240	16.3	1.77
1.15	.223	16.3	2.11
P = 480 psia H_s = 80 Btu/lb_m R_o = 70 lb_m/ft^3 H_c = 16 Btu/lb_m			
1.81	.216	24.50	.252
2.80	.140	9.55	.354
4.62	.097	3.51	1.190
2.56	.147	11.40	.385
P = 495 psia H_s = 80 Btu/lb_m R_o = 70 lb_m/ft^3 H_c = 16 Btu/lb_m			
1.80	.209	23.1	.55
3.23	.134	7.18	1.04
3.58	.118	5.84	1.34
4.45	.105	3.78	1.40
5.17	.088	2.80	1.52
P = 520 psia H_s = 80 Btu/lb_m R_o = 70 lb_m/ft^3 H_c = Btu/lb_m			
1.33	.252	42.40	.865
1.34	.266	41.70	.865
1.90	.204	20.70	1.12
2.06	.186	17.60	1.28
2.50	.134	12.0	1.89

2.87	.115	9.1	1.99
2.32	.155	13.9	1.45
2.70	.119	10.3	2.01
2.63	.122	10.8	2.01
1.24	.262	48.8	.828
P = 525 psia H_s = 80 Btu/lb_m R_o = 70 lb_m/ft^3 H_c = 16 Btu/lb_m			
1.28	.275	45.70	.374
1.37	.262	39.9	.413
1.33	.270	42.3	.169
1.80	.197	23.1	.312
1.98	.189	19.1	.038
1.99	.166	18.9	1.170
2.02	.203	18.4	.104
2.34	.149	13.7	1.26
2.49	.140	12.1	1.26
2.49	.150	12.1	1.01
3.22	.112	7.24	1.43
3.36	.112	6.64	1.45
3.84	.096	5.08	1.40
3.64	.101	5.66	1.42
1.81	.214	22.90	.313
P = 555 psia H_s = 85 Btu/lb_m R_o = 70 lb_m/ft^3 H_c = 16 Btu/lb_m			
2.81	.124	9.50	2.06
1.31	.269	43.7	.523
1.33	.272	42.4	.842

1.34	.253	41.7	1.10
2.00	.170	18.7	1.64
2.10	.173	17.0	1.62
2.10	.163	17.0	1.73
2.36	.134	13.5	2.19
2.47	.124	12.3	2.28
P = 575 psia H_s = 85 Btu/lb_m R_o = 70 lb_m/ft^3 H_c = 16 Btu/lb_m			
1.82	.153	22.6	2.48
1.98	.146	19.1	2.50
1.34	.252	41.7	1.09
1.34	.274	41.7	.725
1.28	.266	45.7	.994
1.25	.295	48.0	.784
1.50	.265	33.3	.765
1.52	.271	32.4	.502
2.06	.185	17.7	1.50
2.36	.143	13.5	2.02
2.58	.128	11.2	2.21
1.76	.166	24.2	2.40
1.86	.159	21.6	2.47

*P = System Pressure H_s = Enthalpy Zero Point

TABLE 4a

EXPERIMENTAL INSTABILITY POINTS FOR CONSTANT PRESSURE TESTS

UTILIZING H_2O AS THE HEAT TRANSFER FLUID

H_2O Experimental Instability Points				
T_8 Inlet Temp ^oF	H_i Inlet Enthalpy Btu/lb_m	ρ Inlet Density lb_m/ft^3	H_o H_s-H_i	ΔP Flow In. H_2O
*P = 1740 psia H_s = 640 Btu/lb_m R_o = 45 lb_m/ft^3 H_c = 60 Btu/lb_m				
424	401	52.6	239	1.90
534	529	46.9	111	1.20
534	529	46.9	111	1.20
518	510	47.8	130	1.20
521	513	47.8	133	1.20
503	492	48.8	148	1.40
499	487	49.0	153	1.45
487	473	49.8	167	1.50
478	462	50.0	178	1.60
462	444	51.0	196	1.75
451	431	50.3	209	1.80
P = 2215 psia H_s = 705 Btu/lb_m R_o = 40 lb_m/ft^3 H_c = 90 Btu/lb_m				
579	588	43.9	117	1.20
559	561	45.2	144	1.30

563	566	45.0	139	1.30
545	543	46.4	162	1.45
517	508	48.1	197	1.60
508	497	48.3	208	1.75
496	483	49.3	222	1.85
506	495	48.8	210	1.75
481	466	50.0	239	2.0

*P = System Pressure H_s = Enthalpy Zero Point

TABLE 4b

EXPERIMENTAL INSTABILITY POINTS FOR CONSTANT PRESSURE TESTS

UTILIZING H_2O AS THE HEAT TRANSFER FLUID

H_2O Experimental Instability Points			
W Power KW	u_∞ Entrance Velocity	g Gravity Parameter	s Subcooling
*P = 1740 psia H_s = 640 Btu/lb_m R_o = 45 lb_m/ft^3 H_c = 60 Btu/lb_m			
16.9	.054	1.51	3.98
4.47	.172	21.8	1.85
5.63	.137	13.7	1.85
6.85	.111	9.3	2.17
7.54	.101	7.65	2.22
8.77	.092	5.66	2.47
9.62	.086	4.7	2.55
10.80	.077	3.73	2.78
11.60	.074	3.03	2.97
12.60	.071	2.74	3.27
14.10	.064	2.19	3.48
P = 2215 psia H_s = 705 Btu/lb_m R_o = 40 lb_m/ft^3 H_c = 90 Btu/lb_m			
5.79	.183	23.1	1.30
6.62	.162	17.7	1.60
7.89	.137	12.4	1.55

9.04	.125	9.49	1.80
10.32	.113	7.28	2.19
11.50	.106	5.87	2.31
12.65	.098	4.84	2.46
13.35	.091	4.35	2.34
14.92	.086	3.43	2.66

*P = System Pressure H_s = Enthalpy Zero Point